DESIGN, IMPLEMENTATION AND ENGINEERING ASPECTS OF TCR FOR
INDUSTRIAL SVC SYSTEMS

A THESIS SUBMITTED TO
THE GRADUATE SCHOOL OF NATURAL AND APPLIED SCIENCES
OF
MIDDLE EAST TECHNICAL UNIVERSITY

BY

HALAS BİLGE MUTLUER

IN PARTIAL FULFILLMENT OF THE REQUIREMENTS
FOR
THE DEGREE OF DOCTOR OF PHILOSOPHY
IN
ELECTRICAL AND ELECTRONICS ENGINEERING

MARCH 2008

Approval of the thesis

DESIGN, IMPLEMENTATION AND ENGINEERING ASPECTS OF TCR FOR INDUSTRIAL SVC SYSTEMS

submitted by **HALAS BİLGE MUTLUER** in partial fulfillment of the requirements for the degree of **Doctor of Philosophy in Electrical and Electronics Engineering Department, Middle East Technical University** by,

Prof. Dr. Canan ÖZGEN
Dean, Graduate School of **Natural and Applied Sciences**   _____

Prof. Dr. İsmet ERKMEN
Head of Department, **Electrical and Electronics Eng. Dept**.   _____

Prof. Dr. Muammer ERMİŞ
Supervisor, **Electrical and Electronics Eng. Dept., METU**   _____

Examining Committee Members :

Prof. Dr.Aydın ERSAK
Electrical and Electronics Eng. Dept., METU   _____

Prof. Dr. Muammer ERMİŞ
Electrical and Electronics Eng. Dept., METU   _____

Prof. Dr. Işık ÇADIRCI
Electrical and Electronics Eng. Dept., Hacettepe Unv.   _____

Prof.Dr. Nevzat ÖZAY
Electrical and Electronics Eng. Dept., METU   _____

Asist. Prof. Dr.İres İSKENDER
Electrical and Electronics Eng. Dept., Gazi Unv.   _____

Date: 07 / 03 / 2008

I hereby declare that all information in this document has been obtained and presented in accordance with academic rules and ethical conduct. I also declare that, as required by these rules and conduct, I have fully cited and referenced all material and results that are not original to this work.

Name, Last name   :   H. Bilge MUTLUER

Signature   :

ABSTRACT

DESIGN, IMPLEMENTATION AND ENGINEERING ASPECTS OF TCR FOR
INDUSTRIAL SVC SYSTEMS

MUTLUER, H. Bilge

Ph.D., Department of Electrical and Electronics Engineering

Supervisor : Prof. Dr. Muammer ERMİŞ

March 2008, 235 pages

Design and implementation of TCR (Thyristor Controlled Reactor) for industrial
SVC (Static VAr Compensator) systems require special design. Both power stage
and control system design and implementation are thoroughly investigated in this
thesis. Engineering aspects of TCR design are emphasized and supported with case
studies. As the first case study; a novel, unified and relocatable SVC for open cast
lignite mining in Turkey is designed, implemented and commissioned. The second
case study is the first 12 pulse TCR design and implementation for ladle furnace
compensation in the world. The SVC simulation results are verified by data acquired
in the field. Real time data are also simulated in EMTDC/PSCAD program to verify
the control system responses of the commissioned systems.

Keywords: TCR, SVC, 12-pulse TCR

ÖZ

ENDÜSTRİYEL STATİK VAR KOMPANZATÖRÜ İÇİN TİRİSTÖR
KONTROLLU REAKTÖR SİSTEMLERİNİN TASARIM, UYGULAMA VE
MÜHENDİSLİK YÖNLERİ

MUTLUER, H. Bilge

Doktora, Elektrik Elektronik Mühendisliği Bölümü

Tez Yöneticisi : Prof. Dr. Muammer ERMİŞ

Mart 2008, 235 sayfa

TKR (Tiristör Kobtrollu Reaktör) tipi SVK (Statik VAr Kompanzatörü) sistemlerinin dizaynı ve uygulaması özel tasarım gerektirmektedir. Hem güç katı hem de kontrol sisteminin tasarımı bu tezde detaylı olarak incelenmektedir. TKR tasarımının mühendislik yanı vurgulanmakta ve örnek olaylar ile desteklenmektedir. Birinci örnek olay olarak açık linyit madeni ocakları için özgün, genelleştirilmiş ve taşınabilir SVK tasarımı, uygulanması ve devreye alınması gerçekleştirilmiştir. İkinci örnek olayda pota ocağı için 12 darbeli TKR tasarımı ve uygulanması dünyada ilk kez gerçekleştirilmiştir. SVK simülasyon sonuçları sahada yapılan ölçümler ile doğrulanmıştır. Ayrıca sahada devreye alınan sistemlerden toplanan veriler EMTDC/PSCAD programında gerçek zamanlı olarak çalıştırılarak kontrol sisteminin tepkileri doğrulanmıştır

Anahtar Kelimeler: TKR, SVK, 12-darbeli TKR

ACKNOWLEDGMENTS

TABLE OF CONTENTS

LIST OF TABLES

LIST OF FIGURES

xvi

NOMENCLATURE

α	Firing delay angle
σ	Conduction angle
a_n	Fourier transformation coefficient of the harmonic number n
B_γ^{ab}	SVC susceptance for phase ab
B_l^{ab}	Load susceptance for phase ab
C_k	Rms amplitude of the $(k)^{th}$ spectral component
$G_{g,n}$	Square root of the sum of the squares of a harmonic
G_l^{ab}	Load conductance for phase ab
I_{dc}	DC component of the current
I_n	Rms value of nth current harmonic
I_h	Instantaneous value of hth current harmonic
I_k	Short circuit current for the point of common coupling
I_l	Load current averaged for 15 minutes
I_{tav}	Thyristor average on state current
I_{Trms}	Thyristor rms on state current
I_+	Positive sequence component of current
$I_{TCR}(\alpha)$	TCR reactor current as a funtction of firing delay angle
K_k	Rate of change of voltage per reactive power
P_{cvalve}	Thyristor valve conduction losses
$P_{E.CR}$	Eddy losses in an oil immersed transformer
P_{hyst}	Iron core reactor (hysteresis) losses
P_k	Power delivered by fundamental component for phase k
P_{kh}	Power delivered by harmonic sources for phase k
P_l	Load power
P_{sn}	Thyristor snubber circuit losses
P_{Tsw}	Thyristor total switching losses

P_{valve}	Thyristor valve conduction losses
P_{vd}	Thyristor equalizing circuit losses
Q_k	Reactive Power delivered by fundamental component for phase k
Q_{kh}	Reactive power delivered by harmonic sources for phase k
Q_l	Load reactive power
R_s	Reistance of the source
S	Apparent power
V_{DRM}	Thyristor repetitive peak off state voltage
V_k	Knee point voltage
V_{RRM}	Thyristor repetitive peak reverse voltage
V_s	Source voltage
V_t	Terminal voltage
V_+	Positive sequence component of voltage
X_L	Impedance of the reactors in the fundamental frequency
X_s	Source reactance
Y_l^{ab}	Load admittance of phase ab
Y_a	admittance of line a
Z_a	Impedance of line a
Z_t	Terminal impedance seen from the load
Z_s	Source impedance

ABBREVIATIONS

CSC	Current Source Converter
CT	Current Transformer
EAF	Electrical Arc Furnace
EMI	Electromagnetic Interference
EMC	Electromagnetic Compatibility
ESL	Equivalent Series Inductance
ESR	Equivalent Series Resistance
FACTS	Flexible AC Transmission Systems
GTO	Gate Turn-Off Thyristor
HF	Harmonic Filter
LF	Ladle Furnace
LTT	Light Triggered Thyristor
LV	Low Voltage
MV	Medium Voltage
PCC	Common Coupling Point
PI	Proportional and integral
PLL	Phase Locked Loop
PT	Potential Transformer
STATCOM	Static Synchronous Compensator
SVC	Static VAR Compensator
Std.	Standard
TCR	Thyristor Controlled Reactor
TS	Transformer Substation
TSR	Thyristor Switched Reactor
TDD	Total Demand Distortion
THD	Total Harmonic Distortion
TR	Transformer

| TSC | Thyristor Switched Capacitor |
| VSC | Voltage Source Converter |

CHAPTER 1

INTRODUCTION

1.1 Overview of TCR Based SVC

The design of the Static VAr Compensator (SVC) has been considered as a challenge since the early 1970s. Nowadays, the power stage has increased from several MVArs up to hundreds of MVArs and the control methods have evolved in a way to keep flicker levels in most of the loads below the required standards. Currently, there are many SVCs all around the world and many are under construction and commissioned. Although it is not a recently developed technology, still there are improvements to be done on this subject.

IEEE defines Static VAR Compensator as a shunt connected static var generator or absorber whose output is adjusted to exchange capacitive or inductive power in order to control reactive power flow [31] in power systems.

There are four main purposes for the installation of a SVC according to Miller [1]:

1. Maintaining Voltage at or near a constant level,

2. Improving Power System stability,

3. Improving Power Factor,

4. Correcting Phase unbalance.

Further objectives are filtering out harmonic currents, power oscillation damping, flicker reduction and sub-harmonic filtering as described in IEEE 1031 [31].

The SVC systems are employed by the transmission authorities and industry. The purposes of the installations may differ in industrial type SVC and transmission type SVC systems. Fig. 1.1 shows various SVC systems.

Fig.1.1. Various SVCs

Industrial SVCs are mainly focused on increasing the production capability in an industrial plant while fulfilling the power quality legislations. Harmonic cancellation and minimization of the flicker are some of the topics that attracted the researchers in early 2000s. TCRs (Thyristor Controlled Reactors) are gradually being

replaced by STATCOMs (Static Synchronous Compensators) [63,64] that have been under development for the last two decades; however, TCR is still a great cost-effective solution for many applications.

The transmission type SVC systems are mainly focused on power stability and voltage control [1,2]. TCR type SVC systems are subsets of the FACTS (Flexible Alternative Current Transmission Systems), which is the recent application of power electronics to the transmission systems. Therefore, transmission type TCR based SVC systems are also under great development [10-15]. High power applications as large as 500MVArs and more have not matched with STATCOM systems yet (in the year 2007).

In Turkey, most of the active SVC installations are composed of TCR based industrial SVC systems in the year 2007.

1.1.1 Other SVC Types

The static shunt compensating devices other than TCR are listed in [1,2] as follows:

1.1.1.1 Saturated Reactor (SR)

Saturated reactor is a shunt-connected iron core reactor. It is a variable (nonlinear) susceptance that is controlled by the terminal voltage. It is connected in parallel to filters or capacitor banks. SR is fixed in value and it is not a flexible solution.

Fig.1.2. 25MVAr 110kV shunt magnetically controlled (Saturated) reactor connected to 32MVAr Capacitor bank, installed in Kudymar Substain,Russia. [65]

1.1.1.2 Thyristor Switched Reactor (TSR)

Thyristor Switched Reactor is a primitive TCR, which has the ability of controlling the reactive power in steps, with just on/off control. It is only suitable for slowly varying loads with fixed capacity, i.e. underground cable compensation.

Fig.1.3. Reactors of a Y-connected TSR installed for Bursaray, Turkey for the compensation of underground cables installed for light railway.

1.1.1.3 Thyristor Switched Capacitor (TSC)

In high power applications, this type of compensator is usually connected as passive shunt filter that is switched by back to back connected thyristors. TSC control is also stepwise as in the case of TSR. When compared to the conventional contactor type filter banks, TSC can be turned on and off in a few operating cycles. However, in a conventional system, a capacitor or filter bank needs to be discharged in the order of minutes in order to be able to reconnect it to the supply safely. Operating characteristics can be found in [1,15,20,30]. In order to limit overvoltages and to balance the load, TSC must be used with other types of SVCs such as TCR or STATCOM [9,10,11].

1.1.1.4 Synchronous Condenser

Synchronous Condenser is the former technology for adjustable compensation. It consists of a synchronous generator and a field control circuitry. It is fully controllable and has low harmonic generation. In a synchronous compensator, reactive power is varied by changing field current. Armature current versus field

current relation of synchronous condenser is given in Fig. 1.4. Its major drawbacks are high maintenance cost, slow response and balanced VAr generation capability.
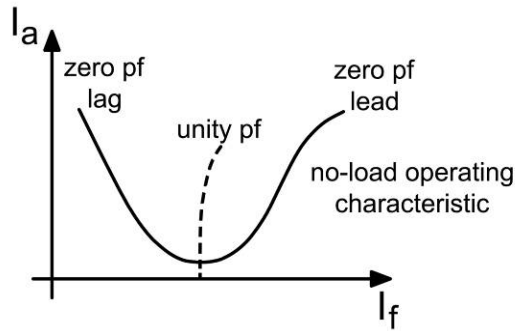
Fig.1.4. Armature Current versus Field Currrent for Synchronous Condenser

1.1.1.5 Static Synchronous Compensator (STATCOM)

In the definitions for the Transmission SVCs [31], STATCOM is defined as a static synchronous generator operated as a shunt connected SVC whose capacitive or inductive output current can be controlled independent from the AC system voltage.

In a Synchronous Condenser type compensator, reactive power can not be controlled fast enough for rapid load changes. Switching power converters can also exchange real power with the ac system if supplied from an appropriate, usually dc energy source. Because of these similarities with a rotating synchronous generator, they are termed as Static Synchronous Generator (SSG). When the active energy source is replaced by a DC capacitor or DC reactor which can not absorb or deliver real power except for short durations, SSG becomes a Static Synchronous Compensator (STATCOM) [63].

STATCOM systems can either be Current Source (CSC) [64], or Voltage Source [63]. These systems can be seen in the Fig. 1.5.

Fig.1.5. VSC and CSC STATCOM systems in KEAŞ, Turkey

1.1.2 Literature Survey on TCR based SVCs

The first industrial TCR based SVC was installed by ABB (former ASEA Co.) in 1972 [27]. It was connected to 20kV with a total reactive power capacity of 60 MVAr. Siemens GmBh built their first TCR in 1974. It was controlled by analog amplifiers with a technique called "Transvector Control" [26]. The TCRs were 3 x 20 MVAr connected to 1kV busbar.

Johnson et al described static high speed VAr control for arc furnace flicker reduction [28] in as early as 1972. In those days, most of the information available about TCR and SVC systems had been published in the ASEA Journals [29]

One of the earliest papers describing the operation principles is the [30], where Gyugyi et al introduced Steinmetz's equations for load balancing and compensation. Meanwhile, ASEA Company and SIEMENS Gmbh had the technical capability to connect TCRs directly to 33kV medium voltage [26,27].

The first TCR standard was published by IEEE in 1991 [31]. The IEEE 1031 offers a guide to the standardization process of TCR design and implementation. Later, this document was revised in 2000.

The theory of the active and reactive power measurement and determination of the susceptances of the phases are given in [1] and [2] as a theory. A practical implementation is described in [41].

Although 12 pulse operational theory [1] and simulation papers [67,77] exist, there is no evidence in the literature that a 12 pulse TCR implementation has been made until 2004. Control system for a 12 pulse TCR is suggested in [67]. Paralleled active filters have been investigated in [66], which can also be implemented in parallel operating SVCs. Generally, most of the known control methods are also applicable to 12 pulse systems with the help of the strategies studied in Chapter 3.

Relocatable systems became realizable with the compact nature of STATCOM systems. ALSTOM Co. developed relocatable STATCOM based SVC systems [76] for the National Grid of UK. The project started in mid 90s and 12 SVC systems were installed in England and Wales.

The instantaneous power theory was first proposed by Akagi and Nabae [69] for usage in shunt active filters. Rapid control of a Thyristor Controlled Series Capacitor (TCSC) is shown in [68] based on instantaneous power theory. The proposed control method can be used for FACTS systems, including TCR.

Voltage stability and power system stability in SVC systems are investigated and analyzed in [1,2]. In [71] IEEE/CIGRE Joint Task Force on Stability Terms and Definitions, the definition and the main criteria of power system stability are proposed as the ability of an electric power system, for a given initial operating condition, to regain a state of operating equilibrium after being subjected to a physical disturbance, with most system variables bounded so that practically the entire system remains intact. Practical simulations and implementations of FACTS systems can be found in [10-15,70,73]. In [70], control system model for transient studies is also introduced.

8

The simulations of the SVC based systems were formerly done by the conventional simulation methods such as Newton-Raphson model in [72]. Nowadays, many simulation tools are available such as EMTDC-PSCAD, MATLAB SIMULINK, EMTP and PSS. Especially EMTDC-PSCAD program includes large SVC libraries and these libraries have been enlarged in the latter versions [75].

The cost analysis of the TCR based industrial SVCs can be found in [74]. It is claimed that an SVC installation to a medium sized steel furnace can pay off in a 15 months time. In [7], installation costs of FACTS systems are compared. It is stated that the installation and infrastructure costs of an SVC system in the range of 100-400 MVAr will cost an investment of 40-100 US $/ kVAr. At the same reactive power level, STATCOM installation cost is given in the range of 60-130 US $/ kVAr.

1.2 Scope of the Thesis

This research work has made the following original contributions to the area of TCR based SVC systems:

- The first unified relocatable TCR based SVC for coal mining has been introduced, designed and developed within the scope of this thesis. The design and development process is summarized in the paper named "A Unified Relocatable SVC for Open-Cast Lignite Mining in Turkey" which was presented at IEEE IAS2002 and also published in IEEE Transactions on Industry applications [3]. There are 7 successive installations of the unified and relocatable TCR based SVC in 5 different TKİ Enterprises. Four of these installations have been relocated in a six-year-period, which proves the necessity of the relocatable and unified design criteria. These works also have given a way to STATCOM based relocatable and unified SVCs later on, which also have been investigated in the Ph.D. thesis of F. Bilgin [32].

- One of the original contributions of this thesis is the first twelve pulse TCR implementation to the industry for ISDEMIR Iron and Steel Works. Although the theory of twelve pulse TCR operation has been a well known technology as mentioned in [1, 67, 77]; however, there had been globally no implementation

of this technology until 2003. This is because of the fact that 12 pulse TCR implementation requires very specific conditions. In a normal application, price increases because of the transformer design. However, in ISDEMIR, 12 pulse configuration was the most suitable solution. Design, implementation and field results have been gathered in "Design and Implementation of a 12-Pulse TCR for a Ladle Furnace in ISDEMIR Iron & Steel Works" [4] and "Two-Folded Implementation of a 12-Pulse TCR with Dissimilar Transformers for a Ladle Furnace: Reactive Power Compensation and Power System Redundancy"[5].

- Within the scope of this thesis, the first investigation and evaluation of interharmonics in TCR based SVCs have been carried out. As it will be mentioned in chapter 2, the interharmonics have a great impact on flicker and harmonic content, which degrades the power quality of the system. After the literature survey, it has been found out that the interharmonics in TCR based SVCs have not been investigated yet. The results of this research work on interharmonics are also investigated in this thesis.

These contributions have been presented in the following conference publicaitons:

- Mutluer, B.; Cadirci, I.; Ermis, M.; Cetin, A.; Ozay, N.; Gultekin, B.; Kose, N.; Ermis, C.; Terciyanli, A.; Unver, O.; Unal, V.; "A unified relocatable SVC for open-cast lignite mining in Turkey" Industry Applications Conference, 2002. 37th IAS Annual Meeting. Volume 1, 13-18 Oct. 2002 pp. 712 - 722

- N. Köse, B. Mutluer, A. Terciyanlı, B. Gültekin, A. Çetin, F. Bilgin, M. Ermiş, S. Hasbay, E. Akgül, Y. Bahtiyaroğlu, T. Ahi, M. Keyifli, 'Design and Implementation of a 12-Pulse TCR for a Ladle Furnace in ISDEMIR Iron & Steel Works, ACEMP 2004, Istanbul, Turkey, May 2004, pp.438-445

- N. Köse, B. Mutluer, A. Terciyanlı, B. Gültekin, A. Çetin, F. Bilgin, M. Ermiş, S. Hasbay, E. Akgül, Y. Bahtiyaroğlu, T. Ahi, M. Keyifli, 'Two-

Folded Implementation of a 12-Pulse TCR with Dissimilar Transformers for a Ladle Furnace: Reactive Power Compensation and Power System Redundancy', IEEE IAS 39th Meeting, October 3-7, 2004, Seattle, USA

The presentation in the 37th IAS Annual Meeting has been selected for publication in IEEE Transactions on Industrial Applications with the following reference:

- B. Mutluer, I. Çadırcı, M.Ermiş, A. Çetin, B. Gültekin, N. Özay, N. Köse, C. Ermiş, M. İnan, Ö.Ünver, V. Ünal, 'A Unified Relocatable SVC for Open-Cast Lignite Mining in Turkey', IEEE Transactions on Industry Applications Vol. 40, no.2, March/April 2004, pp.650-663

The outline of the thesis is given below:

In Chapter 2, theoretical background and analysis techniques are presented for the TCRs and industrial SVCs. Topology and connection types are first investigated, and the operation principles for both six pulse and twelve pulse TCRs are introduced. The nonlinear nature of both TCR and loads is considered in the analysis of harmonics and interharmonics. The standards concerning harmonics and interharmonics are studied and some examples based on the field data acquisition are used for harmonic content extraction. The results are checked by EMTDC-PSCAD simulations. Reactive power compensation, voltage regulation and load balancing concepts are the main installation purposes for an industrial based SVC; therefore, these subjects are also examined in detail. Moreover, other power quality issues including the light flicker are also introduced in order to prepare a basis for the design of the SVC. Chapter 2 concludes with the sizing of the TCR in order to be able to progress into the design stage which will be introduced sequentially in the next chapter.

Chapter 3 is a complete guide for the detailed design procedure of a TCR. As a roadmap in the design, the sequential design steps are introduced graphically. Then, the building blocks of a TCR are introduced. Design method for each building block

is investigated starting with the power stage. Finally, control methods and TCR controller design are studied.

Implementation of a TCR based unified and relocatable SVC is investigated in Chapter 4 as a case study. This chapter contains the detailed design concepts for the unification and transportation concepts as well as other necessary considerations for open cast lignite mining requirements. 7 different implementations installed and commissioned in 2001-2004 are studied for the justification of EMI considerations, unification and easy relocation concepts. Field tests and real time simulations are evaluated and discussed at the end of the chapter.

Another case study within the scope of the thesis is the Twelve Pulse TCR implementation, which is introduced in Chapter 5. Although it is a well known topology, the designed and commissioned system for ISDEMIR A.Ş. is the first 12 pulse SVC ever built. Power system redundancy and the reasons for the 12 pulse implementation are also given. The detailed design considering the harmonics of the load and the SVC is introduced which is also verified by the field measurements and simulations.

Conclusions and recommendations for the further work are given in Chapter 6. All the theoretical and practical considerations of the thesis study is justified and concluded in this chapter once more.

CHAPTER 2

OPERATING PRINCIPLES OF TCR BASED SVC

Thyristor controlled reactor based SVC is a variable shunt susceptance which is mainly installed in order to overcome the power quality issues as mentioned in chapter 1. Typical SVC characteristics are given in Fig. 2.1. TCR is usually connected in parallel with filter groups; therefore, the SVC currents can also be adjusted in capacitive region. There are exceptional cases such as 12-pulse TCR where there is no capacitive current.

The major drawback of the SVC is that the reactive current drawn from or injected to the grid is directly proportional to the grid voltage (Fig. 2.1)

IEEE 1031-2000 [31] gives a detailed list of the main objectives of the Transmission SVC installations. Objectives for the installation of an industrial SVC are more limited when compared to transmission type SVC because power stability is not an issue in the distribution level. The comparison of these objectives is given below in Table 2.1.

Transmission SVC and distribution SVC may be designed to cope with different technical problems. These objectives are mostly determined for the improvement of power quality in a power system. Official legislations about power quality may change from one country to another. Current regulations published by EPDK (Turkish Energy Market Regulatory Authority) define the penalty limits for power quality in transmission and distribution.
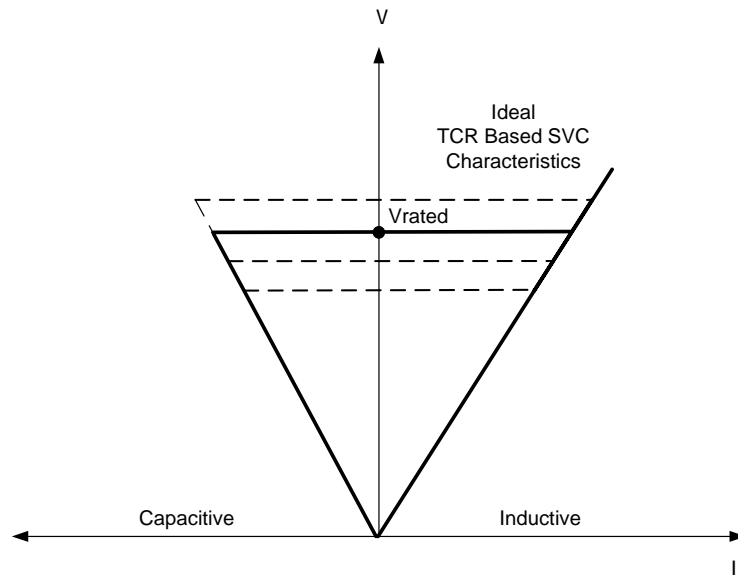
Fig.2.1. Ideal V-I characteristics of an ideal TCR based SVC

Table.2.1. Transmission and distribution type SVC Objectives

	Transmission	Distribution (Industrial)
Steady state voltage control;	√	√
Voltage stability;	√	-
System stability;	√	-
Power Oscillation damping;	√	-
Coordination of VAr contributions from other equipment;	√	-
Fast VAr correction of variable loads;	√	√
Fast correction of power factor;	√	√
The correction of (line current) unbalance;	√	√
Harmonic filtering;	√	√

Electricity Transmission System Supply Reliability and Quality Regulation [33] and Electric Market Network Regulation [34] published by EPDK put forward the limits for power quality, as also described in the international standards. Flicker levels are defined in IEEE 141 [22] and IEC 61000-4-30 [23]. The standard for transmission type SVC design and implementation is IEEE Std 1031-2000 [36],

14

which is the modified version of IEEE Std 1303-1994 [31]. This standard also introduces a guide for SVC field tests.

Maximum allowable current and voltage harmonics and related practices and requirements are defined in IEEE 519-1992 [35]. Table 2.2. contains the limits accepted by EPDK for current harmonic limits for a typical industrial load. In the standard, harmonic current limits are defined for the I_l/I_k ratio. I_l is the load current averaged for 15 minutes, I_k is the balanced three phase short circuit current for the point of common coupling (PCC). In most of the industrial applications, TCR based SVCs are connected to the bus which has high harmonic content and flicker. These busbars are sometimes referred as "dirty bus". Therefore, harmonics should be considered carefully in the design stage. The limits are stricter for the lower I_l/I_k ratios.

Table.2.2.   Limit values defined in IEEE Std.519

Harmonic Order	*154 kV side (%)* *(100<I_l/I_k<1000)*	*34.5 kV side (%)* *(20< I_l/I_k <50)*
2	1.50	1.75
3	6.00	7.00
4	1.50	1.75
5	6.00	7.00
6	1.50	1.75
7	6.00	7.00
8	1.50	1.75
9	6.00	7.00
10	0.69	0.88
11	2.75	3.50
12	0.69	0.88
13	2.75	3.50
14	0.69	0.88
TDD	7.5	8.0

2.1 Harmonics and Interharmonics

2.1.1 Definition of Power System Harmonics and Interharmonics

Whenever an electrical load presents a non-linear impedance to the AC source, it draws distorted current from the source [1]. The distortion occurs in frequencies other than the fundamental frequency, and usually it has different amplitudes and phases at the other frequencies. To investigate the behavior of the distortion, we can use Fourier analysis. It should be assumed that the waveforms under investigation are periodic and the system is at steady state, at least for a reasonable duration during the Fourier analysis. According to [2], the definition of a "Harmonic" is the content of the function whose frequency is an integer multiple of the system fundamental frequency.

"Harmonics" is a major field in power quality and has an important role in the design of most plants. There are standards issued by IEC 61000 series [23,42] and IEEE 519-1992 [35] which contain definition, measurement, and the limitations of the harmonics in the power systems. Turkish Harmonic standard published by TEK [39] and harmonic obligations published by EPDK [33-34] refer to these standards.IEEE 1031-2000 [36], which is a guide in the design of SVCs, also refers to [35] for the "Harmonic Performance" sub-section.

In IEC-61000-4-7 [42]; three different methods of harmonic and interharmonic computation practices are given. In case of fluctuating harmonics and interharmonics, these three methods give close but different results, which may affect the performance of spectrum estimations significantly for different cases of harmonic and interharmonic contents of the signal. These three computation methods, which can also be seen in Fig.2.2, are summarized briefly in the following sub-sections.
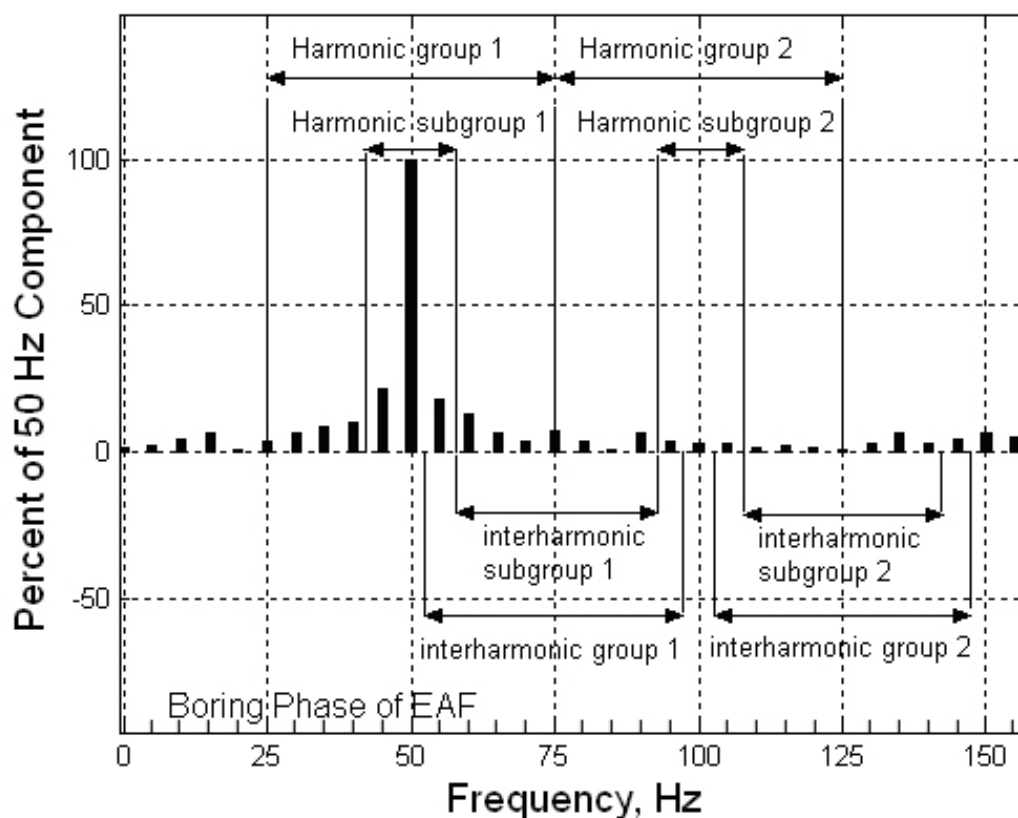
Fig.2.2. Illustration of the harmonic and interharmonic group and subgroup computations according to IEC61000-4-7. The data is acquired from an arc furnace which had just started operation of arcing called the "boring" phase

Table.2.3. Harmonic and interharmonics in Fig.2.2.

	Group		Subgroup	
	Starting Frequency (Hz)	Ending Frequency (Hz)	Starting Frequency (Hz)	Ending Frequency (Hz)
Fundamental	25	75	45	55
Interharmonic 1	50	100	55	95
2nd Harmonic	75	125	95	105
Interharmonic 2	100	150	105	145
3rd Harmonic	125	175	145	155

2.1.1.1 Harmonic and Interharmonic Groups:

Harmonic group denoted by Gg,n is the square root of the sum of the squares of a harmonic and the spectral components adjacent to it within the time window, the equation below is defined:

$$G_{g,n}^2 = \frac{C_{k-5}^2}{2} + \sum_{i=-4}^{4} C_{k+i}^2 + \frac{C_{k+5}^2}{2} \qquad (2.1)$$

For 50 Hz power systems, where Ck is the rms of amplitude of the (k)th spectral component obtained from the Digital Fourier Transformation (DFT) for the (n=k/10)th harmonic component. The resolution is 5Hz and the system frequency is 50Hz and every 10th DFT sample corresponds to a harmonic, i.e. 10th is the fundamental, 20th is the 2nd harmonic, etc… Interharmonic group is defined as:

$$C_{ig,n}^2 = \sum_{i=1}^{9} C_{k+i}^2 \qquad (2.2)$$

for 50 Hz power system, where C$_{k+i}$ is the (k+i)th DFT sample, and they are the DFT samples between the (n)th and the (n+1)th harmonics (for example, 9 adjacent DFT samples between 55 Hz and 95 Hz for the interharmonics between 2nd and 3rd harmonics).

2.1.1.2 Harmonic and Interharmonic Subgroups:

The harmonic grouping considers only the previous and the next DFT components around the harmonic component itself:

$$G_{sg,n}^2 = \sum_{i=-1}^{1} C_{k+i}^2 . \qquad (2.3)$$

In the interhamonic subgroup case, the effects of fluctuations of harmonic amplitudes and phases are partially reduced by excluding the components immediately adjacent to the harmonic frequencies:

$$C_{isg,n}^2 = \sum_{i=2}^{8} C_{k+i}^2 . \qquad (2.4)$$

2.1.1.3 Single line harmonic frequency:

According to [42], single line harmonic frequency is the single line measurement of the current or voltage frequency amplitude component obtained directly from the 5Hz-resolution DFT samples. For instance, 50 Hz fundamental component is computed from the DFT samples evaluated between 47.5Hz and 52.5Hz.

2.1.2 Characterization of Loads in View of Reactive Power, Harmonics and Interharmonics

In a power system, some non-linear or rapidly fluctuating loads need special attention in terms of harmonic and interharmonic investigations. Some of these loads will be presented in the sections 2.4.2.1 – 2.4.2.4 below. It is important to notice that these loads differ from other loads by the speed of power fluctuations and also their harmonic content. Different operational conditions are also investigated in arc furnace plant because load characteristic changes notably during the operation phases.

The measurement data used in the following subsections are acquired in the field by National instrument DAQCard 6036E data acquisition system with SC-2040 S/H (sample and hold) Card. Three phase data is recorded with 3200KS/s sampling rate.

2.1.2.1 Modern Motor Drives

Typical example to this type of load is the 6 pulse converter with neutral point thyristors used in electrical excavators. There are permanently connected shunt harmonic filters on the excavators. The sample characteristics of this load are seen in Fig. 2.3. Typical operation cycle is about 30s. The electrical excavators of this type can be seen in Fig.4.4 and Fig. 4.5.
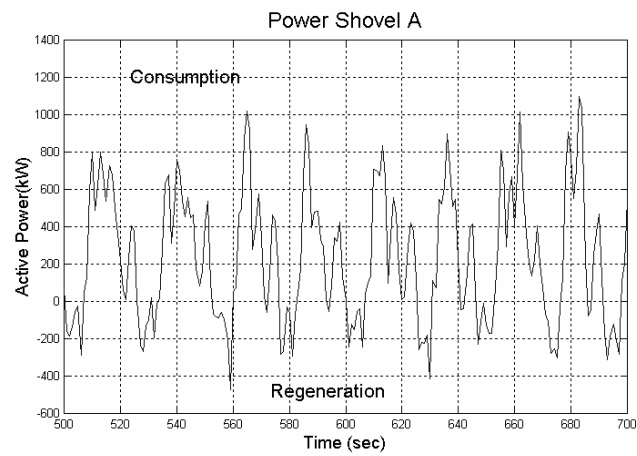
(a)
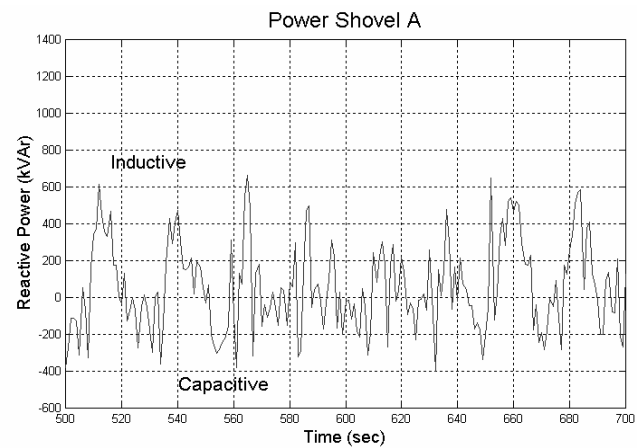
(b)

Fig.2.3. Active and Reactive Power characteristics of a modern motor drive based electrical power shovel

20
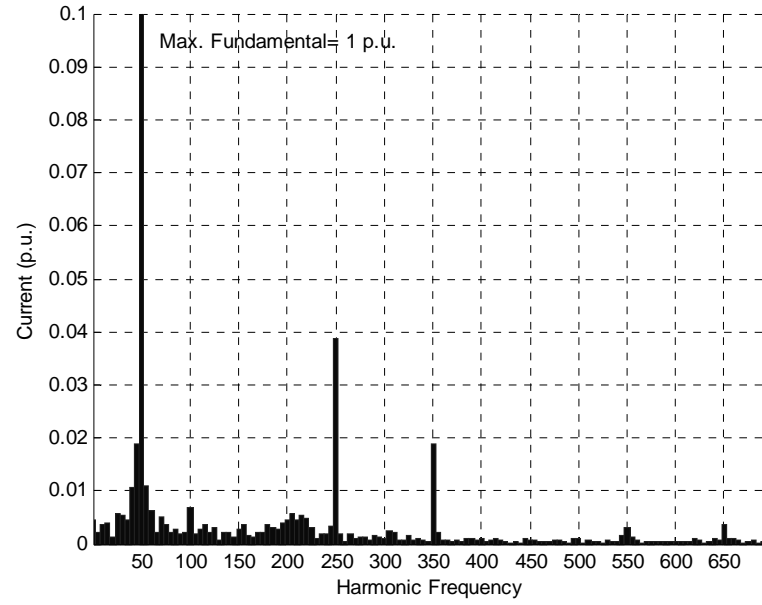
Fig.2.4. Single line harmonics and interharmonics of a modern motor drive current waveform, sampled at 3.2Ks/sec. (10 cycle average)
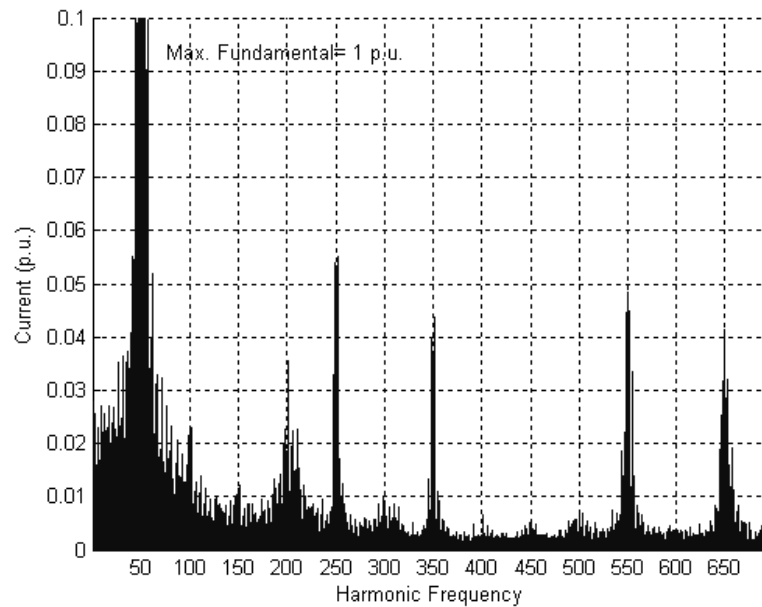
Fig.2.5. Maximum single line harmonics and interharmonics of a modern motor drive evaluated for 1 minute (10 cycle average)

21

2.1.2.2 Conventional Motor Drives

This type of loads does not have a converter and are directly connected to the mains. Typical example is the Ward-Leonard motor drive system which can be seen in the conventional excavator systems. Fixed capacitor type small compensation units on the excavator are common in this type of load. Operation is usually inductive. Current harmonics are much lower when compared to modern motor drive based electrical excavators as seen in Fig.2.7 and Fig.2.8.
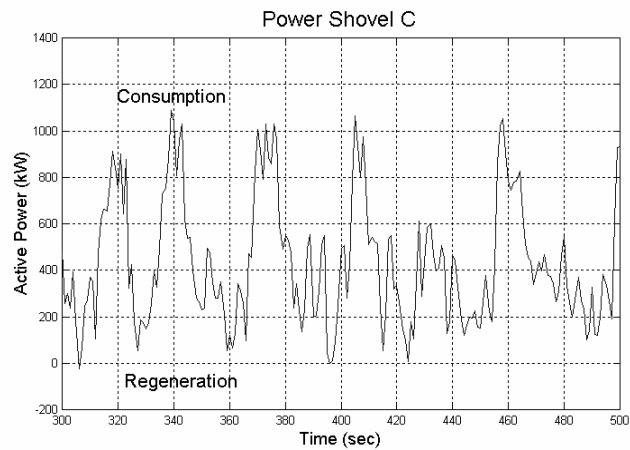
(a)
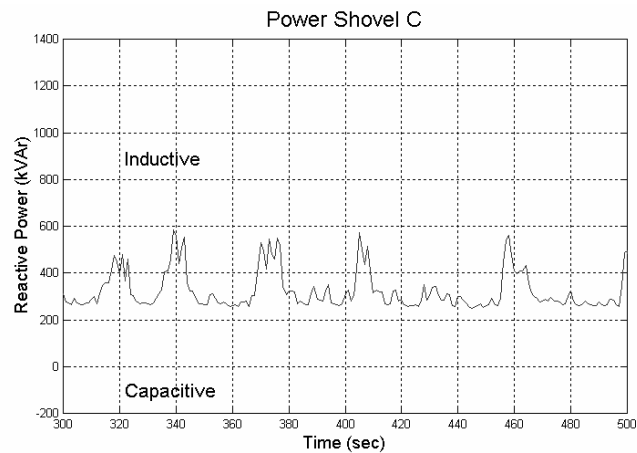
(b)

Fig.2.6. Three phase active and reactive power characteristics of a Ward-Leonard motor drive based electrical power shovel

22
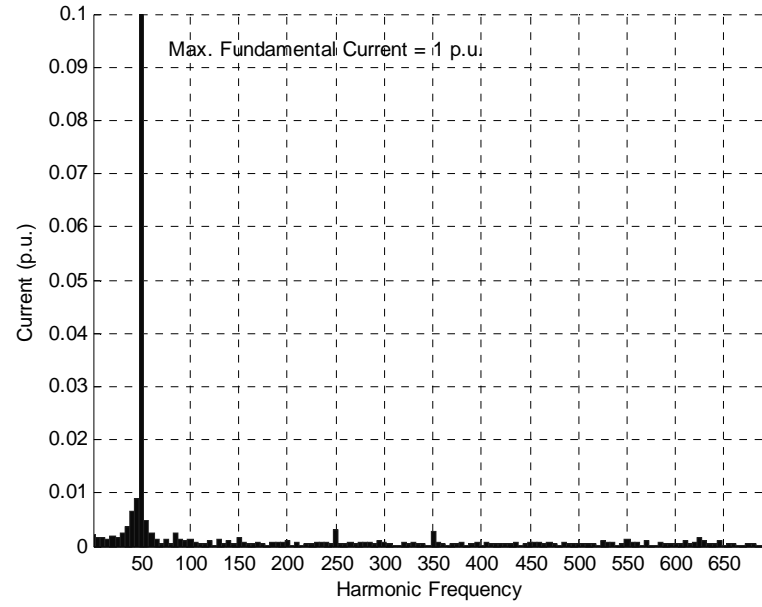
Fig.2.7. Single line harmonics and interharmonics of a conventional motor current waveform, sampled at 3.2Ks/sec. (10 cycle average)
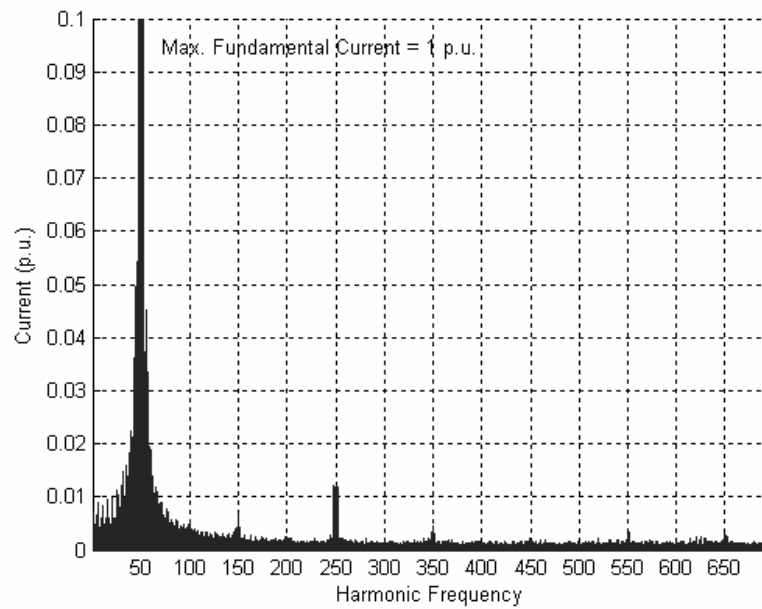
Fig.2.8. Maximum single line harmonics and interharmonics of a conventional motor drive evaluated for 1 minute (10 cycle average)

23

2.1.2.3 Ladle Furnace

Ladle furnace (LF) is a type of electrical furnace to heat up and to homogenize metals, mainly steel. It is also employed in other metal industry plants. Electric energy is transferred to the processed metal by graphite electrodes. A sample ladle furnace operating at ISDEMIR Steel Works Company is seen in Fig. 2.9.

Fig.2.9. ISDEMIR Ladle furnace (120 metric tones) [4]

Active and reactive power demand of the ladle furnace is varying in time as seen in Fig. 2.10.a and b. The current waveform is distorted and may even be unbalanced as seen in Fig.2.11. In Fig. 2.12., sample harmonics and interharmonics spectrum can be seen.

24
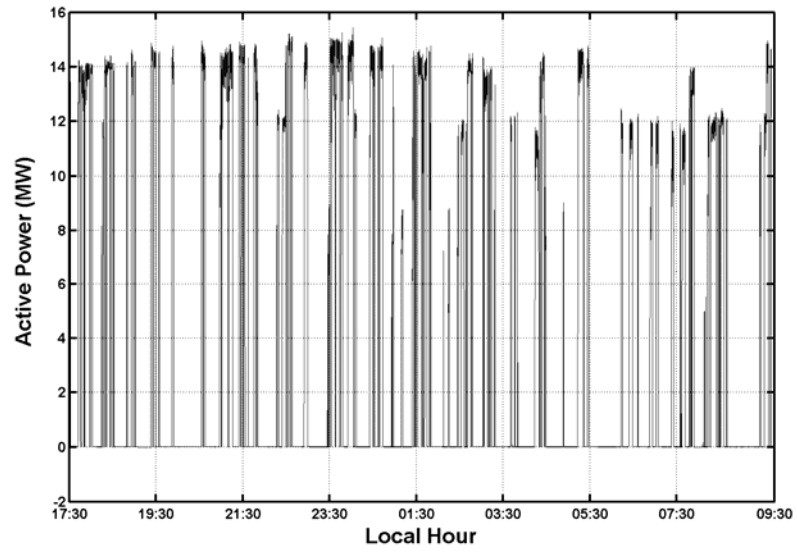
(a)
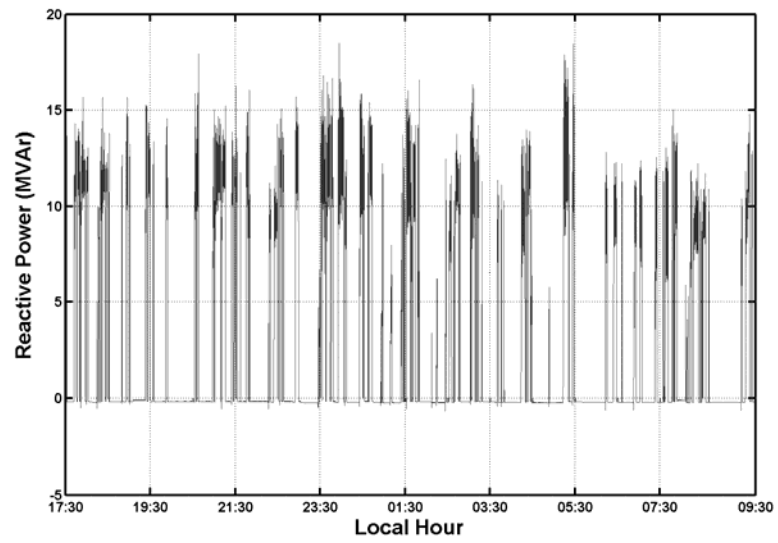
(b)

Fig.2.10. (a) Ladle furnace three phase active power demand, (b) Ladle furnace three phase reactive power demand

25
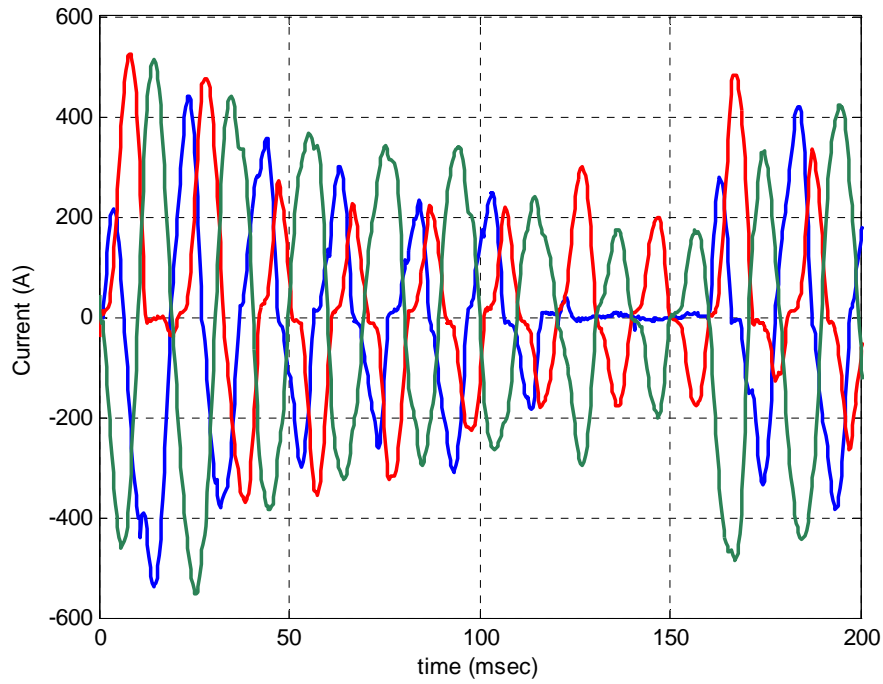
Fig.2.11. Sample three phase current waveforms of a ladle furnace
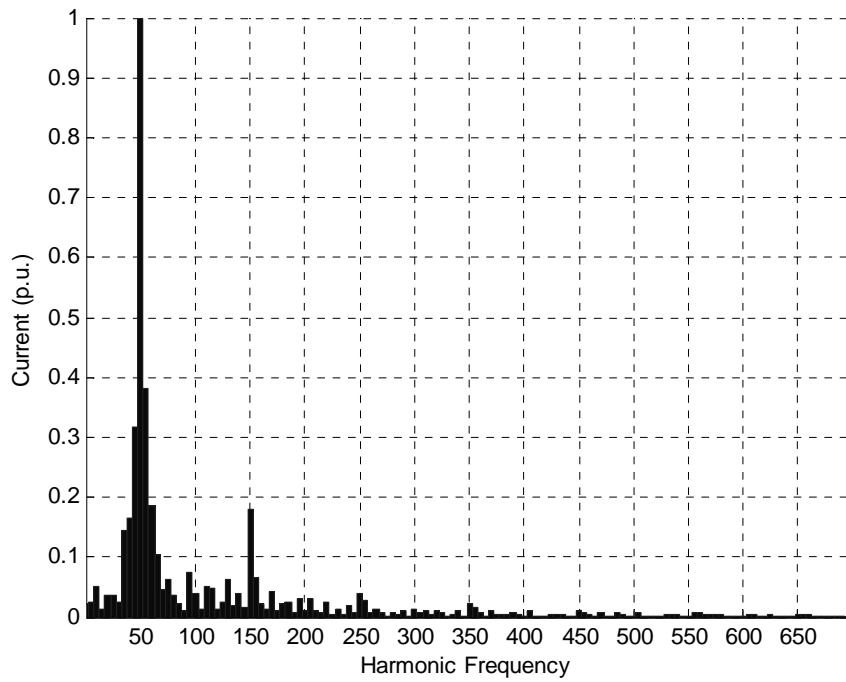
Fig.2.12. Single line harmonics and interharmonics of a ladle furnace current waveform; Current is sampled at 3.2Ks/sec. (10 cycle average)

2.1.2.4 Electric Arc Furnace

Electric Arc Furnace (EAF) is the most difficult load type in electrical distribution system. Electric energy is transferred to metal scrap by arcing over graphite electrodes. It is similar to ladle furnace; however, it demands much more power. Current waveform is non-periodical, pulsed, unbalanced and distorted [35]. This leads to the increase in harmonics and interharmonics. A typical load cycle is seen in Fig. 2.13. The process has four stages; charging, boring, melting and refining. Each state has different load characteristics (Fig. 2.14- Fig.2.19.). "Boring" is the first phase of arc melting and contains high inrush currents and unbalanced operation. In "Melting" phase, the metal in the furnace melts as a result of continuous arcing on the scrap. In "Refining" phase, currents become steady and balanced because all the metal in the furnace melts and surface becomes smooth. The molten metal may heat up to 2000°C.
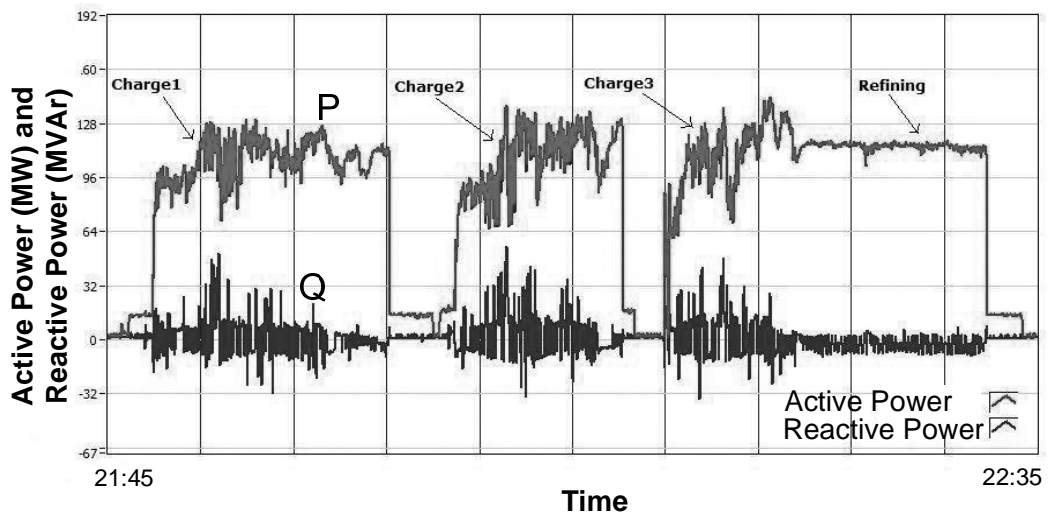
Fig.2.13. Typical tap to tap load characteristics of a bus that contains arc furnace and SVC.

27
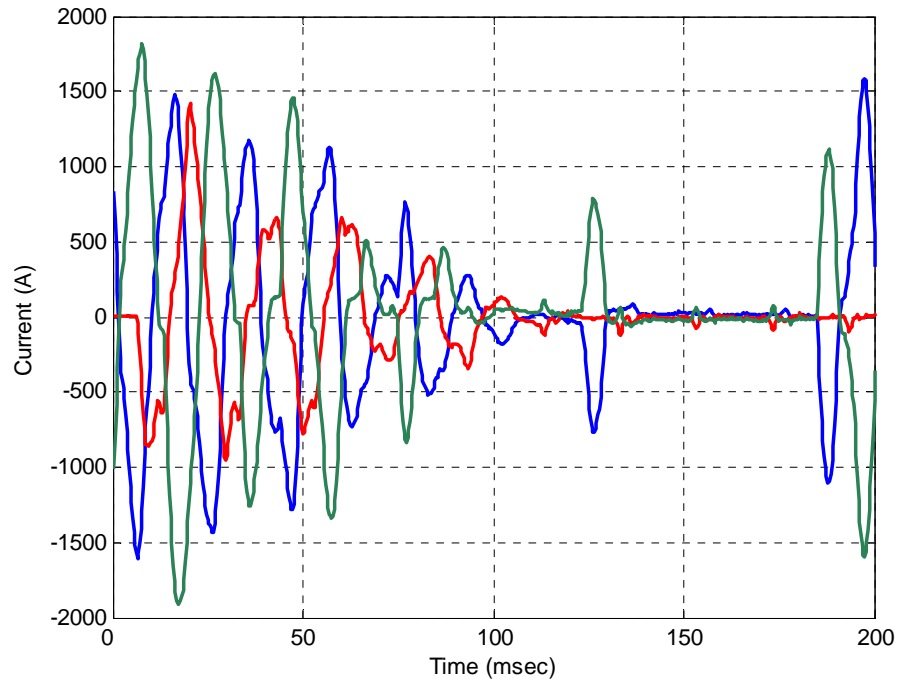
Fig.2.14. Sample three phase current waveforms of an arc furnace during "boring"
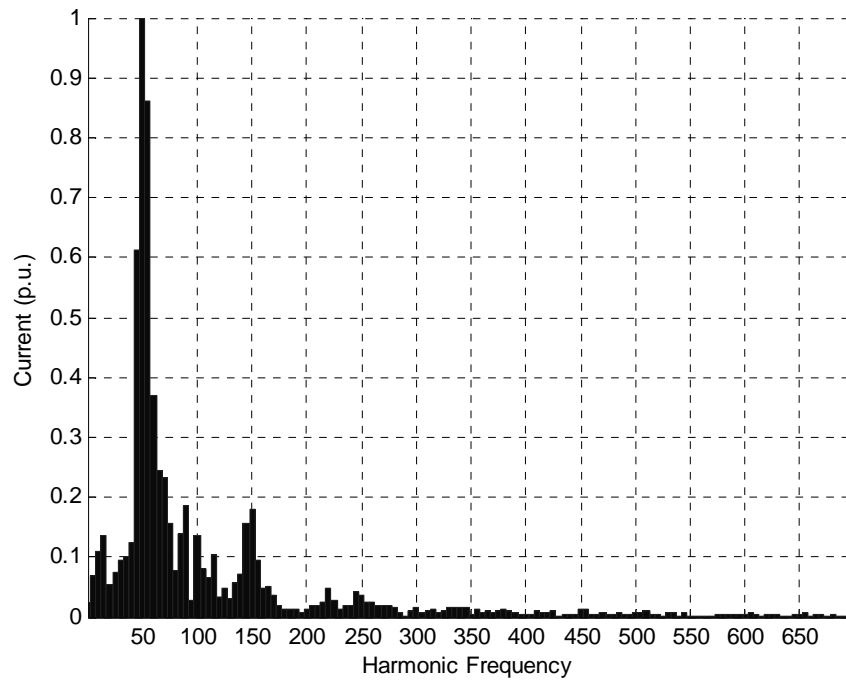
Fig.2.15. Harmonics and interharmonics of an arc furnace current during boring; current waveform is sampled at 3.2Ks/sec. (10 cycle average)

28
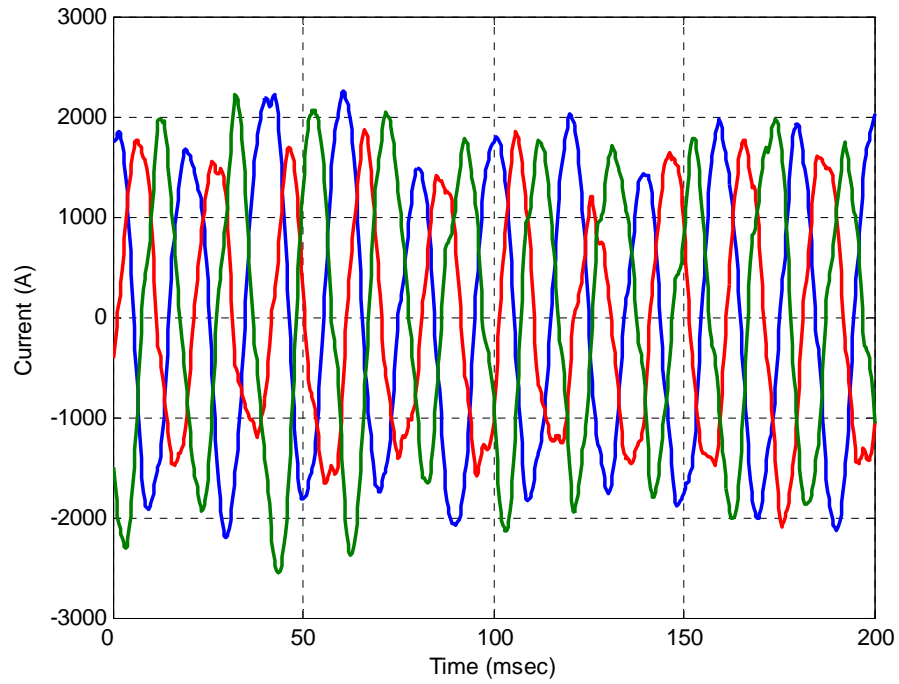
Fig.2.16. Sample three phase current waveforms of an arc furnace during "melting"
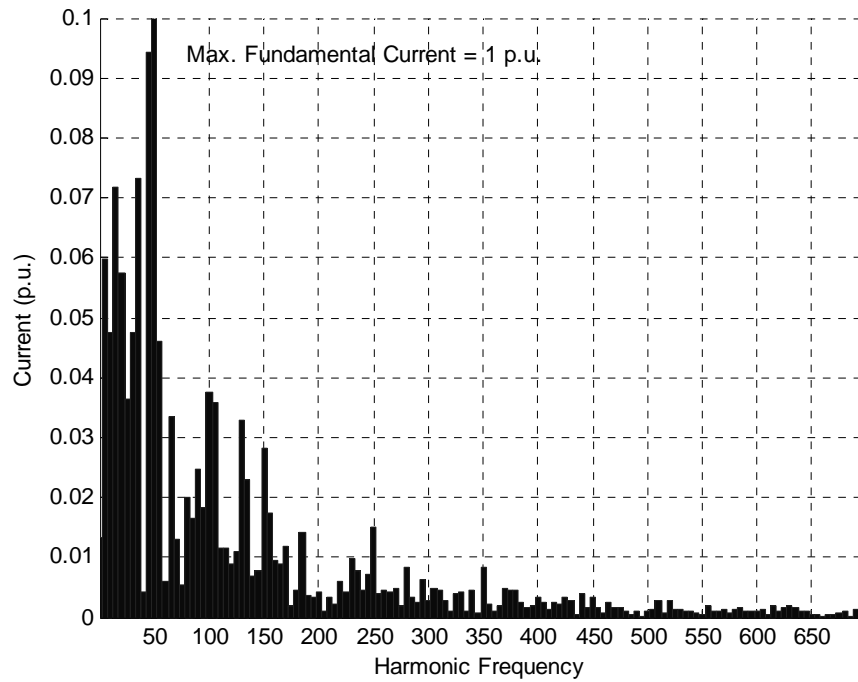
Fig.2.17. Harmonics and interharmonics of an arc furnace current during "melting"; current waveform is sampled at 3.2Ks/sec. (10 cycle average)
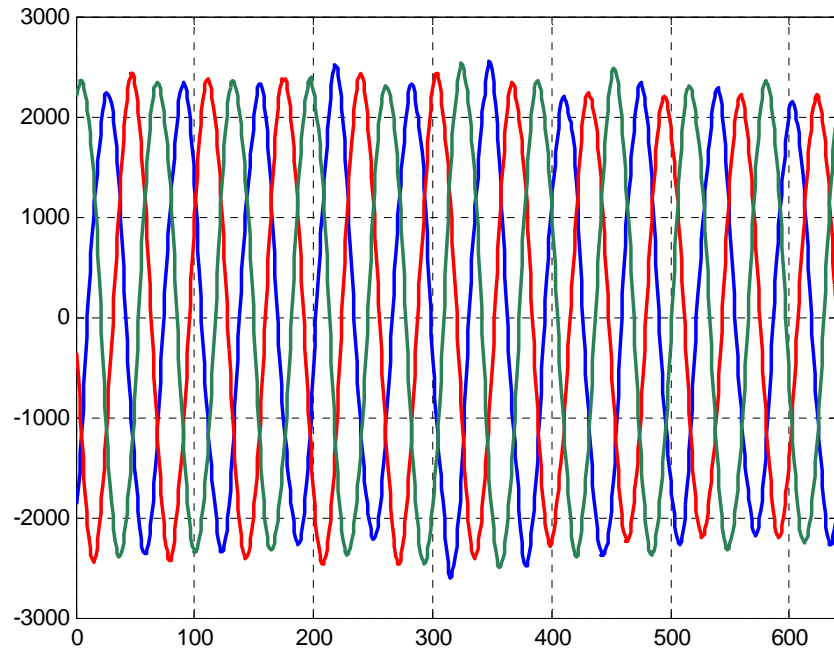
Fig.2.18. Sample three phase current waveforms of an arc furnace during "refining"
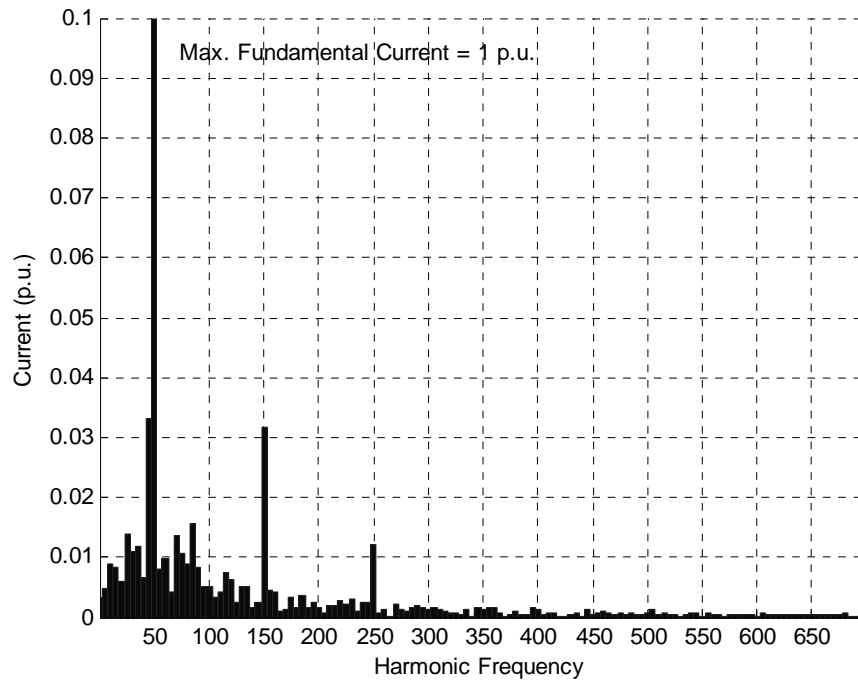
Fig.2.19. Harmonics and interharmonics of an arc furnace current during refining;
current waveform is sampled at 3.2Ks/sec. (10 cycle average)

30

2.2 SVC Connection Types

A typical single line diagram of an industrial TCR based SVC with shunt harmonic filters is given in Fig. 2.20.a. According to the needs of the application, an SVC can be connected to the grid terminals either directly or via coupling transformer. The Point of Common Coupling (PCC) can be the overhead line or a transformer substation, which depends on the location of the SVC. Several connection types can be seen in Fig. 2.21.

The TCR can be connected as delta or wye as seen in Fig. 2.21 (a) and (b). The main differences in delta and wye connections are voltage and current ratings of the power semiconductors as well as the harmonic content of the TCR current. The harmonic components in TCR currents are investigated in Table 2.5. It is certain that line currents in delta configuration contain lower harmonic content in the steady state. In wye connection, voltage across the reactor and thyristor terminals is lower while the current flowing through these components is higher when compared to the delta connection. Delta connection is the most common connection.

As it will be described in section 2.7, the harmonic current minimization can be achieved with shunt connected filters. These filters are also used as capacitive VAR source in a TCR based SVC system. Various connection types are seen in Fig.2.20 (c) – (j). The selection criteria and filter configurations are also described in section 2.7.

Industrial SVCs are most commonly used for arc and ladle furnace compensation. These loads require harmonic filtering. Fig.2.21.(c)-(i) includes possible filter options for load current harmonic filtering.
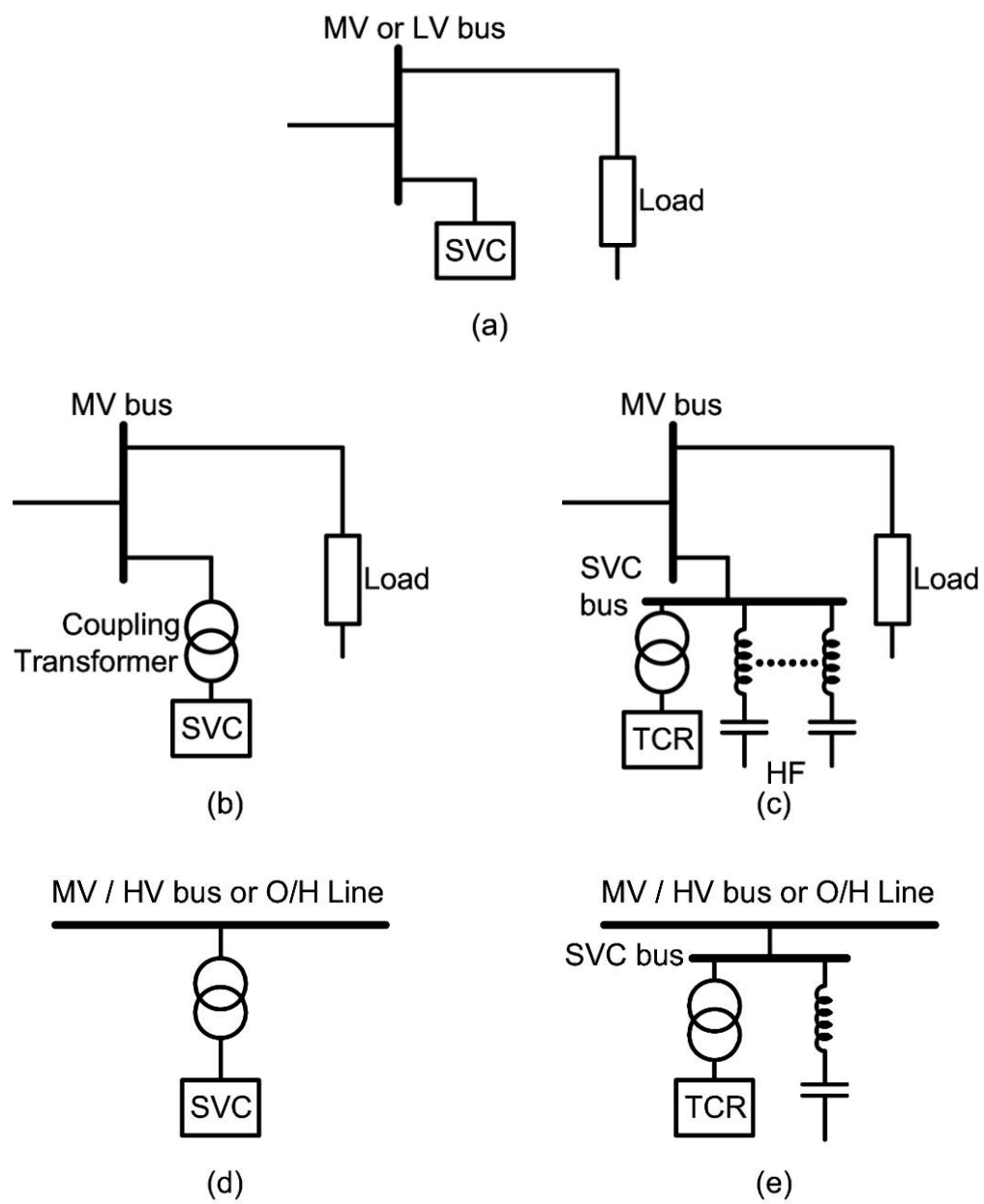
Fig.2.20. SVC connection types.

Table.2.4. TCR based SVC topology selection table

Description	Figure	Typical Compensation Applications
Wye connected TCR without filters connected via coupling transformer	Fig.2.21.a	Public transportation systems in which long underground cables generate nearly constant capacitive VArs while the converters demand fluctuating VArs
Delta connected TCR without filters connected via coupling transformer	Fig.2.21.b	
TCR connected to MV bus where 2nd,3rd,4th,5th and HF harmonic filters are installed	Fig.2.21.c	Feasible for arc and ladle furnace installations.
TCR connected to MV bus where 2nd,3rd,4thand 5th harmonic filters are installed	Fig.2.21.d	
TCR connected to MV bus where 3rd,4th and 5th harmonic filters are installed	Fig.2.21.e	
TCR connected to MV bus / Overhead line where 5th and 7th harmonic filters are installed	Fig.2.21.f	Suitable for 6 pulse motor drives
TCR connected to MV bus / Overhead line where 5th,7th and 11th harmonic filters are installed	Fig.2.21.g	Dominant 12-pulse motor drives, variable frequency motor drives, rolling mill, compressor, fan drives
TCR is coupled to the MV system via transformer, filters are at the MV side	Fig.2.21.h	Suitable for modern industrial motor drives which produce current harmonics
TCR is coupled to the MV system via transformer. Some filters are connected parallel to TCR, some filters are at the MV side	Fig.2.21.i	Conventional motor drives with rapidly varying reactive power consumption PCC may be equipped with a detuned filter.
TCR and the harmonic filters are coupled to the HV/MV system via transformer	Fig.2.21.j	Conventional motor drives connected to harmonic-free bus.
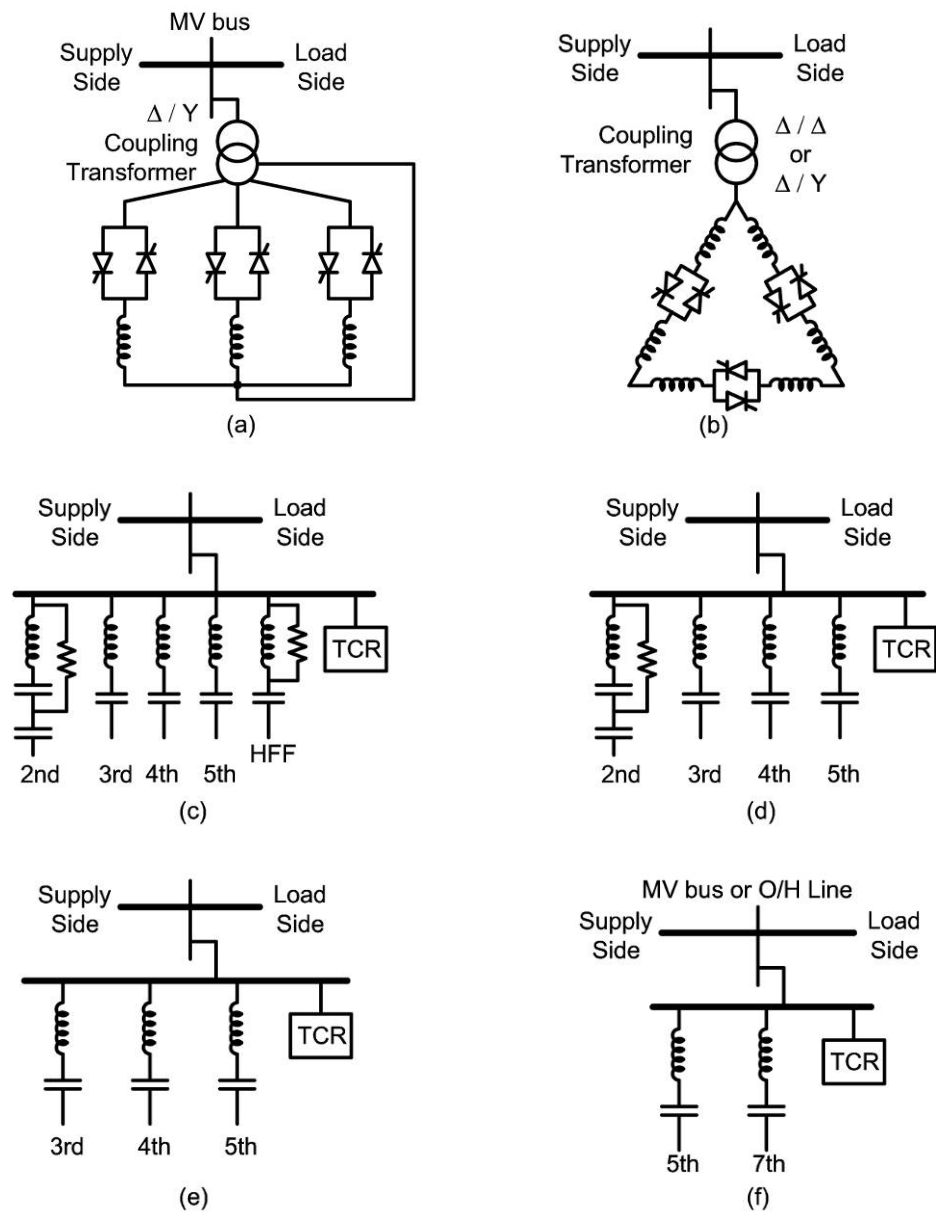
Fig.2.21. Possible SVC configurations defined in Table 2.4
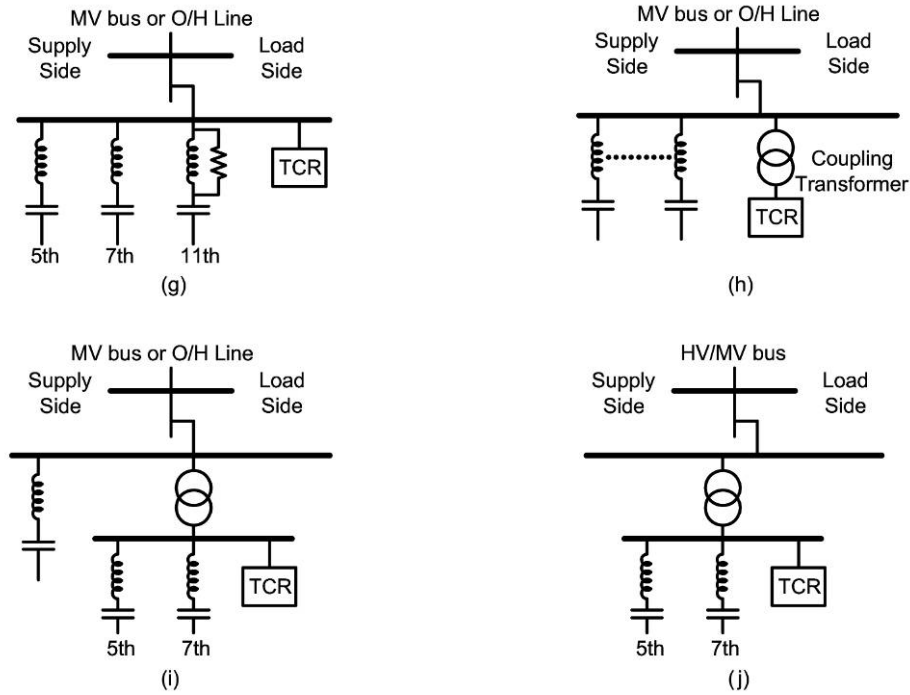
Fig.2.21 (cont'd) Possible SVC configurations defined in Table 2.4

Most common connection type of SVC is seen in Fig.2.2.c. It is possible to filter both TCR and load current harmonics. It is also a cost effective solution, because coupling transformer is omitted by connecting TCR directly to MV bus. 6-pulse TCR is used in nearly all applications. Filter design for the TCR based SVC can be found in Chapter 3.

2.3 Analysis of the Six Pulse TCR

The Thyristor Controlled Rectifier, as the name suggests, consists of two main parts; the thyristor stack and the reactor. The thyristor stack consists of as many thyristors as necessary in order to meet the reverse voltage blocking capacity with an additional safety factor. The thyristors are connected back to back, opposing each other, and conduct on the alternate half cycle of the supply frequency. The current flowing through the thyristors is almost purely reactive, lagging the voltage nearly

35

90$^{\text{o}}$. Due to the power losses in the reactor owing to its internal resistance, there is an in-phase component which may be in the order of 0.5-2% of the reactive power [1]. The arrangement is called six-pulse because there are six thyristor gatings in each and every cycle. This definition is valid even if some or all thyristors are in "off state", which are assumed to be fired with a delay of 180 degrees with respect to the zero cross of the voltage. The firing delay is α, and conduction angle is σ. When the thyristors conduct for 180, they are said to be in "full conduction" and the thyristors act as if they were short-circuited. The reactive power delivered to the supply is maximum and the susceptance of the TCR seen from the supply side is minimum in this condition.

(a)   (b)
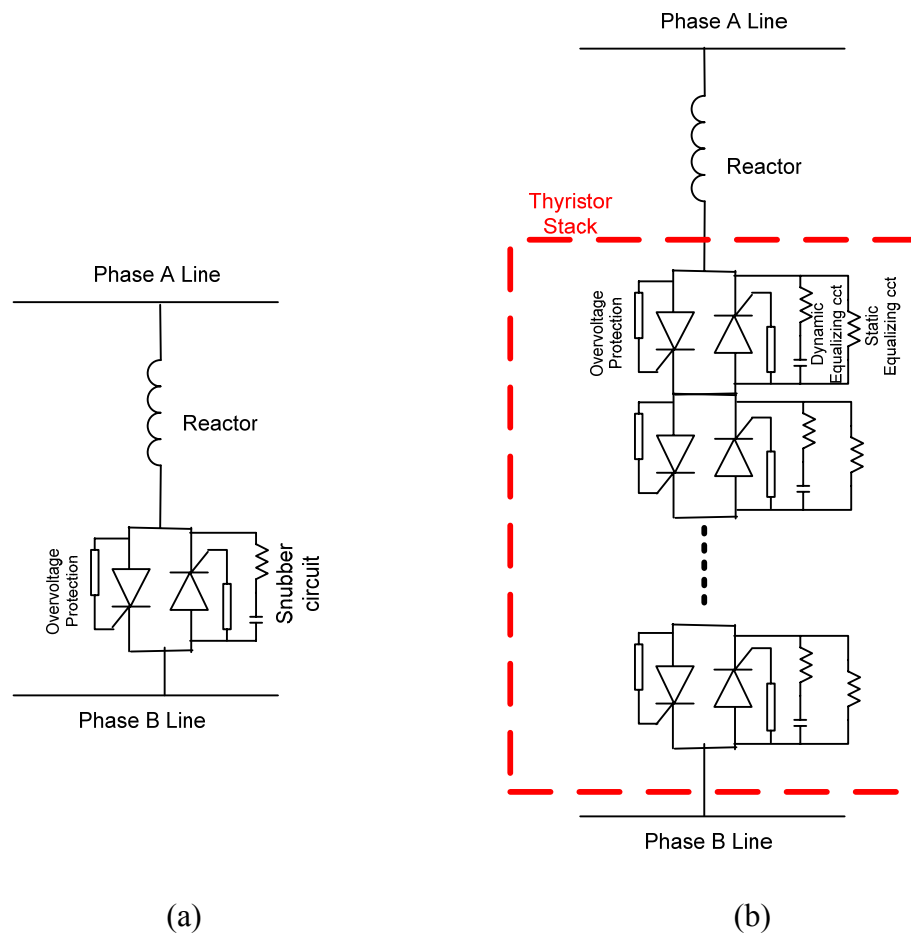
Fig.2.22. Single line diagram of a polyphase TCR (a) with, (b) without series thyristor operation

36
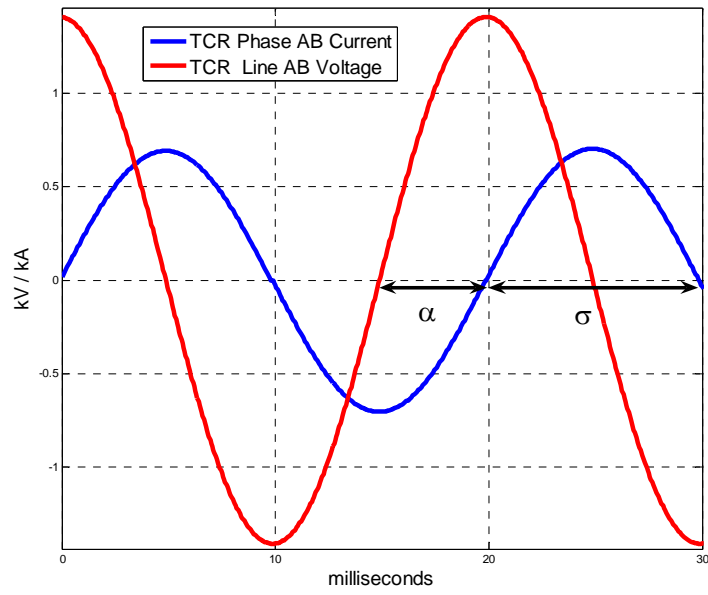
(a)
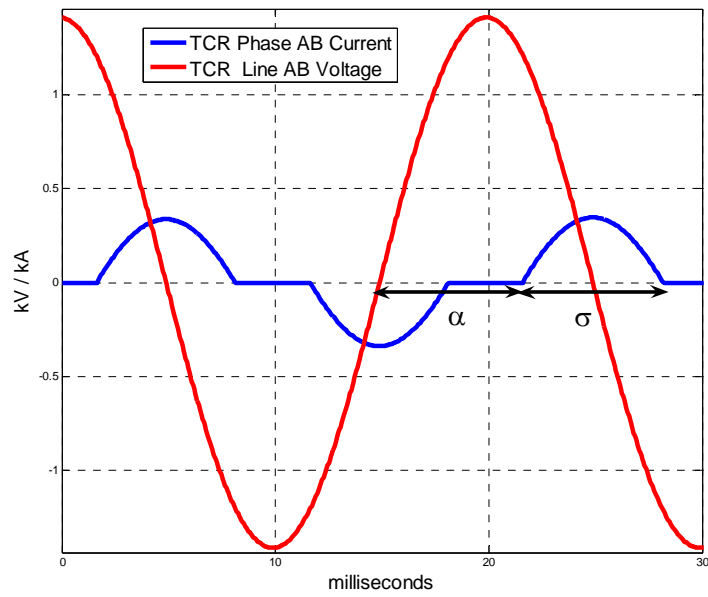
(b)

Fig.2.23. Current and voltage waveforms of a 1.5 MVAr 1 kV TCR obtained by PSCAD Simulation (a) full conduction; (b) 120° firing delay angle (α) and 120° conduction angle (σ).

37

Whenever the firing delay is increased, the rms value of the TCR current decreases because the conduction time reduces. The current waveform is still about 90° lagging, but it becomes chopped symmetrically from the sides as seen in Fig.2.23. The TCR current value can be derived from the Voltage Time Area method:
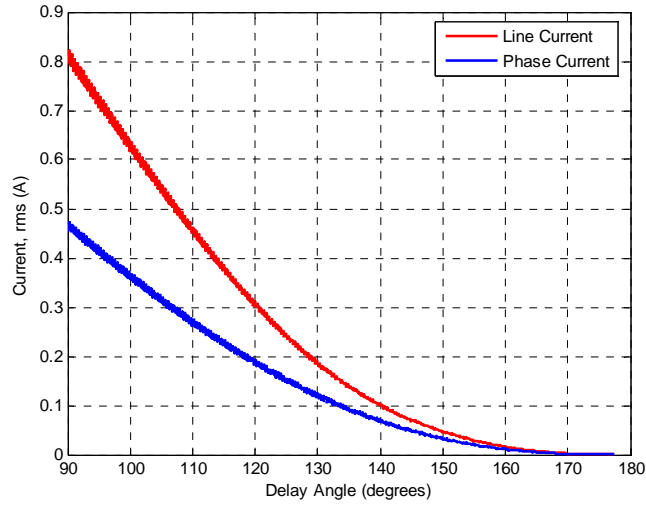
Fig.2.24. Phase and line true-rms currents in a delta connected TCR.

$$i_{TCR}(\alpha) = \frac{1}{L}\int_{\alpha}^{wt} v(\tau)d\tau \qquad (2.5)$$

The instantaneous phase current i(t) is then given by:

$$i(t) = \begin{cases} \dfrac{\sqrt{2}V}{X_L}(\cos\alpha - \cos wt), & \alpha < wt < \alpha + \sigma \\ 0, & \alpha + \sigma < wt < \alpha + \pi \end{cases} \qquad (2.6)$$

Here, α is the firing delay angle and σ is the conduction angle. The voltage V is given in rms value and the X_L is the impedance of the reactors in the fundamental frequency. In order to find the fundamental frequency component of the current

38

waveform, we need to evaluate the Fourier Coefficient of the fundamental component given in equation (2.3)

$$a_n = \frac{2}{T} \int_{-T/2}^{T/2} x(t) \cos\left(\frac{2\pi n t}{T}\right) dt \qquad\qquad \text{for n=1 to } \infty \qquad\qquad (2.7)$$
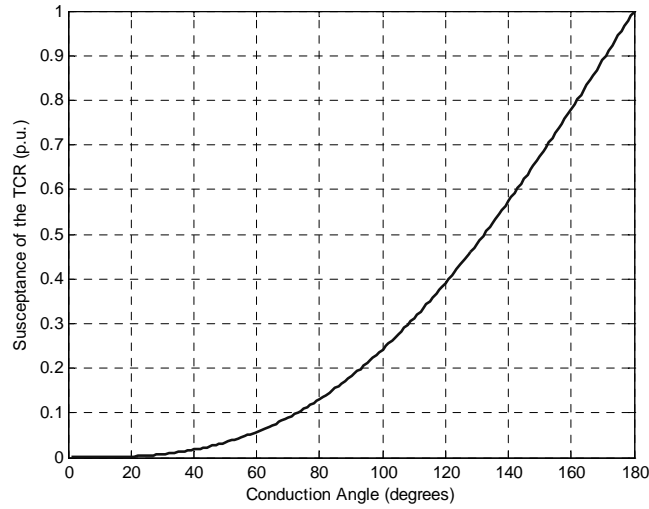
Fig.2.25. Susceptance of TCR per phase (at 50Hz) against conduction angle

2.4 Twelve Pulse TCR

Twelve pulse TCR needs special coupling transformer connections as shown in Fig.2.26. These connection yields 30° phase shift between input voltages of the two 6-pulse TCR groups. The arrangement is called twelve-pulse because there are twelve thyristor gatings in each and every cycle. This definition is valid even if some or all thyristors are in "off state", which are assumed to be fired with a delay of 180 degrees with respect to the zero cross of the voltage. The main reason for using the 12-pulse configuration is the harmonic cancellation for the 5th and 7th harmonics. The harmonic cancellation is valid also for the harmonic numbers that are 6n+/-1 (n=1,3,5…) integer multiple of the fundamental. This is because of the fact that the

39

30 degrees phase shift causes a 180 phase difference in these specific harmonic domains.

(a)   (b)
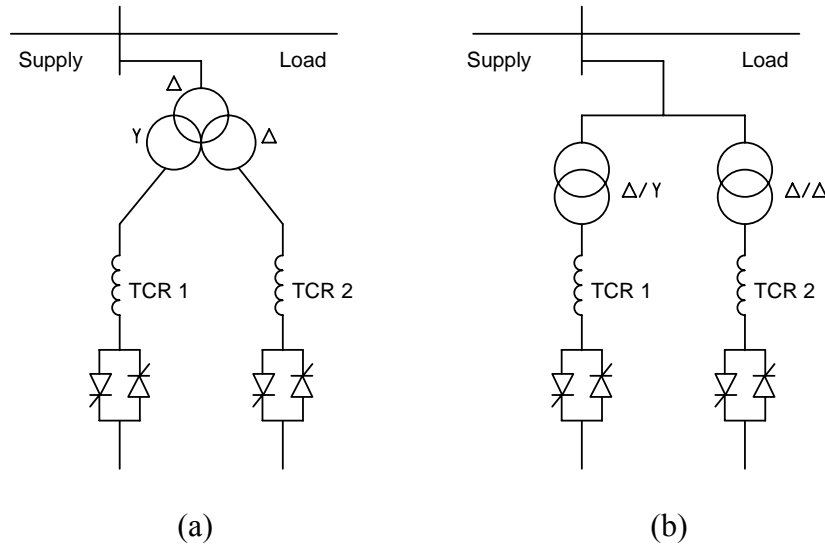
Fig.2.26. Twelve pulse TCR configuration with (a) single transformer, (b) two separate transformers.

2.5 TCR Current Harmonics

2.5.1 Steady State Odd Current Harmonics

The current flowing through the reactor becomes discontinuous by increasing the firing delay angle and eventually reducing the conduction angle. Therefore, TCR generates current harmonics [1]. If the firing pulses of the back-to-back connected thyristors are balanced and the compensation system is in a steady state, all the odd harmonics of the fundamental frequency are generated. The rms value of the nth harmonic (I_n) of the TCR fundamental currents are given in equation (2.8) V is the line voltage and X_L is the inductive reactance of the TCR in full conduction. I_n is derived from the Eqn.2.7.

40

$$I_n = \frac{4}{\pi}\frac{V}{X_L}\left[\frac{\sin(n+1)\alpha}{2(n+1)} + \frac{\sin(n-1)\alpha}{2(n-1)} - \cos\alpha\frac{\sin(n\alpha)}{n}\right] \qquad (2.8)$$

Table.2.5. Maximum amplitude of the steady state balanced current harmonics produced by the TCR (Values in parenthesis do not appear outside the delta)

Harmonic Order	6- Pulse TCR [2] %	12- Pulse TCR, Delta Connected %
1	100	100
3	(13.78)	-
5	5.05	-
7	2.59	-
9	(1.57)	-
11	1.05	1.05
13	0.75	0.75
15	(0.57)	-
17	0.44	-
19	0.35	-
21	(0.29)	-
23	0.24	0.24
25	0.20	0.20
27	(0.17)	-
29	0.15	-
31	0.13	-
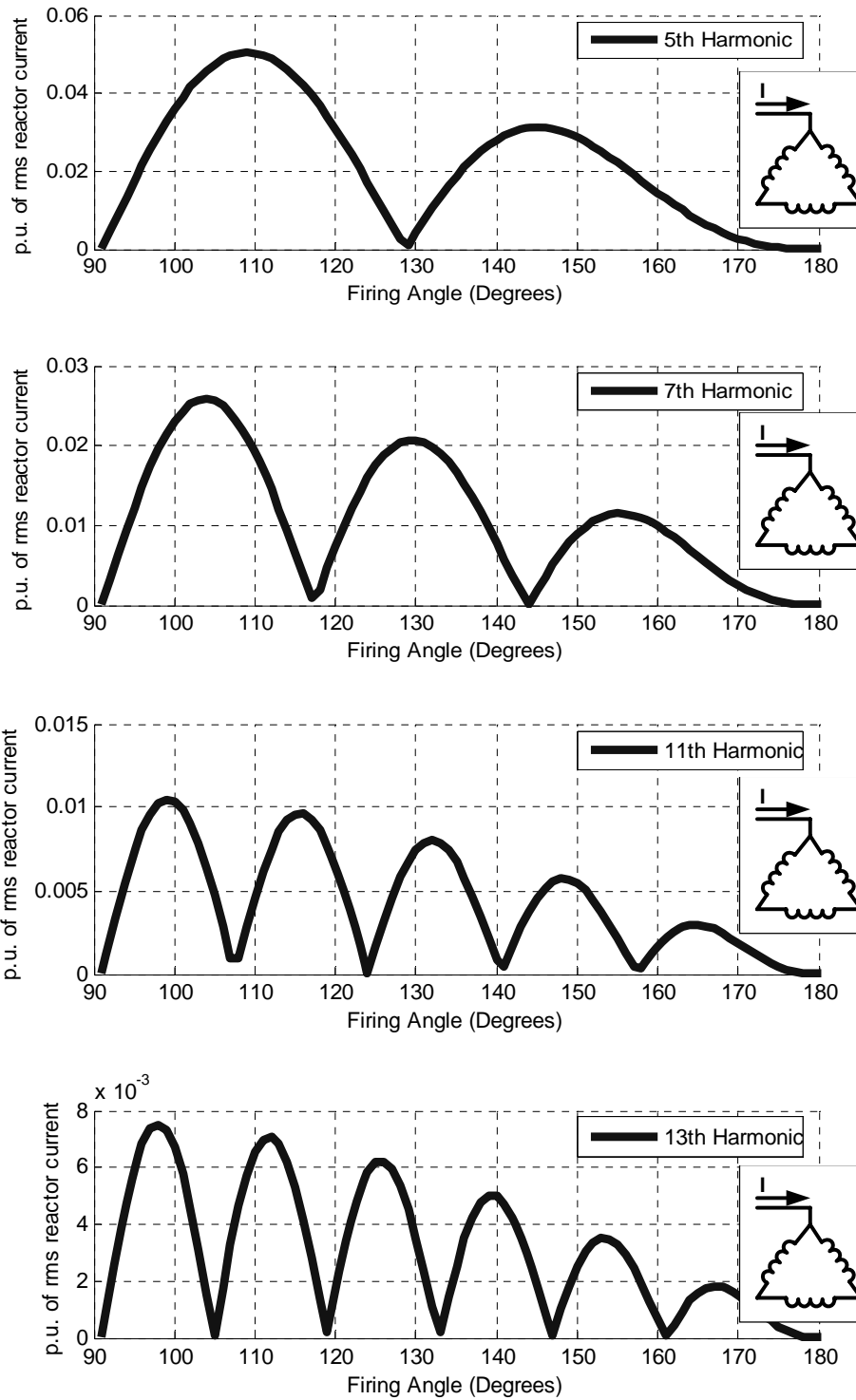
Fig.2.27. rms values of the harmonic current components as a percentage of the maximum rms TCR line current

2.5.2 Even Current Harmonics in TCR

Even harmonics in the current waveform are caused by nonlinear characteristics of the load. The practical sources of the even harmonics can be mainly considered as the rectifiers, converters connected to rapidly changing loads, arc and ladle furnaces, etc… Whenever the two half cycles in a period of the waveform are not symmetrical, the second harmonics are generated [17]. According to [18], the even harmonics can be modeled as in Fig. 2.28.
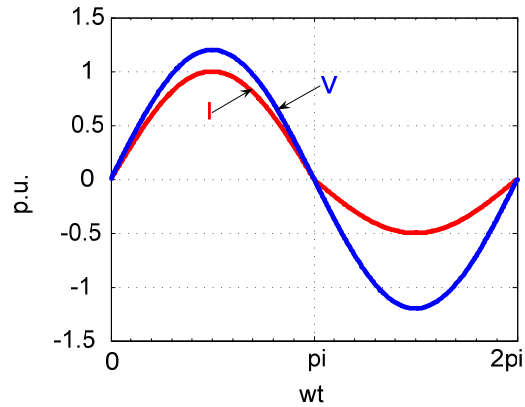
(a)
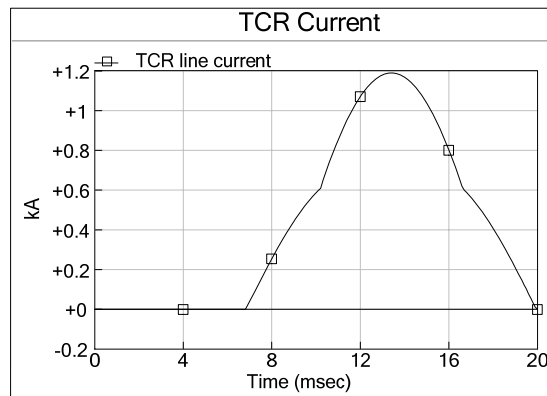
(b)

Fig.2.28. Load with asymmetrical i-v characteristic; (a) i versus v; [18]. Although the voltage waveform is symmetrical, current waveform is not symmetrical. (b) PSCAD simulation result for a 1.5 MVAr TCR, firing delay angle is changed from 180° to 90° in a half cycle

43

Consider:

$$I = G_1 V \qquad V > 0 \qquad\qquad (2.9)$$

$$I = G_2 V \qquad V < 0 \qquad\qquad (2.10)$$

Assume that:

$$G_1 > G_2$$

The current waveform can be decomposed as:

$$I = V\sqrt{2}\left\{ \frac{G_1 + G_2}{2}\sin\omega t + \frac{G_1 - G_2}{\pi}\left[1 - 2\sum_{h=2,4,6\ldots} \frac{\sin(h\omega t)}{h^2 - 1} \right] \right\} \qquad (2.11)$$

It is clear that rapid changes in the conductance increase the even harmonics. TCR control system is designed to follow the reactive power demand changes; therefore, the TCR current set point may change in each half cycle. This results in even harmonic generation in TCR.

It is obvious from the equation (2.11) that the worst even current harmonics occur when G_1 is maximum and G_2 is minimum, or vice versa. This is the case when firing delay is 90° in the first half cycle, and firing delay is 180° in the second half cycle. G_2 is 0 in this case, and G_1 is equal to the reactor susceptance G. Even current harmonics and the dc component in this case become:

$$I_h = \frac{V 2\sqrt{2} G \sin(h\omega t)}{\pi h^2 - 1} \qquad h = 2,4,6\ldots \qquad (2.12)$$

$$I_{dc} = \frac{V\sqrt{2} G}{\pi} \qquad\qquad (2.13)$$

2.6 TCR Harmonics Obtained by Simulations

In order to verify the harmonic current values in [1], a PSCAD simulation is run on the computer. The simulation file just consists of the supply and the TCR. The Figures 2.30-2.36 show the plots for 5th, 7th, 11th and 13th harmonics in the line current. Total harmonic distortion evaluated in the simulation is also plotted in Fig. 2.37. The TCR can not conduct continuously if it is fired at 90 degrees. This is

44

because of the internal resistance value of the reactors. In order to see the full conduction, the simulation is evaluated between 88 – 180 degrees firing delay angles.

2.6.1 Steady State Balanced Operation

By using the circuit in Fig.2.29., all three phases of the TCR are fired with the same delay ranging from 88 degrees up to 180 degrees. Maximum line current during the full conduction is taken as 1 p.u.. The harmonic currents are as expected when compared to Fig.2.27 and Table 2.5 given by [1].

(a)

(b)

Fig.2.29. A six pulse TCR simulation in EMTDC-PSCAD. (a). Voltage source connections (b) Details of TCR Model

Fig.2.30. Fundamental currents versus delay angle for a TCR
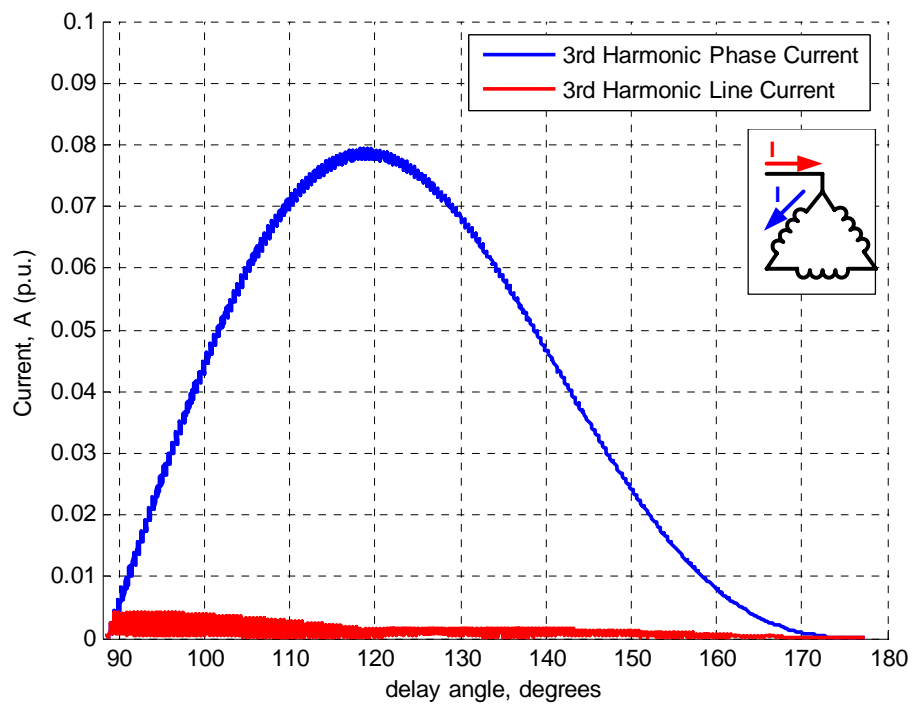
Fig.2.31. 3rd harmonic current components in the TCR currents versus delay angle
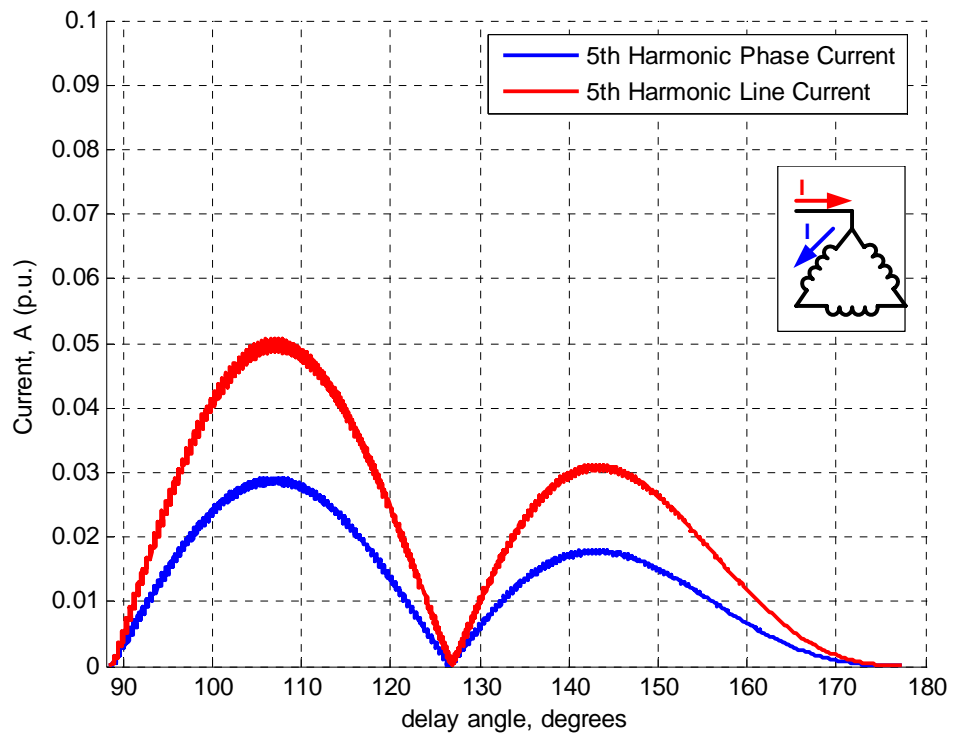
Fig.2.32. 5th harmonic current components in the TCR line current versus delay angle
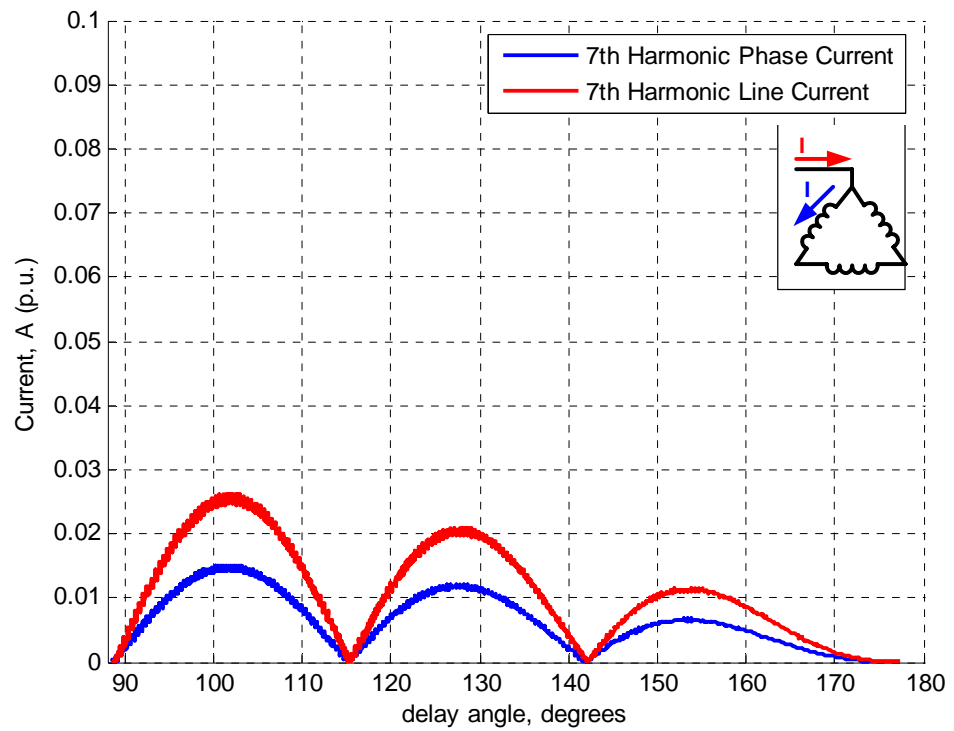
Fig.2.33. 7th harmonic current component in the TCR line current versus delay angle
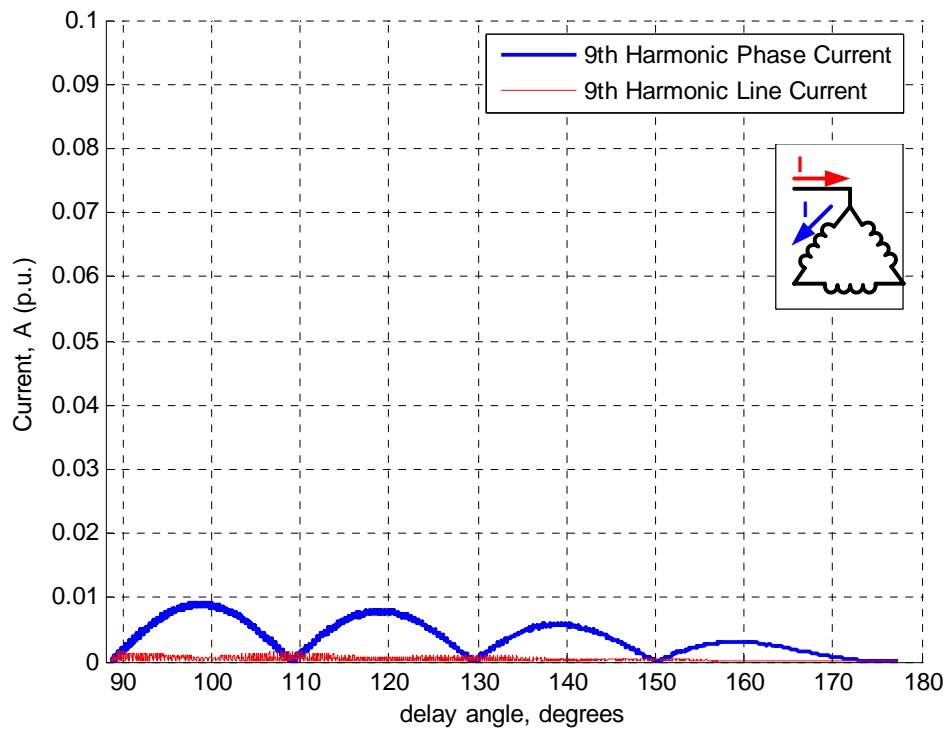
Fig.2.34. 9th harmonic current component in the TCR line current versus delay angle
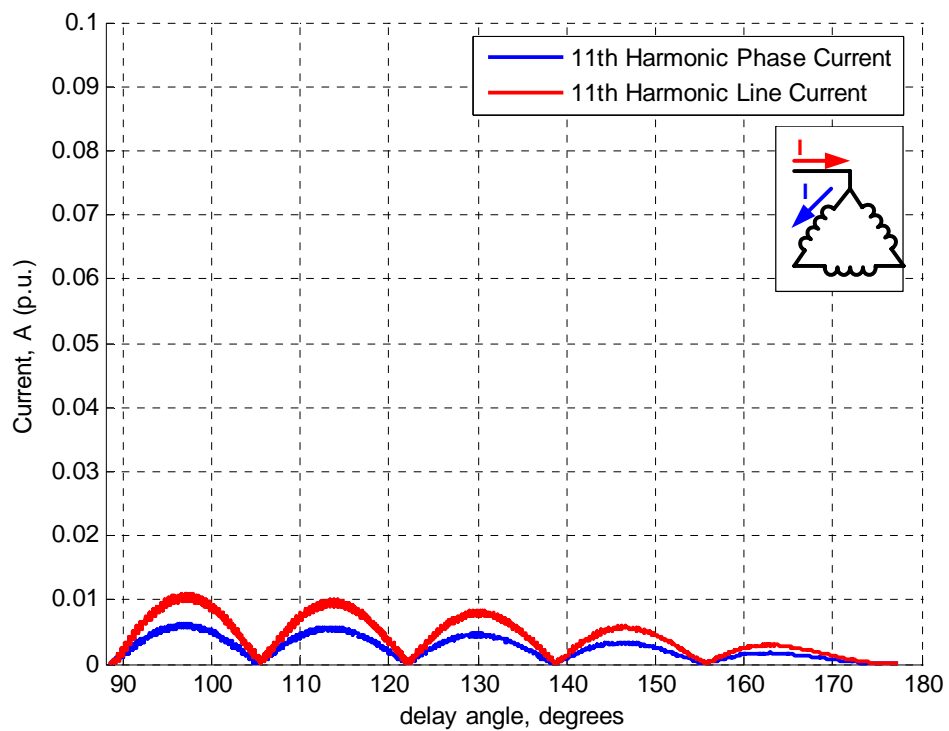
Fig.2.35. 11th harmonic component in the TCR line current versus delay angle

48
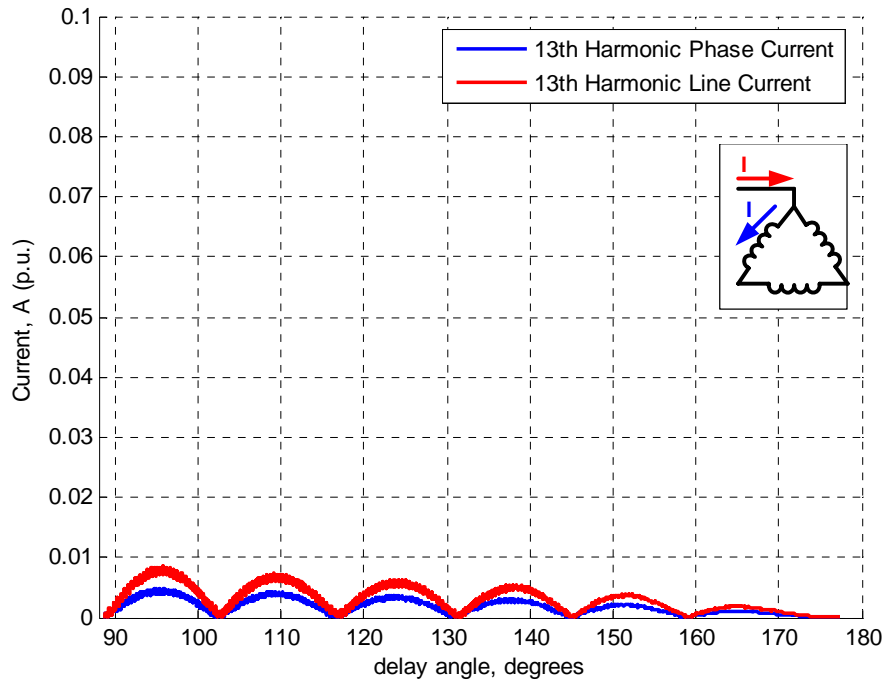
Fig.2.36. 13th harmonic component in the TCR line current versus delay angle
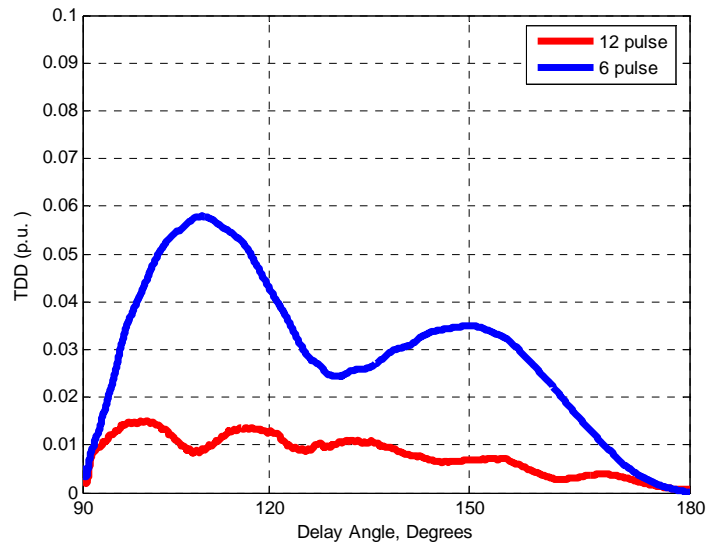
Fig.2.37. Total harmonic distortion versus maximum fundamental current for 6 pulse and 12-pulse TCR based SVC (full conduction for the TCR line currents is taken as 1 p.u. and power rating of both SVCs are equal.).

2.6.2 Steady State Unbalanced Operation

The 6 pulse balanced TCR in Fig.2.29 is modified for the unbalanced operation. The delay for each phase is applied in order to create an unbalance in TCR currents. The results in Fig.2.38 have been obtained for the above cases. In order to see the effect of unmatched firing delay in half-cycles, 3 degrees extra delay is added to the backward connected thyristors in the PSCAD simulation. In Fig.2.39, the results are presented.

Table.2.6.   TCR Firing Delays for each 6 pulse delta connected TCR phase

Case No.	Phase AB, α (Degrees)	Phase BC, α (Degrees)	Phase CA, α (Degrees)
Case 1	180	150	180
Case 2	180	120	180
Case 3	180	90	180
Case 4	180	90	90

In Fig.2.38.a, it is seen that in the unbalanced operation, the 3rd harmonic current to appear in the line current. The other triplen harmonics also appear in the line. Interharmonic currents are low in magnitude, but interharmonics group 1 is a about 1% in case 3 and 4 as seen in Fig.2.38.(c-d). Interharmonic subgroup is also higher than 0.4%.

In the second experiment, in addition to the results obtained in the previous simulation, even harmonics appear in the line currents because of the dissimilar firing delays. 0.7% 2nd harmonic (line harmonic) is also observed in case 2 for 3° of firing delay difference among the backward connected thyristors. Interharmonic groups and subgroups are lower than the first simulation as seen in Fig.2.39.(c-d).
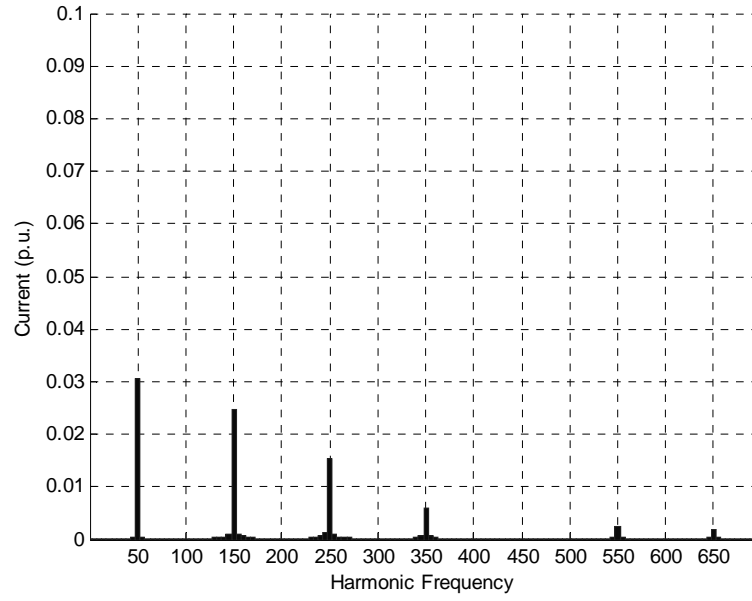
(a)
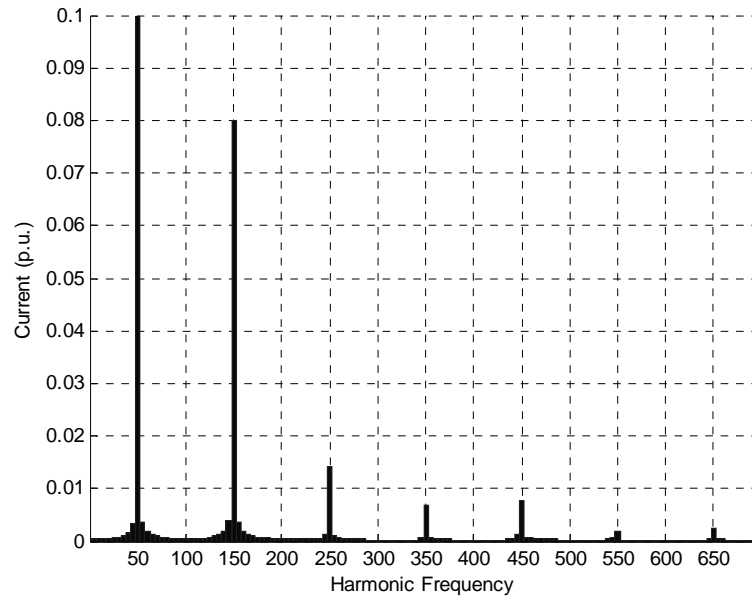
(b)

Fig.2.38. Unbalanced TCR Simulation in Table 2.6. (a) case 1, (b) case 2; fft analysis for line currents for phase B is plotted. Full conduction line current in full conduction is 1 p.u. (Single line, 10 cycle average)

51
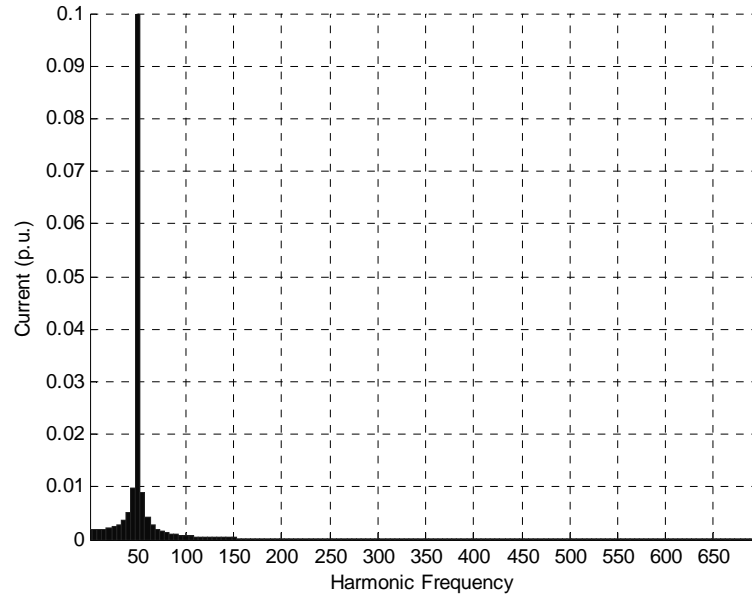
(c)
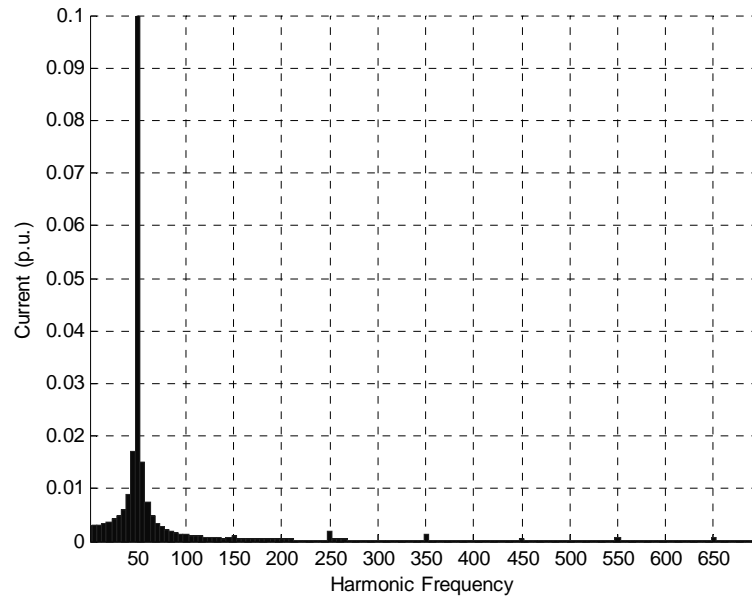
(d)

Fig. 2.38. (cont'd) Unbalanced TCR Simulation in Table 2.6. (c) case 3, (b) case 4; fft analysis for line currents for phase B is plotted. Full conduction line current in full conduction is 1 p.u. (Single line, 10 cycle average)

52
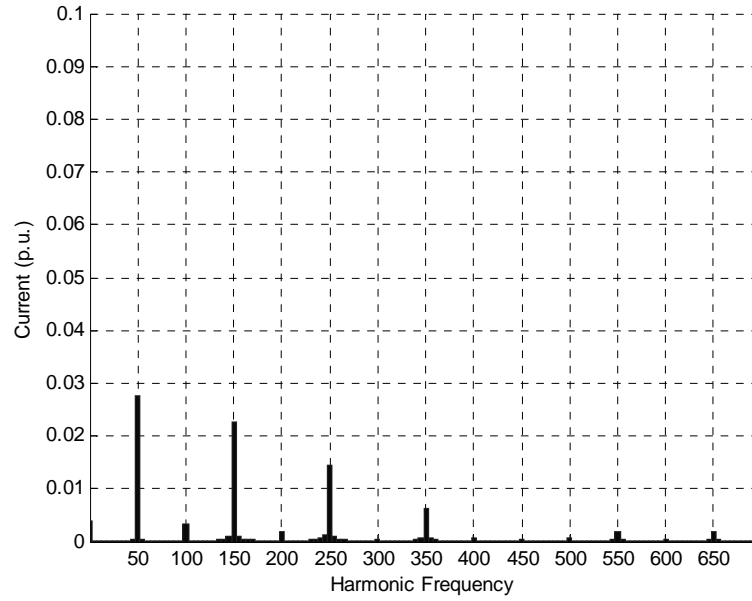
(a)
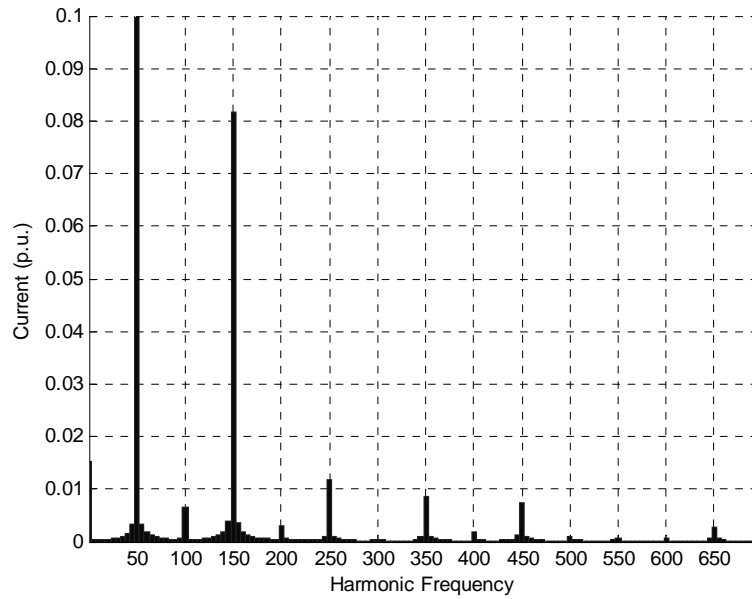
(b)

Fig.2.39. Unbalanced TCR Simulation in Table 2.6 with extra 3 degrees delay imposed to backward connected thyristors. (a) case 1, (b) case 2; fft analysis for line currents for phase B is plotted. Full conduction line current in full conduction is 1 p.u. (Single line, 10 cycle average)

53
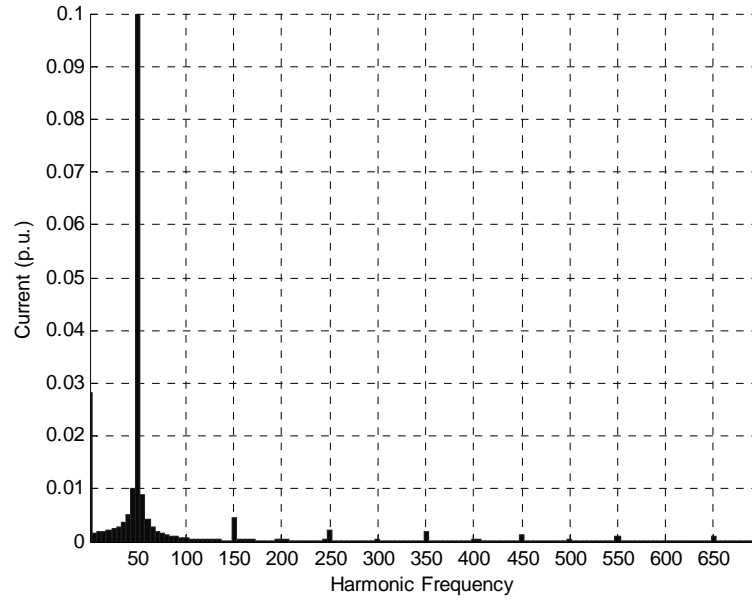
(c)
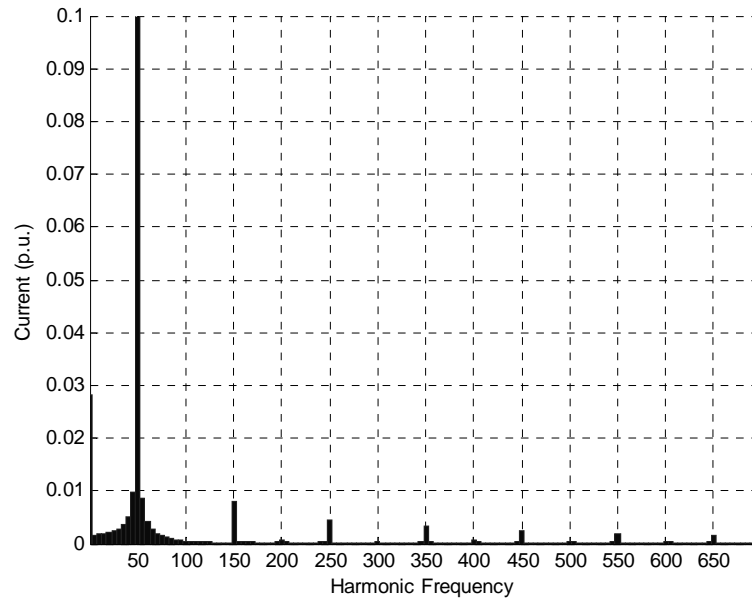
(d)

Fig. 2.39. .(cont'd) Unbalanced TCR Simulation in Table 2.6 with extra 3 degrees delay imposed to backward connected thyristors. (c) case 3, (d) case 4; fft analysis for line currents for phase B is plotted. Full conduction line current in full conduction is 1 p.u. (Single line, 10 cycle average)

54

2.6.3 Transient Operation

The transient operation depends on the load characteristics and the operating mode of the TCR. The worst case will be the load which changes from minimum to maximum in a half cycle. Unbalanced loads make transient operation more complicated because balancing the load may require more reactive power capacity than regular compensation. There are even cases where compensation can not be achieved because of unbalance even though SVC capacity is enough for compensation without balancing.

It is impossible to simulate every possibility of the transient operation because there are infinite combinations, especially in the rapidly fluctuating loads such as an arc furnace. Simulation using the real time data collected by data acquisition systems can be preferred. According to the field results, the load and SVC line currents have high 2nd and 3rd harmonic content SVC currents also have high odd harmonic content due to not only the TCR harmonics but also the load current harmonics. According to the selected topology, TDD in SVC line current differs in similar TCR installations. 'nd harmonic may be a big problem, because current installations in arc furnaces in Turkey do not eliminate 2nd harmonic and sometimes amplify it [37].

Typical case can be seen in Fig.2.40 which contains the 2nd harmonic current of an arc furnace installation in Aliağa region in Turkey. Source current (I_s) is plotted for EAF current (I_{eaf}) and it is seen that 2nd harmonic source current is amplified for the most of the field data ($I_s > I_{eaf}$ for 2nd harmonic). However in Fig.2.41, it is seen that 5th harmonic currents are filtered for the most of the field data ($I_s < I_{eaf}$ for 5th harmonic).
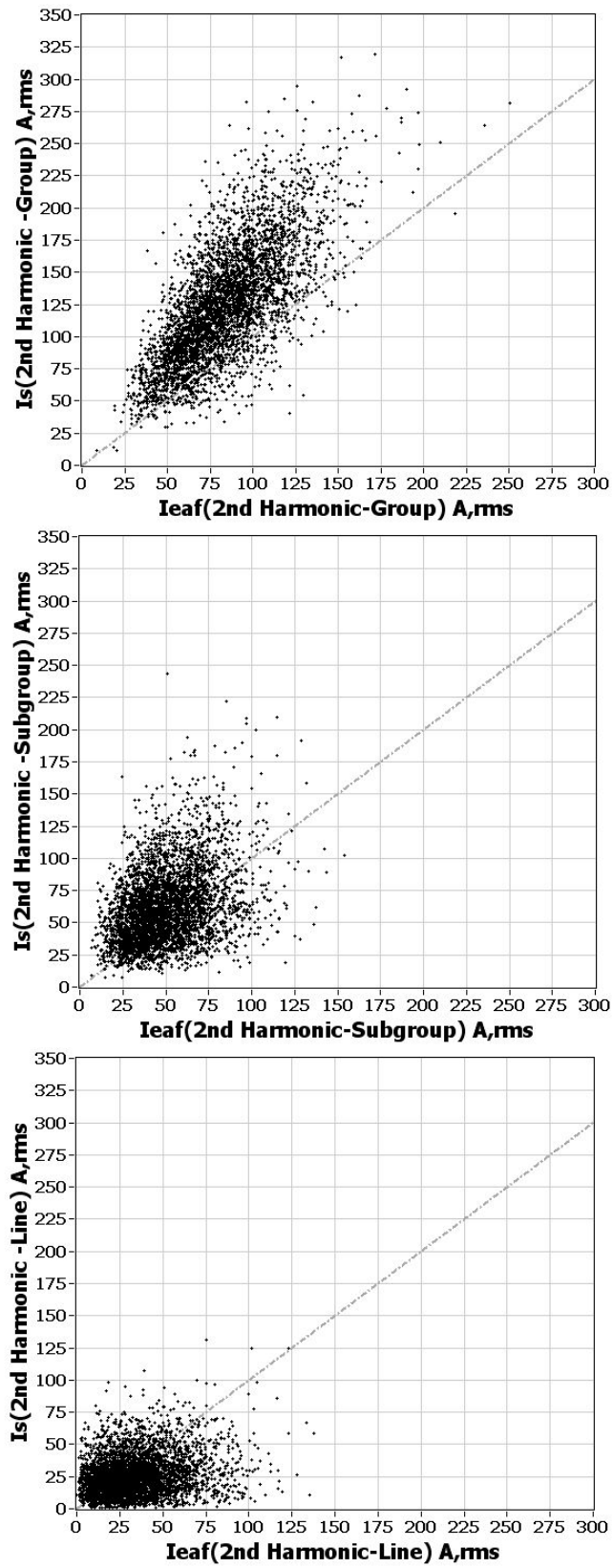
Fig.2.40. 2nd harmonic content, computed for harmonic group, harmonic subgroup and single line

56

Fig.2.40. 2nd harmonic content, computed for harmonic group, harmonic subgroup and single line
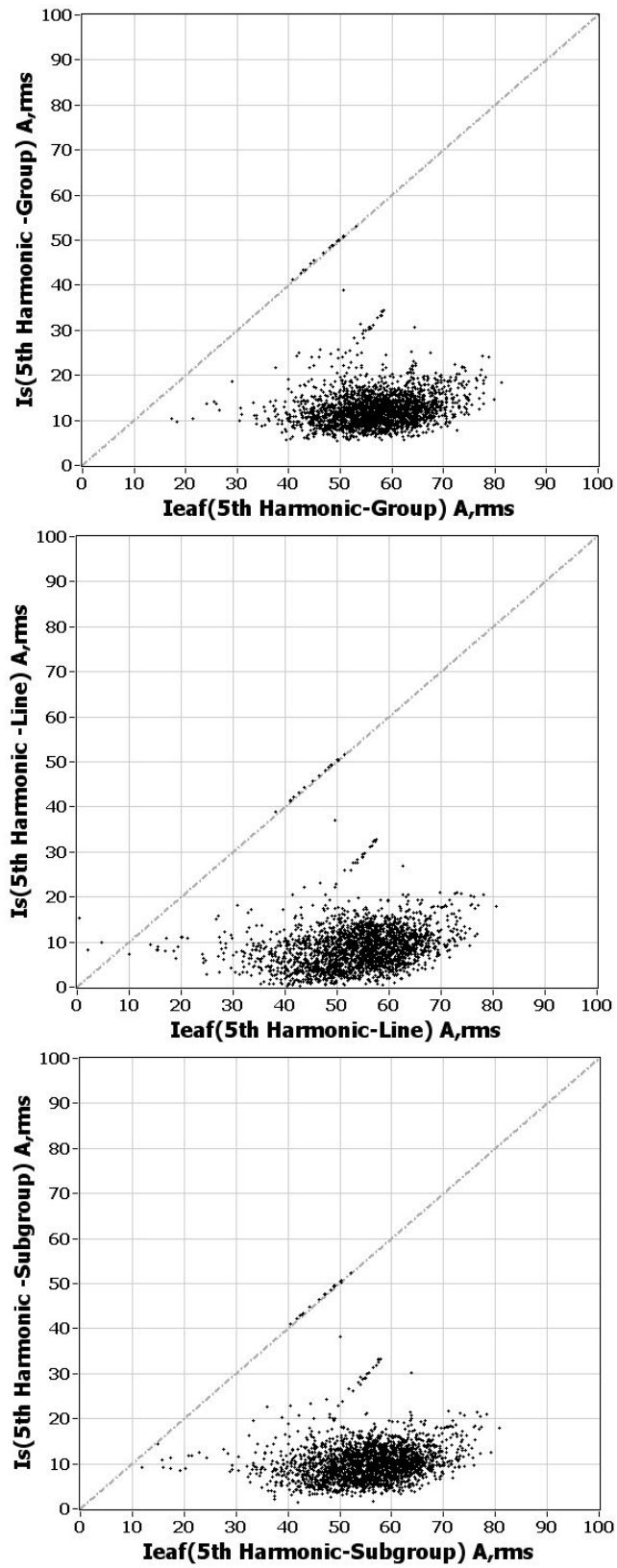
Fig.2.41. 5th harmonic content, computed for harmonic group, harmonic subgroup and single line

57

2.7 Minimization of TCR Harmonics

As mentioned in previous sections, the TCR generates harmonics which may exceed the regulation limits in the country [33-34]. It has to be carefully investigated and evaluated. In order to eliminate the harmonics, there are two different methods proposed in the literature:

a- Filtering of harmonics with a passive or active shunt filters

b- Cancellation of harmonics by phase shifting

2.7.1 Minimization of Harmonics by Passive Shunt Filters

Shunt filters form a low impedance path for the harmonics in the specific frequencies. The ideal shunt filter is short circuit at the tuning frequency, and high impedance at other frequencies. The filter is capacitive below and inductive above the tuning frequency. Therefore, the harmonic currents flow through this path instead of flowing towards the source or other loads. Voltage harmonics may also cause current harmonics to flow in the circuit. In order to cancel voltage harmonics, series type filters are necessary [10-15].

Conventional filter design depends on many criteria. IEEE 519-1992 [35] suggests the methods for harmonic evaluation and cancellation. According to [2], the filter size is defined by the reactive power supplied at the fundamental frequency. In an ideal case, it would be preferred to cancel out all the waveform distortion caused by the harmonics including the radio interference [2]. However, in a practical case, it is almost impossible to design such a filter because of the technical and economical reasons. Therefore, the aim of the design should be filtering the specified harmonics thus bringing them to an acceptable level. Typical characteristics of different kinds of filters are given in Fig.2.42-2.44: The sharpness of tuning depends on the quality of the filter (Q).

58
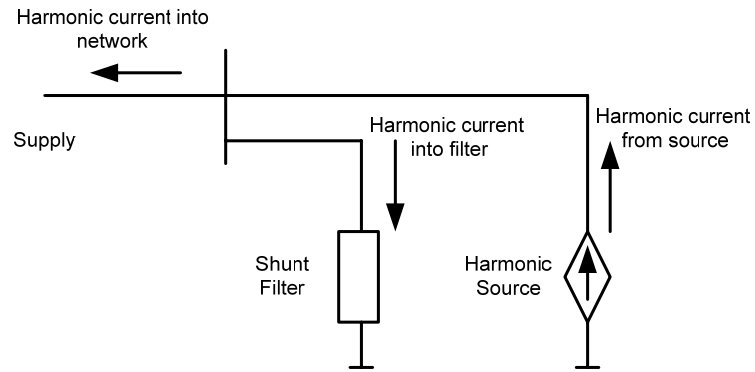
Fig.2.42. Harmonic current flow in an AC network
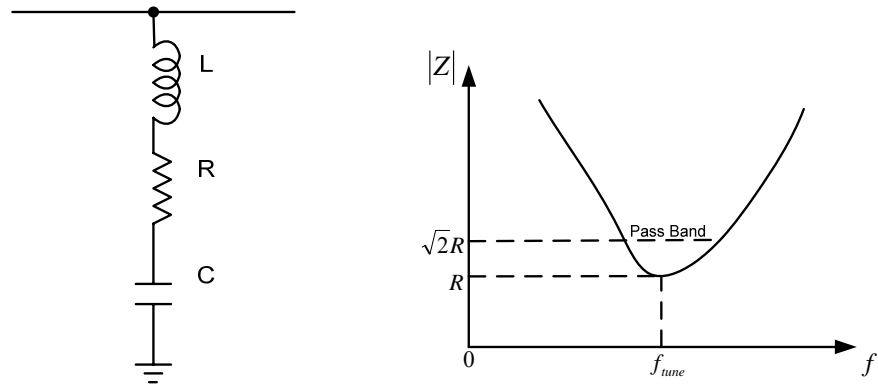
Fig.2.43. Tuned shunt filter and its characteristics.
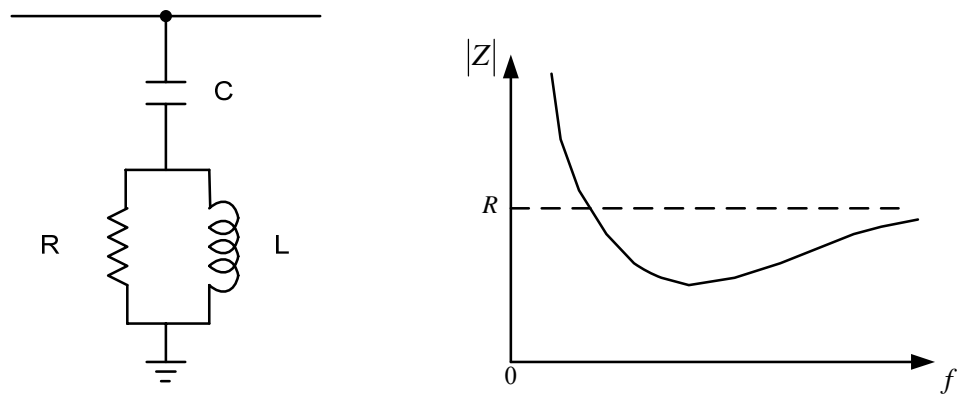
Fig.2.44. Second order damped shunt filter and its characteristics.

59

The design of a harmonic filter may not be straight forward, but complicated. Design of the filters will further be investigated in Chapter 3 in detail. However, measurements at the installations with currently installed filters show that frequency characteristics of a filter may sometimes amplify current harmonics instead of filtering them. In [37], there are examples of 2nd and 3rd harmonic filter banks which amplify the 2nd harmonic and interharmonics of the EAFs and TCRs installed for Turkish steel industry companies. This problem also has correlation with the light flicker. Therefore flicker and harmonic standards can not be fulfilled in this area. One of the reasons for this problem is the selection of primary objectives. In the time where these filters were installed, there were no strict regulations concerning the harmonics. Since the primary objective was reactive power compensation, filters were designed to reduce the costs by reducing filtering capacity. In some cases, 2nd harmonic filter was omitted in order to further reduce the costs. Load balancing capability of the SVCs is also reduced in order to reduce the capacitive banks and TCR size.

2.7.2 Cancellation of Harmonics by Phase Shifting

Instead of filtering TCR harmonics existing in the line current, it is also possible to cancel them before they can reach to the supply. By choosing a 12-pulse topology, as mentioned in section 2.4, the harmonic numbers that are $6n+/-1$ ($n=1,3,5...$) integer multiple of the fundamental cancel each other. The phase shift of $\pi/3$ rad exists between delta and wye connection. This phase shift also reflects to the harmonics. The harmonics that are multiples of $6n+/-1$ ($n=1,3,5...$) of the fundamental are shifted π rad between Δ and Y , while the others do not have a phase difference. This can be achieved by either connecting Δ / Y TCRs as in Fig. 2.45, or by connecting via Δ-Y / Δ-Δ transformers as in Fig.2.46.
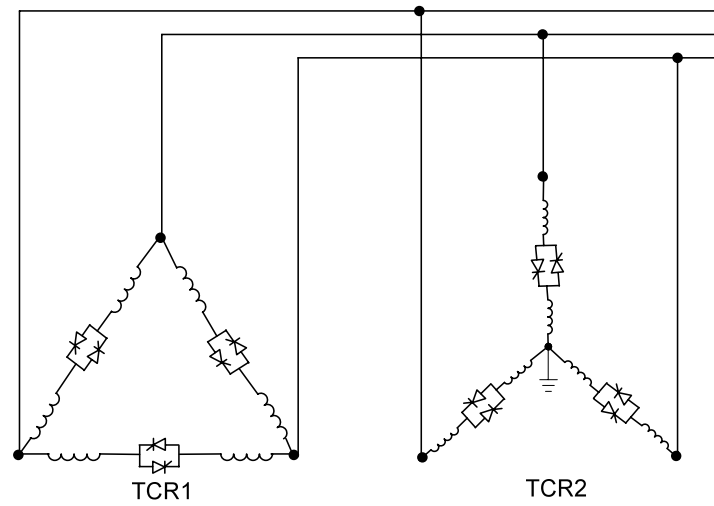
Fig.2.45. Harmonic phase shifting by 12-pulse Δ-Y connected TCR.
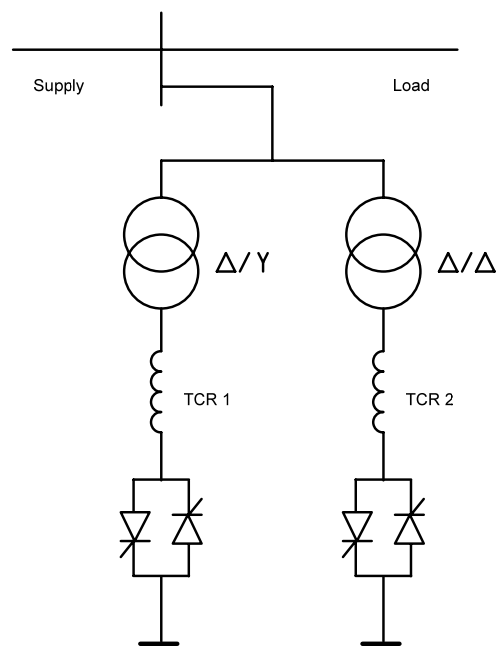
Fig.2.46. Harmonic phase shifting by 12-pulse TCR connected via Δ-Y / Δ-Δ transformers

2.8 Principles of Reactive Power Compensation

In an ideal AC power system, the voltage and current waveforms should be free from harmonics, frequency should be constant at each measurement point and the power factor should be unity [1]. In terms of "quality of supply" and "ideal load" conditions, the fluctuations in voltage and frequency are defined in standards [standards]. However, when the load is not an ideal one, especially in very rapidly changing demand conditions, there will be fluctuations, which may surpass the acceptable limits.

Power factor change in the load also brings an extra burden for the supply in terms of current. Whenever the current increases, losses in the transmission lines increase and voltage regulation worsens.

2.9 Load Compensation

Management of the reactive power to improve the quality of the supply is defined as the Load Compensation [1]. The principles of the load compensation are given below:

2.9.1 Power Factor Correction

Power factor is defined as the ratio of the active power P to the apparent power S. Actually, in an ideal balanced case where there exists no harmonics; this corresponds to the cosine of the displacement angle between phase voltage and phase current. In this ideal case, reactive power Q can be defined as the sine of the displacement angle between phase voltage and phase current

$$power\ factor = \cos(\phi) = \frac{P}{S} \tag{2.14}$$

where:

$$P = \mathrm{Re}(\mathbf{V}^*\mathbf{I}) \tag{2.15}$$

$$Q = \mathrm{Im}(\mathbf{V}^*\mathbf{I}) \tag{2.16}$$
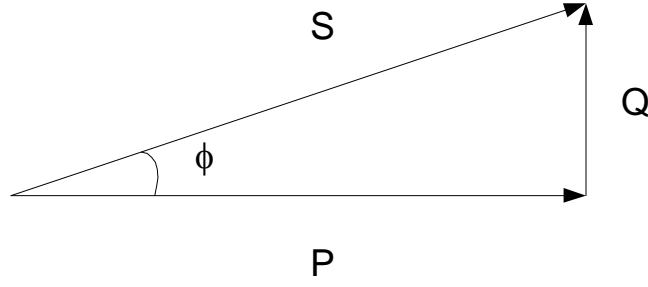
Fig.2.47. Relationship among apparent, active and reactive power.

In a polyphase system, which has k phases that may also be unbalanced, the apparent power becomes:

$$S = \sum_k \sqrt{\left(P_k^2 + Q_k^2\right)} \tag{2.17}$$

Taking harmonics into account, the apparent power becomes:

$$S = \sum_k \sqrt{\left((P_k + P_{hk})^2 + Q_k^2 + Q_{hk}^2\right)} \tag{2.18}$$

In equation (2.17) for each phase k; P_k is the power delivered by fundamental component, P_{hk} is the power delivered by harmonic sources, Q_k is the reactive power caused by fundamental component, and Q_{hk} is the reactive power component caused by harmonics in a polyphase system. Power factor definition still holds after taking harmonics into consideration.

It is important to note that $\cos\phi$ is the fraction of the apparent power, which can be usefully converted into other forms of energy [1].

Consider that the linear load admittance is defined by:

$$Y_l = G_l + jB_l \tag{2.19}$$

Power equation of the load is given by:

$$S_l = \mathbf{VI}_l^*$$
$$\tag{2.20}$$

63

Substituting the equation (2.19), we see that

$$S_l = P_l + jQ_l = V^2 G_l - jV^2 B_l \tag{2.21}$$

The main principle of power factor correction is to compensate for the reactive power, which requires a local compensator with a purely reactive susceptance $-B_l$.

It is usually an engineering compromise between the cost and total compensation because it may be too expensive to compensate the load completely. Reactive energy penalty limits in the country determine the necessary reactive power needed to successfully compensate the load over a defined period of time.

2.9.2 Voltage Regulation

AC transmission lines are electrical networks that can be characterized mainly by per-unit series inductances and shunt capacitances. Any change in the load and load power factor results in voltage alterations along the transmission line which may lead to large amplitude differences in the sending and receiving ends. Electrical Loads are usually not tolerant to voltage variations. Undervoltage conditions result in degradation of performance whereas overvoltage causes magnetic saturation and causes harmonics as well as failures because of insulation breakdown. In the extreme case, a large load change may cause the receiving end voltage to collapse, which is defined as voltage instability [T1].

Miller defines the Voltage regulation as the proportional (or per unit) change in supply voltage magnitude associated with a defined change in load current [1]. In the following equations, bold capital letters denotes the phasors. Fig.2.48 shows the simplified single line diagram of a typical power distribution system. V_s is the supply voltage while the V_T denotes the terminal voltage which is affected by source current I_s and terminal impedance X_T. The terminal impedance includes the source impedance, transmission impedance and distribution impedance. For the sake of simplicity, resistive components are neglected. The parameters are assumed to be lumped. Load impedance is denoted by Z_L and load current is denoted by I_L. The ideal compensator can be represented by a shunt susceptance X_K connected to the load terminal.

64
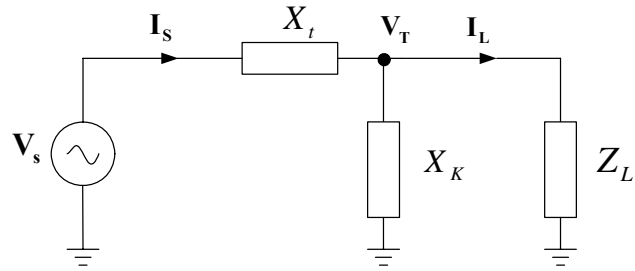
Fig.2.48. Equivalent single line diagram of a transmission system connected to a load.
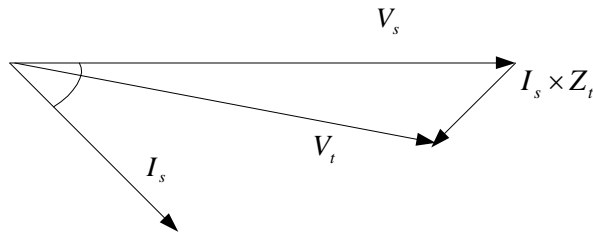
(a)
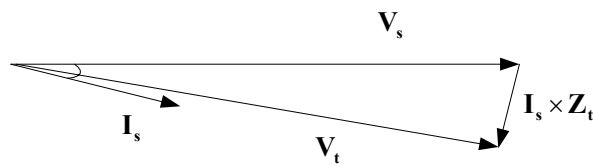
(b)

Fig.2.49. Phasor diagram for the (a) uncompensated system and (b) compensated system

$$\Delta V = V_s - V_l = Z_s I_L \qquad (2.22)$$

In order to regulate the voltage, the compensator needs to alter the voltage at the load terminals which satisfies the condition $|\mathbf{E}|=|\mathbf{V}|$. After the addition of the compensator, the reactive power becomes $Q_s=Q_k+Q_l$ which is composed of compensator and load reactive power respectively. Load active power is assumed to be constant and it is denoted by P_l. Assuming that the compensator is purely reactive:

$$= (R_s + jX_s)\left[\frac{P_l - jQ_l}{V_t}\right] \tag{2.23}$$

$$= \frac{(R_s P_l + jX_s Q_l)}{V_t} + j\frac{(X_s P_l - jR_s Q_l)}{V_t} \tag{2.24}$$

Rewriting the Phasor equations, we find that:

$$|V_s|^2 = \left[V_t + \frac{R_s P_l + X_s Q_s}{V_t}\right]^2 + \left[\frac{X_s P_l - R_s Q_s}{V_t}\right]^2 \tag{2.25}$$

In order to find the solution where $|\mathbf{E}|=|\mathbf{V}|$, we need to solve the above equation for Q_s assuming the active power is constant at the load for the voltage variation:

$$Q_s = \frac{-2V_l^2 X_s \pm \sqrt{4V_t^4 X_s^2 - 4(R_s^2 + X_s^2)\left[(V_t^2 + R_s P_l)^2 + X_s^2 P_l^2 - V_s^2 V_t^2\right]}}{R_s^2 + X_s^2} \tag{2.26}$$

This proves that there exists a solution for complete voltage regulation; however, load compensation cannot be achieved since Q_s is not zero.

66
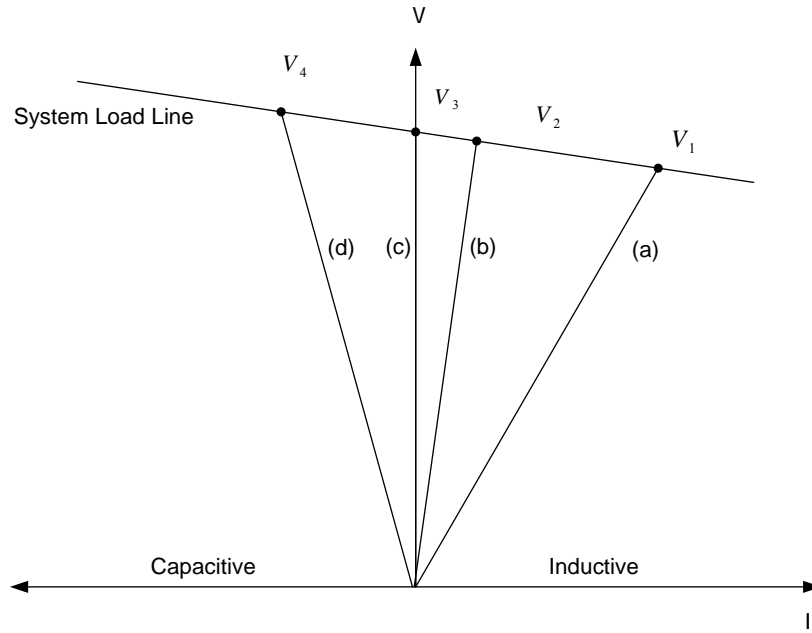
Fig.2.50. Typical voltage/current characteristics of an inductive electrical load for cases: (a): Uncompansated, (b): Compensated, (c):Compensated for unity power factor, (d): Overcompensated

The voltage / reactive power characteristics are defined by [1]:

1. The knee point voltage V_k

2. The maximum or rated reactive power Q_k for phase k

3. The gain K_k

$$K_k = \frac{dQ_k}{dV} \tag{2.27}$$

Therefore voltage characteristics can be found by:

$$V = V_k + \frac{Q_k}{K_k} \tag{2.28}$$
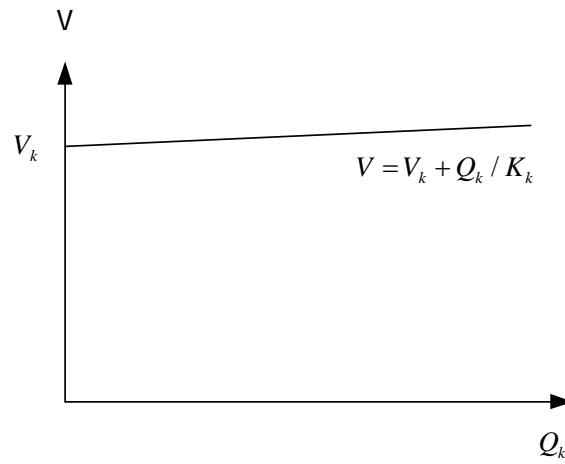
Fig.2.51. Typical voltage/reactive power characteristics of a compensator

2.9.3 Load Balancing

2.9.3.1 Theory of Load Balancing
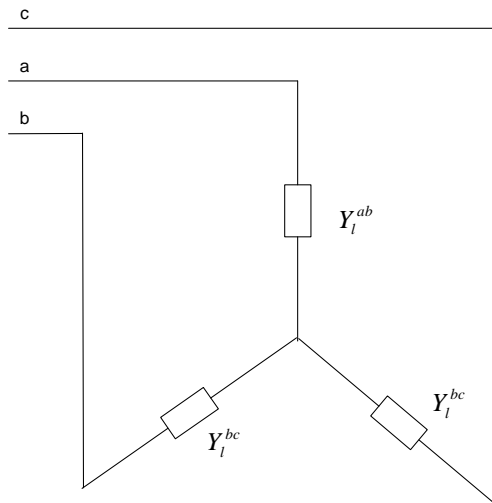
Fig.2.52. Three phase unbalanced load.

68

In Fig.2.52, a network of Y connected admittances is given. It is clear that there exists an unbalance if Y_l^{ab}, Y_l^{bc} and Y_l^{ca} are complex and unequal. In order to balance the load, it is necessary to balance or eliminate the reactive components. By connecting a compensator parallel to each phase (Denoted by $B_k{}^{ab}$, $B_k{}^{bc}$ and $B_k{}^{ca}$), imaginary component of the admittance can be eliminated as seen in Fig.2.53.
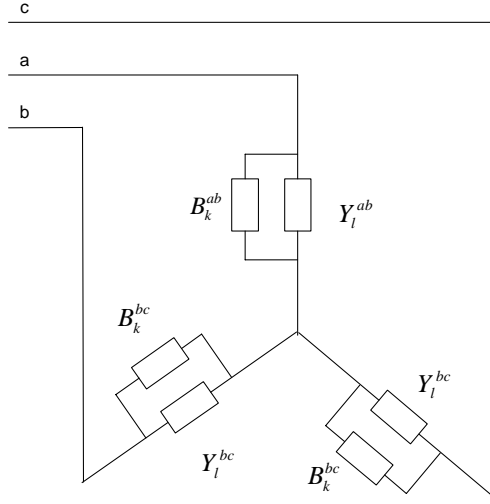
Fig.2.53. Eliminating the susceptance, thus eliminating the reactive power

In order to make admittance purely real the negative of the phase susceptance B_l^{ab} is connected parallel to the phase admittance:

$$Y_l^{ab} = G_l^{ab} + jB_l^{ab} \tag{2.29}$$

Therefore, the compensator susceptance B_γ^{ab} is:

$$B_\gamma^{ab} = -B_l^{ab} \tag{2.30}$$

The load given in Fig. 2.54 will further be balanced by using the same compensator. Each phase will be balanced individually; hence, we will focus on a single phase.
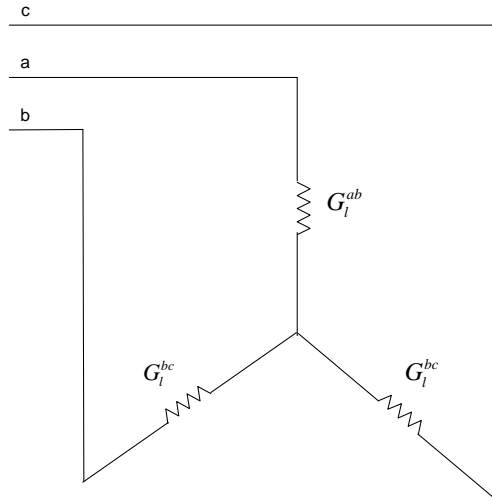
Fig.2.54. Unbalanced load with unity power factor.
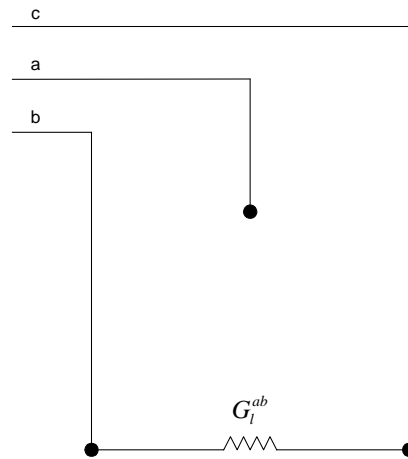
Fig.2.55. Single phase unbalanced load with unity power factor.

In order to balance the real load, we will add a capacitive susceptance between the phases b and c:

$$B_\gamma^{ab} = \frac{G_l^{ab}}{\sqrt{3}} \tag{2.31}$$

In addition to this, we will add the following inductive susceptance between the phases a and c:

$$B_\gamma^{ab} = -\frac{G_l^{ab}}{\sqrt{3}} \tag{2.32}$$

The circuit becomes as seen in Fig. 2.56.
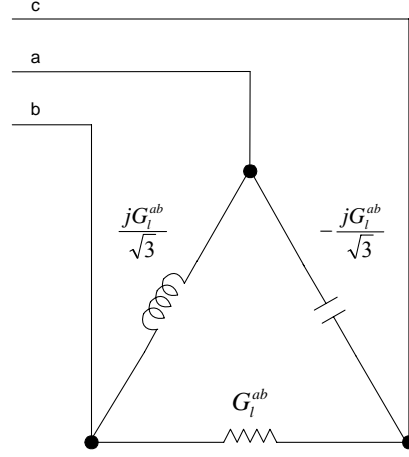
Fig.2.56. Positive sequence balancing of the single-phase unity power factor load.

By making a Delta-Wye transformation of the circuit:

$$\frac{1}{Y_a} = \frac{\dfrac{1}{Y_{ab}} \times \dfrac{1}{Y_{ca}}}{\dfrac{1}{Y_{ab}} + \dfrac{1}{Y_{ca}} + \dfrac{1}{Y_{bc}}} \tag{2.33}$$

$$\frac{1}{Y_a} = \frac{\dfrac{1}{G_l^{ab}} \times \dfrac{1}{j\dfrac{G_l^{ab}}{\sqrt{3}}}}{\dfrac{1}{G_l^{ab}} + \dfrac{1}{j\dfrac{G_l^{ab}}{\sqrt{3}}} + \dfrac{1}{-j\dfrac{G_l^{ab}}{\sqrt{3}}}} \tag{2.34}$$

71

$$\frac{1}{Y_a} = \frac{\sqrt{3}}{-jG_l^{ab}} \qquad (2.35)$$

$$Y_a = \frac{-jG_l^{ab}}{\sqrt{3}} \qquad (2.36)$$

Similarly:

$$Y_b = \frac{jG_l^{ab}}{\sqrt{3}} \qquad (2.37)$$

$$Y_c = \frac{G_l^{ab}}{3}$$

(2.38)

For a symmetrical components transformation, the transformation matrix is:

$$\mathbf{C} = \frac{1}{\sqrt{3}} \begin{bmatrix} 1 & 1 & 1 \\ 1 & h & h^2 \\ 1 & h^2 & h \end{bmatrix} \qquad (2.39)$$

$$\mathbf{C^*} = \frac{1}{\sqrt{3}} \begin{bmatrix} 1 & 1 & 1 \\ 1 & h^2 & h \\ 1 & h & h^2 \end{bmatrix} \qquad (2.40)$$

where $h = e^{j2\pi/3}$.

Since:

$$\mathbf{V} = \mathbf{ZI} \qquad (2.41)$$

$$\mathbf{V'} = \mathbf{C^* ZCI'} \qquad (2.42)$$

Assuming that Z_a, Z_b and Z_c are the complex impedances of the three phases, the symmetrical components impedance matrix becomes:

$$\mathbf{Z} = \frac{1}{3} \begin{bmatrix} Z_a + Z_b + Z_c & Z_a + hZ_b + h^2 Z_c & Z_a + h^2 Z_b + hZ_c \\ Z_a + hZ_b + h^2 Z_c & Z_a + Z_b + Z_c & Z_a + hZ_b + h^2 Z_{c3} \\ Z_a + h^2 Z_b + hZ_c & Y_1 + h^2 Y_2 + hY_3 & Z_a + Z_b + Z_c \end{bmatrix} \qquad (2.43)$$

If negative sequence and zero sequence voltages are zero in the supply, the positive sequence voltage V_+ is written in terms of current sequence components I_+, I_- and I_0 (positive, negative and zero sequence respectively):

$$\begin{bmatrix} V_+ \\ 0 \\ 0 \end{bmatrix} = \frac{1}{3} \begin{bmatrix} Z_a + Z_b + Z_c & Z_a + hZ_b + h^2 Z_c & Z_a + h^2 Z_b + hZ_c \\ Z_a + hZ_b + h^2 Z_c & Z_a + Z_b + Z_c & Z_a + hZ_b + h^2 Z_{c3} \\ Z_a + h^2 Z_b + hZ_c & Y_1 + h^2 Y_2 + hY_3 & Z_a + Z_b + Z_c \end{bmatrix} \begin{bmatrix} I_+ \\ I_- \\ I_0 \end{bmatrix} \quad (2.44)$$

Therefore for the positive sequence:

$$[V_+] = \frac{1}{3} \begin{bmatrix} Z_a + Z_b + Z_c & Z_a + hZ_b + h^2 Z_c & Z_a + h^2 Z_b + hZ_c \end{bmatrix} \begin{bmatrix} I_+ \\ I_- \\ I_0 \end{bmatrix} \quad (2.45)$$

Substituting the eqn. (2.36),(2.37) and (2.38) into (2.45):

$$V_+ = \frac{1}{3} \left[\frac{3}{G_l^{ab}} + \frac{\sqrt{3}}{jG_l^{ab}} - \frac{\sqrt{3}}{jG_l^{ab}} \right] I_+ \quad (2.46)$$

The circuit becomes a wye circuit in Fig. 2.57 for the positive sequence voltages and positive sequence current I_+ eventually becomes:

$$G_l^{ab} V_+ = I_+ \quad (2.47)$$

Evaluating this operation for all three unbalanced phases, we get a balanced three phase system as seen in Fig. 2.57.

$$G = G_l^{ab} + G_l^{bc} + G_l^{ca}$$
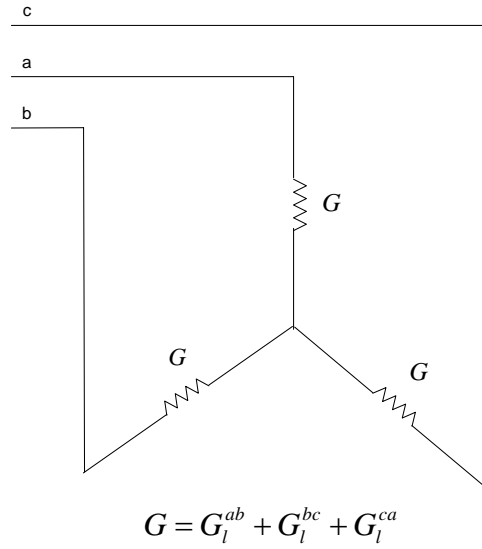
Fig.2.57. Positive sequence wye equivalent of the single phase unity power factor load.

Therefore, the Phasor diagram for the positive sequence becomes balanced. Assuming that there exists no negative sequence and no zero sequence components in the source voltage, only the positive sequence currents will flow (Fig. 2.58):
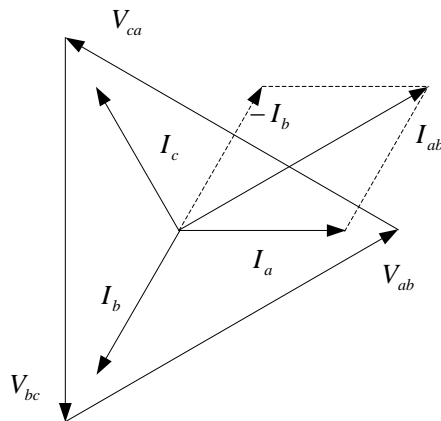
Fig.2.58. Positive sequence Phasor diagram of the single phase unity power factor load.

74

It is important to note that the overall power is still $G_{ab}|V|^2$, where $|V|$ is the amplitude of the line-to line voltage. The added inductance and reactance cause reactive power to flow through the delta; however, they cancel each other when observed from outside the delta.

2.9.3.2 Unbalanced Operation

If the firing pulses of the back-to-back connected thyristors are not balanced or the compensation system is not operating in the steady state, then it performs an unbalanced operation. Unbalanced operation is in the nature of an SVC because load balancing or voltage regulation requires the generation of negative sequence currents and unbalanced SVC currents.

Sometimes unbalance condition may be a sign of a fault in the SVC control system. It is easy to identify such a fault by firing the SVC at constant angle for all phases and observing the current waveforms. A typical case is introduced in section 2.7.

In a delta connected TCR, zero sequence currents can not flow in the delta connection. However, any negative sequence voltage appearing on the terminals of the TCR will force a negative sequence current in the TCR and load phases. If the TCR is designed to balance voltage, the control system will immediately respond to negative sequence voltage. If the control system is in the linear control range, in other words if conduction angle satisfies $0 < \sigma < \pi$, then the firing delay angles will shift towards a susceptance value that will confront and minimize the negative sequence voltage. However, in full conduction mode or no-conduction mode, the TCR will not be able to reduce the voltage unbalance.

On the other hand, an SVC designed only for load balancing and reactive power compensation can not regulate terminal voltages completely. Instead, negative sequence in the load current will be reduced, and cancelled in the ideal case. Therefore, only the negative voltage sequence component is prevented that can be

caused by voltage drop on the supply impedance by the negative sequence load current.
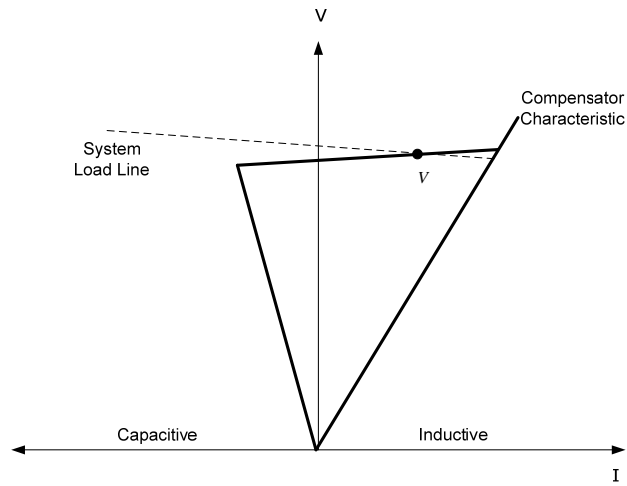
Fig.2.59. System load line versus compensator characteristics for the voltage balancing.
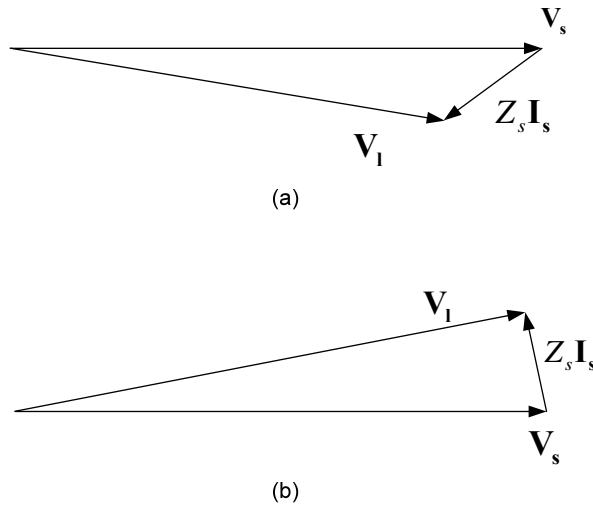
Fig.2.60. Voltage Phasor diagram for voltage balancing for (a) uncompensated system, and (b) compensated system; the circuit diagram in Fig.2.48 is assumed for each of the three phases.

76

In order to achieve voltage regulation, load balancing and reactive power compensation all at the same time, a reactive power compensator with voltage regulating control system biased to maintain a long-term unity power factor is proposed [1]. It is certain that voltage-regulating system cannot maintain unity power factor all the time, as seen in Fig. 2.60, but it can be adjusted to keep the power factor at a certain level.

2.9.3.3 Balancing the Unbalanced Load

As described in Chapter 1 and Chapter 2, by applying the Steinmetz's Equations to the system, we can evaluate the necessary susceptance values for the compensator. A PSCAD simulation example is given below for a system fed by a 34.5kV bus with a 3790 MVA short circuit value as seen in Fig. 2.62.

An unbalance is created by inserting a 5 Ohm resistance between phase B and C. Therefore, the necessary inductance of 0.0276mH is calculated between A and B, while 366.6uF capacitance is needed across C and A to balance the load.

In Fig. 2.59, the system is started in unbalance state, and later balancing susceptances are switched on by a circuit breaker. As seen in Fig.2.63, the supply current waveforms become balanced.

Load balancing is necessary for equalizing the line currents and for the reduction of flicker [1]. Balanced loads are easy to compensate, and they reduce the losses in the conductors as well as in the magnetic circuits such as transformers.
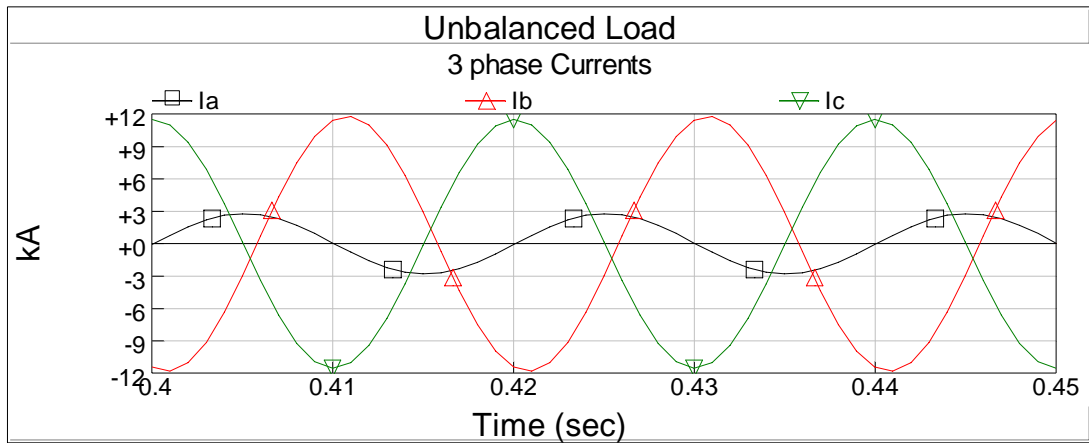
(a)
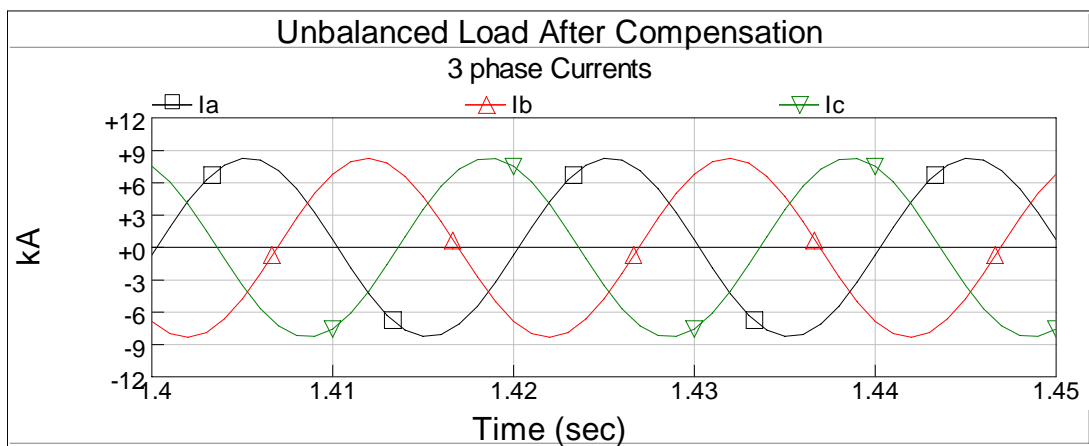
(b)

Fig.2.61. PSCAD simulation results (a) unbalanced load, (b)after the load balancing
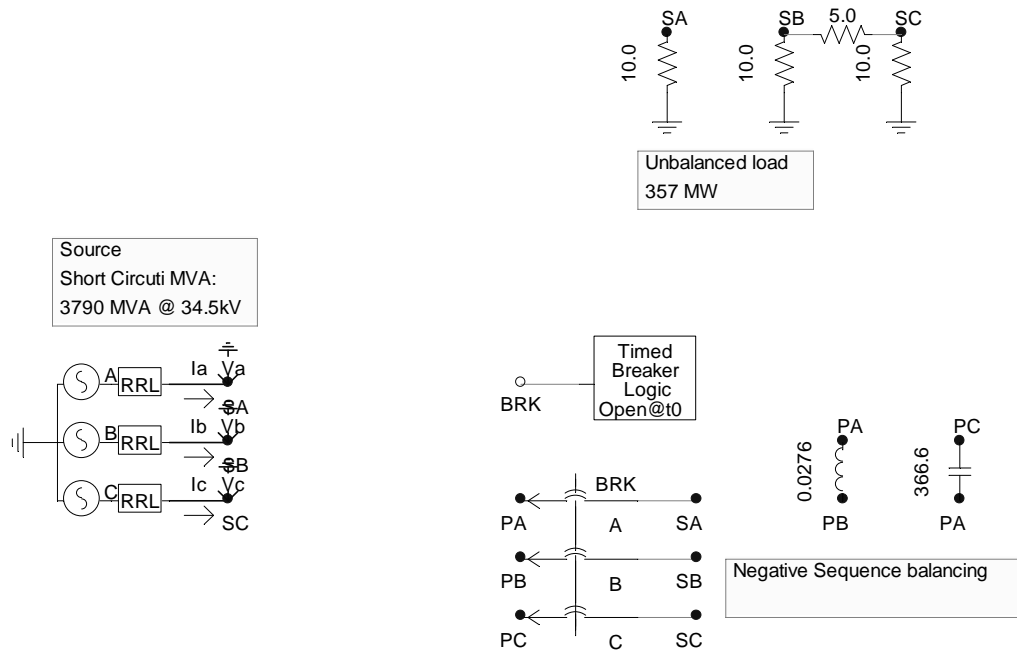
Fig.2.62. PSCAD simulation for balancing an unbalanced load

In order to decide on the sizing of the compensator, load characteristics are investigated. Instant power factor and instant reactive power demand per phase should be determined for the design of the TCR based SVC in order to be able to compensate successfully. The maximum values should be evaluated in the Steinmetz equation (2.48):

$$B_\gamma^{ab} = -B_l^{ab} + (G_l^{ca} - G_l^{bc})/\sqrt{3}$$
$$B_\gamma^{bc} = -B_l^{bc} + (G_l^{ab} - G_l^{ca})/\sqrt{3} \qquad\qquad (2.48)$$
$$B_\gamma^{ca} = -B_l^{ca} + (G_l^{bc} - G_l^{ab})/\sqrt{3}$$

For example, a three phase load is designed for 31 different cases with a power factor of 0.7 as seen in Fig. 2.64. The results are obtained by using (2.48) and they can be seen in Table 2.7. The two different operation types, Reactive Power Compensation (RPC) only and RPC with load balancing, are compared and it is found out that both filter and reactor sizes need to be increased for the same load. Moreover, in order to achieve load balancing, reactor size should be greater than the filter size.
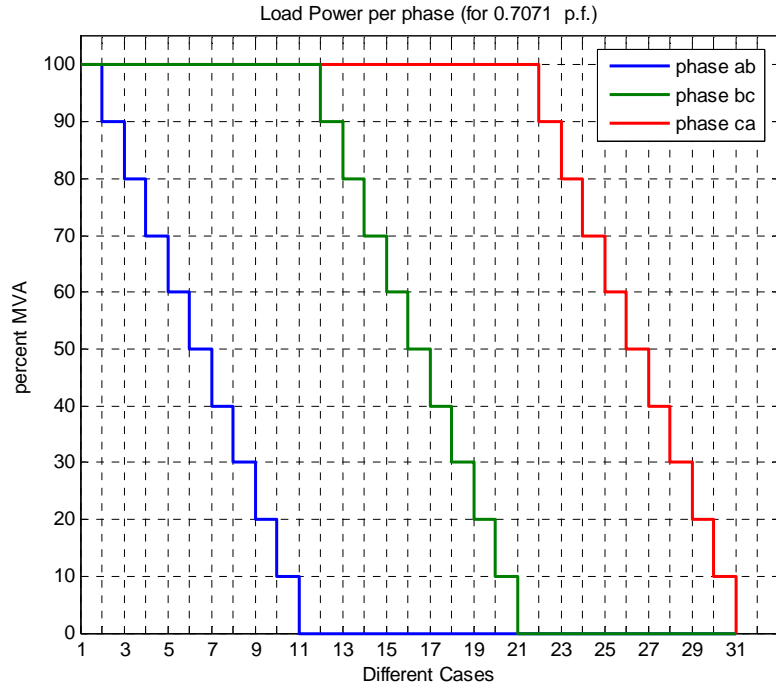
Fig.2.63. Load power in terms of percent of load MVA for each phase to be used in the selection of TCR and harmonic filter sizing
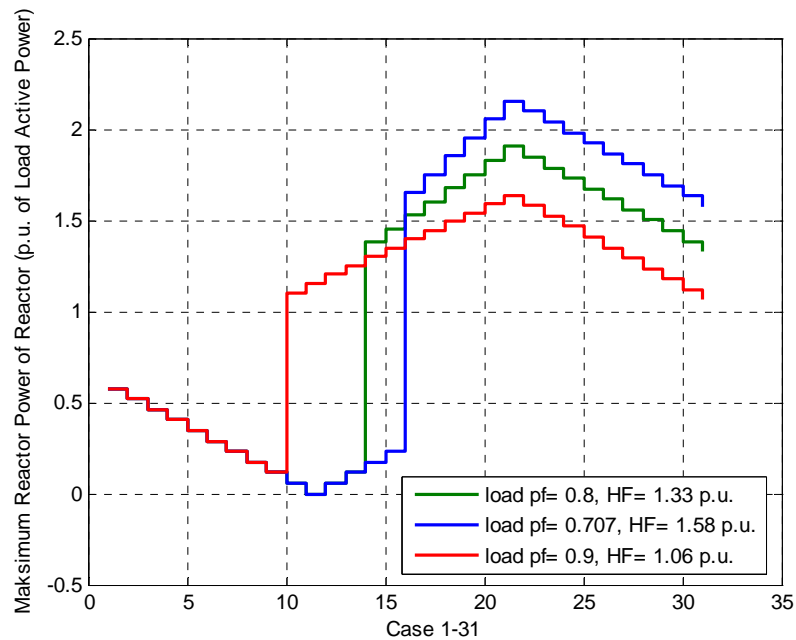
Fig.2.64. Different reactor installations required for both reactive power compensation and load balancing for the cases given in Fig. 2.63. The results are evaluated for three different load power factors (0.707, 0.8 and 0.9) and three different shunt filters.

Table.2.7.   Harmonic Filter and TCR Sizing for a load with 0.7071 p.f.

Case	With Load Balancing (p.u.)		Without Load Balancing (p.u.)	
	TCR	HF	TCR	HF
1	0.577	-1.000	0.000	-1.000
2	0.519	-1.058	0.033	-0.967
3	0.462	-1.115	0.067	-0.933
4	0.404	-1.173	0.100	-0.900
5	0.346	-1.231	0.133	-0.867
6	0.288	-1.289	0.167	-0.833
7	0.231	-1.346	0.200	-0.800
8	0.173	-1.404	0.233	-0.767
9	0.115	-1.462	0.267	-0.733
10	0.057	-1.520	0.300	-0.700
11	0.000	-1.577	0.333	-0.667
12	0.057	-1.520	0.367	-0.633
13	0.115	-1.462	0.400	-0.600
14	0.173	-1.404	0.433	-0.567
15	0.231	-1.346	0.467	-0.533
16	1.654	-1.289	0.500	-0.500
17	1.754	-1.231	0.533	-0.467
18	1.854	-1.173	0.567	-0.433
19	1.954	-1.115	0.600	-0.400
20	2.054	-1.058	0.633	-0.367
21	2.154	-1.000	0.667	-0.333
22	2.097	-0.900	0.700	-0.300
23	2.039	-0.800	0.733	-0.267
24	1.981	-0.700	0.767	-0.233
25	1.923	-0.600	0.800	-0.200
26	1.866	-0.500	0.833	-0.167
27	1.808	-0.400	0.867	-0.133
28	1.750	-0.300	0.900	-0.100
29	1.692	-0.200	0.933	-0.067
30	1.635	-0.100	0.967	-0.033
31	1.577	0.000	1.000	0.000

As seen in Table 2.7; in order to compensate and balance the load (with 0.707 p.f.), 2.154 p.u. of load active power is needed for TCR and 1.577 p.u. of of load active power is needed for HF sizing. However, 1 p.u. of load active power is sufficient for both TCR and HF sizing for compensation without load balancing.

2.10 Suppression of Flicker

2.10.1   Theoretical Considerations

The flicker defines the limits for voltage fluctuations at different frequencies. The standards for flicker exist both in IEEE [22] and IEC [23]. IEC [23] standards include a complete flickermeter definition.

In the early flicker-related experiments, "flicker fusion boundary" is defined as the limit frequency above which the flickering is not recognized [21]. During the experiments in the early 20th century, it was found out that around 6 Hz the sensitivity to the flicker becomes maximum. Half a century later, investigations on human eye behaviour and its response to flicker gave way to a filter for the light fluctuations.
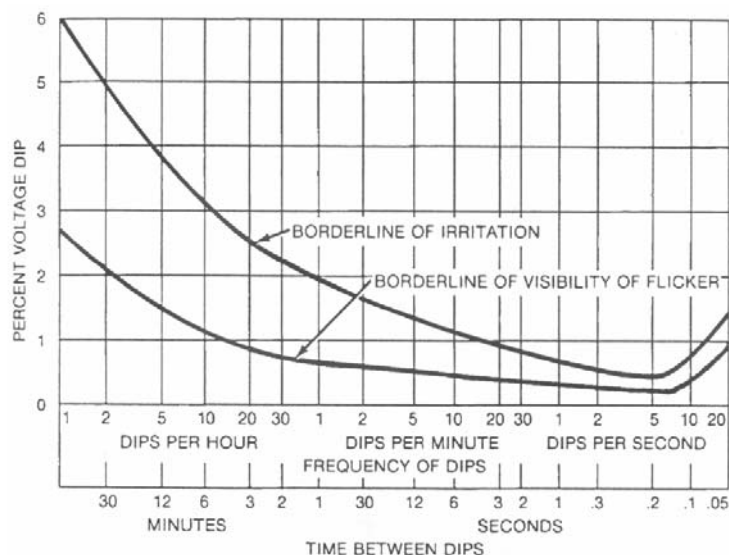
Fig.2.65. Range of observable and objectionable voltage flicker versus time [22]

82

It is also noted in [21] that the human response to flicker may change with stress and tiredness which makes the definitions more complicated. It is also found out that different lights such as fluorescent lamps and incandescent bulbs cause different flicker results for the same voltage. Lately, other measures have been taken into account for the observable and objectionable voltage flicker. A sample graph can be seen in Fig. 2.67 according to [22].

The measurement of flicker is achieved through statistical methods. RMS values acquired from AC voltage are sorted and statistical distribution is evaluated. According to [23], P_{st} is a value measured over 1-5-10-15 minutes that characterizes the likelihood that the voltage fluctuations would result in perceptible light flicker. A value of 1.0 is designed to represent the level that 50% of people would perceive flicker in a 60 watt incandescent bulb. It can be evaluated in 1 or 5 or 10 or 15 min intervals. P_{lt} is derived from 2 hours of P_{st} values (12 values combined in cubic relationship, cubic mean square). Average of at least 1008 P_{st} values (7 days of 10min-Pst) is necessary to conclude the flicker condition of the power system.
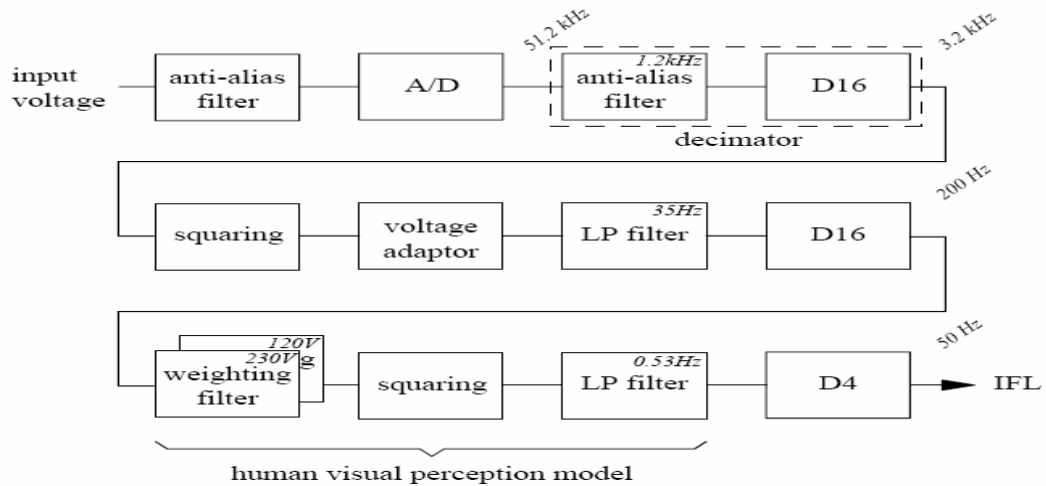
Fig.2.66. The digital flicker-meter implementation [21]

83
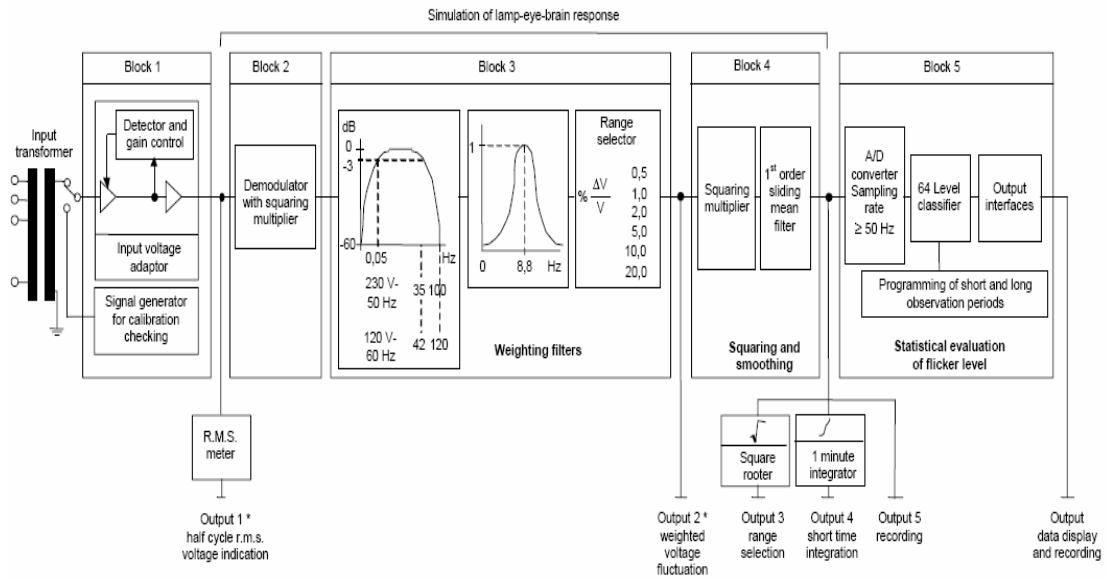
Fig.2.67. Complete implementation of flicker measurement [21]

2.10.2   Common Practice in Flicker Compensation

According to Miller [1], the ways of reducing the flicker especially in a busbar with arc furnace must be chosen from the following solutions:

- Reducing the furnace load,

- Stiffening the supply (increasing the short circuit MVA)

- Installing compensation equipment.

Different kinds of compensation techniques have different flicker results. Some systems may have drawbacks in terms of economics, technical and reliability aspects.

There are two factors affecting the compensator performance in terms of flicker reduction:

- Compensation Ratio

- Speed of Response

Compensation ratio C defined in (2.49) is the controllable part ratio to the total reactive power fluctuation in the load, i.e. arc furnace.

84

$$C = \frac{Q_{\gamma c}}{\Delta Q_l} \qquad\qquad (2.49)$$

The ratio C is greater than 1 in the installations where the compensator is required to correct the unbalance. Choosing C>1 also improve the voltage stability at the PCC while improving the compensation for the voltage drop on the main supply transformer.

In Fig.2.68, flicker intensity in a busbar where many steel manufacturers are connected is recorded by using data acquisition. When the other companies cease activity, only the plant under observation operates with and without its SVC. Note that P_{st} reduces dramatically when SVC is turned off (including HFs). This SVC had been installed by a multinational company, with a C-type 2nd harmonic filter and tuned 3rd and 4th shunt harmonic filters. Further investigation on harmonic characteristics showed that harmonic subgroup 1 is amplified as well as the 2nd harmonic as seen in Fig. 2.69.
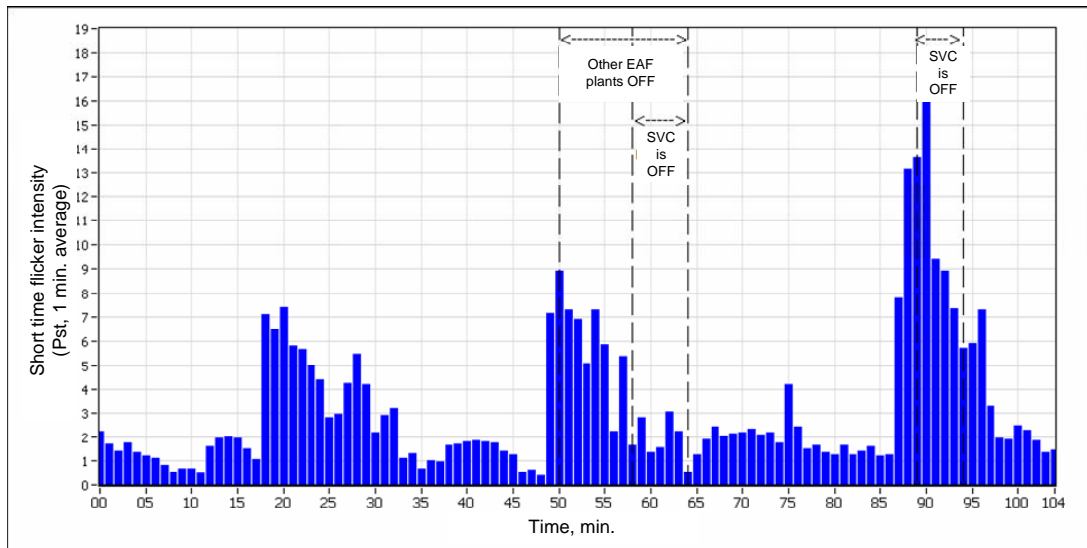
Fig.2.68. Amplification of flicker by SVC while compensating the EAF, recorded in the field.
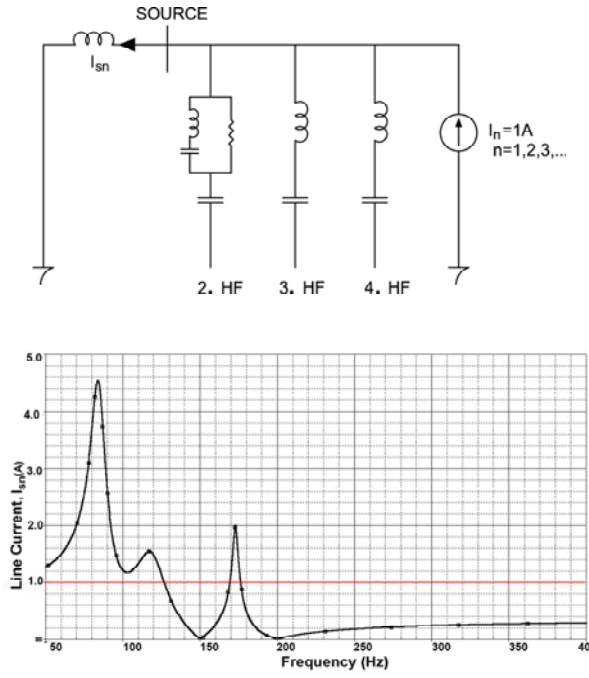
Fig.2.69. Simplified SVC circuit of the arc furnace installation used in the ORCAD simulations and harmonic characteristics of the SVC filters obtained by the ORCAD simulations; I_{sn} represents the harmonic current flow towards the supply; I_n is the harmonic current injected from the load

As discussed in [37], flicker and interharmonics are related. After the investigation of harmonic characteristics, it is possible to say that the unsuitable design in this plant makes the flicker more problematic. Therefore it is concluded that this specific SVC design is not suitable for flicker reduction. It also shows the importance of consideration of interharmonics for the HF design of industrial SVCs.

2.11 Discussions on Operating Principles of TCR

In this Chapter, 6-pulse and 12-pulse TCR operation is investigated for steady state, transient and unbalanced operations. It is worth noting that triplen harmonics and even harmonics that are not expected in steady state have impact on the TCR currents in the transient and unbalanced operation.

A complete set of equations are derived to explain the Steinmetz equations (2.48) for load balancing. In order to be able to balance and compensate an

unbalanced load, simulations have been carried out. It is seen that A higher harmonic filter installation than maximum reactive power demand of the arc furnace (nearly 1.577 times) is required. In addition, installed TCR capacity should be higher than the installed harmonic filter capacity (nearly 2.154 times reactive power demand of EAF).

The definition of harmonics in various harmonic standards such as [33], [34], [35],[39] and [42] is not clear. However, IEC Std. 61000-4-7 [42] divides harmonics into three classes: Single line, group and subgroup. It has been assumed for the rapidly changing loads that the penalty limits specified in many harmonic standards should be applied in the sense of harmonic subgroup as defined in [42]. However without load balancing, TCR and harmonic filter size can be selected equal to the load reactive power for complete compensation. Reactor size is also as important for the reduction of flicker as the response delay of the TCR control system.

Wye connected TCR is has high 3rd harmonic line current component in the steady state. Also other triplen harmonics increase the TDD of the line current both in the steady state and transient state. Therefore delta connected TCR topologies are selected for SVC implementations. However the wye-connected topology can be suitable for TSR applications because it is possible to control the power circuit by using 2 back-to-back connected thyristor stacks instead of 3 stacks [79].

12-pulse TCR implementation has clear TDD advantages when compared to conventional 6-pulse TCR systems. The maximum TDD is reduced 407 times by choosing a 12-pulse topology. However, the 12-pulse TCR requires special conditions to make up for the cost disadvantage.

TCR based SVC for Transmission and Distribution (Industry) may have different objectives. The transmission type SVCs are mainly focused on power system stability and voltage regulation, while industrial SVCs are mainly focused on reactive power compensation, load balancing, flicker reduction and harmonic filtering. In this thesis, TCR based industrial SVCs are investigated; therefore, the objectives of transmission SVCs will not be investigated. However, IEEE Guide for the Functional Specification of Transmission Static VAr Compensators [36] is still valid for most of the issues in industrial SVC design.

CHAPTER 3

DESIGN METHODOLOGY FOR AN SVC

3.1 Preliminary Design

Preliminary design is the most important part of the design process, because any specific error in the preliminary design and specifications in requirements documents may end up with great amount of money, labor and time loss. The following subjects have to be investigated thoroughly in order to finalize the preliminary design of an SVC:

3.1.1 Power Quality and Legislations

Power quality of the supply busbar is determined by field measurements. The standards concerning power quality and SVCs given in [25, 31, 35, 40, 42] should be investigated in order to define and consider any power quality issues. Currently valid legislations for reactive energy limits and other power quality issues may differ from one country to another.

3.1.2 Load Characteristics

The load characteristics of specific loads that need SVC type compensation in view of current harmonics are mentioned in Section 2.4.2. The active and reactive power variations are also given in that section. Whenever a TCR based SVC project is initiated, it is necessary to define the load characteristics clearly. The precise load characteristics are evaluated by using:

1- Field measurement by data acquisition
2- Monthly electrical energy bills

Variations in both active and reactive power are important as mentioned in Chapter 2. Flicker performance, shunt filter and reactor sizing depend on these

variations. If the load is varying slowly, the control system design does not have a great impact on the design. However, if load is varying rapidly, then both control and measurement systems have to be designed accordingly.

Duty cycle and load unbalance also plays a significant role in the design. The negative sequence compensation is a challenge in TCR design as mentioned in [1, 2]. The methodology of load identification is also advised in the standards [31] for Transmission SVCs.

3.1.3 Project Requirements

The customers may require some flexible solutions because of the future plans for the enterprise that the SVC is installed. Capacity of the plant may change so that a modular/flexible SVC may be required instead of a fixed installation capacity.

Location may also change in the time, e.g. open cast mines, therefore the customer may demand a re-locatable solution instead of a permanent one.

3.1.4 Environmental and Operational Conditions

The following environmental conditions are needed to be considered for the robustness of the SVC installation:

1- Maximum and minimum values of ambient temperature
2- Humidity
3- Snow load
4- Pollution level
5- Probable risks of coal/iron powder and acid rain

Unmanned operation in hardly accessible regions may be required. In order to overcome such a difficulty, re-closing and remote monitoring options should be considered. Local and remote alarm tools are also necessary for the sake of continuous operation.

3.2 General Design Methodology

A basic flowchart for design, installation and commissioning of an SVC is given in Fig.3.1.
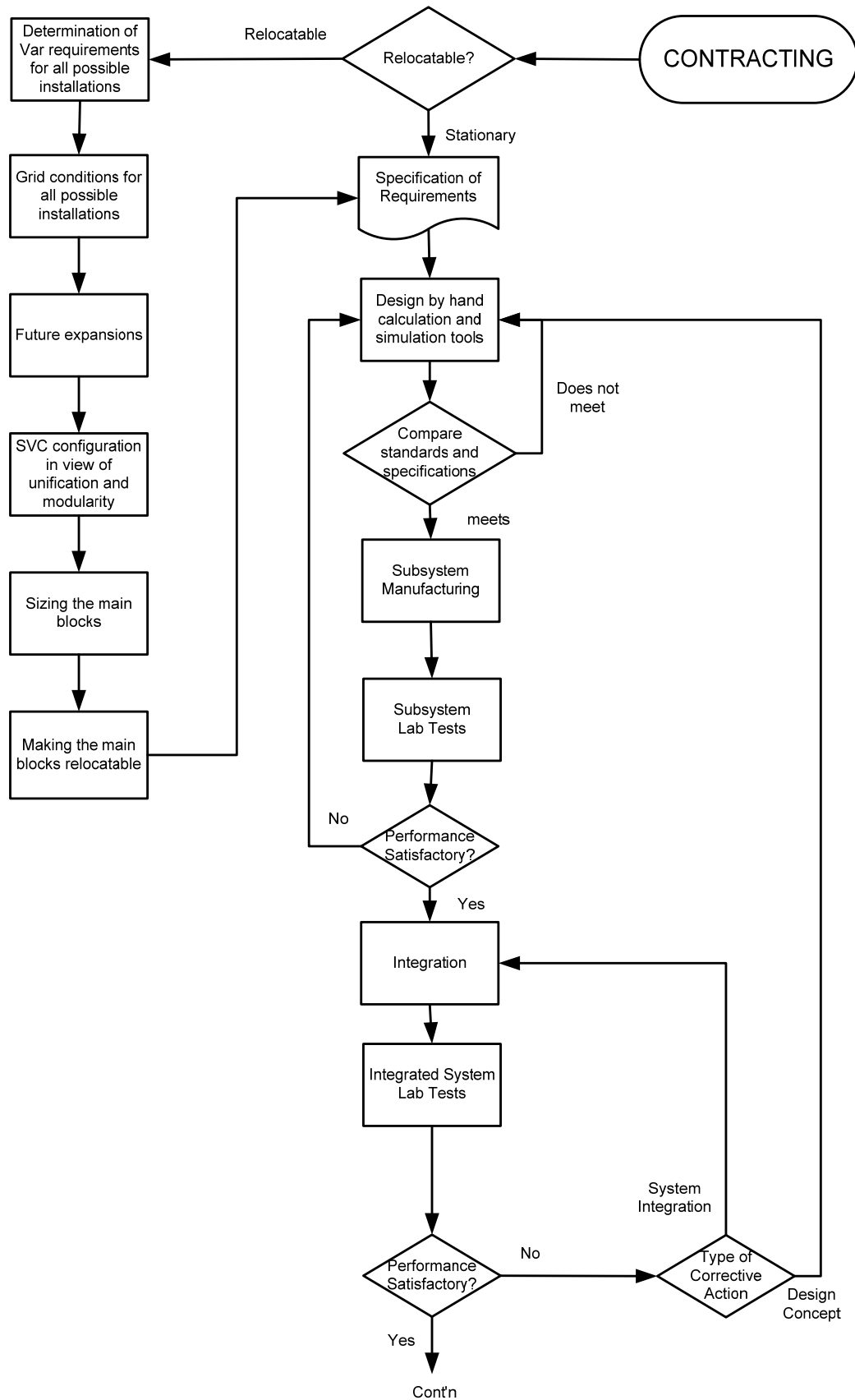
Fig.3.1. General design methodology flowchart

90
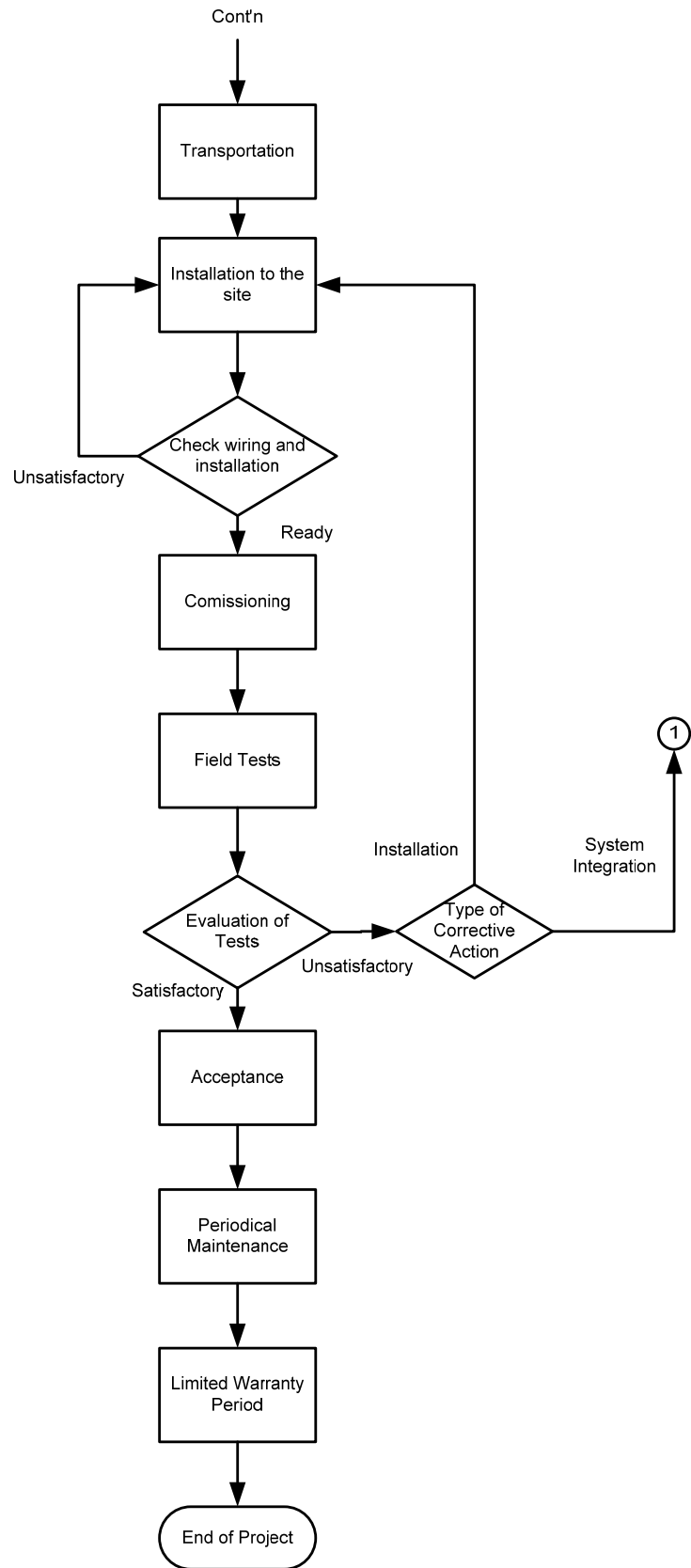
Fig.3.1. . **(Cont'n)** General design methodology flowchart

91

3.3 Design of the Power Stage

3.3.1 Single Thyristor Operation

The Thyristor is the "static switch" part of a TCR based SVC. The current flowing through the reactors is adjusted by thyristor valves. They are connected back-to-back and may share the same snubber. Selection of the thyristors and snubbers depends on many parameters. In order to verify the selection, a computer simulation is appropriate. In Fig.3.2, a typical thyristor valve can be seen. A thyristor needs to be triggered into conduction, therefore the electronic triggering circuit design is also important as well as the thyristor selection. Some failures may occur if triggering circuit is not designed carefully.

A detailed thyristor selection analysis can be found in [38]. In order to be able to select the thyristors, the following information in thyristor data sheets, such as the one in[43], should be investigated:
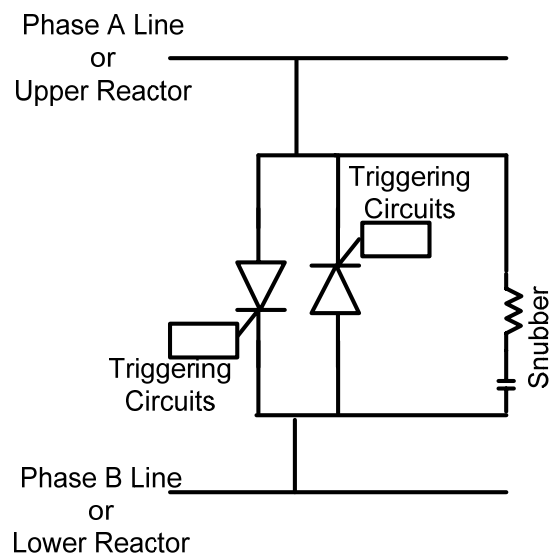
Fig.3.2. A typical back to back connected thyristor valve

3.3.1.1 Mean on state current

I_{TAV} is defined as the maximum value of continuous on-state current for the current waveforms, temperatures and cooling conditions stated, with no margins for overload [43]. I_{TAV} is dependent on the frequency and the cooling thermal impedance; therefore, curves are usually available in datasheets for the selection. In [36] Annex C, the average thyristor current in a TCR based SVC is defined as:

$$I_{TAV} = I_{TCR} \times \frac{\sqrt{2}}{\pi} \times \left[\sin(\pi - \alpha) - (\pi - \alpha)\cos(\pi - \alpha) \right] \qquad (3.1)$$

Where, I_{TCR} is the fundamental rms-current for a fully conducting thyristor valve and α is the firing angle ($\pi/2 - \pi$ rad).

It is advised in [43] that I_{TAV} should be derated to 80% because of the local heatings and unusual changes in weather conditions.

3.3.1.2 RMS current

Given the type of cooling current conduction angle, waveform (including any power frequency harmonics) and cooling conditions, I_{TRMS} is the absolute maximum value of the true-rms current flowing through a single thyristor. In [36] Annex C, the rms thyristor current in a TCR based SVC is defined as:

$$I_{TRMS} = I_{TCR} \times \sqrt{\frac{(\pi - \alpha) \times \left[1 + 2\cos^2(\pi - \alpha)\right] - 1.5\sin\left[2(\pi - \alpha)\right]}{\pi}} \qquad (3.2)$$

3.3.1.3 Non-repetitive On State Current

I_{TSM} is 10ms duration single half wave maximum peak value of the thyristor current. It is also guaranteed by the thyristor producers that the thyristor will withstand the maximum peak reverse voltages stated in the datasheets.

3.3.1.4 Off State and Reverse Blocking Voltage

V_{DRM} is the repetitive peak off state voltage and V_{RRM} is the repetitive peak reverse voltage. V_{DRM} and V_{RRM} can be different from each other according to the thyristor selected.

93

3.3.1.5 di/dt

During the triggering of the thyristor, the region of the gate connection carries the thyristor current and then spreads over the whole wafer area. In order to avoid excessive dissipations during this operation, the amplitude of this current should be limited. di/dt is defined for the switching instants, and once the conduction starts, it is not limited to a specific value. Operating frequency, peak value of permissible on state current for half sine wave, gate triggering current and the rate of rise of gate current are given in datasheets for the definition of di/dt

3.3.1.6 dv/dt

If the dv/dt value defined by the producers is exceeded, the thyristor self triggers which lead to a break down in the wafer. Therefore, dv/dt should be limited to a safe value by using passive devices such as snubbers.

3.3.1.7 Cooling Method

Cooling method is selected according to the level of power dissipation and available resources. The major cooling types are:

1- Natural air cooling

2- Forced air cooling

3- Liquid based cooling (de-ionized water or other coolant)

Heatsink selection depends on the cooling method. The heatsinks carry the thyristor current; therefore they are selected from good electrical and heat conducting materials, usually aluminum or copper.

3.3.1.8 Thermal Considerations

Theoretically, a TCR produces reactive power only. However in the practical implementation, there are many sources of dissipation. In addition to the copper losses of reactor banks, thyristor stack is also source of dissipation, not only because of the voltage drop on the thyristors, but also because of the passive elements connected to the stack. The main sources of dissipation can be classified as:

1- Thyristor losses (conduction, switching and off state losses)

2- Snubber losses

3- Equalizing resistor losses

4- Valve reactor losses (if present)

5- Protection circuit losses

6- Gate triggering circuit losses

7- Bus bar or cable losses

The method of calculating the thyristor valve losses are defined in [36] Annex C. In this standard, however protection circuit, gate triggering circuit and bus bar losses are omitted in the calculation of thyristor valve losses because in high power applications these issues are negligible. Therefore, thyristor valve total power loss, P_{valve} , is given in [36] as:

$$P_{valve}= P_{cvalve} + P_{Tsw} + P_{vd} + P_{sn} + P_{hyst} \qquad (3.3)$$

P_{cvalve} is thyristor valve conduction losses, P_{Tsw} is thyristor total switching losses, P_{vd} is equalizing losses, P_{sn} is snubber circuit losses, and P_{hyst} is reactor (hysteresis) losses.

Prolonged thermal stress on the thyristors is not desired. The effects of such thermal stress can lead to thermal fatigue, or an earlier failure of the thyristor, which is discussed in [46].

3.3.1.9 Snubber Circuit

The series inductance of the circuit, combined with the rate of rise of the current, produces transient voltage peaks across the thyristor terminals. If voltage exceeds the thyristor ratings, it may lead to the destruction of the device permanently. Therefore, in order to dampen the voltage overshooting a parallel R-C snubber circuit is connected as a general practice [1].

The snubber values are usually selected to keep the circuit response critically damped. Increasing the damping level leads to more dissipation. A detailed snubber design can be found in [38].

3.3.1.10   Triggering Circuit

Triggering circuits usually have dual tasks, primarily isolation and secondarily supplying the gate current necessary to switch on the thyristor.

The isolation can be achieved by magnetically or optically. Pulse transformers suitable for transmitting high current and high frequency pulses are may be used for magnetic isolation.

In medium voltage applications pulses are usually transmitted to the gate by a ferrite core placed around a single wire carrying the low voltage side current. There is isolation material around the primary conductor.

Optical isolation is achieved through optical fibres (F/O). However triggering circuit with F/O requires a gate energy circuit in order to be able to supply the current pulse necessary for the gate. [1] suggests a gate energy circuit that transforms both Anode-Cathode voltage and thyristor current into low voltage DC that does not exceed the thyristor gate ratings.

Typical gate characteristics of a thyristor, Dynex DCR 1596SW thyristor is given in Fig. 3.3. The gate design concepts are discussed in [47]. The thyristor rating given in datasheets defines only the safe operation limits. It is often up to the designer to optimize the triggering circuit.
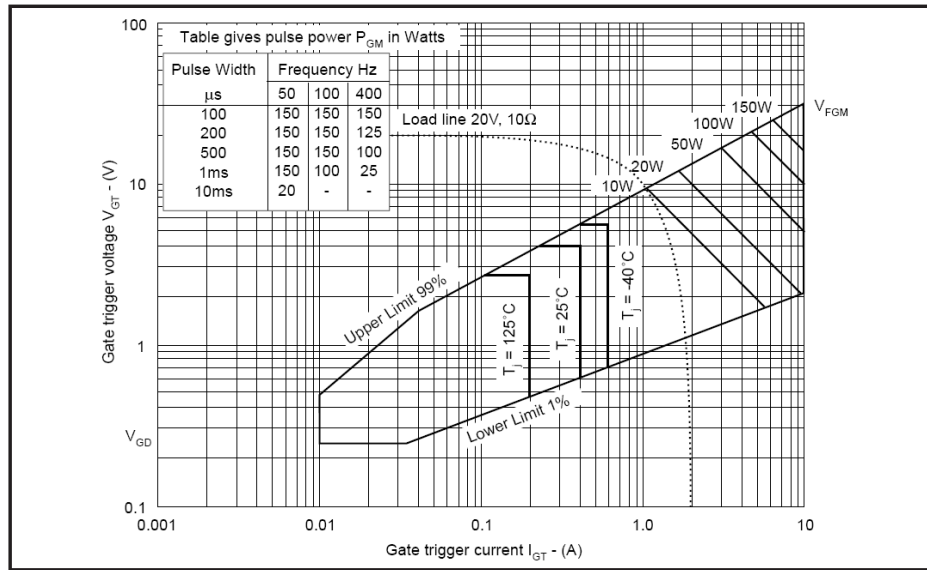
Fig.3.3. Gate (I_{GT}-V_{GT}) characteristics of a thyristor, Dynex DCR 1596SW thyristor[47]

3.3.1.11   Overvoltage protection

Overvoltage in an SVC system usually occurs in a temporary fault condition such as a lightning surge. Temporary overvoltage cases needs fast interaction and protection, therefore they are handled by the overvoltage protection circuits which are usually placed in or near the thyristor triggering circuits.

In a series thyristor operation, equalizing resistor circuits or some of the series thyristors may breakdown. This may impose overvoltages on the remaining of the valve circuit. Overvoltage protection triggers rest of the thyristors to conduction thus protecting them against the overvoltage.

Breakover diodes (BOD), avalanche type diodes or metal oxide varistors (MOV) are used in overvoltage protection circuits. Such implementations can be found in [44] with a BOD, and in [38] with a MOV.

Continuous operating voltages may sometimes rise above the standard levels defined in [45]. If such an overvoltage occurs, the control system must react to this type of fault.

3.3.2 Design Example, TKİ Unified and Relocatable TCR Based SVC Thyristor Stack

The TCR based SVC systems designed within the scope of this thesis are described in Chapter 4. The natural-air-cooled thyristor stack designed for unified and relocatable SVC systems for TKI is shown in Fig. 3.4. The thyristors are mounted in a cabinet with the help of insulators on the back side of the heatsinks. The snubbers are mounted on the right side of the heatsinks and triggering circuits with over-voltage protection are on the front side. The voltage across thyristor terminals are monitored by the use of Hall Effect type voltage sensors placed over the thyristor stack. Hall effect sensors prevent the thyristors from misfiring. They are also useful for monitoring the thyristors during operation which helps finding a failure in the power or control circuits.

Fig.3.4. A single back to back three phase thyristor stack configuration

3.3.3 Series Thyristor Operation

In addition to the specifications discussed in the previous section, series thyristor operation requires additional design work. Connecting semiconductor devices in series or in parallel requires special attention on voltage and current sharing. A failure in balancing the current or voltage may lead to the failure of the whole stack.

(a)   (b)
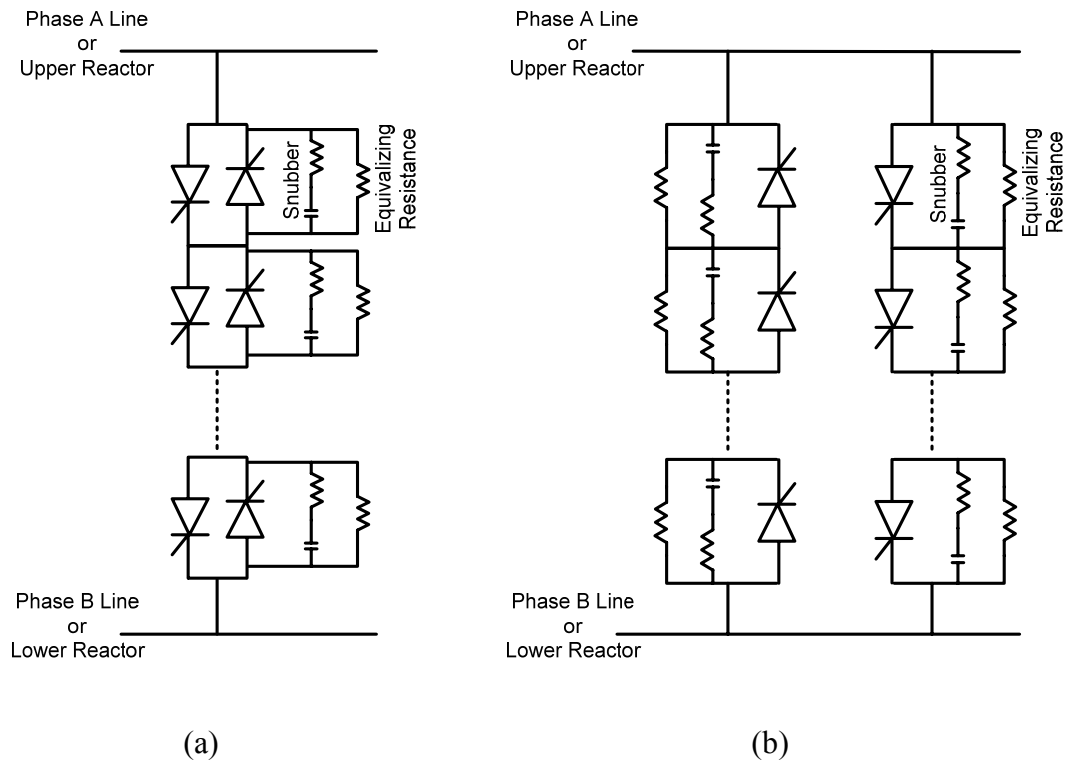
Fig.3.5. A thyristor stack which consists of series connected thyristors. (a): with anti-parallel connected switches (b): with positive and negative thyristors grouped

Design and implementation of series operation of thyristors are discussed in [38]. The same design is also used in the utilization of the ISDEMIR ladle furnace compensation system. In Fig.3.5. the series-connected thyristors are seen. Cooling water flows through the heatsinks, not only cooling the thyristors but also cooling the snubber circuits. The operation voltage of 6.3kV requires special attention to the

99

insulation. The distance between the high voltage switches and other equipment is selected by considering the safe values, and pulse transformers are placed at the back of the insulating separator thus avoiding flashovers to the control circuit.

Fig.3.6. A series operation of back to back three phase thyristor stack configuration

3.3.4 Single Piece / Two Pieces Reactor Arrangement

In order to protect the Thyristor valves against a short circuit, the reactors can be divided into two series reactors having the same total phase reactance. Connecting the Thyristor valves in between these series reactors will limit the maximum fault currents. If one reactor is short circuited, the fault current will be limited. If phase is short circuited, no fault current will flow through thyristors. In order to observe a total short circuit current, each reactor placed on top of one another should be

separately short circuited, which has a very low probability in a TCR installation because of the geometry.

(a)   (b)
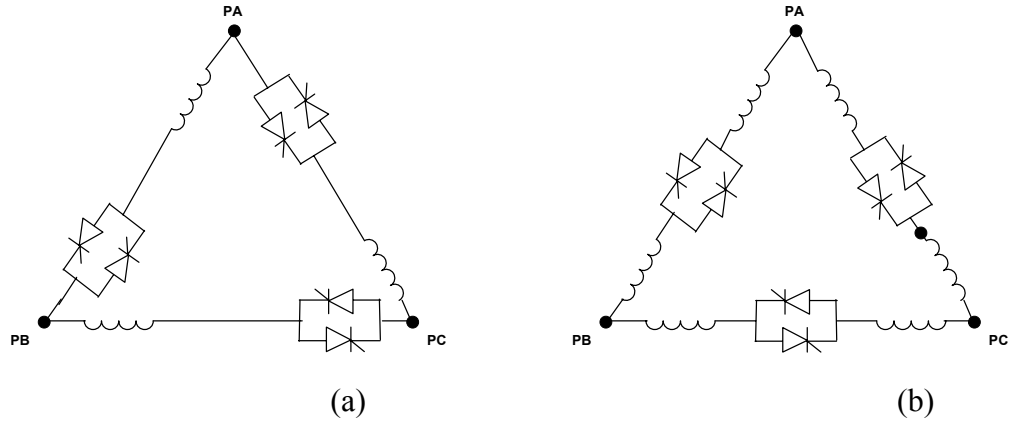
Fig.3.7.   Reactor arrangement; (a) Single piece, (b) two pieces

Several fault cases that can appear in a delta connected TCR are given in Fig. 3.9., 3.10 and 3.11 These cases are simulated for a 1 kV 1,5 MVAr TCR + 0,75 kVAr Filtre installation with a short circuit 525 MVA . Filters consist of three 5th harmonic and three 7th harmonic tuned filters at 1 kV side. A feature of PSCAD called "Multirun" is used for multiple simulations. The results are given in Table 3.1. The worst case is found to be a short circuit across the upper or lower piece of the reactor.
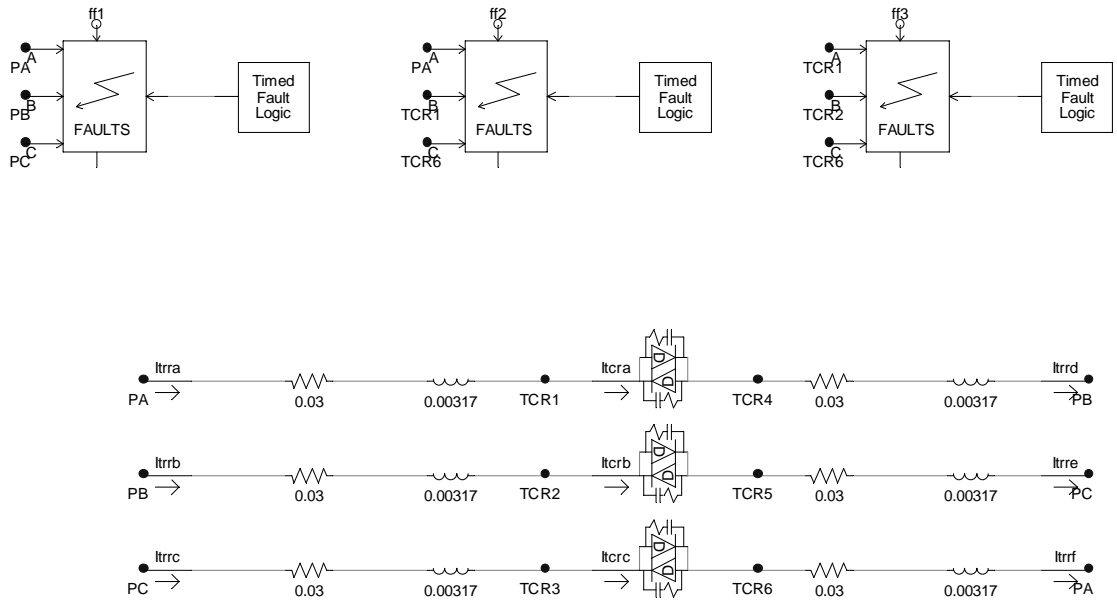
Fig.3.8. PSCAD Multirun (Multiple Simulation) for different fault types
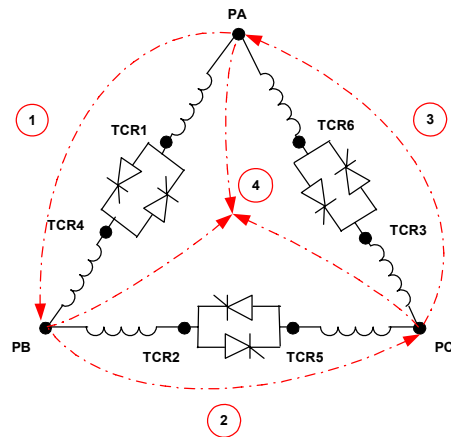
Fig.3.9. Fault cases simulated in PSCAD concerning three phase connections
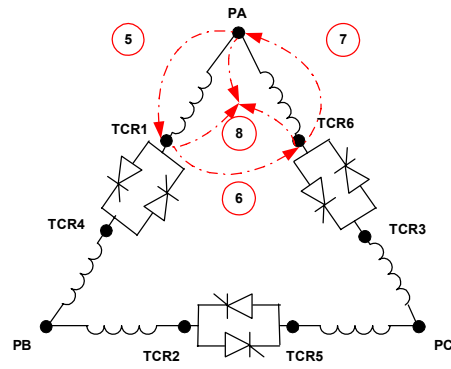
Fig.3.10. Fault cases simulated in PSCAD concerning one phase and two thyristor terminal connections belonging different phases
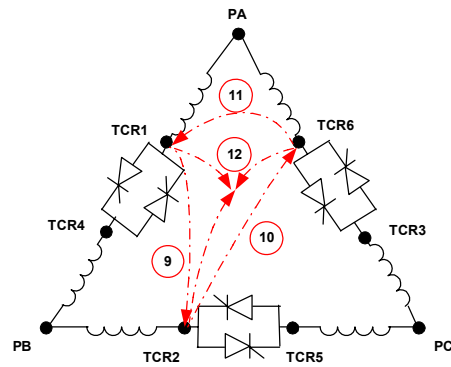
Fig.3.11. Fault cases simulated in PSCAD concerning three thyristor terminals belonging different phases

Table.3.1. PSCAD Multirun simulation results

Case	Maximum 5th Harmonic Filter Current (kA)	Maximum 5th Harmonic Filter Capacitor Voltage (kV)	Maximum 7th Harmonic Filter Current (kA)	Maximum 7th Harmonic Filter Capacitor Voltage (kV)	Maximum TCR Line current (kA)	Maximum TCR Thyristor current (kA)
1	0,4760	0,9582	0,4296	1,0245	26,7383	0,7590
2	0,1383	0,5457	0,0927	0,5009	33,7312	0,9013
3	0,1276	0,8337	0,0832	0,8152	27,5715	0,7833
4	0,2920	0,4659	0,2629	0,4559	39,4042	0,6918
5	0,1333	0,8257	0,0877	0,8005	1,4378	1,6126
6	0,1260	0,8171	0,0826	0,7959	1,7268	1,8834
7	0,1277	0,8336	0,0832	0,8151	1,0207	1,0602
8	0,1300	0,8090	0,0855	0,7799	2,5117	1,8673
9	0,1266	0,8253	0,0828	0,8054	1,1658	1,1886
10	0,1277	0,8336	0,0832	0,8151	1,0207	1,0602
11	0,1303	0,8294	0,0853	0,8070	1,0265	0,7659
12	0,1281	0,8252	0,0836	0,8029	1,2619	1,0690

3.4 Reactor Design

Reactor design for the SVC TCR and shunt filters require special attention to current harmonics and voltage harmonics levels because dissipations in the reactors may be higher than the standard shunt reactors. The Standard IEC 289 [55] gives the definitions and suggestions for shunt reactors. IEEE standards [50-54] give detailed information on reactors and their requirements. IEEE Std C57-120-1991 [54] contains the loss calculations while [52] proposes the test procedures for reactors.

Thyristor Controlled Reactor sizing is investigated in Chapter 2. Given the rated voltage and current, the reactor value in Henrys will be determined. However, the design of such a reactor is a detailed procedure. Turns ratio, insulation, width, height, conductor specifications, supporting material, etc… are all know-how of the manufacturers. The following should be conducted by the customer to the manufacturer when a reactor is to be designed:

- Standard (generally IEC 60289)

- air-cored / iron cored

- Frequency (50 Hz, between 49.8 and 50.2 Hz in Turkey [33])

- Rated voltage (line-line or phase, rms, default IEC 38)

- Max.continuous operating voltage (kV)

- Rated inductance per phase (mH)

- Rated continuous current (kA)

- Max. continuous current (kA)

- TDD

- Short circuit power before reactor (short cct. MVA or current in kA)

- Outdoor/indoor installation

- Insulation class

- Cooling type (Natural air, forced air, oil impregnated…)

- Max. ambient temperature(^{o}C)

- Tuning frequency (If connected in a shunt filter, Hz)

- Quantity and construction details (including terminal connections and mounting style such as top-to-top or independent)

The reactor ratings should be verified by a power system simulation tool. In the simulation, worst case scenarios such as misfiring (where conduction per thyristor is longer than 180°) and short circuits can be investigated.

The manufacturers determine the minimum safe distance to other magnetic material and closed loop conductors. These magnetic clearances around the reactor depend on the individual reactor design and. should be taken into account in the layout of the overall system.

3.5 Harmonic Filter Design

After the determination of the MVAr installed capacity of shunt HFs as described in Chapter 2, the filtering needs should be decided for specific harmonics that exists both in the load and in the TCR. The SVC topology is important in the decision for filtering. Various topologies and connection types are described in Section 2.1. According to the purpose of installation, harmonic filter type may also

differ as described in Section 2.7.1. Therefore, the complete SVC topology should be selected before starting the frequency response analysis.

3.5.1 Frequency Response of the Filters

As stated in Chapter 2, Thyristor controlled reactor (TCR) acts as a harmonic current source and produces its own odd harmonic current components (3rd, 5th, 7th, 9th, 11th, etc.) for symmetrical triggering in the steady-state. However, during control, firing angle will change from positive half-cycle to negative half-cycle resulting in production of even harmonics (2nd, 4th, etc.). These even harmonics are taken as temporary overloads on filter reactors and capacitors. In a delta connected TCR, triplen harmonics do not appear in the line currents for symmetrical triggering in the steady state. They will circulate through the delta connected reactor bank. However, in transient state owing to control, unbalanced portion of triplen harmonics will be reflected to the line side. These temporary overloads on filter elements are taken into account by safety margins in the design.

An important phenomenon of TCR operation during firing angle control from positive half-cycle to negative half-cycle is the generation of direct current component. This may move the magnetic operating point on the B-H characteristics of SVC transformer and thyristor controlled reactors for the iron core case. Therefore, the linearity of TCR core is essential for iron-core solution.

Simulations should be carried out according to this assumption in order to find out harmonic loadings on filter elements. Filter circuits can be designed according to the rules described in IEC 61642 [57]. The loads are taken as harmonic current sources in simulation, which inject 1.0 A rms at all harmonic frequencies. The associated frequency characteristics are given in Figure 3.12.
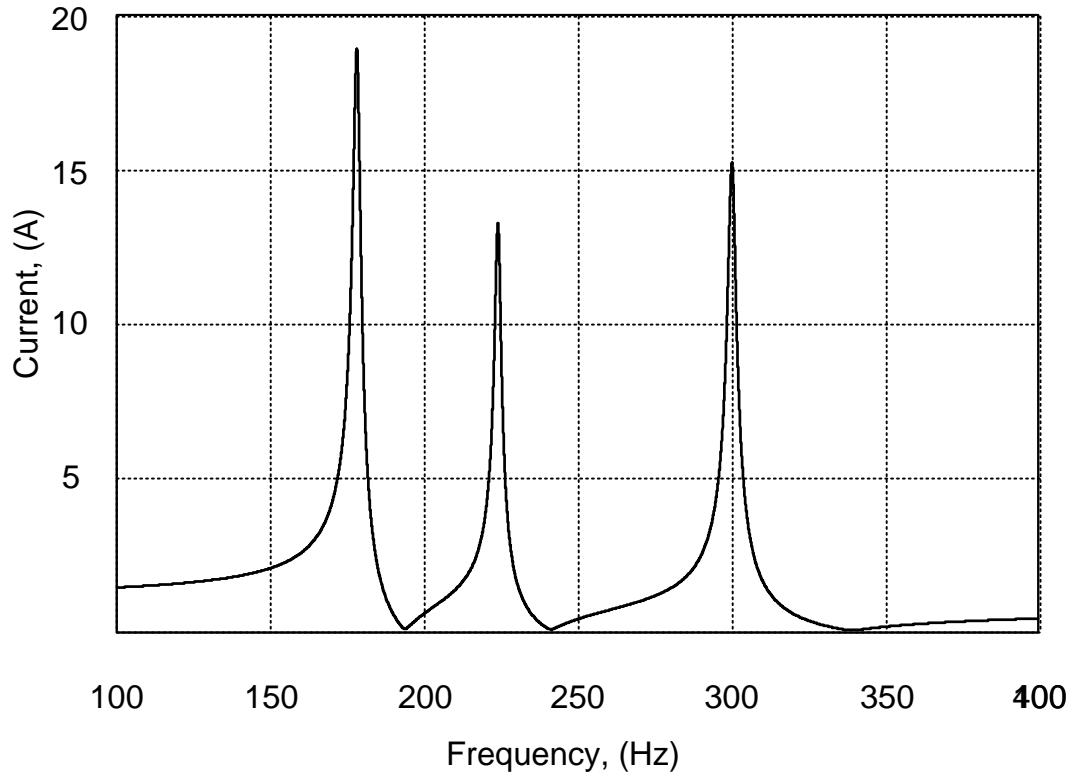
Fig.3.12. The frequency response of a sample circuit designed for TKİ YLİ with 4th, 5th and 7th harmonic filters. The response is seen from the supply side, the injected load current is 1A.

As seen from Figure 3.12., almost all dominant TCR harmonics (5th and 7th) will close their paths through SVC filter circuits. This is because SVC transformer reactance presents a high impedance path to these harmonics. Some of the even harmonics and unbalanced portion of the triplen harmonics produced by TCR may be subject to magnification but this occurs temporarily only in the transient state during control. No harmful effects on filter elements due to these temporarily occurring overloads are expected. A careful monitoring may be needed.

Current through filter reactors ($\sqrt{I_1^2 + I_5^2 + I_7^2 + ...}$) and voltage across the capacitor (algebraic sum of rms harmonic voltage components in the worst case) can be computed from SPICE simulation results for the worst case. These steady-state values are also compared with the results of power system simulation (i.e.EMTDC/PSCAD) of the overall 3-phase system.

107

3.5.2 Specification of Capacitor Bank

The following parameters should be conducted to the producer for the filter capacitor bank(s):

- Quantity of capacitor units
- Standard (default is IEC 60871 above 1kV, however IEC 60831 and IEC 60931 are applicable below 1kV for self healing and non-self healing types respectively)
- Rated Power
- Rated Voltage (kV)
- Withstand Voltage (1min 50Hz, kV)
- Bushing BIL level (peak, kV)
- Rated Capacitance (μF)
- No. Of phases (Single Phase units, three phase units, including capacitor bank construction details)
- Rated frequency (50 Hz, between 49.8 and 50.2 Hz in Turkey [33])
- Capacitance value tolerance (%, according to)
- Fusing (No fusing/Internally fused/Externally fused)
- Discharge resistance (internal/external/none)
- Ambient temperature
- Number of bushings

3.6 Protection and Switchgear Systems

The operation of an SVC may sometimes be interrupted because of temporary and permanent faults. These faults may usually be detected before it can cause damage. In order to take action in the case of such faults, a protection system is designed as it is described in this section.

Protection Systems of TCR based SVCs are described in [1] and start stop sequences are also described. The SVC Standard published by IEEE [31] gives detailed description of monitoring and protection. According to [31], there are two levels of alarms; first level alarms lead to a warning and second level alarms lead to a shutdown. Protection system needs a complete design including the relay sequencing

and timing. For the protection of the main components, sensors should be connected to protective relays or the control systems directly. Table 3.2. Shows the possible required protections, which are also suggested by [31].

Table.3.2. SVC Protection Types for Most Common SVC Sub-systems

	Main Transformer	Main Reactors	Filter Banks	Main Bus	Thyristor Valves
Overcurrent	X	X	X	X	X
Overvoltage				X	X
Differential protection	X				
Ground Fault	X		X	X	
Overtemperature	X				X
Sudden pressure/ gas accumulation	X				
Unbalance / Neutral unbalance			X		

Internal fault detection in the control system is also needed to prevent the wrong operation of SVC. The loss of control may lead to misfiring described in Section 2.13. Therefore control power, power supplies and critical synchronization signals should be monitored for failure. A sample protection system designed for TKİ SVC systems is given in Fig.3.13

Supply Side

O/H Line (34.5 kV or 15 kV)

Load Side

MOV

CT

34.5 kV Bus

PT

CONTROL and PROTECTION SYSTEM

SF6 Circuit Breaker
36 kV 630 A 16 kA

CT

Compensator Transformer
34.5 or 15 kV/1.0 kV, 1.5 MVA,
5.0%Uk, DYn-5

1kV Compensator Bus

PT

Auxilliary Transformer
1.0/0.4 kV, 7.5 kVA
DZn-11

MV Air Ballast CB
1 kV,1600 A,20 kA

TCR Bus

Filter Bus

3.17 mH/ph- Δ
I₁=563 A
Irms=610 A/50 Hz

H.E.D.

3.17 mH/ph- Δ

Ls=0.903 mH

L7=0.674 mH

Ls=0.903 mH

L7=0.674 mH

Cs=162 uF/ph- Δ

C7=108 uF/ph- Δ

Cs=162 uF/ph- Δ

C7=108 uF/ph- Δ

5th Harmonic Filter

7th Harmonic Filter

5th Harmonic Filter

7th Harmonic Filter

Filter Bank 1 (250 kVAr,1 kV/50 Hz)

Filter Bank n (250 kVAr,1 kV/50 Hz)

<Up to five Filter Banks>

Fig.3.13. SVC protection and Control system designed for TKİ SVC systems

The Switchgear systems should be able to clear faults, withstand the maximum defined voltages and currents in an SVC bus. If there is a coupling transformer, then the both sides of the transformer should be equipped with appropriate switchgear. Sample SVC switchgears which are used in TKİ SVC Systems can be seen in Fig.3.14 a and b.

It is important to investigate the low power factor operation of the switchgear because some switchgear has lower current ratings in the low power factor regions, which is the case in a SVC. Especially purely capacitive and purely inductive currents may cause re-striking which imposes high voltage surges because of arcing. In such cases, a damping or snubber circuit may be necessary [79].

<center>(a)   (b)</center>

Fig.3.14. (a)Low voltage SVC switchgear, (b) Medium (High) Voltage SVC switchgear

3.7 Coupling Transformer Design

The differences between a regular power transformer and a SVC coupling transformer are as given in Table 3.3. As well as the given standards, academic research on thermal capability of power transformers is also described in [60,61].

The nature of TCR operation requires the generation of the harmonic currents in both the steady state and the transient state. These harmonics flow through the transformer towards the supply if not properly filtered. It is uneconomical and unpractical to filter all the harmonics generated. Therefore, TCR currents cause both dissipation in the transformer and deviation from the 50 Hz B-H characteristics of the transformer core.

According to [2], power system harmonics result in additional heat generated by the losses caused by the harmonic content of the load current. Furthermore, there may also be a resonance between the transformer inductance and the system

<center>111</center>

capacitance. The temperature cycling and small core vibrations may also cause mechanical stress on winding and lamination insulation [2].

Table.3.3. Comparison of Regular and SVC Coupling Transformers
(Oil Immersed)

	Conventional Power or Distribution Transformers	SVC Coupling Transformer
TDD	Limits defined by [23,35,42]	High if filters are mostly at the primary side
Even Harmonics in the load (and SVC)	Limits defined by [23,35,42]	Higher than limits
DC Current	None	Depends on controller, may be excessive in misfiring conditions
Voltage Fluctuation	Limits defined in [22,23]	Depends on loadbus, mostly higher than regular
Transformer Design	IEC 76,ANSI C.57 [58,59]	IEC 76,ANSI C.57; with minor additions
Core Size and Physical Dimensions	Regular	Core and case dimensions are bigger for the same MVA
Overloads	Rare, depending on load busbar	Usual, depending on load busbar
Load Fluctuation	Low	High, especially in arc furnace applications
Saturation	IEC 76	Needs extra precautions
Hot spot probability	IEEE/ANSI C.57.91-1995 [59]	IEEE/ANSI C.57.91-1995 [59]

The losses in the transformer due to the harmonics can be generalized into copper losses, hysteresis and eddy current losses.

Copper losses are caused by the harmonic current flow through the transformer windings. I^2R losses will eventually increase because of the harmonics, which is by a factor more than the increase in the rms current. Eddy current loss contributes to the I^2R losses proportional to frequency-squared and stray load losses contribute by an amount proportional to the first power of frequency [1]. These losses may even cause unexpected hot spots in the transformer tank.

Triplen frequency zero sequence currents tend to circulate through the delta-connected windings and they should also be taken into consideration while designing in order not to overload the windings [2].

DC component existing in the load current saturates the core which results in an increase in the harmonic content of the excitation current of the transformer [2].

According to the investigations on the effects of harmonics to the transformer, there are suggestions based on the de-rating of the transformer by a factor. The ANSI/IEEE standard C57.110 [39] defines a K factor expressed as:

$$K = \sqrt{\frac{\sum_h (I_h^2 h^2)}{\sum_h I_h^2}} \qquad (3.4)$$

Then, using the above K factor, the maximum allowed current is calculated in (3.5). $P_{EC.R}$ is defined as the eddy losses divided by I^2R losses of the given transformer.

$$I_{max} = I_R \sqrt{\frac{1 + P_{EC.R}}{1 + K P_{EC.R}}} \qquad (3.5)$$

In the case studies discussed in the chapters 6 and 7, a specially designed, oil-insulated, out-door type power transformer is used as the compensation transformer to allow the connection of SVC to any medium-voltage level.

Δ-Y connected transformer with an isolated neutral point is chosen for the case studies where unified and re-locatable systems are developed [3]. In the

selection of connection type for the primary and secondary windings, the undesirable effects of unbalanced operation of the load on the performance of TCR as well as the penetration of harmonics produced by TCR to the supply side have been investigated. It is found out that Δ-Y connection gives much better results than Δ-Δ connection at the expense of more sophisticated electronic circuit implementation for the phase-wise measurement of reactive power. This is because the integer multiples of the third harmonic, i.e. the triplen zero sequence current harmonics, will not propagate through the transformer.

In order to prevent the coupling transformer from undesirable effects of direct current component and harmonics generated by TCR, the magnetic operating point can be placed to the linear portion of the B-H characteristics. B_{op} can be selected below 1.6Wb/m^2 instead of 1.8 Wb/m^2 used normally for distribution transformers. Typical B-H characteristics of an M3 type Steel Core can be seen in Fig. 3.15. For the balanced operation in the steady state, triplen current harmonics generated by TCR will close their paths through delta-connected TCR. However, for unbalanced operation, these will be partially reflected to the primary side of SVC transformer. Passive filters shunt-connected to the low-voltage side will satisfactorily filter out 5th and 7th current harmonics generated by TCR.
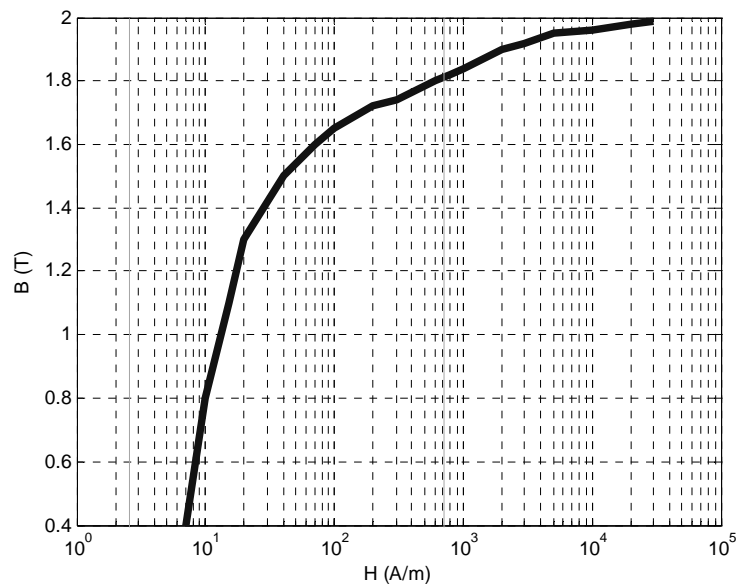
Fig.3.15. B-H Characteristics of an M3 type Steel Core

A further benefit of the isolated neutral point on the secondary side of the transformer is the safety for human life. In the case of a line-to-ground fault, the fault current will be essentially zero, which means that ground potential rise is also zero.

The dc biased transformer behavior is investigated in [62,78]. In [78] unmatched thyristor forward conduction voltage drops cause DC currents on the coupling transformer of a TSR. [62] is mainly focused on the geomagnetically induced currents and claims that current harmonics appear in the transformer due the DC bias.

3.8 TCR Control

Thyristor controlled reactor is a variable susceptance that can be controlled by triggering delay of the thyristor gate signals. The control system differs according to the desired method of TCR implementation. These methods are discussed in the following section.

3.8.1 Control System Overview

Control system that is only designed for reactive power compensation is a simple controller that calculates the necessary firing angle of each phase. It is also acceptable if all three phases are fired with the same angle. This type of control achieves reactive power compensation; however it is capable of neither load balancing nor voltage regulation. Control system design can easily be implemented by using proportional-integral (PI) controller in such an SVC. This type of control can be seen in Fig.3.16. In order to be able to achieve load balancing, the negative sequence of the load current must be eliminated completely.
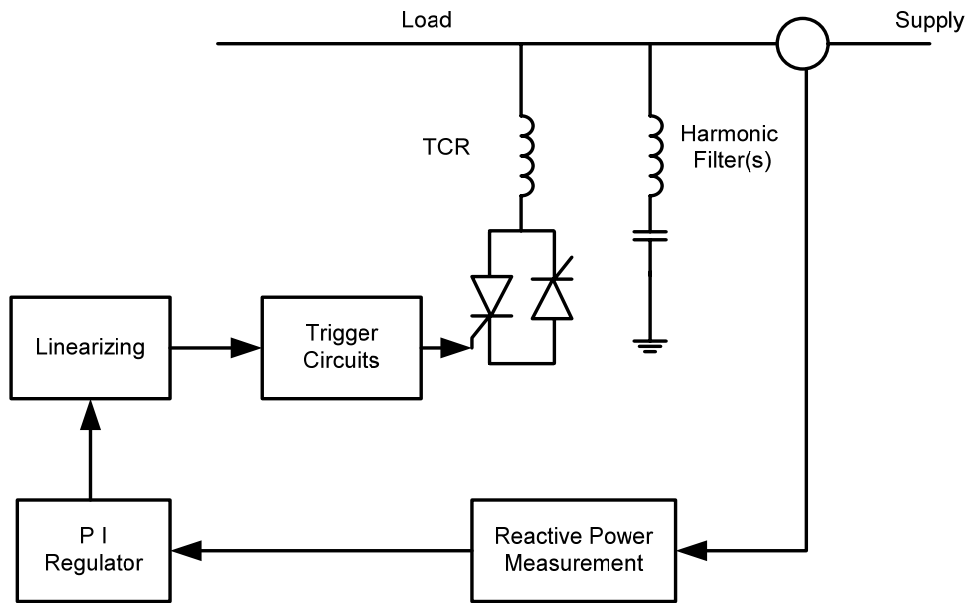
Fig.3.16. Simple reactive power compensation by PI controller
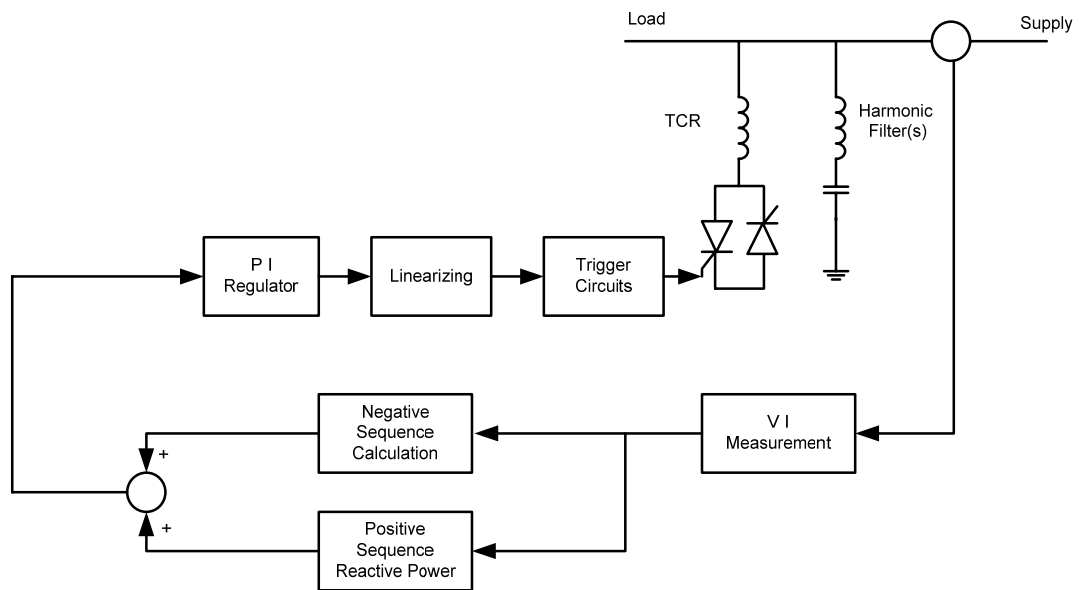
Fig.3.17. Reactive power compensation with load balancing by PI controller
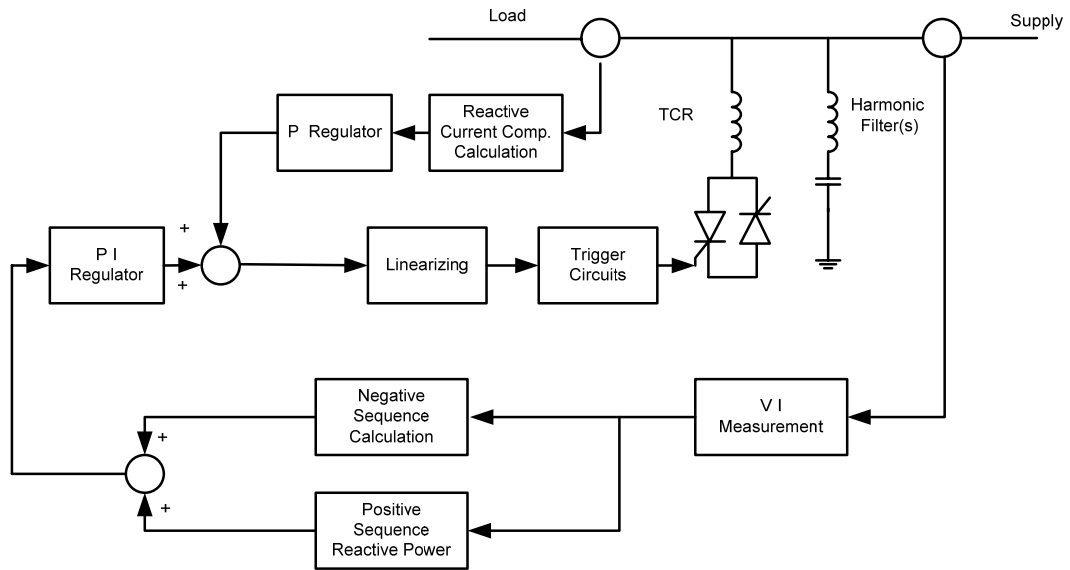
Fig.3.18. Flicker Compensation System with feed-forward and feed-back control

Reactive current component calculation and reactive power calculations can be evaluated by using 50 Hz averaging and 50 Hz d-q transformations. The two methods will cause different responses in the TCR because 50Hz averaging method will require time to take the average value of the signal. The d-q transformations are instant but they have two serious drawbacks:

1-   The d-q transformation requires a robust phase locked loop (PLL) circuit and may cause instability in a variant frequency bus where the frequency stays in the limits but varies very fast within the boundary.

2-   The transformations are valid for 50Hz, and oscillations will be observed in the d-q plane because of the harmonic components and negative sequence component. Therefore the current signal needs to be filtered for only 50Hz.

These drawbacks are verified in a PSCAD simulation and the results can be seen in Fig 3.20 (a-d).

117
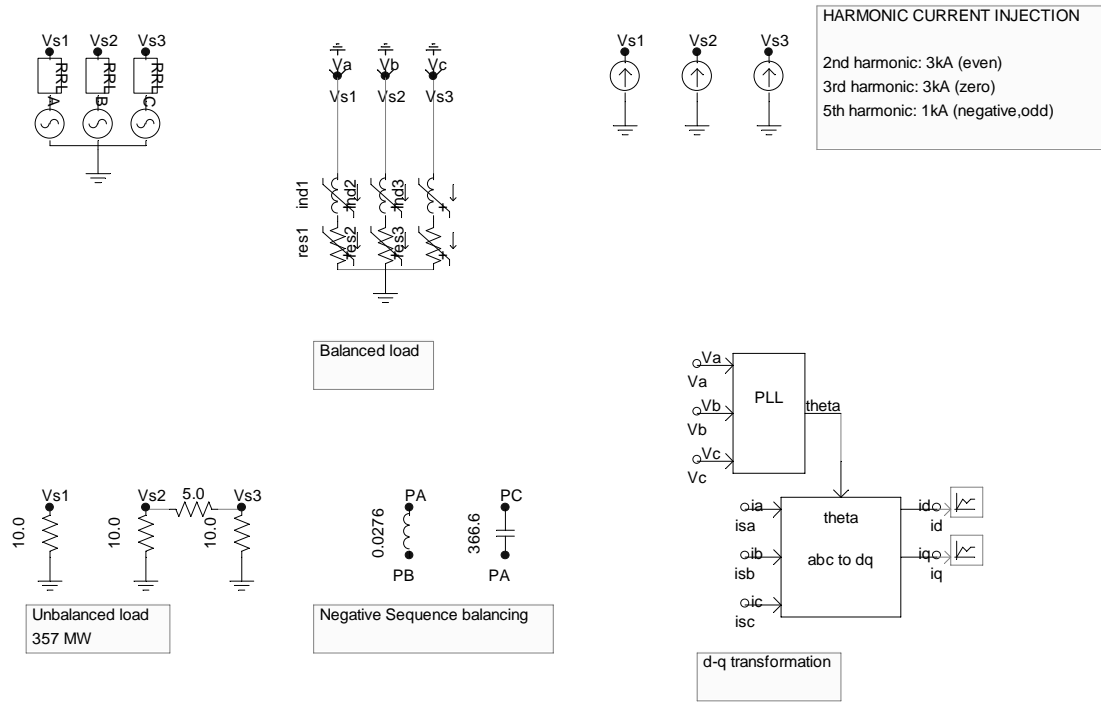
Fig.3.19. Simulation used in the verification of d-q transformation

The firing references of a TCR can be updated in each half cycle. Updating the references in every two (or more) half-cycles can be a choice for an attempt in the reduction of even harmonics of TCR. However, this will result in a delay in response time. Moreover it will not change the harmonic current level in some loads, especially medium to slowly varying loads. Instead of applying such a method, increasing the PI regulator time constant may be a better solution. PI regulator time constant evaluation needs to be done for each plant type because unexpected responses such as an oscillation or under-compensation may be observed. The control parameters also need to be verified by data acquisition in the field tests.
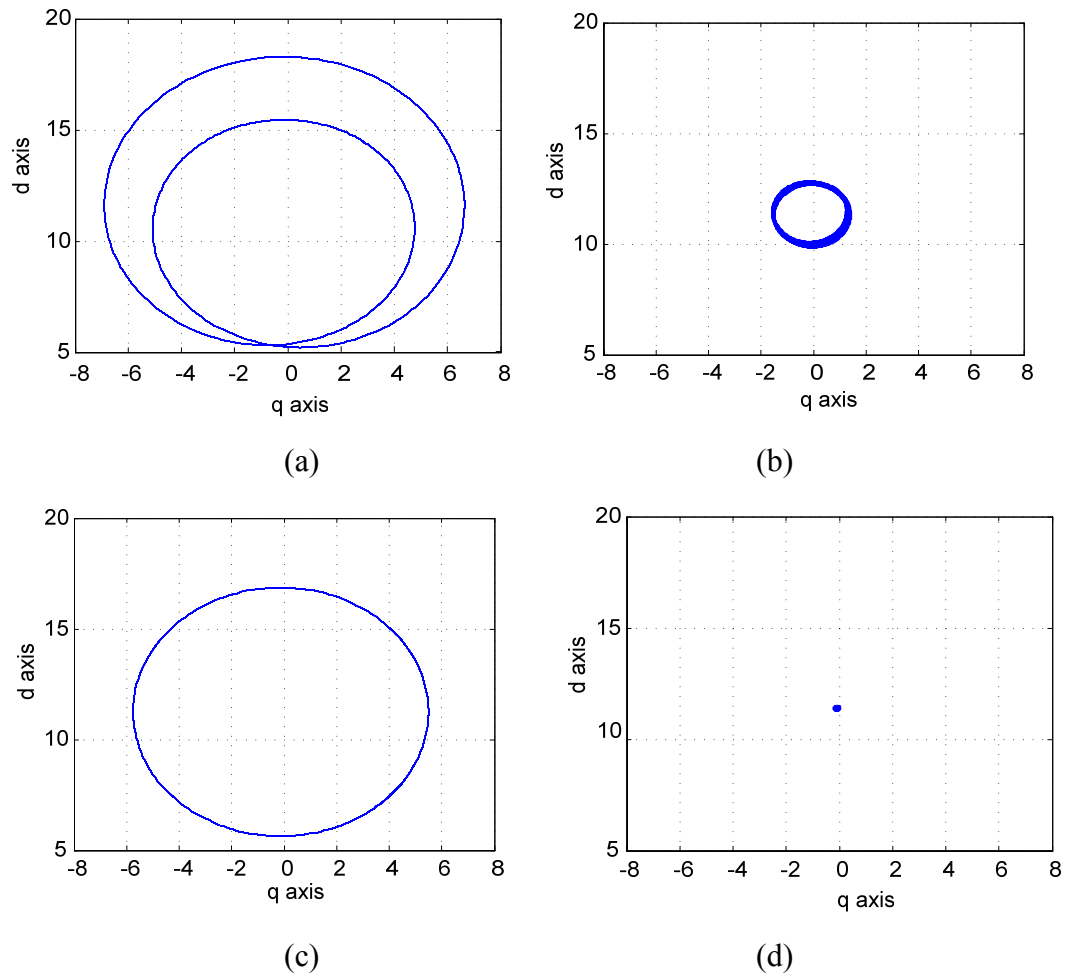
Fig.3.20. Results given in kA for: (a): Current trajectory after d-q transformation for source current with harmonics & negative sequence (b): Current trajectory after d-q transformation for source current with only odd harmonics (c): Current trajectory after d-q transformation for source current with only negative sequence (d): Current trajectory after d-q transformation for source current with no harmonics & no negative sequence (fully compensated)

The TCR control circuit measures reactive power in a half cycle which is 10mS in 50Hz system as seen in region 1 of Fig.3.21. The TCR firing circuits will respond to new delay settings in 0.1 - 10 mS as seen in region 2 of Fig.3.21. Finally feed forward and PI regulator of the TCR responds to the change of reference in 30-100mS according to the default control parameters which coincide with region 3 of Fig. 3.21. Therefore overall response can be in the range of 40 – 120 mS according to the controller settings.
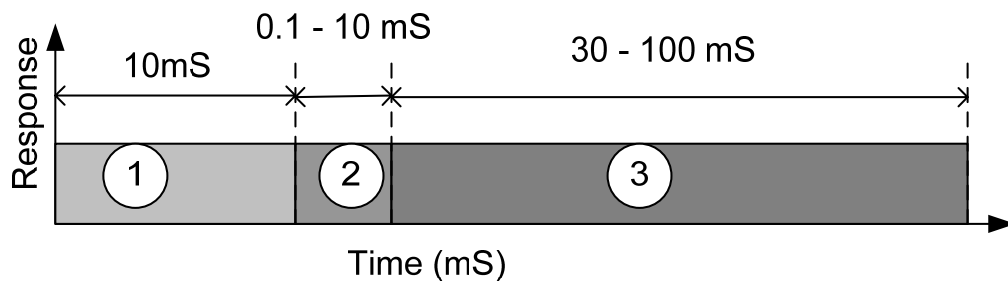
Fig.3.21. TCR control circuit response graphic

3.8.2 Control Strategies in 12 Pulse TCR or parallel connected SVC's

In a TCR based SVC system, if there are purposes other than reactive power compensation, a control strategy must be implemented. There are long term strategies for voltage regulation and load balancing which are described in the previous chapter.

Harmonic minimization or load sharing in 12 pulse systems requires short-term strategies. The 12-pulse TCR can be operated according to one of the following control strategies:

1. Sequential Load Sharing
2. Equal Load Sharing
3. Independent Load Sharing

3.8.2.1 Comparison of Control Strategies

The two control strategies described above will be compared in this section in view of harmonic content of the total current in 12-pulse TCR lines and I^2R losses of air-core reactors [5]. In the simulations, the ladle furnace is represented by a variable RL load and all other system parameters are integrated into PSCAD-EMTDC program in detail. Figs. 3.22 and 3.23 show the variations in capacitive reactive power produced by 12-pulse TCR, which is controlled according to Sequential Load Sharing.

Sequential Load Sharing in which one of the 6-pulse TCR groups is first loaded until its full capacity is used while the other one is kept idle and then the second 6-pulse TCR group is loaded gradually in the range from 0.5 p.u. to 1 p.u. of the reactive power compensation demand.

Equal Load Sharing is the one in which the reactive power demand of the load + fixed shunt filter(s) is equally shared among the two 6-pulse TCR groups at any time.

The above analysis has been repeated for Equal Load Sharing control strategy for the 12-pulse TCR and the results are given in Fig. 9. Both of the above simulations carried out for identical TCRs (6+6MVAr) connected to identical Δ and Y connected transformer secondaries. It can be concluded from these results that Equal Load Sharing strategy yields superior 5th and 7th harmonic cancellation properties in the line current waveforms of 12-pulse TCR over Sequential Load Sharing.

The simulation of Equal Load Sharing control strategy has been repeated for two identical 6-pulse TCRs supplied from two dissimilar and separate Δ and Y connected transformer secondaries (12.5MVA, 8MVA) as implemented in ISDEMİR project. The simulation results are given in Fig. 10.

A comparison of results given in Fig. 3.22 and 3.23 shows that the use of two dissimilar transformers instead of a single transformer with two identical secondaries in a 12-pulse TCR circuit for harmonic elimination purposes would not cause a significant increase in the 5th and 7th harmonic contents of line current waveforms. In order to verify these theoretical results, a test has been conducted in the field on the implemented 12-pulse TCR system. In this test, the reference value of reactive power

signal for the 12-pulse TCR has been increased in steps in the range from 0-12 MVAr manually as shown in Fig. 11.a and three line current and the three line-to-line voltage signals are recorded by the data acquisition system.

A comparison between Fig. 3.22 and Fig. 3.23 shows that field data are nearly the same with simulation results. Furthermore, 12-pulse TCR operated according to Equal Load Sharing Strategy eliminates 5th, 7th, 17th and 19th current harmonics as expected even though two identical 6-pulse TCRs are coupled together by the use of two separate and dissimilar Δ/Δ and Δ/Y connected transformers for the purpose of redundancy in the ladle furnace power system. In order to stress the benefits of 12-pulse TCR in the elimination of 5th and 7th harmonics, a single 6-pulse TCR rated at 12 MVAr is assumed to be connected to ISDEMIR Ladle Furnace Bus and its harmonic current content are obtained by PSCAD-EMTDC simulations. Fig. 12 shows the variations of 5th and 7th harmonic components produced by 12 MVAr, 6-pulse single TCR. If a 6-pulse TCR were used in ISDEMIR upgrading project 5th and 7th harmonic components in TCR line currents would respectively be 4.5% and 2.3% in comparison with negligibly smaller (0.3% and 0.2% respectively) 5th and 7th harmonic current content of implemented 12-pulse TCR.
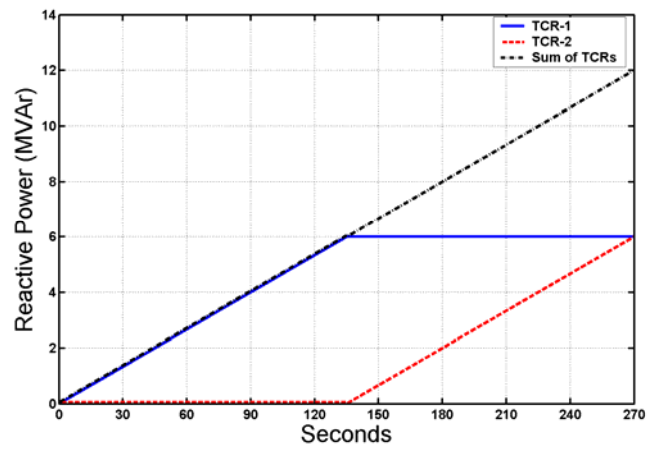
a. Reactive power variation
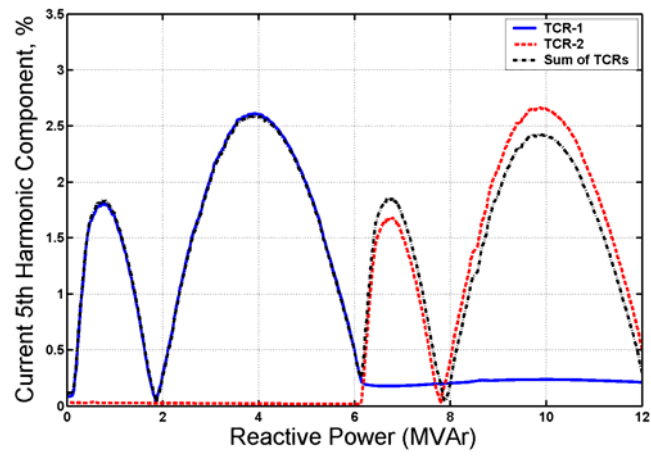
b. 5th harmonic current
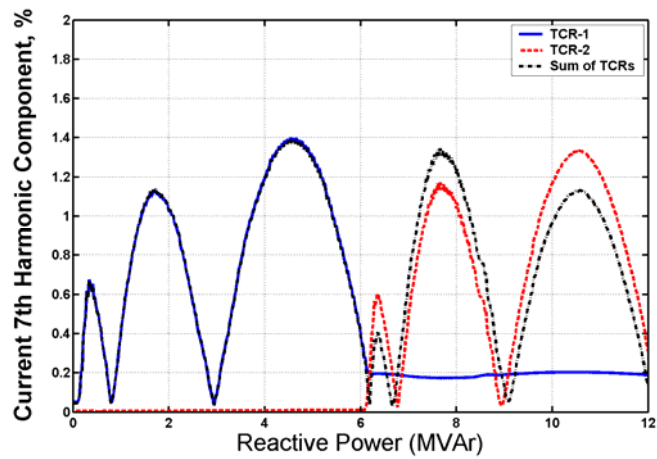
c. 7th harmonic current

Fig.3.22. Sequential Load Sharing for 12-pulse TCR (simulation)

123
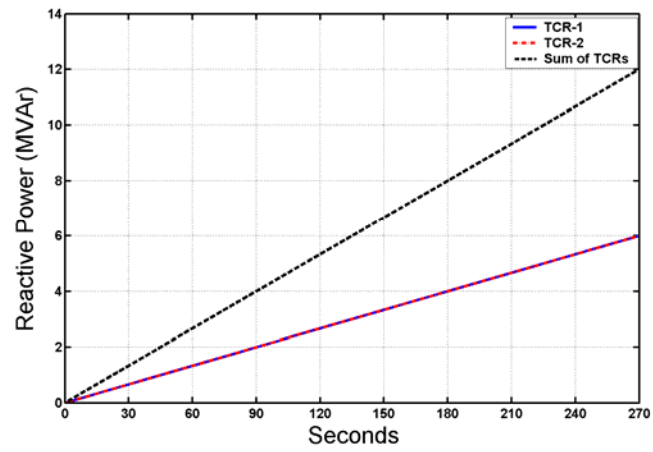
a. Reactive power variation
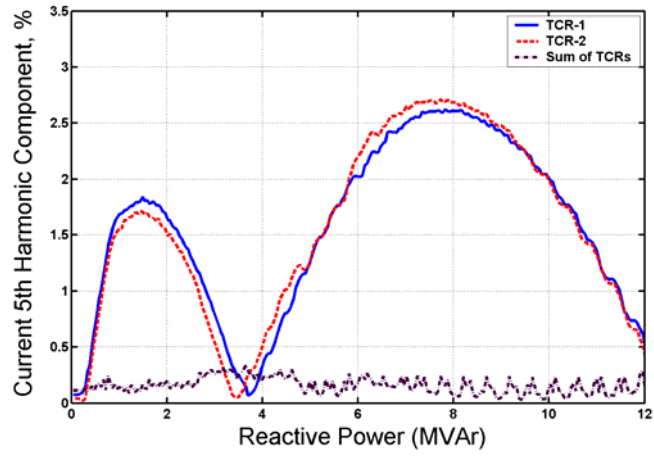
b. 5th harmonic current
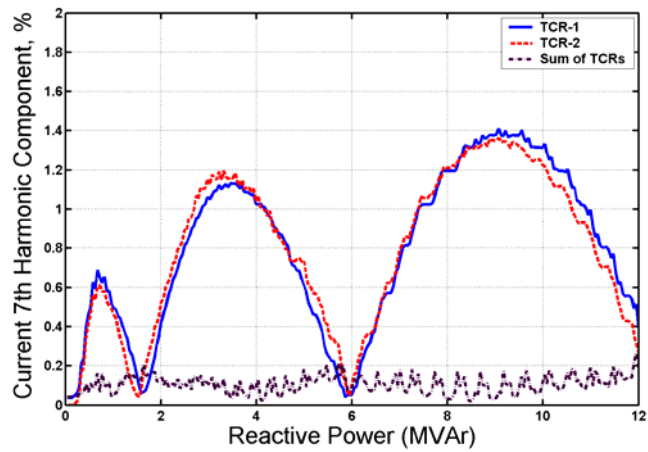
c. 7th harmonic current

Fig.3.23. Equal Load Sharing for 12-pulse TCR (simulation)

124

3.9 Thyristor Valve Control and Misfiring

Ideal TCR line currents are 90° displaced from the line voltage and they are symmetrical and balanced if the firing delay angle is in the range of 90°-180° for positive e half cycle and 270°-360° in the negative half cycle. These are the safe operating regions of TCR, which are the 2nd and the 4th regions shown in Fig.3.24. Whenever the conduction angle of a thyristor exceeds 180°, a DC current component exists. Moreover, the backward connected thyristor may not be triggered into conduction because the other thyristor has not commutated yet.

In a non-ideal TCR which includes an internal resistor, the firing delay angle can be reduced below 90°. The exact angle can be calculated from the inductive reactance and the resistance of the TCR.
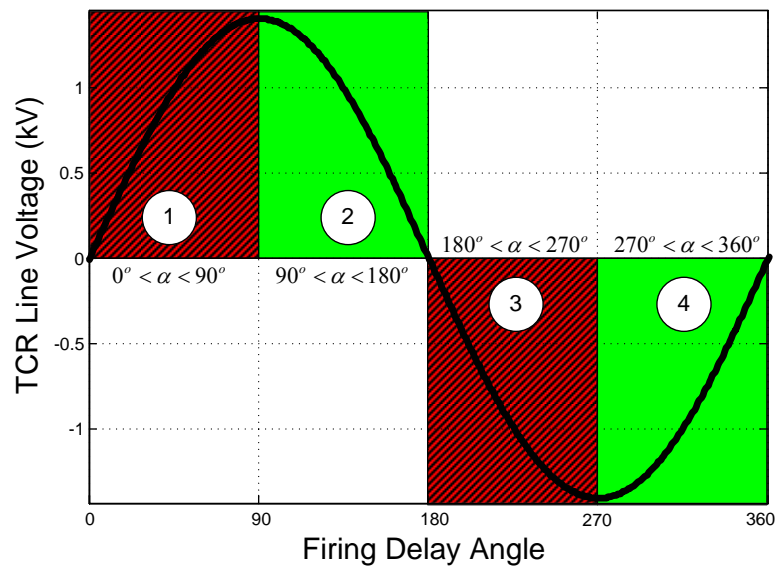
Fig.3.24. Firing Delay Angle (α) versus TCR line voltage. The safe operating regions 2 and 4 of TCR are marked with gren color Unsafe operating regions 1and 3 are marked with red color

Misfiring is an unwanted event in TCR based SVCs. It is the case where one or more than one thyristors are fired at the wrong instant, or the thyristors are not fired at all. There may be several reasons for misfiring.

3.9.1 Misfiring Due to Wrong Reference

Although in SVCs thyristor firing is not allowed before the fundamental line voltage reaches to the maximum value, which indicates that wt is $\pi/2$, there are some cases in which a firing may occur before this instant. Any noise injected in the control system over the reference voltages or the loss of reference signal may cause misfiring. Any firing before wt=$\pi/2$ causes DC component in the line current as well as even harmonics. Injection of unwanted DC and even current harmonics disturbs the power system, as well as SVC itself. SVC transformer may go into saturation, capacitors may cause over-voltages and control system may totally lose synchronization.

Fig.3.25 is an example of misfiring recorded in the field on 4 Oct. 2001. An unwanted voltage noise causes reverse conducting thyristor to be fired in two consequent cycles. The conduction angle for the thyristor exceeds $7\pi/4$ radians. The system recovers from misfiring; but, because of this error, the system gives fault indication and ceases operation.

The easiest way to avoid misfiring in such cases is to inhibit firing pulses for the risky firing angles. However, any noise that is conducted by thyristor gate triggering circuit may cause a misfiring. Therefore, using fiber optical or shielded cables reduces the probability of such cases. Fig.3.26 represents a typical inhibition of firing pulses near π radians.
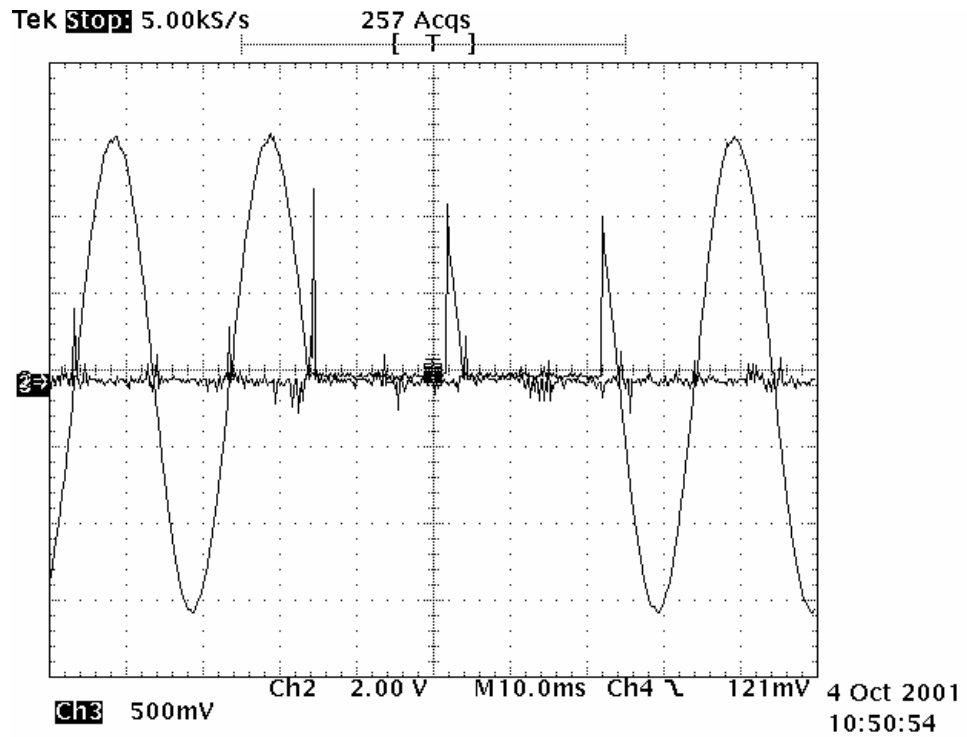
Fig.3.25. Misfiring observed in a TCR system. The voltage across the thyristor valves is zero during conduction.
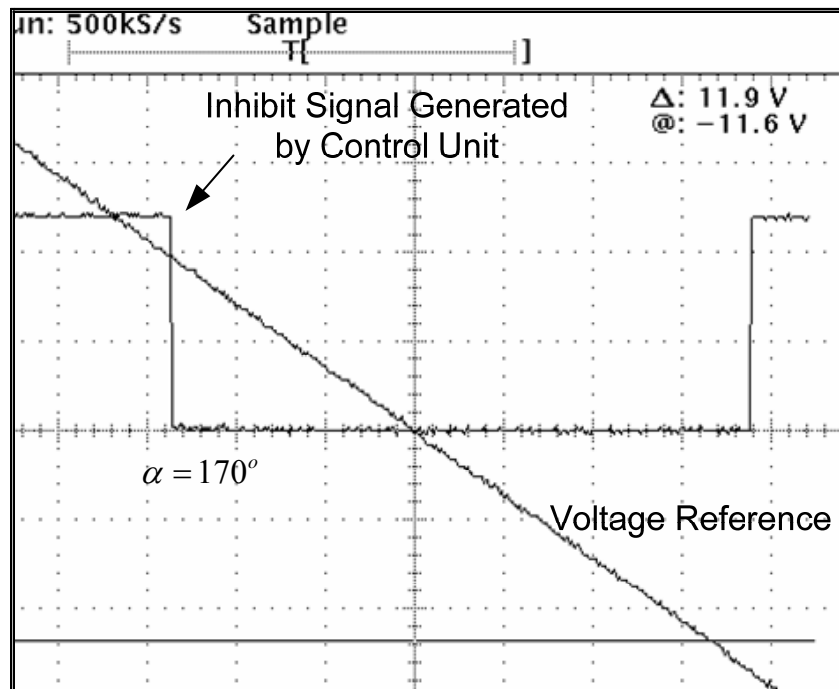
Fig.3.26. Protection against misfiring by inhibiting firing pulses.

In 1996 a case of misfiring occurred in ISDEMIR Laddle Furnace SVC system. Because of the fault in the voltage measurement transformers, the control system lost the voltage reference and started firing the thyristors with a random firing delay angle. Because of this, the reactors started to heat. There wasn't netiher a detection system for the continuous DC current component, nor a reactor heat detector. Eventually reactors were heated up because of excessive dissipation and permanently damaged as seen in Fig.3.27. For the latter modernization project, several precautions were taken to prevent such a case. Heat detectors were installed near reactors. Voltage loss protections were also added to control system.
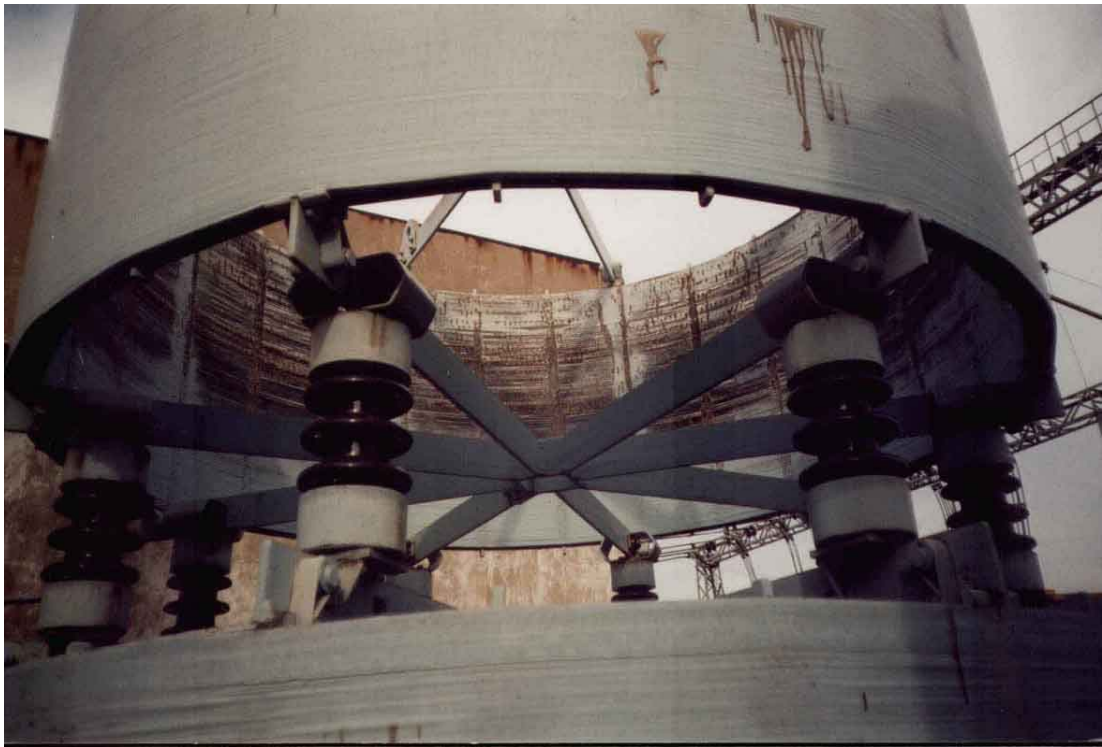
Fig.3.27. Permanent damage by overheating after the loss of control of the TCR, ISDEMIR 1996

3.9.2 Misfiring Due to Thyristor or Control System Failure

Whenever the control system loses one of its references such as set point, firing voltage reference, phase lock loop angle, etc... the thyristors may be triggered

in a wrong instant. This is obvious because triggering the thyristors before the voltage peak of the fundamental will cause a conduction angle above 180 degrees for an ideal TCR. Therefore, the backward connected Thyristor will have less than 180 degrees of conduction, or may even be unable to trigger into conduction. This is dangerous because there will be a high DC component in the current waveform. The current will also tend to rise above the safe limits whenever the firing delay angle approaches to the zero cross point of the voltage.

An example is given in Fig.3.28. The TCR used in the Fig. 3.8 is fired with a delay angle around 30 degrees. Note that the forward Thyristor can not conduct because the backward Thyristor conducts about 150 degrees. The phase and line currents have DC and even harmonics.
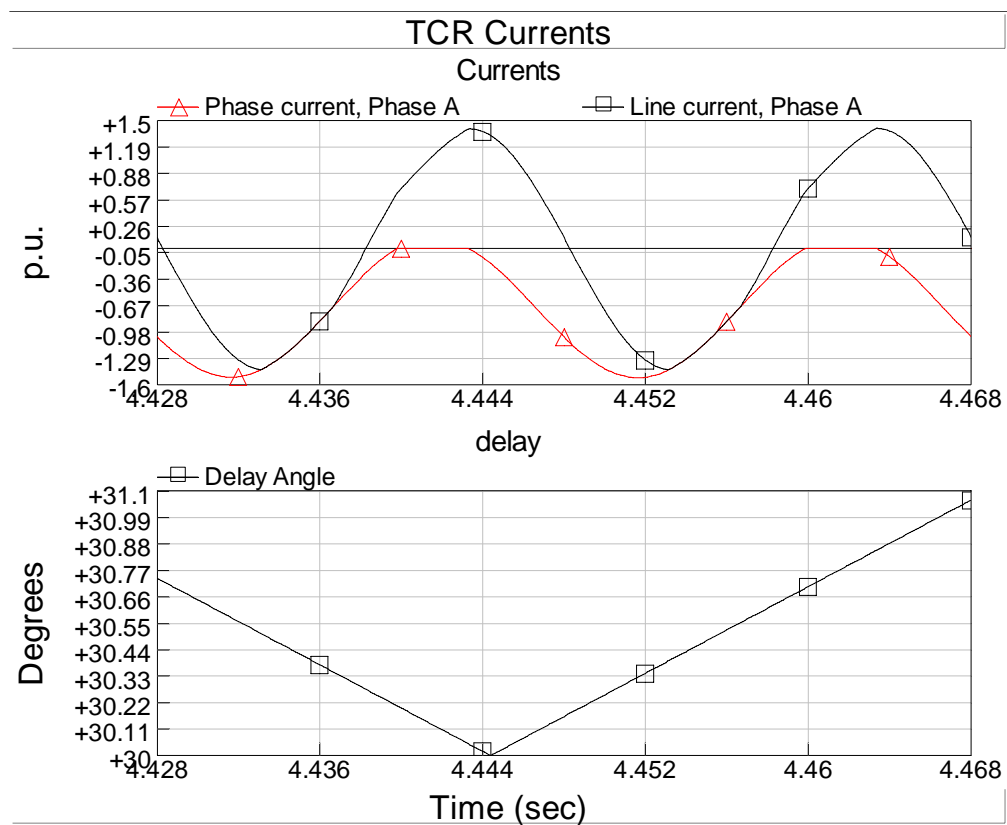
Fig.3.28. An Example of a misfiring simulated in the PSCAD

CHAPTER 4

CASE STUDY 1 : UNIFIED RELOCATABLE SVC FOR OPEN CAST LIGNITE MINING IN TURKEY

4.1 Design Considerations for Unified and Relocatable SVC Concept

The single line diagram of the unified, relocatable SVC is as given in Fig.4.2. The SVC described in this paper is a combination of Thyristor Controlled Reactor and Fixed Shunt Capacitors designed as 5th and 7th harmonic filters. As a derivative of the original system, some of these shunt filters may be implemented as thyristor switched filters (TSF) in the future expansion of SVC, thus keeping the installed TCR capacity the same. Fig. 4.3 shows the general view of various SVCs on the site after erection. The footprint of each SVC is as given in Fig 4.1. Each relocatable SVC is composed of seven building blocks:

- Power cable connection to the overhead line or load bus including a current transformer set to measure load current after VAr compensation and surge arresters (MOV type).

- A Compensator Transformer which allows the connection of SVC to the required medium voltage level (34.5kV or 15kV)

- A Switchgear Container, which includes metal enclosed type switchgear equipment (bus riser, SF_6 circuit breaker, load disconnect switch, earthing switch, potential transformers and their protection and mounting accessories). It is the heaviest part of the system (nearly 4 Tons).

- A Low-Voltage Equipment Container which includes the 1 kV Distribution Enclosure, an Auxiliary Supply and Systems Enclosure, a Measurement and Monitoring Enclosure, Thyristor-Stacks Enclosure, the Control and Protection Enclosure, and Shunt Filters Enclosure(s).

- Air-core type Thyristor Controlled Reactors, with each phase of delta-connected bank being split into two parts for short-circuit current limitation purpose. It includes the necessary mechanical mounting and electrical connection accessories.

- A Mounting Platform, which is built up of high quality concrete with partial reinforcement. Power and signal cables are laid in cable ducts formed in the mounting platform.

- A Lighting mast containing audio-visual alarm system and also acting as a lightning terminator.
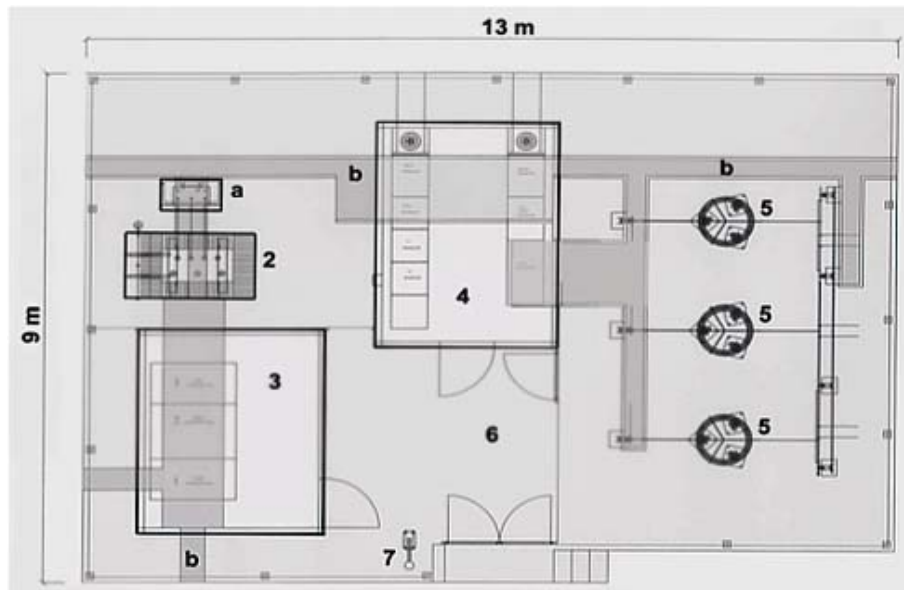
Fig.4.1. Mounting Platform: 1a- Auxiliary Transformer, 1b- Cable Ducts, 2- Compensator Transformer , 3- Switchgear Container, 4-Low–Voltage Equipment Container, 5- Air – cored Reactors, 6- Mounting Platform, 7- Lighting Pole & Lightning Rod

130
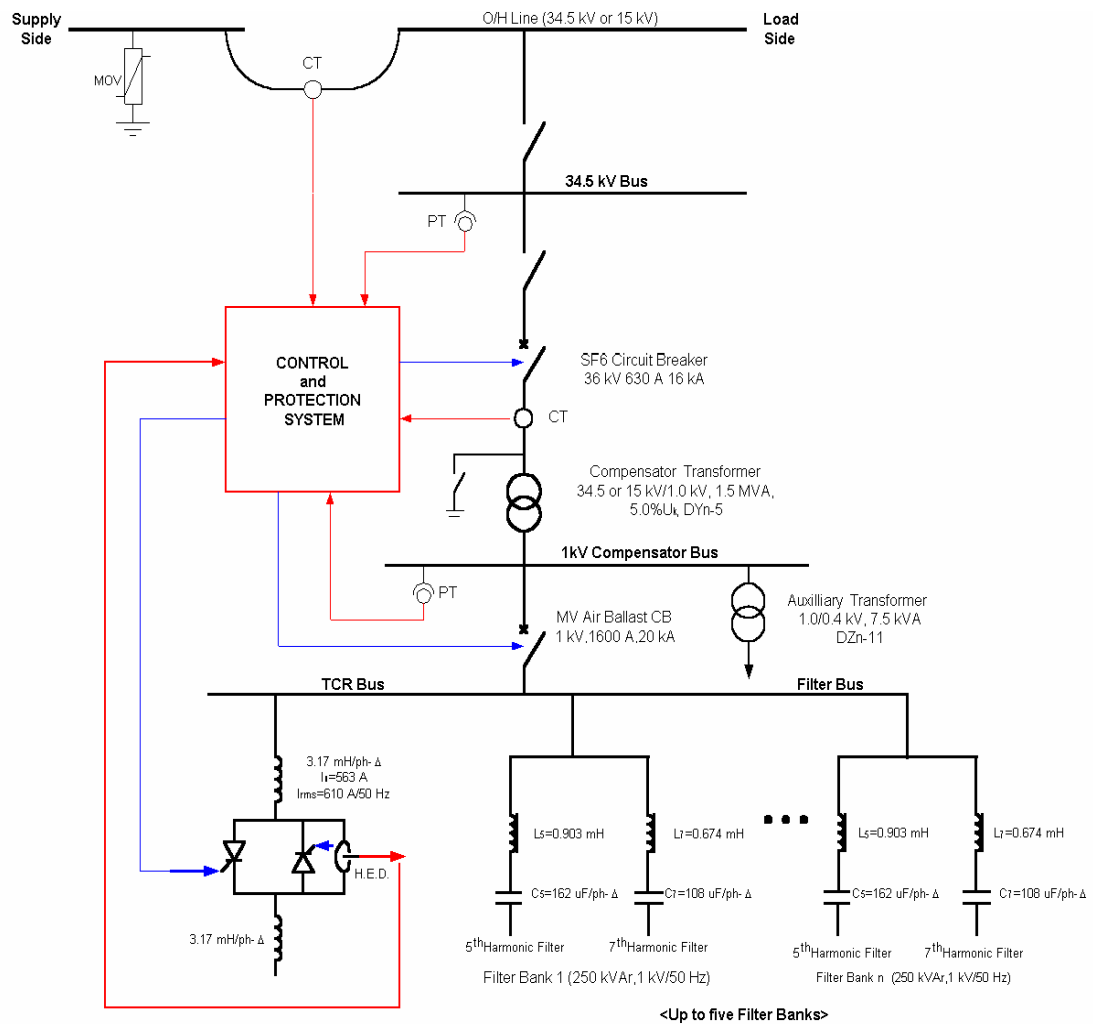
Fig.4.2. Single line diagram of a typical unified and re-locatable SVC

The Unified SVC is a relocatable system. In the case where coal reserve at a certain location runs out, the associated SVC can be transferred to the new location in a short time including demounting, transportation, erection and commissioning works. Since each container has its own internal wiring, only the electrical connections among containers, compensation transformer and reactors are to be made at the new site.

In Table 4.1 the SVC installed capacities are given. Component sizing of these systems are given in Table 4.2. Transformer size is chosen according to the maximum future expansions. These expansions are limited by the reactor, therefore the reactor sizing is very important for the flexibility of the system.

Table.4.1. Table of the TCR based SVC systems designed for TKI General Directorate (until 2005) *: The values in the parentheses will be installed by the end of 2007 in order to increase the controllable range of SVCs, which is necessary to meet the new reactive energy ratios imposed by EPDK.

Enterprise and SVC name	Voltage Level	Installed Capacity	TCR Transformer	TC Reactor Power	TCR Filter Power
TKİ ELİ Işıklar	34,5 kV	20 MVA	1500 kVA	1500 kVAr	750 (+1250) kVAr
TKİ ELİ Deniş	34,5 kV	8 MVA	1000 kVA	1000(+500) kVAr	250 (+250) kVAr[*]
TKİ ELİ Sarıkaya	15 kV	12 MVA	1000 kVA	1000 kVAr	500 kVAr
TKİ ÇLİ TEAŞ	34,5 kV	16 MVA	1500 kVA	1500 kVAr	250 kVAr
TKİ BLİ TEAŞ	34,5 kV	12 MVA	1500 kVA	1500 kVAr	500 (+250) kVAr[*]
TKİ YLİ Sekköy	31,5kV	16 MVA	1600 kVA	1500 kVAr	750 (+250) kVAr[*]
TKİ GELİ Eskihisar	31,5kV	13 MVA	2000 kVA	2000 kVAr	1750 kVAr

Table.4.2. Table 4.2. TCR Subsystem ratings and installed locations

Subsystem	Ratings	TKİ Enterprise
Thyristor Controlled Reactor	1 kV,1 MVAr, 4,7 mH x 2, air core	ELİ
	1 kV,1,5 MVAr, 3,17 mH x 2, air core	ELİ,ÇLİ,BLİ,YLİ
	1 kV,2 MVAr, 2,39 mH x 2, air core	GELİ
Thyristors	Dynex DCR1476SY34, Itav=2223A, Vdrm=3400V, Natural air cooled stack	All Enterprises
CB Switched Detuned 5th HF	1.25 MVAr 31.5kV	GELİ,ELİ
4th H.F. (Permanent)	150 kVAr, 1kV	YLİ
5th H.F. (Permanent)	150 kVAr, 1kV	All Enterprises
7th H.F. (Permanent)	100 kVAr, 1kV	All Enterprises
Thyristor Switched 5th HF	500 kVAr, 1kV	YLİ,BLİ
SVC Transformer	1000 kVA, 34,5 kV/ 1 kV, Dyn-11, Uk=5,50	ELİ
	1000 kVA, 15 kV/ 1 kV, Dyn-11, Uk=5,50	ELİ
	1500 kVA, 34,5 kV/ 1 kV, Dyn-11, Uk=5,30	ELİ,ÇLİ,
	1600 kVA, 31,5 kV/ 1 kV, Dyn-11, Uk=4,80	YLİ
	2000 kVA, 31,5 kV/ 1 kV, Dyn-11, Uk=5,00	GELİ
	7,5 kVA 1kV / 0,4 kV, Yzn-11 Auxillary Transformer	All Enterprises
MV Switchgear	36kV, 72kV peak, 630A, 16kA short cct breaking capability	All Enterprises

133

Fig.4.3. The TCR based SVC systems designed and installed for TKİ (a) ÇLİ TEAŞ 34.5kV SVC System (b) ELİ Deniş 34.5kV SVC System, (c) ELİ Sarıkaya 15 kV SVC System, (d) ELİ Işıklar 34.5kV SVC System (e) BLİ TEAŞ 34.5kV SVC System, (f) GELİ Eskihisar 31.5kV SVC System, (g)

4.2 Engineering Aspects

4.2.1 Load Identification

There are 15 enterprises of General Directorate of TKI which are all engaged in lignite mining business by the use of 90 excavation machines in addition to underground mining facilities. At the present time, 82 of Power Shovels with a capacity of 10-20 cubic yrd, and 8 Draglines with a capacity of 20-70 cubic-yrd are in operation [3]. A very high percentage of electricity consumed by TKI is demanded by these electric excavators. Types of motor drives, electric power demands, and built-in compensation facilities for these machines are given in Table 1. As an ideal solution to the compensation problem, each machine should be equipped individually with new or additional compensation facilities to meet the requirements of new regulations. However, this is found to be impractical and uneconomical because of large amounts of compensation capacity needed, space considerations, and vibratory mechanical environment of excavation machines.

The group compensation technique is, therefore, chosen as a practical and economical solution to the problem. These machines are acting as rapidly fluctuating loads (intermittent loads) and have the active and reactive power demands as summarized in Table 4.3. Active and reactive power consumptions of these machines for a few operating cycles are obtained by processing data collected by National Instruments data acquisition system.

135

Table.4.3.   Electrical excavators as a load on the network

Excavator type	Drive Type	Power Demand From the Supply		Integrated Var Compensation Facility	Duration of Operating Cycle, Sec (Typical)
		Active Power	Reactive Power		
Power Shovel A	DC motors fed from 4-Q, 6-pulse thyristor converters with neutral thyristors	Consumption and regeneration	Inductive and Capacitive	Fixed 5th and 7th shunt harmonic filters	30-45
Power Shovel B	DC motors fed from 4-Q, 6-pulse Thyristor Converters	Consumption and regeneration	Inductive and Capacitive	Fixed 5th and 7th shunt harmonic filters, only one group is thyristor switched	30-40
Power Shovel C	Ward-Leonard Drive, Induction Motor on the supply side.	Consumption and regeneration	Inductive only	Fixed, shunt connected plain capacitors	30-40
Dragline	Ward-Leonard Drive, Synchronous Motor(s) on the supply side	Consumption and regeneration	Inductive and Capacitive, depends on the field exciter settings	Non-Existent	65-120

Fig.4.4. Buserus Dragline

Fig.4.5. Marion 191 Power Shovel

The preliminary design work has been based on the following considerations:

- A single line diagram of the distribution system including the parameters of the utility grid is obtained first to determine the possible connection points of SVC for group compensation.

- Monthly electric bills for at least one year in the past (a sample graph obtained from the bills is as given in Fig.4.7; penalty limits for inductive and capacitive reactive energy consumptions according to the new regulations are also marked on the same graph.

- Daily active and reactive power demands of each load bus, and harmonic voltage and current components are obtained by processing the raw data collected in the field by National Instruments data acquisition system. A sample waveform set obtained in this manner is as shown in Fig.4.8 .a and b.

- Detailed information about electric motor drives, transformers, and their operating cycles.

- Investigations of low-voltage shunt compensators and medium voltage capacitors available at each bus.

- Future production plans and machine stocks.

Preliminary design work gives sizes and ratings of main parts of each SVC and investigates the possibility of series and parallel resonance. Sizing of each SVC is based on daily active and reactive power demand curves in Fig 4.8.a and b, and achieved on a PC by the use of a custom developed program. The variations in reactive power consumption of Çan Lignite Enterprise after compensation by 1.5MVAr TCR and 0.25MVAr F is estimated as given in Fig 4.8.c.

(a)   (b)

Fig.4.6.   (a) Data acquisition system (b) Connection of data acquisition system to the SVC
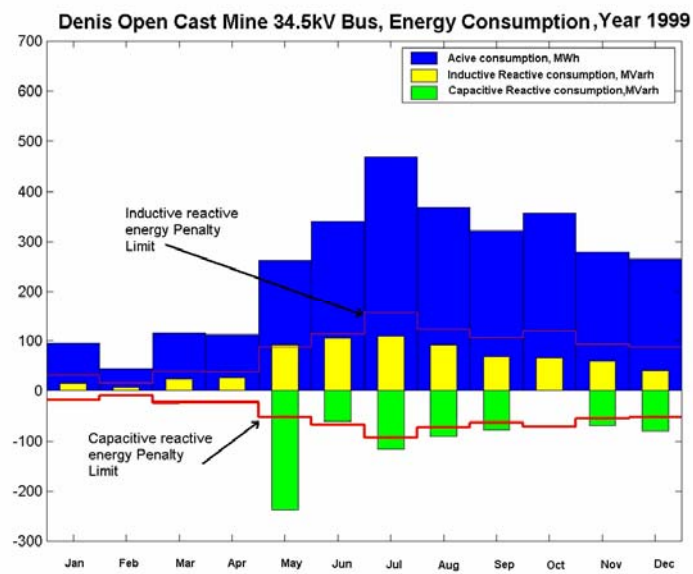
Fig.4.7.   A sample Energy Consumption analysis of a load bus.
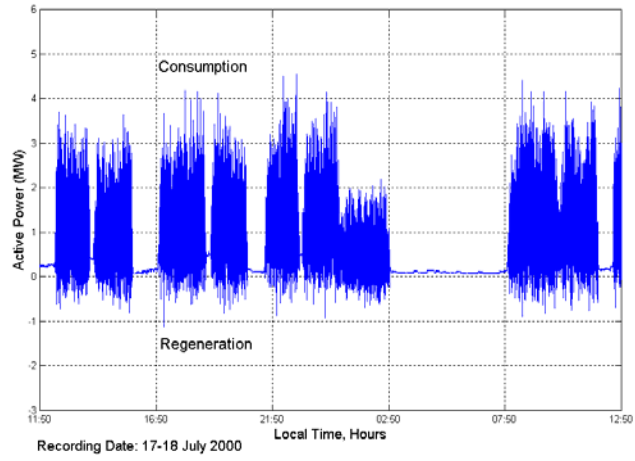
(a)
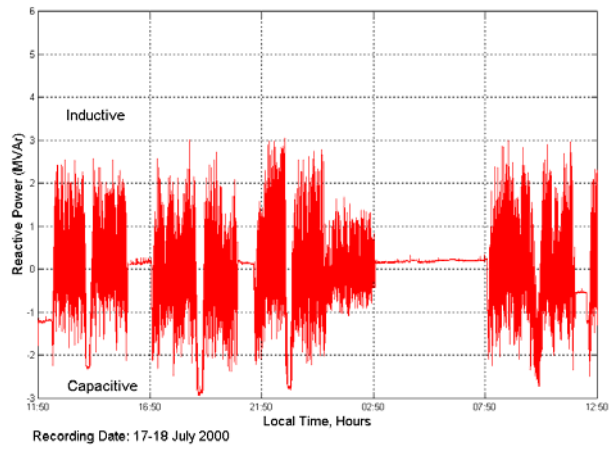
(b)
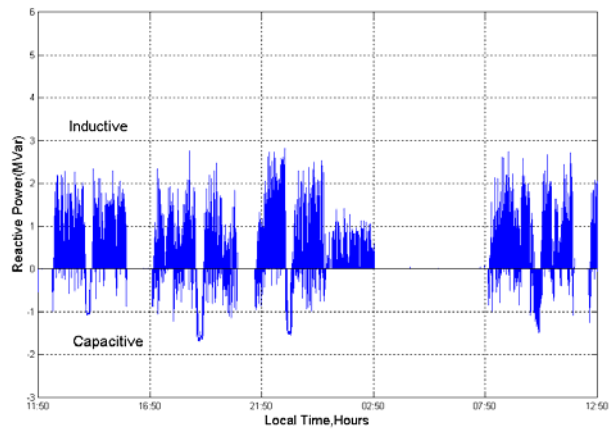
(c)

Fig.4.8. TKİ ÇLİ enterprises busbar(a)Active power demand ,(b) Reactive Power demand, (c) reactive power after compensation (theoretical)

140

Determination of ratings and resonance analysis has been carried out by Spice by the use of single line diagram for each load bus. Since the installed capacity of each SVC is relatively lower in comparison to those in common industrial applications, the operating voltage of TCR and F is chosen to be 1 kV line-to-line according to IEC Standard voltages[25], thus eliminating the need for series thyristor operation. For the chosen voltage value, 5MVAr TCR units employing single back-to-back connected thyristor stacks can be realized with the present semiconductor technology.

4.2.2 Distribution System Types

All TKI Enterprises are supplied either from the nearest thermal power plant or national grid via medium voltage single- or double-circuit O/H lines, some of which may be dedicated for TKI utilization only.

These are of radial type, which transmit electrical power at a higher voltage level (34.5 kV or 15 kV), and stepped down to a lower voltage level of 6.3 kV in the transformer sub-stations (TS). Power is transferred from TS to switching sub-stations (SS) through O/H lines and from SSs to individual excavating machinery loads through EPR type cables laid on the ground. The feeding and energy measurement arrangement of the distribution systems can be grouped essentially in three different forms as illustrated in Fig 7.

The first system (Fig.4.9) is a dedicated line on which there are various step-down transformer sub-stations to supply the nearby loads. The measurement of energy is done at the sending end of the feeder on the utility premises. The factors to be considered are the active and reactive energy consumption, generation by the individual loads connected to step-down transformers and the comparatively higher diversity factor involved between different sub-stations. The second system (Fig.4.9) is a step-down transformer sub-station at the end of an O/H line, where the energy metering is carried out within the transformer sub-station. The measuring CTs and PTs are located conveniently within the sub-station on the incoming line. The third system (Fig.4.9) is similar to the second system except that instead of one

transformer sub-station, there are as many as required along the line. Each has its own measurement system.

It should be noted that the latter two systems do not enjoy the full benefits of power generation that takes place on the load side as the meters are designed to operate only in one direction. Furthermore, the diversity factor is lower compared to the first system [3].
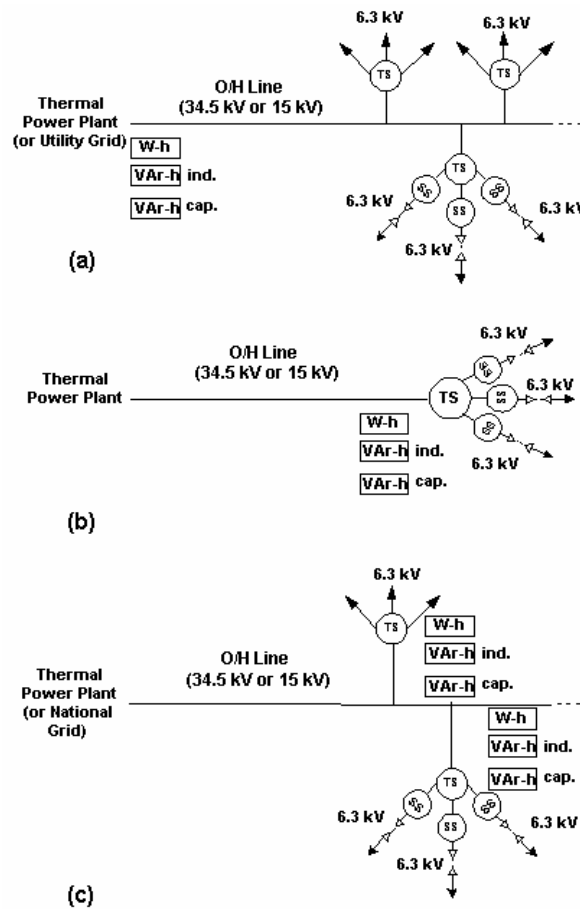
Fig.4.9. Feeding and energy measurement arrangements of radial distribution systems in TKI Enterprises. TS: Transformer Sub-station; SS: Switching sub-station, (a) Energy measurement on the utility premises for a dedicated line, (b) A single TS with its own energy measurement, (c) Individual energy measurement in TSs for groups of loads

142

Fig.4.10. (a) installation of underground power cables (b) Installation of current transformers and power cables to 15 kV overhead line. (c) Mounting the bases for current transformers on a 34.5kV double circuit tower. (d) Installation of current transformers on a 34.5kV double circuit tower

An SVC may be connected to an O/H line or a load bus available within a transformer sub-station which may have different voltage levels (34.5kV and 15kV) and supply conditions. PTs for measurement (monitoring) and control are located in SVC Switchgear Container with connection made to the supply side (or on the supply side of CBs).

Supply specifications according to the Turkish Standard TS 831 [45] are as given in Table II. The supply frequency varies in the range of 50±0.5 Hz. The three-phase balanced short-circuit current varies in the range from 4 kA to 14 kA at the bus-bars belonging to TKI. In view of these, metal-enclosed type 36kV switchgear

143

equipments are chosen even for 15kV SVC system (which is to be abandoned in favor of 36kV in very near future). The SF_6 circuit breakers have a breaking capacity of 16kA to match the short circuit MVA of all possible connection points in TKI system in the future.

Each SVC should be connected to a point between energy-meters and the load and as close as possible to load terminals. SVC should, therefore, be connected directly to the single-circuit or double-circuit O/H line for the distribution system configuration in Fig 4.9 and to the load bus existing in transformer sub-station for system configurations given in Fig 4.9.

For system configurations in Fig 4.9.b and c, the location of SVC, which will perform group compensation, is fixed. That is, it should be connected to the load side of measuring current transformers existing in the TS. However, for system configuration in Fig 4.9.a, SVC should be connected to the O/H line somewhere between sending end and the first TS on the feeder. Connection to the sending end takes into account full compensation requirements while connection just before the first TS minimizes the O/H line losses and results in better voltage regulation.

In the case where the continuity of the supply is important, a double-circuit O/H line is normally used, thus permitting the transformer substations to be switched on to either of these lines (Fig. 4.10). In order to minimize the losses occurring on the transmission lines, the two circuits are evenly loaded during normal operation. However in case one of the lines is faulted, all TSs are transferred to the healthy line. At a first glance, one would require two separate SVCs connected in the same manner as given above, further these SVCs should be oversized by a factor of two for successful compensation in the event of a fault on one of the lines. It is obvious that such a solution would not be economical.

By considering the method of energy measurement at the sending end of the double-circuit O/H line which takes place at the utility premises (Fig. 4.11), an ingenious solution has been found as illustrated in Fig. 4.11. The energy measurement system utilizes two sets of current transformers, one set for each line as well as a summation CT to obtain the total current for the double-circuit O/H line as given in Fig.10. If the total VAr demand and power factor of the double-circuit O/H

144

line is known, then it is sufficient to connect only one SVC to any one of these circuits sized for the total power demand (Fig. 4.11). In this case, reactive power demand of SVC connected line will have its reactive power from the SVC directly, while the reactive power demand of the other line will first go to the sending end bus-bar, and then to the loads connected to the second circuit. In the operation, the reactive currents are in opposite directions in the two sets of current transformers as shown in Fig.4.11. These would be cancelled in the summation transformer and the kVArh measuring units will not be able to detect the flow of reactive power through sending-end bus bars.
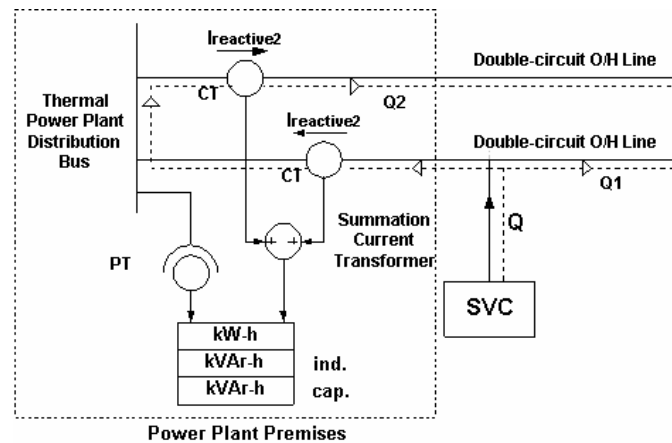
Fig.4.11. SVC operation in double-circuit dedicated feeder

If the reactive power measurement of the double-circuit O/H line can be made at the utility premises and transmitted to SVC by an appropriate data transmission system for control purposes, this would be an ideal solution. The only requirement is the accessibility of the connection of SVC to either one of the lines in case the other is faulted. However, it is essential that the SVC is connected to one of the lines only, and some means of interlocking between the switching schemes to the lines, is necessary.

In order to have a self contained and independent SVC system, it is preferred to measure the total reactive power demand of double circuit O/H line within the SVC. Therefore, as in the previous case of a single line system, current transformers are mounted on the tower tops, two current transformers for each circuit (Fig. 4.10.c).

The total current is then measured by the use of summation current transformers. However, only the O/H line voltage to which SVC is connected can be measured within the SVC. If the lines are unequally loaded, this would result in a small error in the reactive power measurement as the two circuit voltages will vary slightly. This error was made negligibly small by installing the SVC to a point as close as possible to the source

4.2.3 System Sizing and Determination of Ratings for Main SVC Components

The preliminary design of each unified, relocatable SVC has been finalized by the use of PSCAD/EMTDC. For this purpose, the 3-phase equivalent circuit of the system including the loads and the mains is first obtained. Two different approaches have been used in the simulation of rapidly changing loads. These are:

1. The use of standard 6-pulse ac-dc converter, transformer and electrical machine tools available in PSCAD. In this approach, the rapidly changing loads are represented by current and voltage data collected in the field by data acquisition system at a sampling rate of 3.2kS/s, thus replacing the load models in (a). The file containing current and voltage data is then integrated into PSCAD/EMTDC, and real time data are synchronized with the time base in simulation.

2. The ratings of various SVC components are determined from the results of simulation by considering all the possible load busses for connection and the worst operating conditions. Among all possible load busses for the connection of all possible SVC configurations (1.5 or 1.0 MVar TCR installed capacity, 250-1250 kVar shunt filter installed capacity) when the mains voltage is at its maximum continuous operating value, the maximum filter-capacitor voltage,

and maximum TCR current, and filter-reactor current values are determined for the choice of component ratings. The thyristor ratings are also obtained from the results of simulation by considering all possible short-circuits which may occur in TCR and misfiring of naturally-cooled thyristors for the worst operating conditions.

(a)   (b)

(c)   (d)
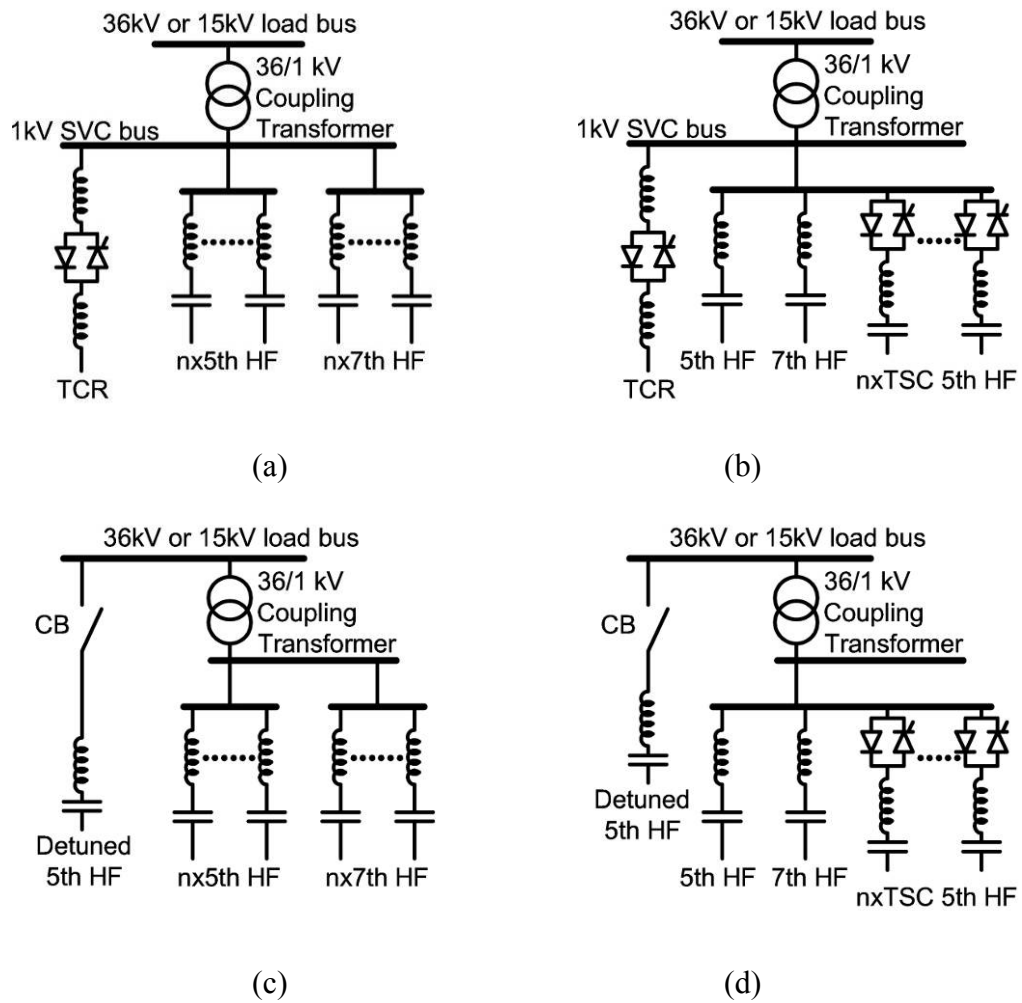
Fig.4.12. Various filter configurations
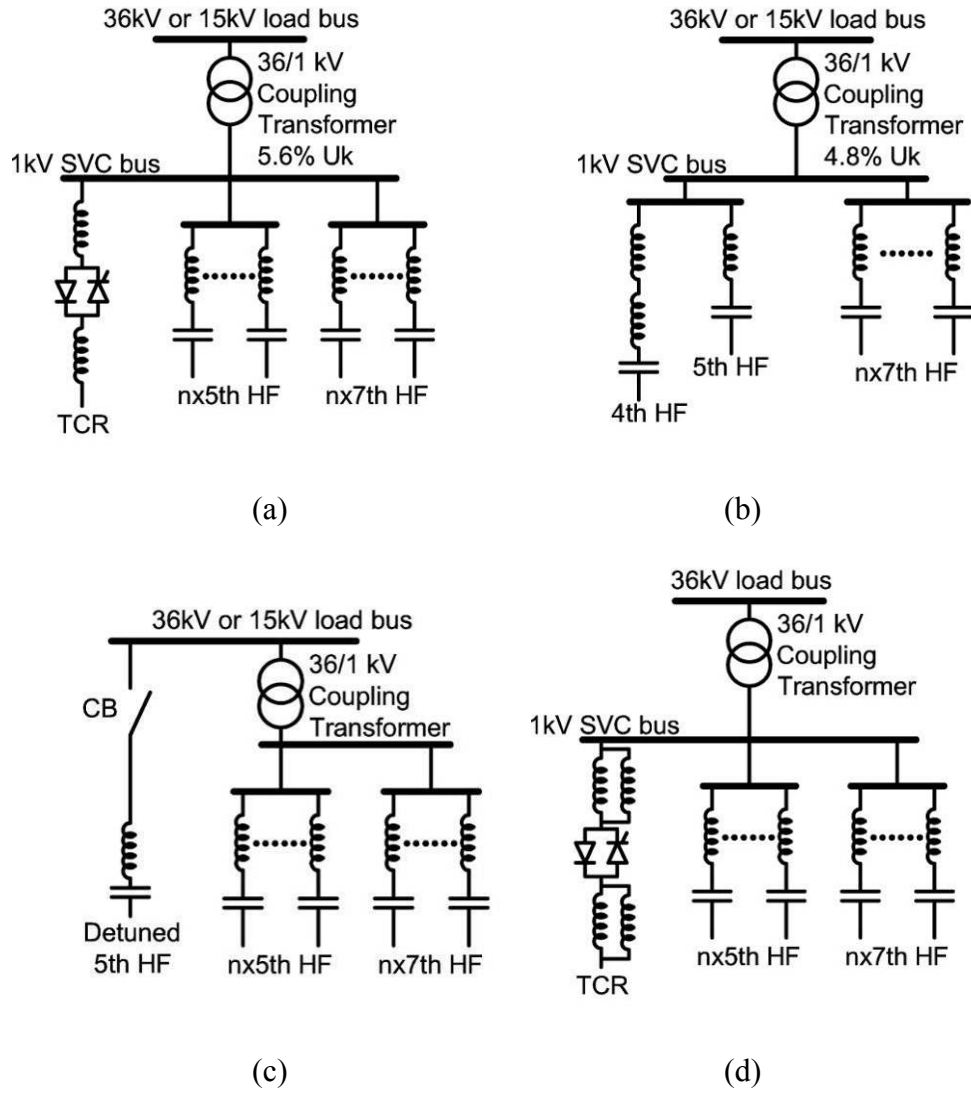
Fig.4.13. Modernization of filters in 2007 (a) Addition of filters to 1kV side , (b) addition of 4th harmonic filter in YLİ (c) Detuned filter added to 34.5kV in ELİ Işıklar (d) Additional reactors for ELİ Deniş

Back-to-back connected thyristor stacks cool down naturally provided that internal air temperature of the associated container is kept at a temperature not higher than 5K above ambient by adequate ventilation. The worst unusual operating conditions for each thyristor stack are:

Whenever a short-circuit occurs between the terminals of the reactor half, to which the thyristor stack is connected; since firing pulses are applied for a period of 1ms to each thyristor, backward thyristor does not trigger into conduction for this condition. The thyristor stacks are chosen to withstand these currents for a period of 2 seconds.

The sizing study of each SVC is finalized by using the results of simulation. The TCR operation has been verified by the use of actual data collected in the field, after the installation of associated SVCs, as will be presented in the next section.

4.2.4 Filter Design

In order to eliminate 5th and 7th harmonics generated by TCR, two types of modular shunt connected filter types are developed. Shunt filter design parameters are verified by EMTDC PSCAD simulations. The current and voltage values are determined as in Table 4.4. and Table 4.5. respectively.

Table.4.4.   Current loading of filter reactors.

Filter element	rms current, A			True rms value of total current, A
	50 Hz	250 Hz	350 Hz	
L_5	110	26	1	115
L_7	71	4	13	75

Table.4.5.   Filter Capacitor Voltages.

Filter element	rms voltage, V l-to-l			Algebraic sum of harmonic voltages, l-to-l rms V
	50 Hz	250 Hz	350 Hz	
C$_5$	1225	60	2	1300
C$_7$	1206	12	32	1250
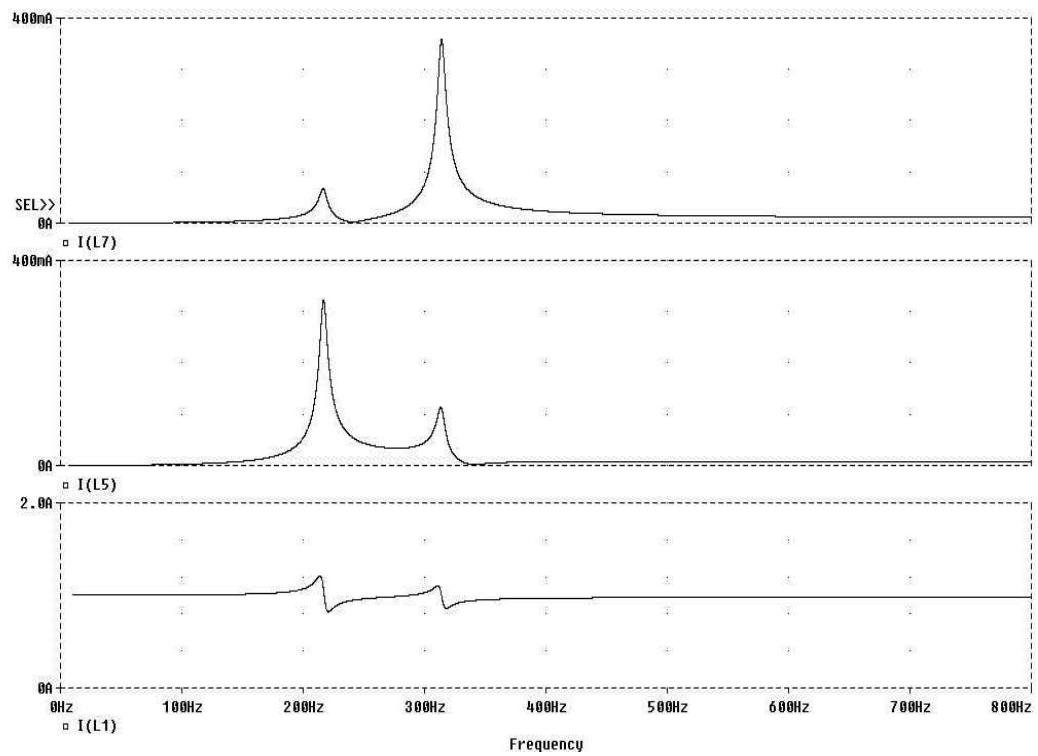
Fig.4.14. Filter characteristics for 1A current injected from the load side, simulated in ORCAD
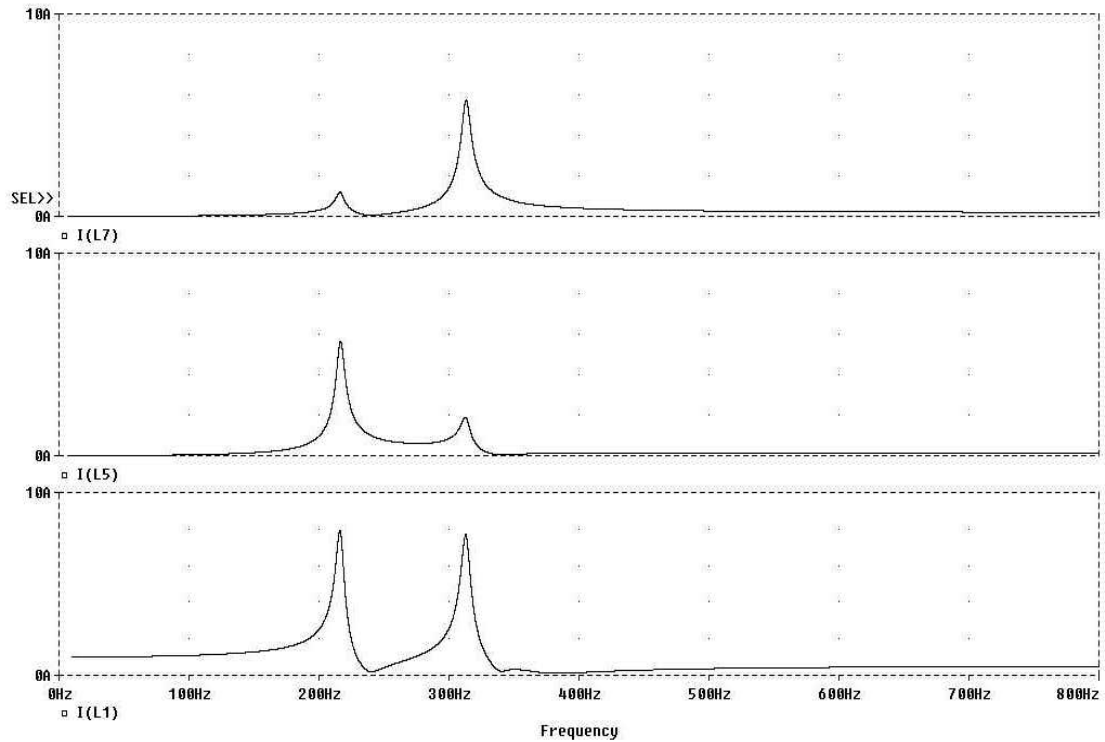
Fig.4.15. Filter characteristics for 1A current injected from the TCR side, simulated in ORCAD

The SVC filter characteristics are simulated in ORCAD in order to determine the frequency response characteristics. The results are seen in Fig.4.14 and Fig. 4.15. It is seen that a very small content of load 5th and 7th harmonics are filtered. It is also seen that 5th and 7th TCR current harmonics are filtered effectively, while 4th and 6th TCR current harmonics are amplified 2.8 and 3 times respectively.

4.2.5   SVC Coupling Transformer

In this project, a specially designed, oil-insulated, outdoor type power transformer is used as the compensation transformer to allow the connection of SVC to any medium-voltage level (Fig. 13). It is connected in Δ-Y with unearthed and unused neutral point. In the selection of connection type for the primary and secondary windings, the undesirable effects of unbalanced operation of load on the

performance of TCR as well as the penetration of harmonics produced by TCR to the supply side have been investigated.

It is found out that Δ-Y connection gives much better results than Δ-Δ connection at the expense of more sophisticated electronic circuit implementation for the phase-wise measurement of reactive power.

In order to prevent the compensation transformer from undesirable effects of direct current component and harmonics generated by TCR, the magnetic operating point has been placed to the linear portion of the B-H characteristics (B_{op}<1.6Wb/m^2). For the balanced operation in the steady-state, triplen current harmonics generated by TCR will close their paths through Δ-connected TCR. However, for unbalanced operation, these will partially reflect to the compensation transformer. 5th and 7th current harmonics generated by TCR will be satisfactorily filtered out by passive filters shunt-connected to the low-voltage side. However, this system will operate in transient state performing unbalanced operation for the vast majority of time owing to the intermittent characteristics of excavation machines. This type of operation for TCR will produce direct current component and even current harmonics in addition to the odd ones.

4.2.6   Environmental and Climatic Conditions

Environmental and Climatic Conditions are specified as follows:-20/+40°C ambient temperature range; high humidity; 50 cm. max. snow load; air pollution at some places (including acid rain); 1500 m altitude (max); erection at rural area; unmanned operation; very poor road infrastructure. To cope with these difficulties:

1.   A simple and reliable air ventilation system is chosen for containers. The fans are only kept in operation at ambient temperatures above 0°C. The switchgear equipment is continuously heated in order to prevent them from the risk of condensation. Pre-heating is applied in the internal medium of containers before start-up (after long mains interruptions).

2.   Conformal coating techniques are to be applied to electronic PCBs together with the use of special connectors and bare terminals.

3. Reasonable container sizes are needed to allow their transportation by the use of ordinary trucks (Fig. 4.16.a). Other parts are also modular and easily transported, installed and disassembled as seen in Fig.4.16.a and b.

4. Each SVC is to be equipped with an automatic re-closing system against system trips due to supply failures, disturbances coming from the supply, and internal faults. It reconnects the SVC to the mains only one time after disconnection. In case of persistent abnormal operating conditions, the system is locked out in the open condition and audio/visual alarm system is activated.

(a)   (b)

Fig.4.16. (a) After mounting the switchgear and TCR 1kV systems to containers, they are transported to field, (b) Installation of the air-core reactors in ELİ 15kV SVC

Fig.4.17. Audio-visual alarm systems, red-flashing light and an audible alarm mounted right at the bottom of it on the light post.

4.2.7 Control System

Control System developed for the TKİ Unified and Relocatable Systems is a combination of flexible analog main board and peripheral systems. The main board in Fig 4.18 was designed and developed in less than 3 months time because of the project time considerations in 2001. Analog cards are replaced by recent versions in two modernization projects. In the latest control systems, PLC usage becomes more common for the ease of user interface and alarm logging. With the increased employment of PLC and other digital subsystems, software has become rather complex. In addition to these, a GSM based remote sensing and data acquisition will be added in 2008.
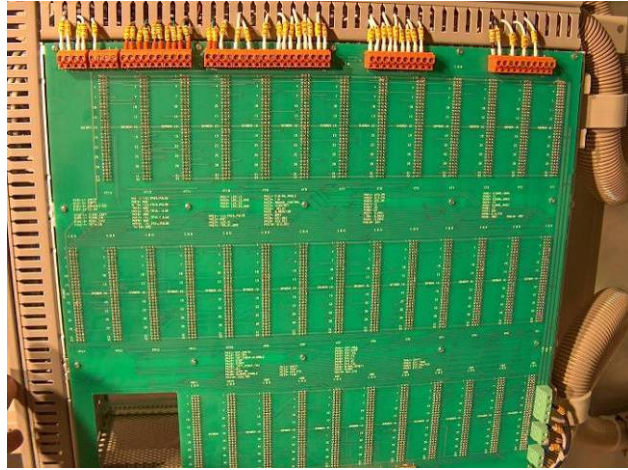
(a)

(b)

Fig.4.18. Inside the control cabinet, (a): Motherboard, (b): Peripheral electronic susbsystems and PLC

Fig.4.19. Control panel designed for YLİ SVC system.

4.3 EMC Considerations

4.3.1 Avoiding Loop Formation in Electromagnetic (EM) Environment

Air-core type thyristor-controlled reactors are mounted on the platform as in Fig.4.20. These reactors constitute the major artificial electromagnetic source on the platform. An illustration of the magnetic field distribution around outdoor type air-core reactors is given Fig.4.20. They are mounted side by side with magnetic directions so as to provide flux cancellation at fundamental frequency for balanced operation in the steady state (Fig.4.21). Unfortunately, the air-core reactors perform unbalanced operation in the transient state for vast majority of the time owing to the rapidly fluctuating character of the electric excavators. Around SVC system and under each reactor, formation of closed loops is, therefore, not allowed.

156
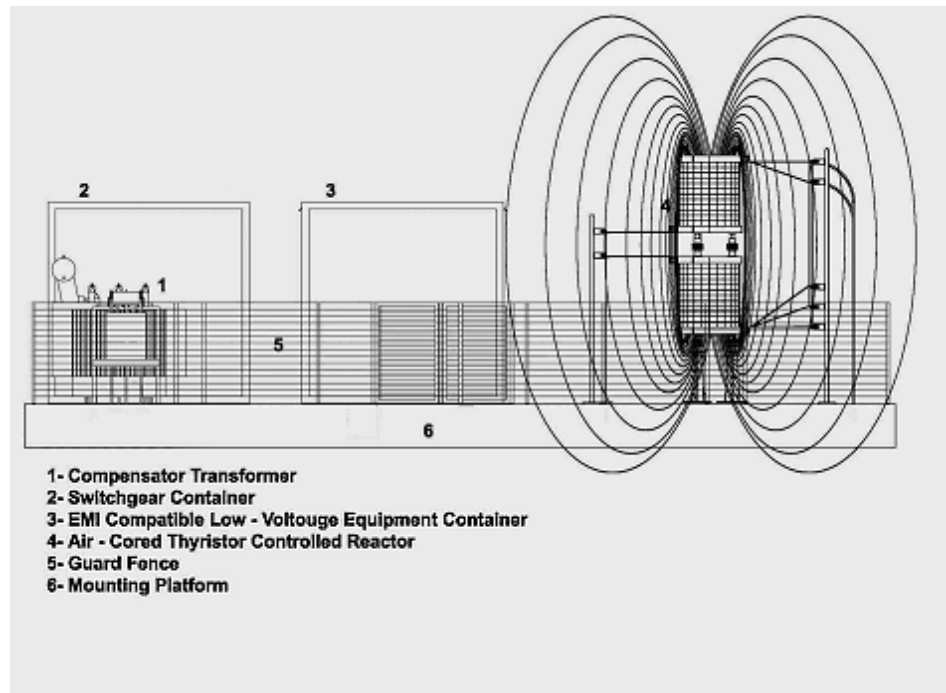
Fig.4.20. Air-core reactors mounted on platform and illustration of their magnetic field distribution

(a)
Fundamental flux components when current in phase-B is positive maximum

(b)
Third harmonic flux components
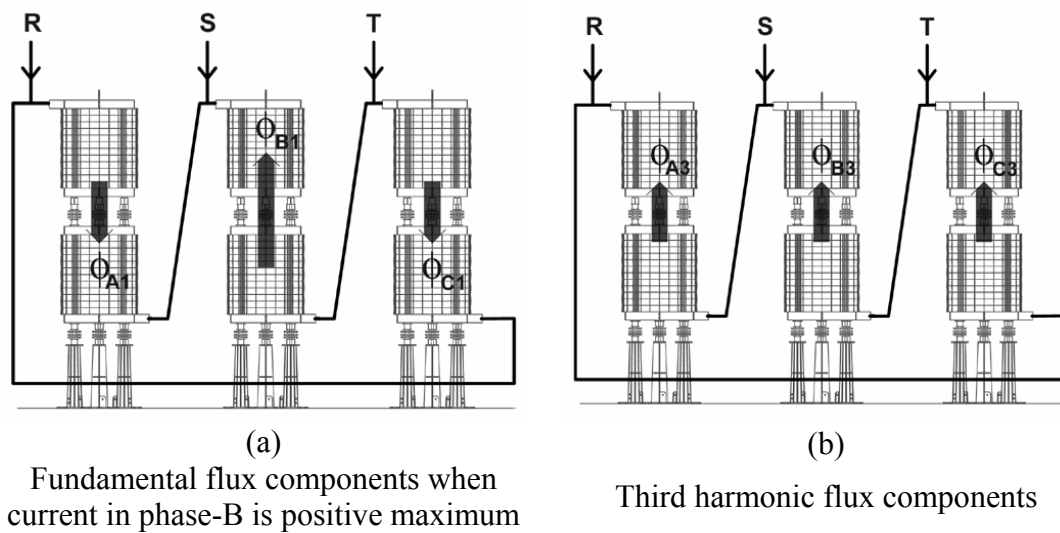
Fig.4.21. Positioning of Δ-connected Thyistor Controlled Reactors for cancellation of fundamental flux component

Under each reactor, a high quality concrete platform with partial reinforcement is present. Reinforcing bars are furnished with plastic tubings in order to eliminate formation of closed-loops within the foundations under air-core reactors. The mounting platform is surrounded by an electrically conductive guard fence and also by copper grounding bars and conductors. If both ends of these parts were electrically connected, they would act as a closed-loop around the air-core reactor system thus carrying significant loop currents at harmonic frequencies as well as at fundamental frequency although it is located at a position sufficiently far from the artificial electromagnetic sources in view of the minimum clearances as recommended by the reactor manufacturer. This is because, especially in transient state, the sum of the fluxes produced by air core reactors would not be zero resulting in a time varying flux linked by the guard fence on one hand and grounding bars on the other hand. This is avoided by replacing a small part of the guard fence by an electrically non-conductive concrete column designed as a mounting surface for the system nameplate (Fig.4.22).

Equipment grounding copper bars are fixed to the surface of the mounting platform by the use of a nailing-gun. All metallic parts of the system are connected to the grounding bars by flexible connectors and stainless steel bolt and nuts resulting in a tree of grounding bars thus avoiding a closed loop and making sure that the length is kept minimum. Here again close loop formation in the major grounding bars is avoided by the aid of concrete column formed on the surface of the mounting platform. The loop formed by copper grounding bars and guard fence and surrounding the SVC installation entirely is named the major loop.

4.3.2 Medium Voltage Equipment Grounding System

The design of the grounding system has been carried out according to the present regulations. Before designing the grounding system special attention should be paid to the accurate assessment of the site's soil conditions. For some sites of TKI Enterprises, the surface is covered by limestone. However, in some others, surface is covered by high quality agricultural soil. Dealing with high soil resistivity and sites having limestone is an expensive and time-consuming task. Attempts in obtaining a successful grounding system usually fail (Fig. 4.23).
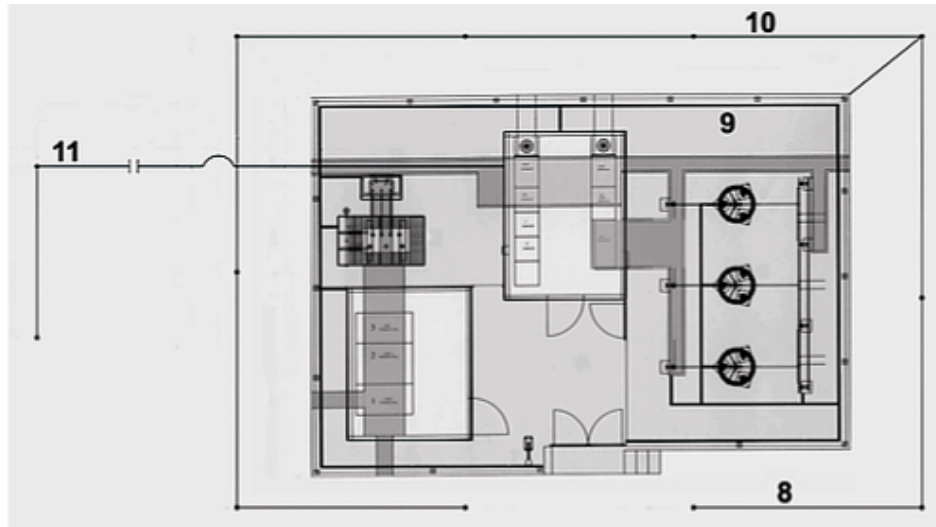
Fig.4.22. Grounding System 8- Medium Voltage Equipment and Electronic Grounding Systems, 9- Grounding Bars on the Platform, 10- MV Equipment Grounding system, 11- Connection to Electronic Equipment Grounding system

Grounding rods, 2.5 m in length, ¾" in diameter, have been used in the grounding system with a displacement of 5 m. First, the soil is drilled by a drilling machine thus forming a hole with a diameter of 30 cm and filled with coal powder and agricultural soil mixture as shown in Fig.4.23. The ducts containing 50 mm^2 copper grounding wires are also filled with this mixture.

Fig.4.23. Drilling holes for grounding rods

The grounding resistance of the each system was measured by the use of fall of the potential method using three probes. High grounding resistance was measured in the range from 13 to 15 ohms for the limestone sites. In order to have lower grounding resistance values, additional grounding elements (ground lattice in combination with chemical enhancement material-GEM) had been installed to these sites. Furthermore, soil conditioning had been achieved by spreading right amounts of salt (NaCl) onto the surface of the grounding area and watering. One year later, only a minor improvement was observed. Grounding resistance was measured to be 10 Ohms.

Fig.4.24. Ineffective attempts to reduce ground resistance for surface limestone sites

Following this experience, in the other sites of TKI Enterprises, first soil resistivity was measured. For sites having low quality soil was replaced entirely by a mixture of agricultural soil and coal powder or only the interfacing cylinder around the rod was conditioned by the same mixture. Grounding rods installed one by one following a measurement until a satisfactory ground resistance has been obtained. By this way, reasonably low grounding resistance values have been obtained in the range from 0.4 to 2.5 Ohms.

4.3.3 Other Measures Against EMI

Low voltage and medium voltage equipments have been placed into two separate EMI compatible containers, each of which acts as a Faraday's cage. In order to prevent interference from the operation of circuit breakers on both medium and low voltage sides, circuit breakers are also placed in metal cubicles well away from the SVC elements.

Operation of the semiconductors in SVC yields smooth current waveforms due to TCR nature and applied control philosophy. Only power frequency component and its even and odd harmonics are present. Shielded power and signal cables have been used. Shields have been grounded on one side to avoid loops. All cables used for measurement and control signals were twisted pairs. Special attention has been paid to the routing of gate cables, which carry high frequency firing pulses. Critical control cards and all switched mode power supplies were inserted into box type plug-in units.

Against transient over-voltage components owing to the conventional circuit breaker action and lightning surges, all electronic cards and the outputs of the measuring devices are equipped with MOVs and semiconductor type suppressors.

4.3.4 EMI Field Tests and Interpretation of Results

After installing the first SVC System, a series of measurements have been carried out in the field to test EM immunity of the system layout. Magnetic field distribution at different points on the surface of the mounting platform has been obtained by the use of a search coil (Coil data: N=500 turns, A=150 cm^2). Induced voltages across the terminals of the search coil are measured for a thyristor conduction angle of 180° (resulting in purely sinusoidal current waveforms). A typical induced emf waveform is as shown in Fig.4.26 for a thyristor conduction angle of 120°. The dominant component is the fundamental component (50 Hz) as expected for the specified operating conditions of TCR. Search coil voltages are measured at various points.

(a)   (b)

Fig.4.25. Measurement of the (a) Closed loop (b) Magnetic field on the SVC platform
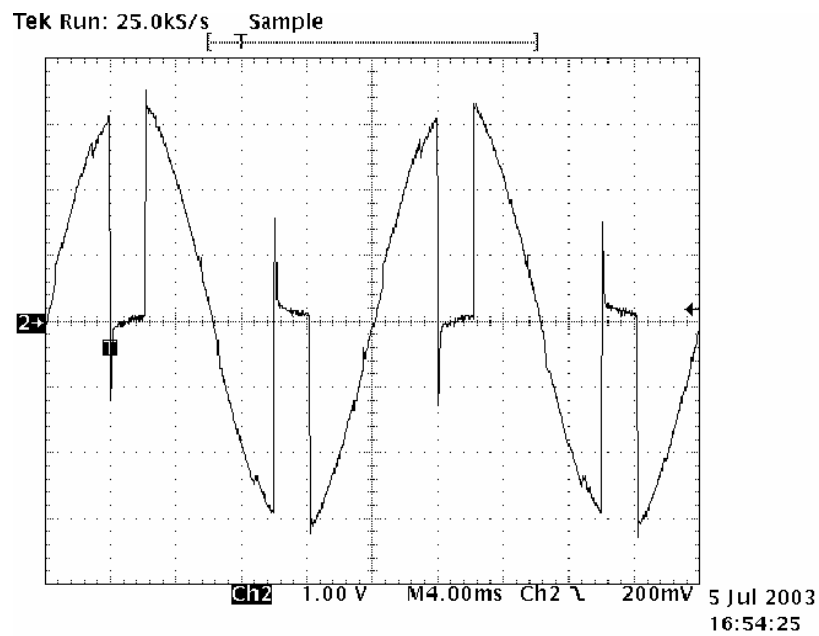
Fig.4.26. A typical induced voltage waveform (50 Hz) across the search-coil under the center of outermost reactor for a thyristor conduction angle of 120°

4.4 Field Tests

The performance of SVCs has been tested in the field since November 2001. The success of sizing study was evaluated by using the active and reactive energy consumptions given in the electricity bills belonging to the last seven months. It is found out that "inductive reactive energy / active energy" and "capacitive reactive energy / active energy" ratios of systems compensated by 1.5 MVAr SVC units are varying in the ranges of 3–21 % and 4–15 %, respectively. These variation ranges for 1 MVAr SVC units are 5–22 % and 3–16 % respectively for inductive and capacitive energy. 2 MVAr SVC unit installed in TKİ GELİ Enterprises keeps the variation of reactive energy ratio in the range of 0.2–3 % and 0.5-5 % respectively for inductive and capacitive energy. In view of new penalty limits of 33.3 % and 20 % respectively for inductive and capacitive reactive energy consumptions on monthly basis, SVC performances are found to be satisfactory in the compensation of rapidly fluctuating loads.

Fig.4.27 shows the variations in reactive power produced by SVC in comparison with the demand of the load bus. This five minute data have been collected in the field by data acquisition system and then processed. A similar record of SVC and load reactive power variations is given in Fig.4.27. As it can be seen from these waveforms, each SVC frequently works at its limit values. This is because each SVC has not been sized for full compensation but only for keeping active to reactive energy ratios on monthly basis within the penalty limits specified by utility authorities. It is also observed from the data collected in the field that each SVC can follow satisfactorily the variations in the reactive power consumption of the associated load bus.

163
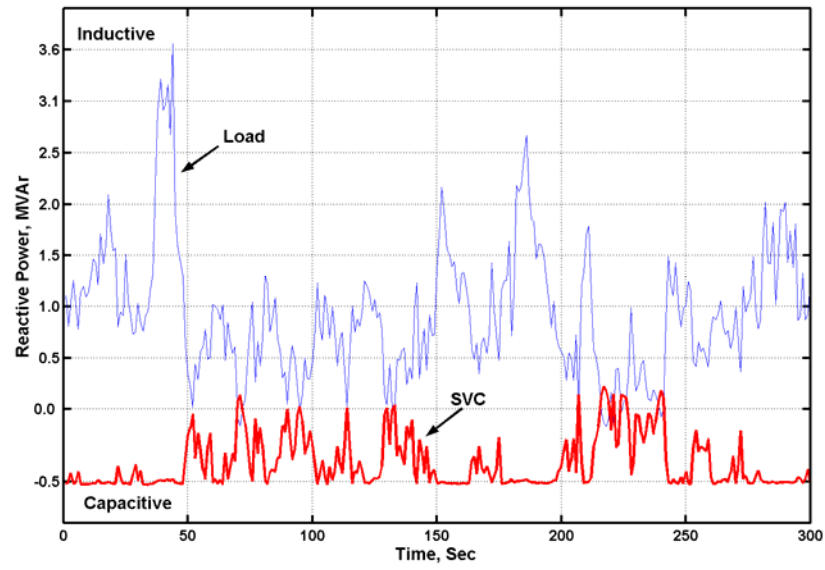
Fig.4.27. Variations in Reactive Power for Load and SVC (measured field data)
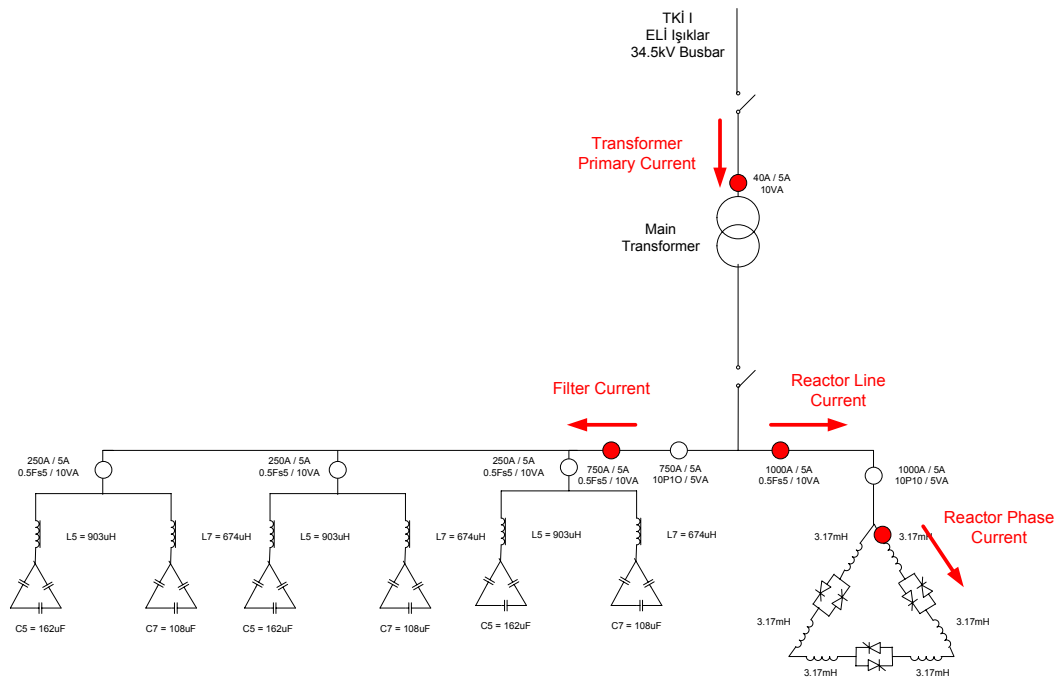
Fig.4.28. The data acquisition points in TKİ ELİ 34.5kV SVC System

In order to determine the harmonic content, the current waveforms of the 34.5kV SVC system in TKİ ELİ are recorded in the field. The existing current transformers in Fig.4.28 are used for data acquisition. The firing delay of the SVC is changed from 90° to 180° linearly in 90 seconds. The current harmonics are plotted in Fig. 4.29. Balanced operation and steady state conditions are assumed in this experiment.

Table 4.6 consists of the 5th and 7th harmonics existing in the waveforms. It is concluded that the 5th and 7th harmonics generated by TCR are mostly filtered by the 5th harmonic filters. It is also seen in Fig. 4.29.b that higher harmonics are also filtered up to 48% for 11th harmonic and 46% for 13th harmonic.

Table.4.6.   Maximum 5th and 7th harmonic currents in the system according to the field data

	Transformer Current referred to 1kV	Filter Current	Reactor Line Current	Reactor Phase Current
5th Harmonic current (rms)	34 A	49 A	46 A	26.7 A
7th Harmonic current (rms)	9.6 A	25 A	22.3 A	13.8 A

It is observed that in Fig.4.29.a, transformer currents have 3rd harmonic components especially when the firing delay angle is closer to 90°. It is because of the fact that the thyristor firing circuits have up to 2% of tolerance because of the measurement sensors and electronic components. This results in the slight angle computation differences in each phase of the TCR. When the firing delay is closer to 90°, the rate of change of the susceptance is high. As a result 3rd harmonic current is observed up to 1% of the maximum reactor line current because of the unbalance. The remaining part of the 3rd harmonic current is resulting from the 3rd harmonic in the medium voltage.
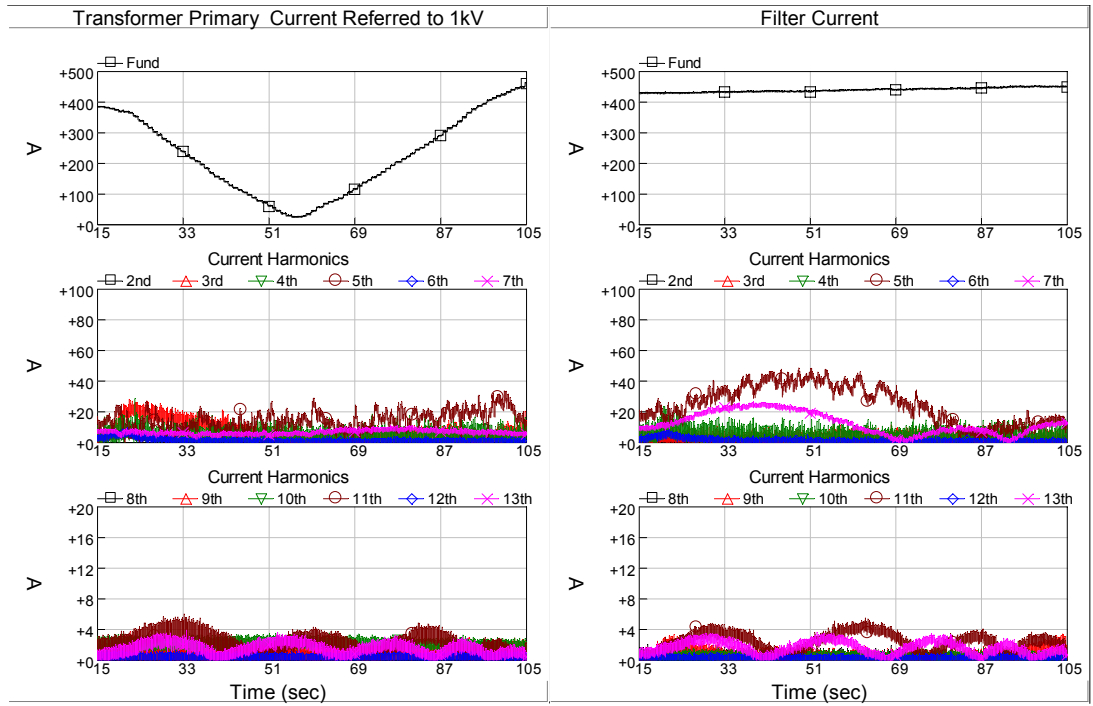
(a) (b)
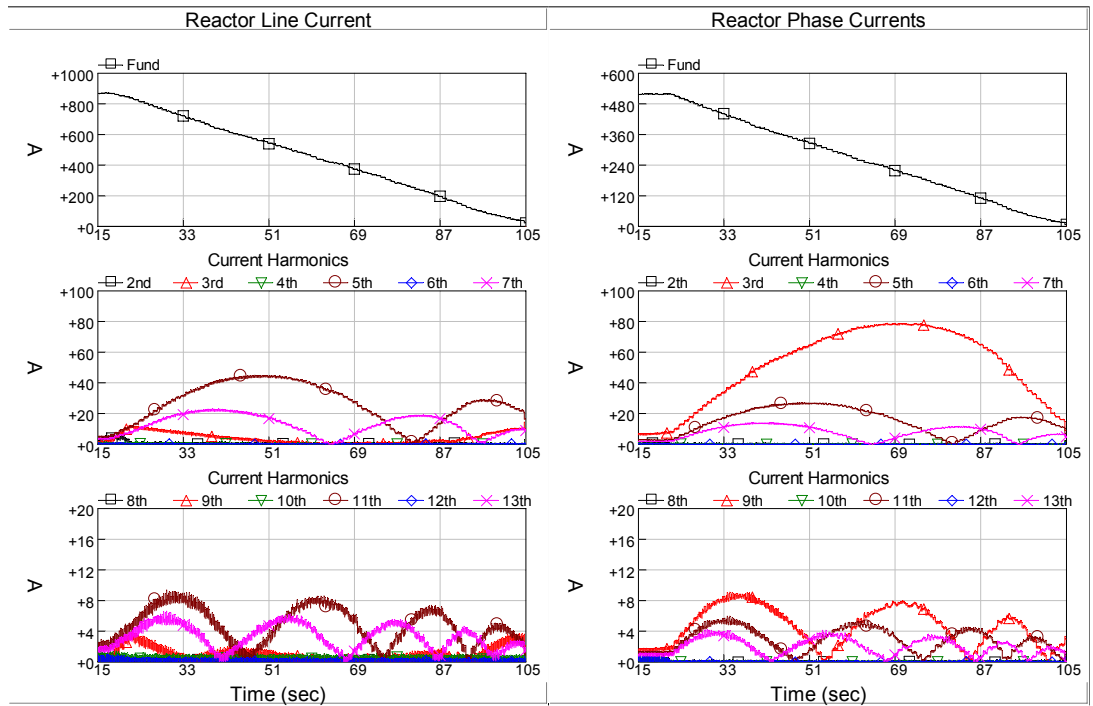
(c) (d)

Fig.4.29. : Rms current magnitudes for ramp reference change between 90°-180° firing delay angle in ELİ Işıklar 34.5kV SVC System

166

Individual 5th and 7th harmonic filter currents are investigated in BLİ 34.5kV SVC using the measurement points in Fig.30. It is seen that the 5th harmonic filter conducts 5th harmonic current flowing from the load through the coupling transformer up to a magnitude of 12% of its fundamental current. 7th harmonic filter conducts 7th harmonic current flowing from the load through the coupling transformer up to a magnitude of 9% of its fundamental current. The SVC filters therefore filter not only the TCR harmonics but also the harmonic currents flowing from the load as seen in Fig.31. Even harmonics and higher order harmonics are also filtered as seen in Fig.36 and Fig.38.

Although the current waveforms are distorted, the SVC still complies with the harmonic standards in the steady state operation. The harmonic currents sometimes flow from the supply side, which are produced by other customers connected to the same overhead line. In this case, harmonic currents of these customers should also be measured in order to investigate the real content of the TDD resulting from the electrical excavators in TKİ enterprises.
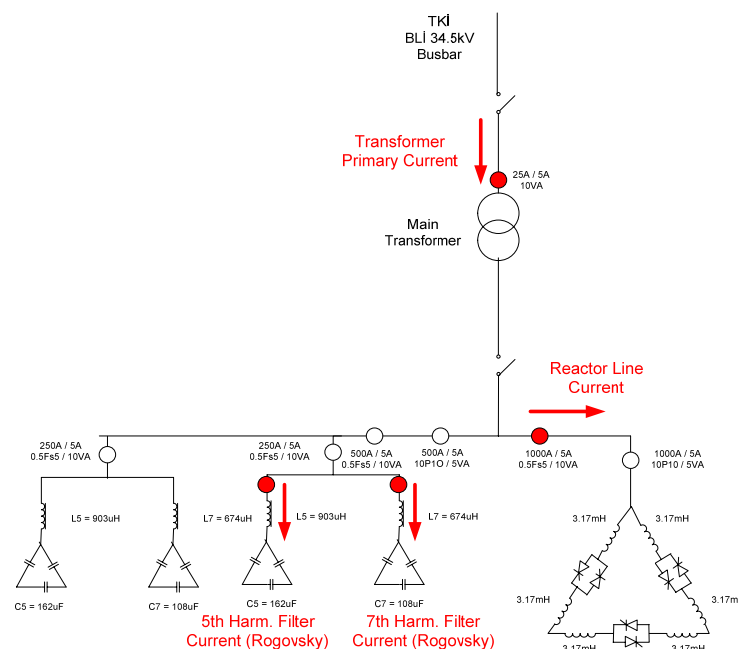
Fig.4.30. Measurement points for the investigation of individual filter currents in BLİ 34.5kV SVC
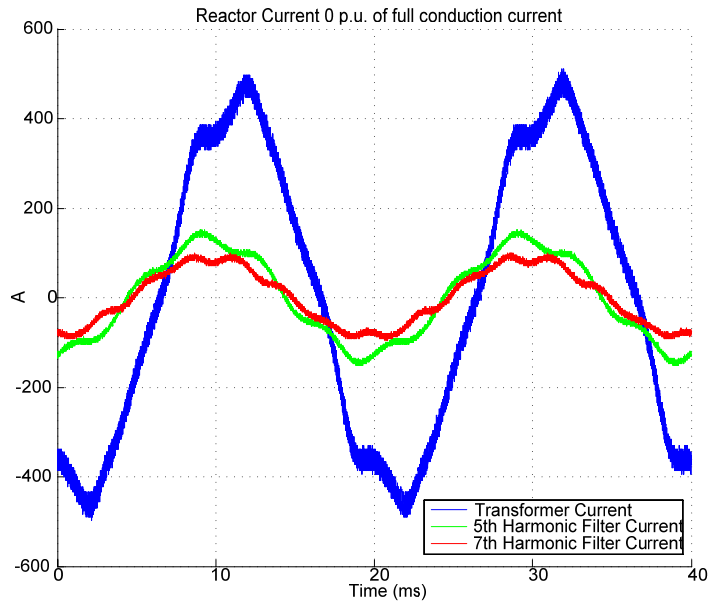
Fig.4.31. Measured currents for 0 p.u. of full conduction current of TCR
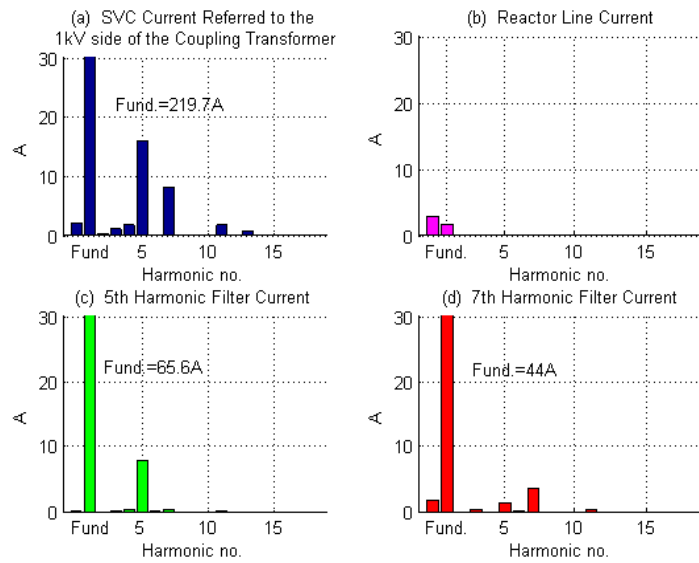
Fig.4.32. Harmonic analysis of the currents in Fig4.31.
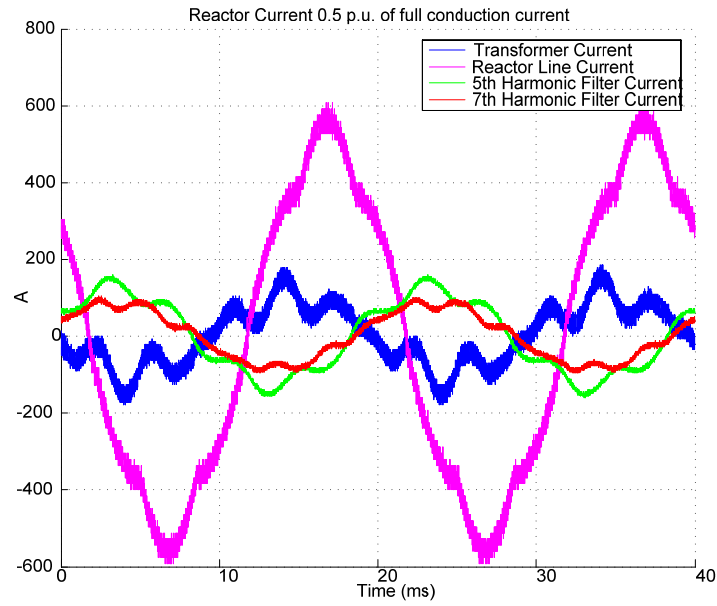
Fig.4.33. Measured currents for 0.5 p.u. of full conduction current of TCR
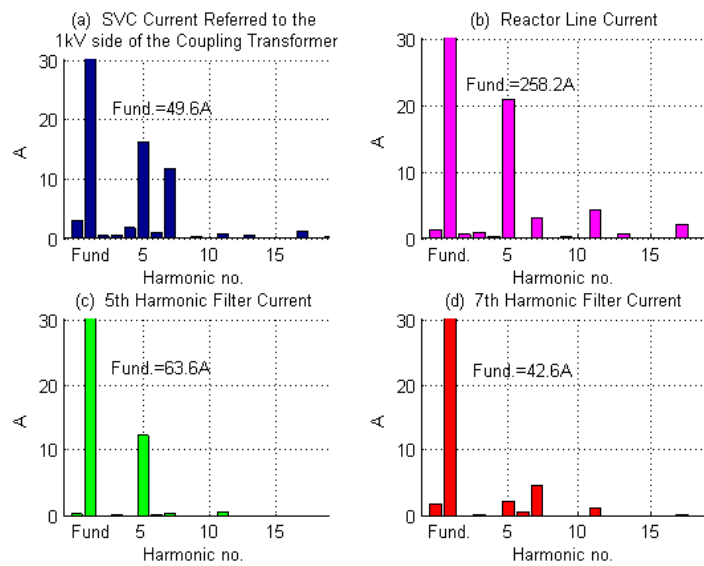
Fig.4.34. Harmonic analysis of the currents in Fig4.33.

169
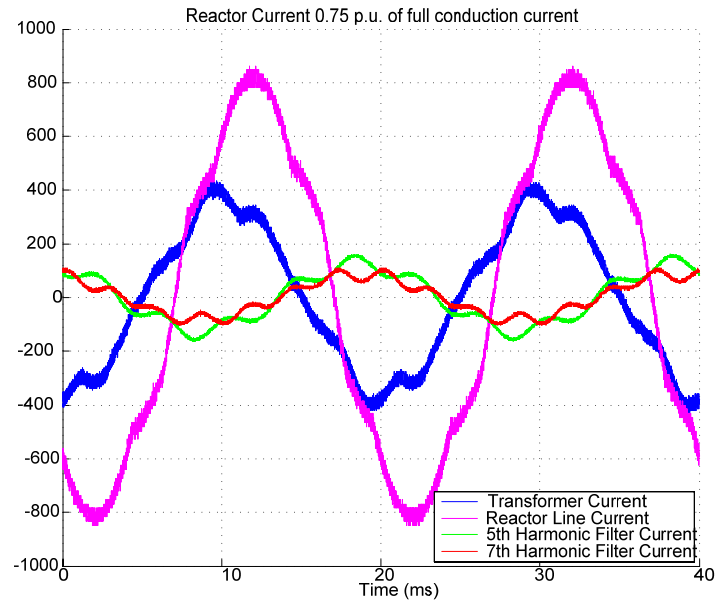
Fig.4.35. Measured currents for 0.75 p.u. of full conduction current of TCR
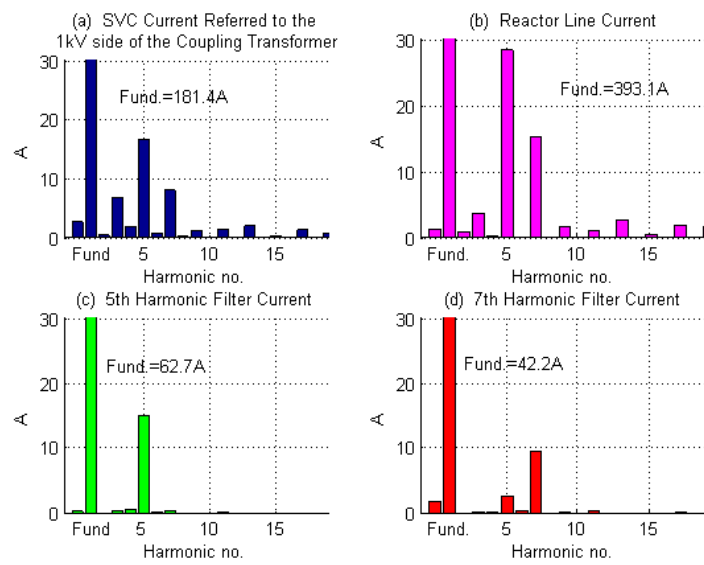
Fig.4.36. Harmonic analysis of the currents in Fig4.35.

170
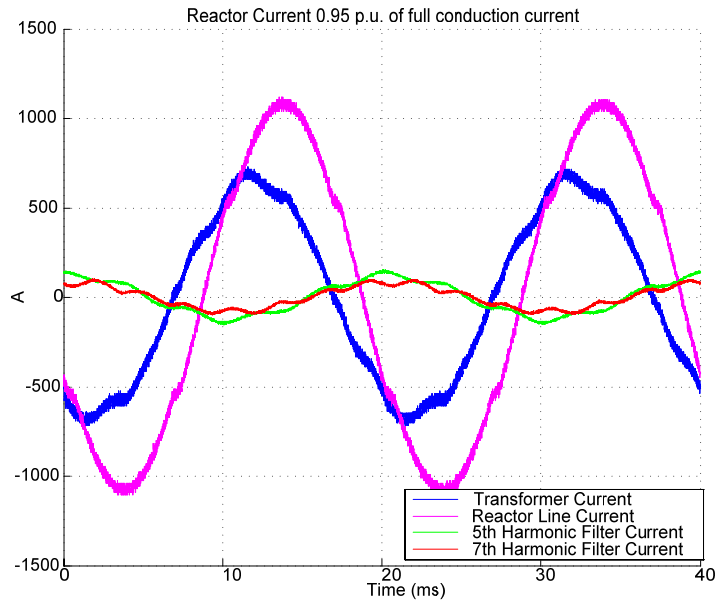
Fig.4.37. Measured currents for 0.95 p.u. of full conduction current of TCR
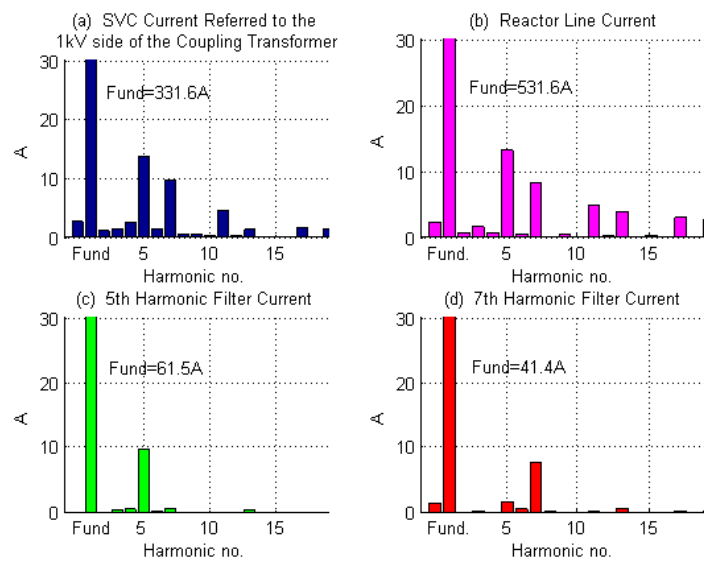
Fig.4.38. Harmonic analysis of the currents in Fig4.37.

The voltages across the terminals of the thyristor and reactor currents are recorded using an oscilloscope as seen in Fig.4.40 – Fig.4.42. The TCR current is changed manually and waveforms for 25%, 50% and 95% of the full conduction current are captured as seen in Fig.4.40, Fig.4.41 and Fig.4.42 respectively. When the thyristor line commutation occurs, there is an overshoot across the thyristor stack because of the snubber currents in the thyristor reverse recovery period. The snubber voltage is initially a few Volts and whenever the thyristor commutation starts, a step voltage with a magnitude equal to the line voltage is seen at the terminals of the thyristor stack. The R-L-C circuit formed by the snubber components and the air core reactors cause limited voltage overshoots as a function of conduction angle and line voltage. In the 1.5 MVAr BLİ SVC system, these overshoots are 129% of the peak line voltage as seen in Fig.42, which is acceptable according to the stack design. The DYNEX DCR1476-SY thyristors used in the stack have 3400V reverse blocking voltage. The snubber circuit displays an under-damped response. Choosing a damping factor of 0.5-1.0 is a common practice in the snubber design because low damping factor causes large overshoot of the transient voltages [38]. In 1.5MVAr thyristor stacks used in the SVCs the damping factor is 0.79. Over-damped snubbers are not preferred because of the excessive losses. A typical snubber current and snubber current in the transient can be seen in Fig.45 and Fig.46 respectively.
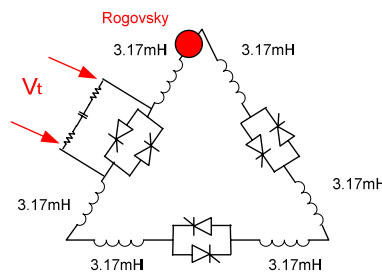
Fig.4.39. Measurement points for the investigation of Thyristor Voltage and Phase Current
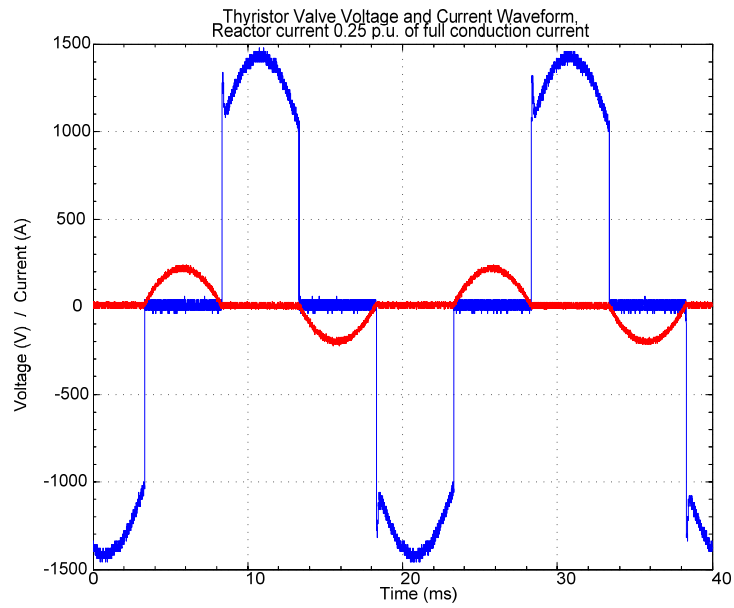
Fig.4.40. Thyristor terminal voltage and reactor phase current recorded for 0.25 p.u. of the full conduction current.
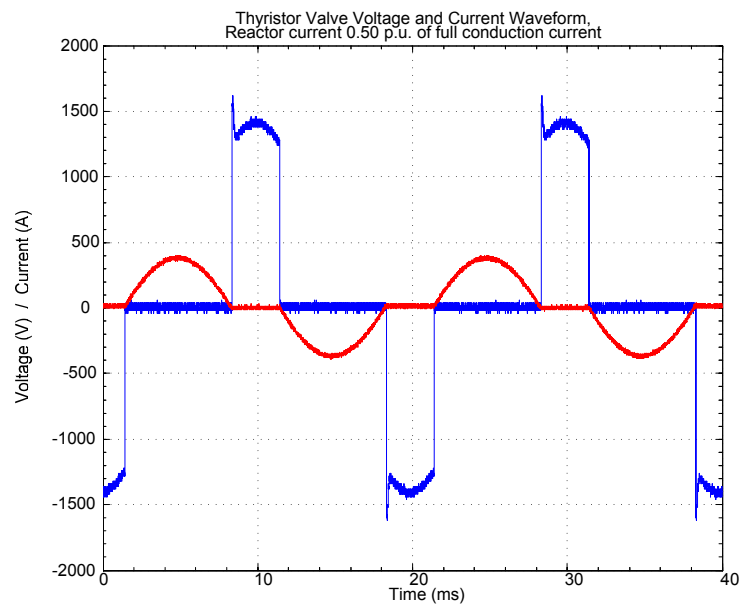
Fig.4.41. Thyristor terminal voltage and reactor phase current recorded for 0.50 p.u. of the full conduction current.

173
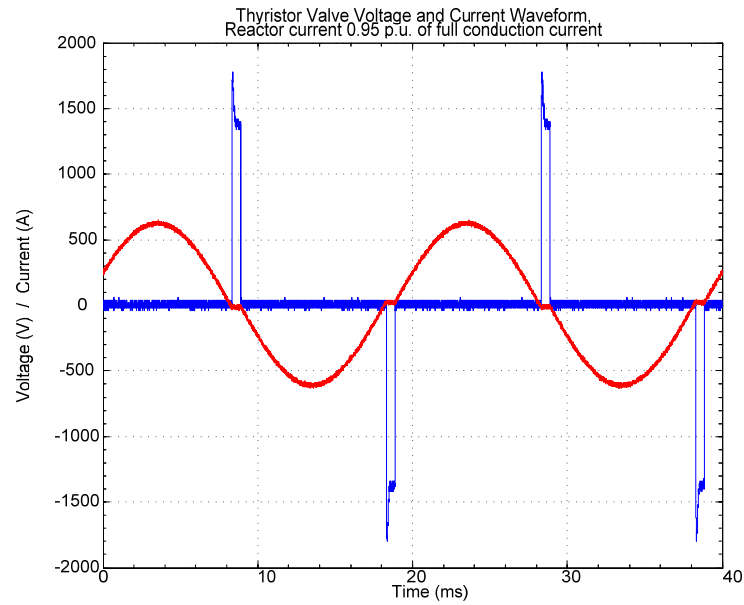
Fig.4.42. Thyristor terminal voltage and reactor phase current recorded for 0.95 p.u. of the full conduction current.

The transient operation of the SVC is observed in TKİ BLİ 34.5kV SVC system. The load and SVC currents are seen in Fig.4.43.a and Fig.4.43.b respectively. 1-minute current recording is analyzed for harmonics and interharmonics and results are plotted persistently in Fig.4.43.c and Fig.4.43.d. It is seen that interharmonic content of the SVC is proportional to the load current. It is observed that the interharmonic components are lower than 46% of the load current interharmonics.

174
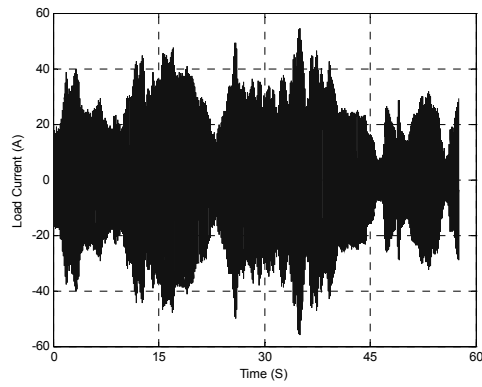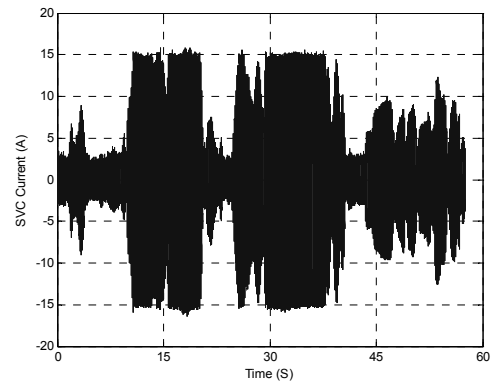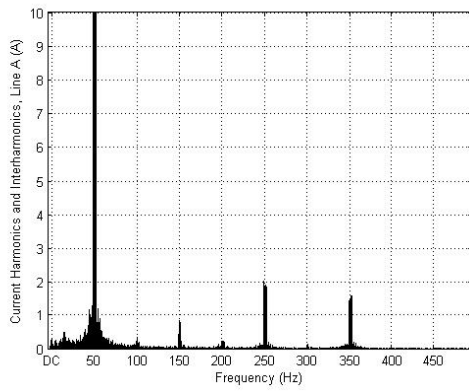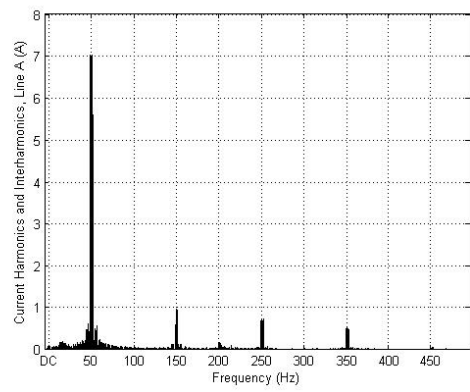
Fig.4.43. Load and SVC currents in view of harmonics and interharmonics in TKİ BLİ 34.5kV SVC; (a) Load Current, (b) SVC Current; (c) Load current persistent harmonic spectra (1 minute); (d) SVC current persistent harmonic spectra (1 minute)
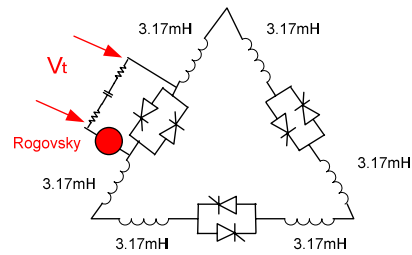
Fig.4.44. Measurement points for the investigation of Thyristor Voltage and Snubber Current
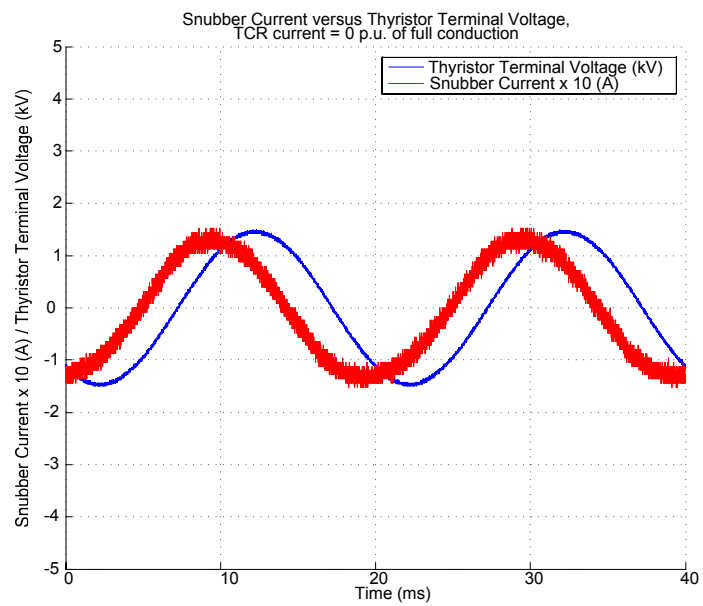
Fig.4.45. Thyristor terminal voltage and snubber currents, TCR current is 0 p.u. of full conduction current, the TCR firing is halted.
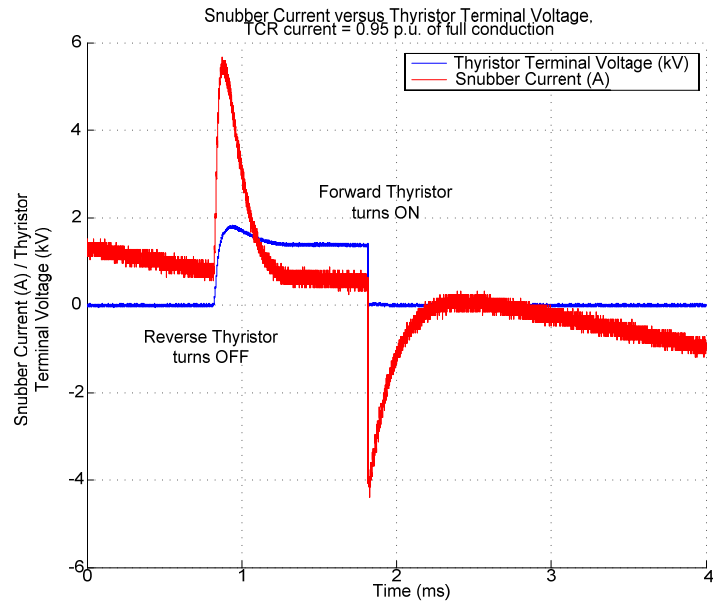
Fig.4.46. Thyristor terminal voltage and snubber currents, TCR current is 0.95 p.u. of full conduction current

The control circuit is first simulated in the PSCAD with the real time currents and voltages recorded in the field in order to investigate the TCR performance prior to installation. The simulation is prepared in PSCAD and the field data are converted to the acceptable data format of PSCAD. TCR system designed for ÇLİ Enterprise is modeled in PSCAD. The TCR rating is 1.5 MVAr and the HF rating is 0.25 MVAr. The SVC coupling transformer is chosen ideal with a U_k rating of 5%.
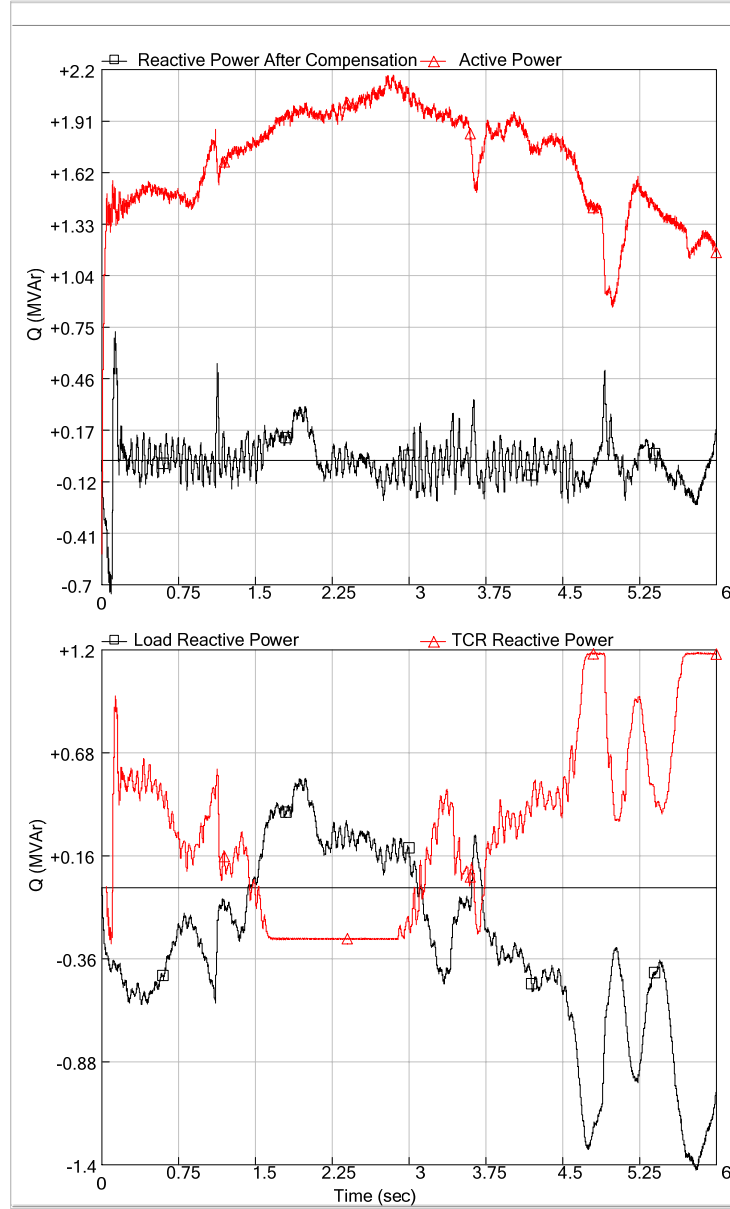
Fig.4.47. . Evaluation of Modelled SVC in TKİ ÇLİ 34.5kV SVC system.

As seen in Fig.4.54, the compensation of the load is analyzed by using the data recorded in the field. It is seen that SVC PI control time constant set to 38ms is sufficient for the compensation, keeping the ratio of inductive reactive energy to active energy less than 11.3% and the ratio of capacitive reactive energy to active energy less than 3.4% in this case.

With the help of simulations, the time constant of the PI regulator is chosen as 38ms in the SVCs designed for the compensation of open cast lignite mines. Proportional gain is 0.2, Integral gain is 0.45 and the feed-forward gain is 0.133. Increasing the proportional gain over 1 led to oscillations and unnecessary overshoots in the TCR response in the simulations.

After the systems are installed, response characteristics of the TCR are also verified by the field data acquisition. In order to be able to obtain the TCR response, the control circuits of the TCR are modified as seen in Fig.47. Feedback loop is modified because the load current will not be evaluated in the step response tests. In order to investigate Open loop characteristics seen in Fig.48, firing delay angle set is directly given to the control circuit. It is observed that TCR reached 90% of the reference in 13ms. In order to be able to investigate PI regulator response with the default time constant settings, a step reference input is fed to the system as seen in Fig.47. Just for the first part of this experiment, feed-forward is disabled. By this way, a step change of load in the modified scheme can be simulated by external reference square wave input. It is seen in Fig.49 that the TCR reactive power reaches steady state in 140ms.

Feed-forward is enabled again to see the real performance of the control circuitry. With default settings, where PI time constant is 38ms, the step response of TCR is about 120ms. In order to see a faster response, time constant of the PI regulator is reduced to 25ms. The new response of the system is seen in Fig.51. The response time reduced to 90ms. The time constant is further reduced to 15ms to obtain the response waveforms in Fig. 52. It is seen that the response time reduces to less than 60ms with the PI time constant setting of 15ms.
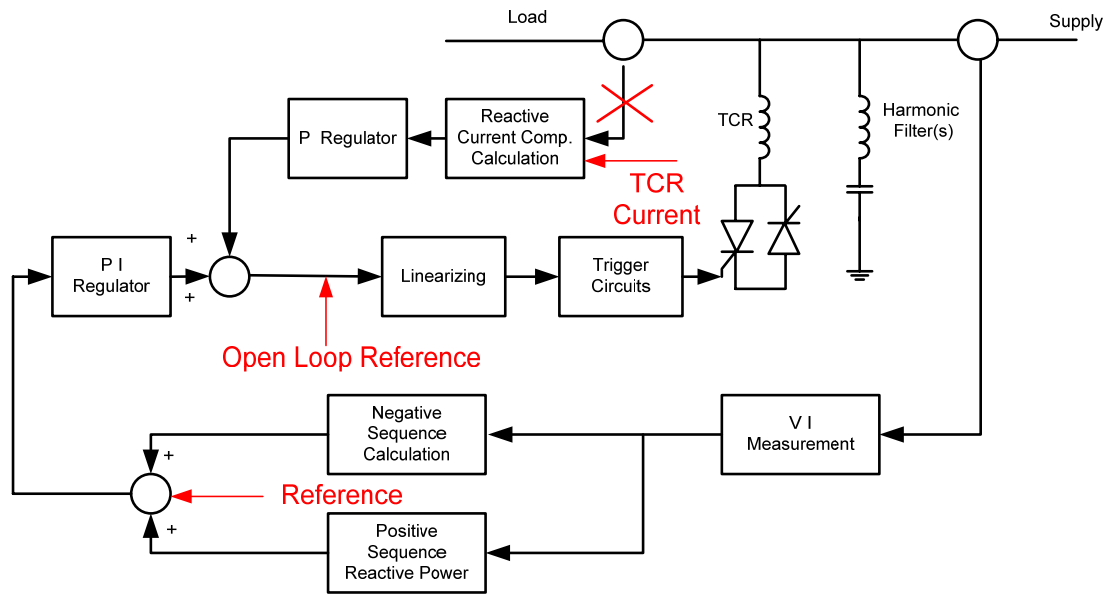
Fig.4.48. Modifications in the control system for measurement of TCR Response
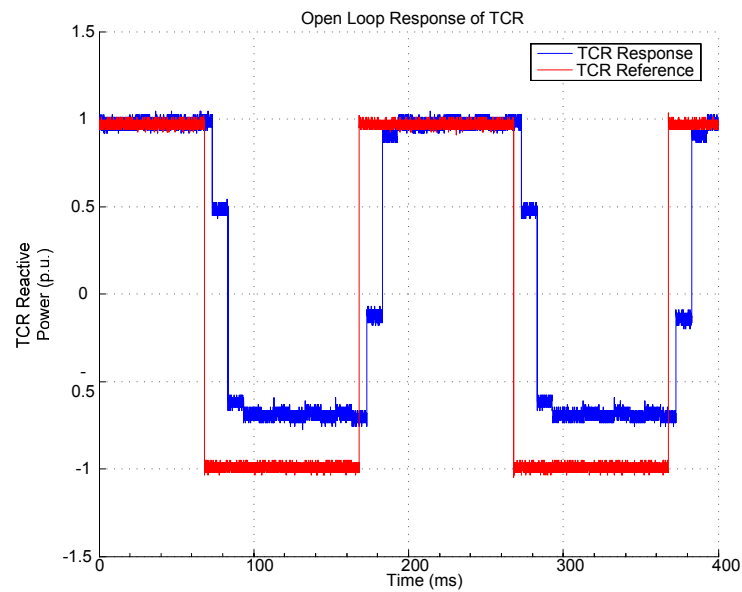
Fig.4.49. Investigation of Open Loop response of the BLİ 34.5kV TCR by applying the necessary modifications in Fig.4.47.
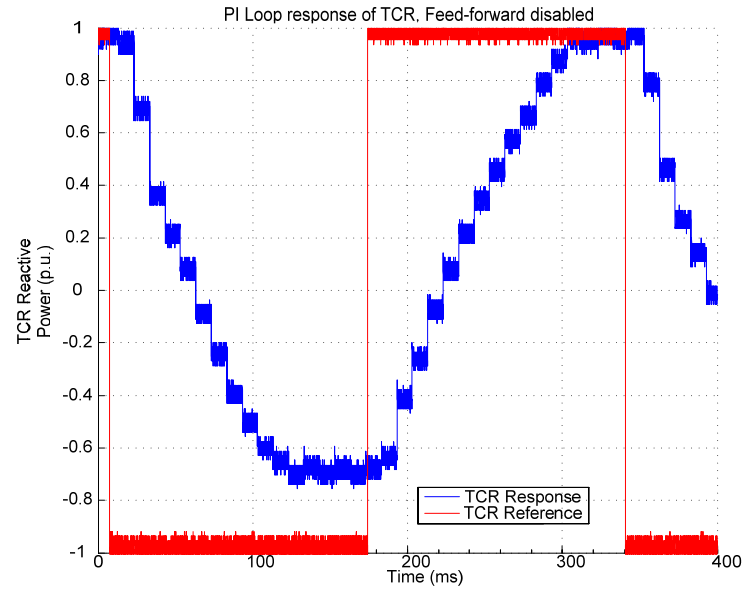
Fig.4.50. Closed Loop PI regulator response of the BLİ 34.5kV TCR, the feed forward is disabled by applying the necessary modifications in Fig.4.47
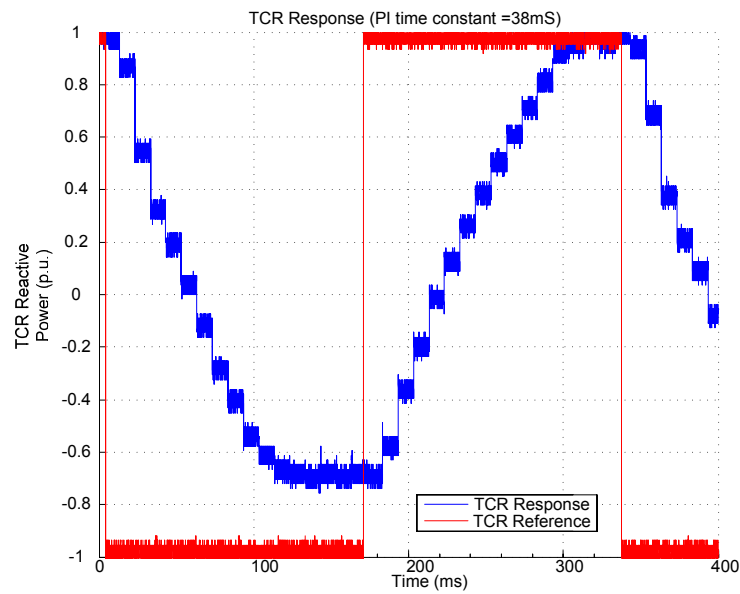
Fig.4.51. Closed Loop response of the BLİ 34.5kV TCR, both feed forward and PI regulator are enabled. PI time constant is set to 38ms.
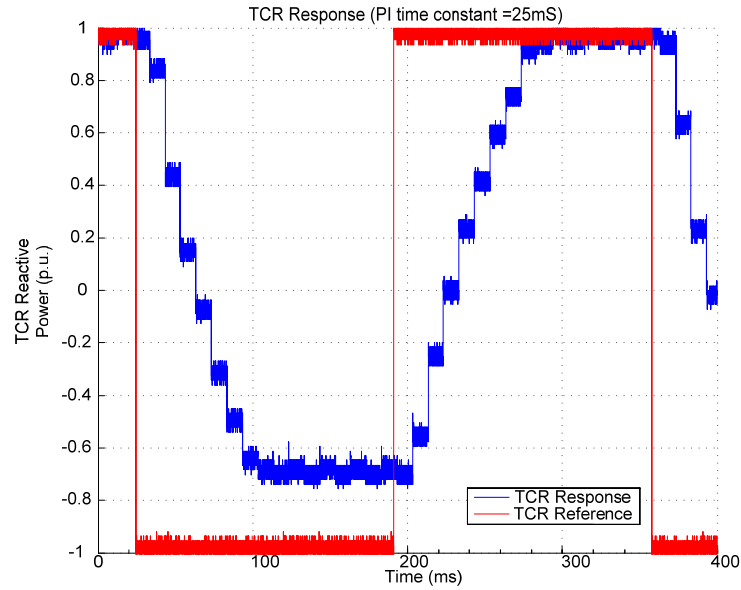
Fig.4.52. Closed Loop response of the BLİ 34.5kV TCR, both feed forward and PI regulator are enabled. PI time constant is set to 25ms.
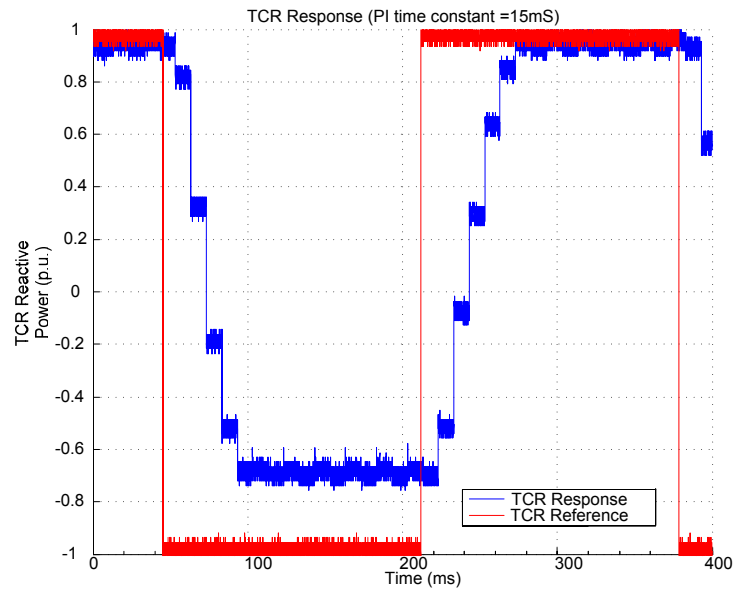
Fig.4.53. Closed Loop response of the BLİ 34.5kV TCR, both feed forward and PI regulator are enabled. PI time constant is set to 15ms.

The system sizing and field result verification are achieved by the simulations evaluated in EMTDC PSCAD program. For this purpose, the 3-phase equivalent circuit of the system including the loads and the mains is first obtained. Two different approaches have been used in the simulation of rapidly changing loads. These are:

a-   The use of standard 6-pulse ac-dc converter, transformer and electrical machine tools available in PSCAD.

b-   In this approach, the rapidly changing loads are represented by current and voltage data collected in the field by data acquisition system at a sampling rate of 3.2kS/s, thus replacing the load models in (a). The file containing current and voltage data is then integrated into PSCAD/EMTDC, and real time data are synchronized with the time base in simulation.
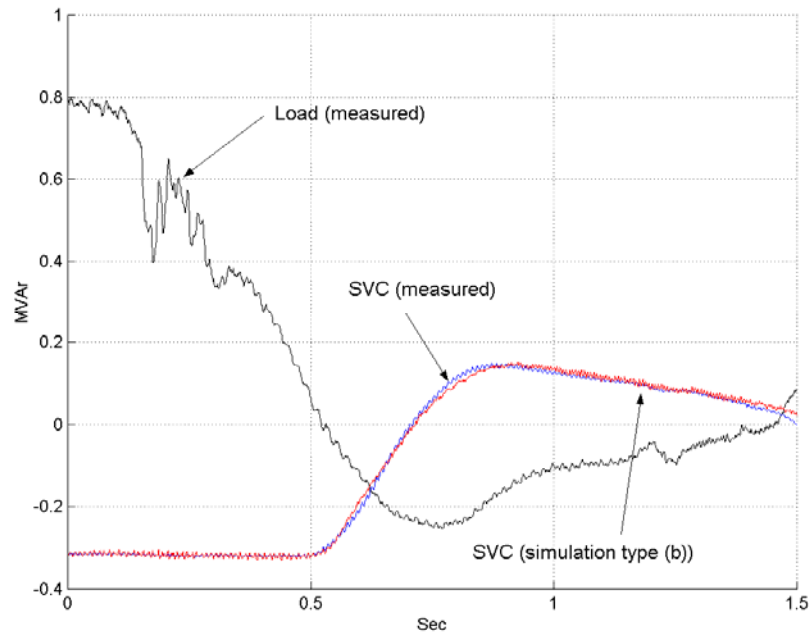
Fig.4.54. Theoretical and experimental response of SVC to measured load data in TKİ Deniş 34.5kV SVC system. (evaluated in PSCAD Simulation)

The response time of each SVC has been adjusted to an optimum value thus reducing direct-current and even order harmonic components that will appear in SVC lines. In order to test the validity of simulation approach (b), the theoretical results are compared with data collected in the field. A sample waveform segment is given in Fig. 4.53. A good correlation between actual SVC variations and the results of simulation type (b) has been observed

4.5 Relocating the SVC

The need for relocation in the open cast lignite mines may be required because of the landslides and other natural disasters. Underground mines also cause cracks on the surface, which is called "Tasman Cracks". Because of the nature of the lignite mines, four SVC systems had to be relocated due to the landslides within 2001-2007. Fig.4.55 shows the great natural disaster occurred in BLİ Lignite Mine. A huge amount of land slipped into the mine, including the BLİ transformer substation. Thanks to the modularity and ease of relocation, SVC had been demounted and transported within just 6 hours. The relocation process is shown in Fig.4.56.

The new concrete platform had been prepared before the process began. All the connection points and any new supporting equipment were prepared at the new location site in BLİ. Typical steps in the re-location are as follows:

- De-energizing and grounding (Fig 4.56.a-b)),

- Labeling of the main parts, busbars, cables and supporting materials (Fig.4.56.c),

- Cables and busbars are disassembled, (Fig.4.56.d)

- Reactors are disassembled (Fig 4.56.e),

- Medium voltage current transformers are replaced by jumpers or other equipment and medium voltage connections are terminated,

- Container connections are extracted,

184

- All equipment is transported to the new installation site and placed on the new platform, (Fig.4.56.f-g)

- Main parts, busbars, cables and supporting materials are mounted and connected,

- Medium voltage current transformers are mounted,

- System tests are carried out,

- System is energized and commissioned as stated in the documentation.

(a)

(b)

Fig.4.55. (a) Landslide near TKİ BLİ SVC System (b) Tasman cracks and partial landslide near TKİ ELİ SVC Systems

Fig.4.56. Step by step relocation of the SVC system in TKİ BLİ because of the landslide (a-h).

4.6 Discussions

Design and implementation of unified, relocatable and extendable static VAr compensators have been carried out successfully on various open-cast lignite mining enterprises in Turkey. Ease of demounting, transportation, erection, and commissioning constitute the major features of the system as a relocatable compensator. The unified compensator can be connected to an overhead line or load bus of different voltage levels with minor modifications, and it is designed to operate satisfactorily under different environmental/climatic conditions. The system is designed to be a flexible and extendable one in order to meet the possible future needs of the enterprises. Reactive power demand of each load bus before and after compensation has shown the validity of the proposed design method based on PSCAD/EMTDC simulations of various excavator loads of enterprises, using actual data obtained by means of a data acquisition system in the field.

The steady state and transient performance of the TCRs are investigated in the field tests. It is verified that the response of TCR is adequate to successfully compensate the electrical excavator type loads operating in open cast lignite mines. Monthly energy-meter readings have been far below the penalty limits until 2008 where stricter penalty limits are imposed by the EPDK. Thanks to the modularity of the SVCs, the systems are easily upgraded to meet the new regulations.

Response time of the TCR control system is verified in the field and gave satisfactory results. The response time can further be reduced below 60ms for faster loads. Excavator loads with thyristor controlled rectifier units have shorter time constants but still they are bounded by the mechanical time constants of the DC motors which may be up to a few hundred milliseconds. Ward Leonard drives have softer characteristics. Harmonic filtering is not considered because there are 5th and 7th harmonic filters on the excavators with thyristor based motor drives. Ward-leonard type excavator currents have slight 2nd and 3rd harmonics but they usually don't need filters.

In the steady state of the TCR operation odd harmonics are as expected as seen in the field tests. However in the dynamic operation, even harmonics and interharmonics are observed, which also contributes to flicker problem. 4th harmonic

187

component was the most effective even harmonic because the modular 5th harmonic filter units have a parallel resonance path which amplifies the 4th and the 6th harmonic. Because of the unbalanced transient operation, TCR generates even harmonics. These even harmonics flow into the filters and the supply. In figure 4.57, L_s is the source inductance, L_t is the transformer inductance and the filter impedance is decomposed into R-L-C components for the simulation of the harmonic flow. Each system has different L_s and L_t. According to the simulations 4th harmonic can be amplified up to 13 times as seen in Fig.4.58.
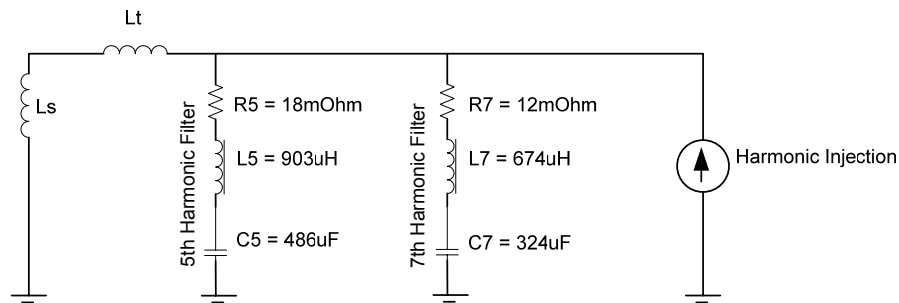
Fig.4.57. Parallel resonance circuit composed of filter, transformer and supply reactance, L_s is the source inductance, L_t is the transformer inductance

In order to reduce the harmonic amplification and to filter 4th harmonic, a permanent 4th harmonic filter to the SVC installed in the YLİ. In the other SVC systems, the 4th harmonic and 6th harmonic currents were below the design specifications.
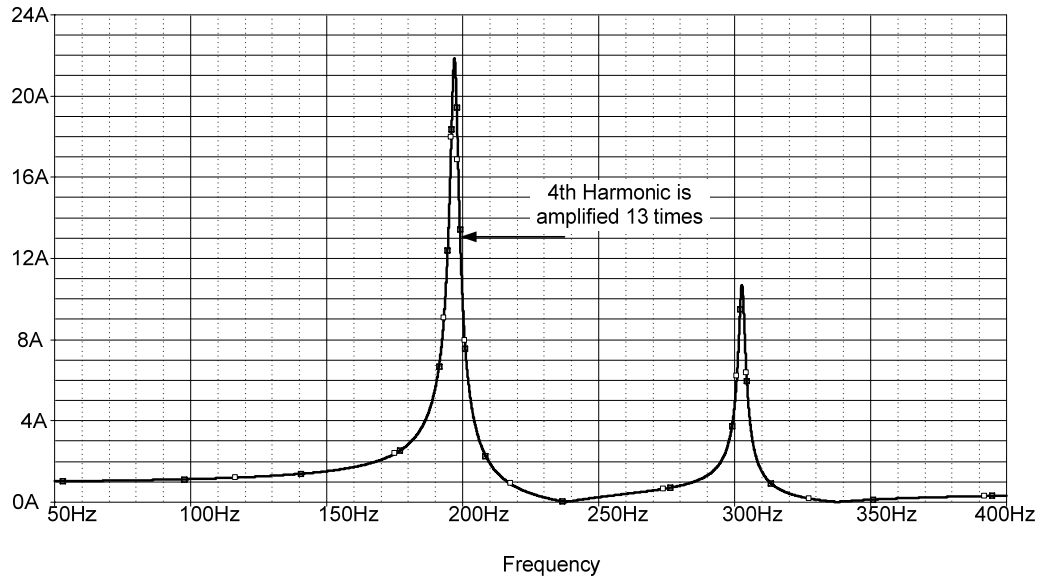
Fig.4.58. Frequency analysis of the YLİ 5th and 7th HF groups.

Because of the landslides, Tasman cracks and modernization purposes, the systems were relocated several times. Relocation of the systems was successful In 2-4 days, the whole SVC system can be relocated and commissioned. In order to reduce this time, mobile systems can also be designed. Penalty limits are not reached in one month time period by decommissioning the SVC up to 5 days, therefore mobile system is not a necessity at this time. TCR air core reactors can be replaced with iron core reactors and placed in the cabin but heat and saturation problems have to be considered.

CHAPTER 5

CASE STUDY 2 : 12 PULSE TCR OPERATION FOR LADLE FURNACE COMPENSATION AND POWER SYSTEM REDUNDANCY

5.1 Design Considerations for 12-pulse TCR Operation in Heavy Industry

Owing to non-linear and stochastic nature of the electric arc furnace (EAF) as a load, various furnace parameters such as the furnace voltage and current, the real and reactive power as well as the furnace resistance and reactance exhibit significant and sudden variations in time, especially during the scrap melting [5]. These variations cause harmonic and flicker problems at the Point of Common Coupling (PCC) which can be overcome by increasing the short-circuit MVA of the PCC and/or using flicker compensation systems.

However in a ladle furnace; flicker, reactive power, unbalance, and harmonic problems are not as severe as those of AC EAFs. If the short-circuit MVA rating of the bus bar to which the ladle furnace is connected is high enough, then only harmonic and reactive power compensation problems arise. The use of permanently connected shunt harmonic filters tuned to second and third harmonics together with 12-pulse Thyristor Controlled Reactor (TCR) can be a simple and low-cost solution to this problem. A 12-pulse TCR does not produce theoretically the most significant odd current harmonics such as 5th, 7th, 17th and 19th owing to delta and wye connected transformer secondaries [3-5].

The 20 MVA ladle furnace in Iskenderun Iron and Steel Works Inc. (ISDEMIR) is equipped with a 13 MVAr permanently connected shunt harmonic

filter (HF) tuned to 150 Hz and supplied from 154 kV dirty bus via 40 MVA, 154/34.5 kV power transformer. Within the scope of an upgrading work, 2x6 MVAr, 12-pulse TCR system has been designed and implemented for connection to the 34.5 kV ladle furnace bus. This upgrading work resulted in a low cost solution because some of the infrastructure and system components such as circuit breakers, disconnectors, and air core reactors, etc. which are present in ISDEMIR but not in use are employed in this work. The two 6-pulse TCRs are connected to 34.5 kV ladle furnace bus via two separate dissimilar transformers. One of the transformer is chosen with a sufficiently large rating in order to allow supplying the ladle furnace from an alternative path in emergency or during maintenance periods of main power transformer resulting in a redundant power system. The performance of the resulting system in the field is found quite satisfactory from the viewpoint of harmonic standards [35,39] and reactive energy regulations [33,34] currently in use in the country.

(a)

(b)

Fig.5.1. (a) The Ladle Furnace (120 metric tones) (b)Molten steel towed out of the furnace

Fig.5.2. Upgraded Power Distribution System of Ladle Furnace

192
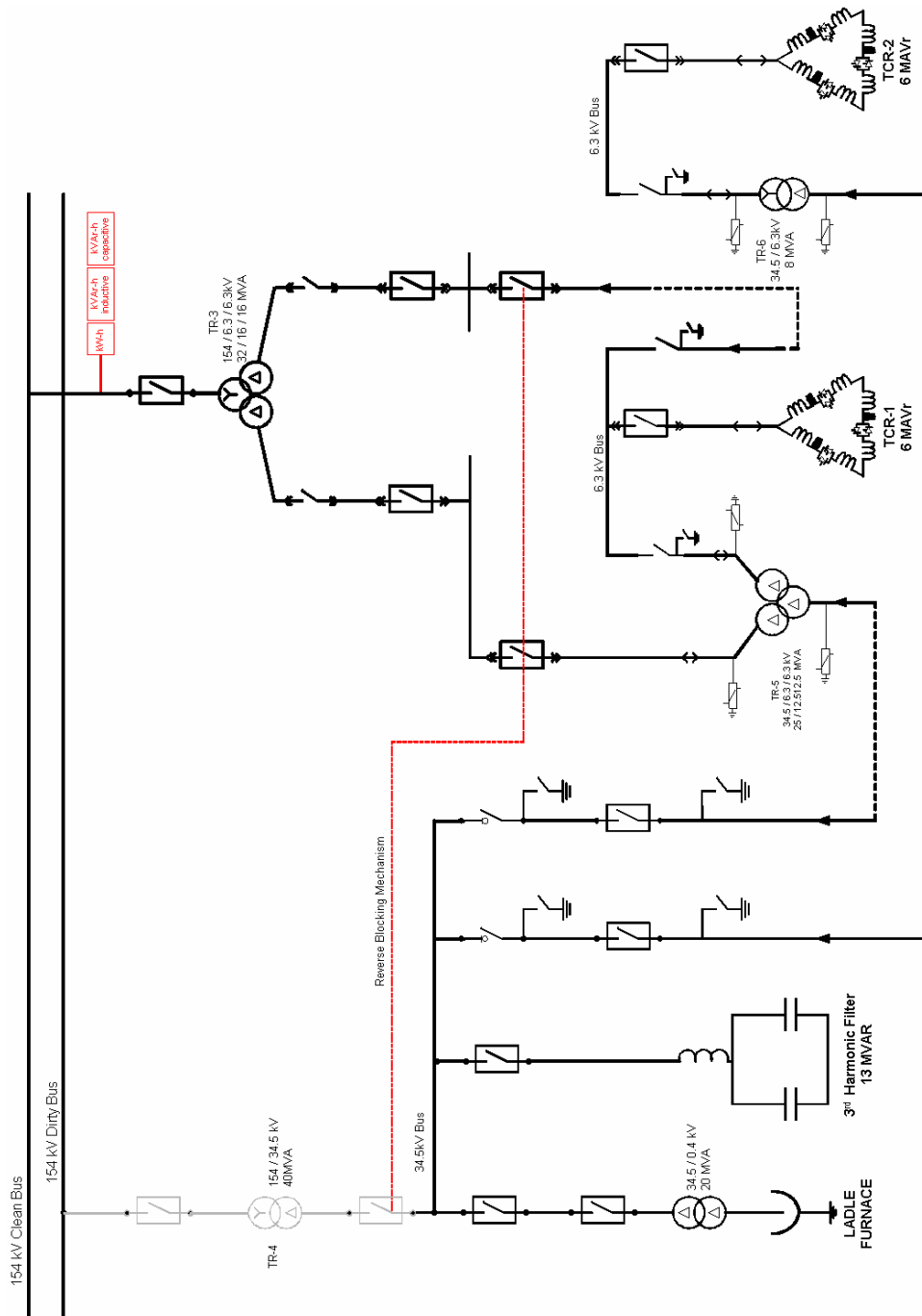
Fig.5.3. Emergency Supply Scheme

193

Fig.5.4. Existing 13 MVAr 3rd Harmonic filter of LF.

5.2 Engineering Aspects

5.2.1 Load Identification

Iskenderun Iron and Steel Works is one of the largest iron and steel plants in Turkey. Throughputs of blast furnaces are partly processed metallurgically before tapping by a ladle furnace, which is supplied from 154 kV main bus via a 40 MVA, 154/34.5 kV Y/Δ connected power transformer and 20 MVA, 34.5/0.4 kV Δ/Δ connected furnace transformer (Fig.5.2). The 154 kV main bus can be taken as Point of Common Coupling (PCC) for the dirty load and other clean loads. The ladle furnace had been originally equipped only with a permanently connected 13 MVAr, 34.5 kV 3rd harmonic shunt filter (Fig. 5.4).

According to the regulations in 2001-2007, the inductive reactive energy and capacitive reactive energy consumptions in monthly electric bills should not exceed respectively one-third and one-fifth of the associated active energy consumption. In the year 2003, this made necessary keeping the average power factor of the industrial plant on monthly basis between 0.95 lagging and 0.98 leading. Penalty limits

computed from new regulations for inductive- and capacitive-reactive energy on monthly basis are also marked on Fig. 5.5. At the present time according to a national regulation, there is no pecuniary penalty for the violation of harmonic limits [39], but the local electricity authority may refrain from selling electricity to the consumer which violates harmonic limits. Therefore, it is not possible to solve the reactive power compensation problem of the ladle furnace by disregarding harmonics.

Table5.1. Energy Consumptions of Ladle Furnace (Field data).

Status of Ladle Furnace System		Reactive energy as a percentage of active energy, %	
		Inductive	Capacitive
Before Compensation	Without Filter	78.5	3.6*
	With Filter	0.1	329.1
After Compensation (With Filter)		8.1	4.7
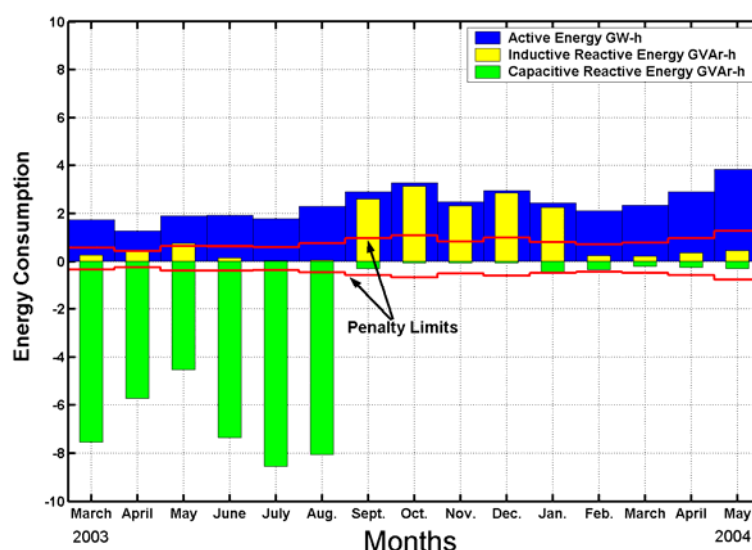
Fig.5.5. Monthly active and reactive energy consumptions of the ladle furnace (penalty limits are also marked)

5.2.2 System Sizing and Current Harmonics Considerations

Current harmonics injected into the distribution system by the ladle furnace are also obtained from the line current measurement carried out at Measurement Point M2 marked on Fig. 5.2. Their most expected values and maximum values are given in Table 5.2. These are 3 second averaged data according to the Turkish Harmonic Standard [33]. As it can be understood from harmonic values given in Table 5.2, 2nd, 3rd and 4th harmonic current limits are exceeded for the unfiltered ladle furnace. Beyond the significant variations in the amplitude of each current harmonic component during operation of the ladle furnace, their phases with respect to the ladle furnace bus voltages are also changing drastically. This conclusion is drawn from the Fourier Series Expansion of the three line-current and three line-to-line voltage data for the ladle furnace collected by the data acquisition system (at point M2 in Fig. 5.2).

Power quality problems such as reactive power compensation, flicker and harmonics which arise from the operation of the ladle furnace can be solved by using the TCR based schemes given in Fig. 5.2. The success of the solution depends on several factors such as power system layout, system parameters, short circuit MVA rating of the supply, size and operation strategy of the ladle furnace, reactive energy and harmonics regulations and standards currently used in the country.

Table.5.2. Harmonic Current Spectrum of Ladle Furnace (Field Data), single line harmonics

Harmonic Order	Ladle Furnace, %		Ladle Furnace with 3rd Harmonic Filter, %		Overall System after Integration of TCRs, %		Limits according to IEEE Std.519 and Turkish Harm. Std.
	The Most Expected	Maximum	*The Most Expected*	Maximum	*The Most Expected*	Maximum	*Limit*
2	2.0	6.0	3.0	8.0	4.5	8.0	1.5
3	5.5	8.5	3.5	7.0	3.5	7.0	6.0
4	1.5	3.5	1.0	3.0	2.0	3.0	1.5
5	2.5	4.5	2.0	3.5	3.5	4.0	6.0
6	0.8	2.5	0.5	1.5	0.7	1.5	1.5
7	1.4	1.8	1.0	1.5	1.4	2.0	6.0
8	0.6	1.2	0.5	1.0	1.1	1.2	1.5
9	0.7	1.0	0.5	0.8	0.5	1.0	6.0
10	0.5	0.8	0.4	0.8	0.4	0.7	0.7
11	0.5	0.8	0.3	0.8	0.7	0.8	2.8
12	0.4	0.6	0.2	0.6	0.2	0.7	0.7
13	0.5	0.7	0.3	0.7	0.3	0.7	2.8
TDD*	7.0	10.0	6.0	10.0	7.0	10.0	7.5

The following simulations have been carried out in order to find out the maximum ratings of the system:

5.2.2.1 Load Sharing of Coupling Transformers

Ladle furnace simulation for the steady state has been carried out by a PSCAD Simulation for minimum and maximum loading conditions. The results are seen in Table 5.3. The reactors and capacitors are the former equipment used in the

modernization of the SVC system. In simulations, it is assumed that the coupling transformers are identical.
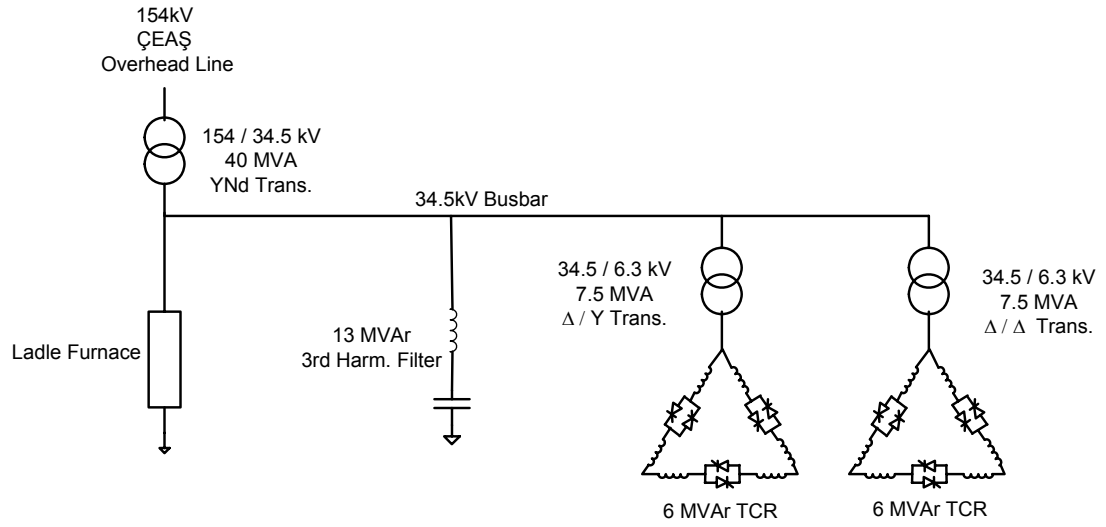
Figure 5.6. SVC Model used in the simulations

Table 5.3. SVC System Simultaion result for maximum and minimum loads
*Load Reactance :   90.16 Ohm (13.2MVAr @ 34.5kV), Load Resistance :79.35 Ohm (15MW @ 34.5kV)Normal Firing

	Main Busbar P (MW)	Main Busbar Q (MVAr)	Busbar Voltage kV	Q (TCR) MVAr	Q (Filter) MVAr	I (Reactor) A
31.5kV No Load	0,051	-0,2	31,62	10,78	10,99	312
34.5kV No Load	0,064	-0,2	34,61	12,96	13,18	343
36kV No Load	0,084	-0,188	36,1	14,15	14,34	354
31.5kV No Load Transformer Commutator Set: -7.5%	0,114	0,064	31,57	10,96	10,97	292
34.5kV No Load Transformer Commutator Set: -7.5%	0,029	0,061	34,56	13,16	13,17	319
36kV No Load Transformer Commutator Set: -7.5%	0,062	-0,112	36	14,3	14,33	332
31.5kV Loaded*	12,24	0,3	31,24	0,47	10,83	0
34.5kV Loaded*	14,72	0,386	34,33	0,84	13,01	0
36kV Loaded*	16	0,45	35,8	0,123	14,16	0

5.2.2.2 Simulation of the Normal Operation of 12-Pulse TCR

The simulation of the circuit in Fig. 5.6 is simulated for firing delay angles that ramp down from 180° to 90°. The TCR currents are seen in Fig. 5.7. The harmonic currents of individual 6-pulse TCRs are in Fig.5.8, and harmonic spectrum of the overall system is in Fig.5.9. Harmonic content matches the theoretical results given in Chapter 2.
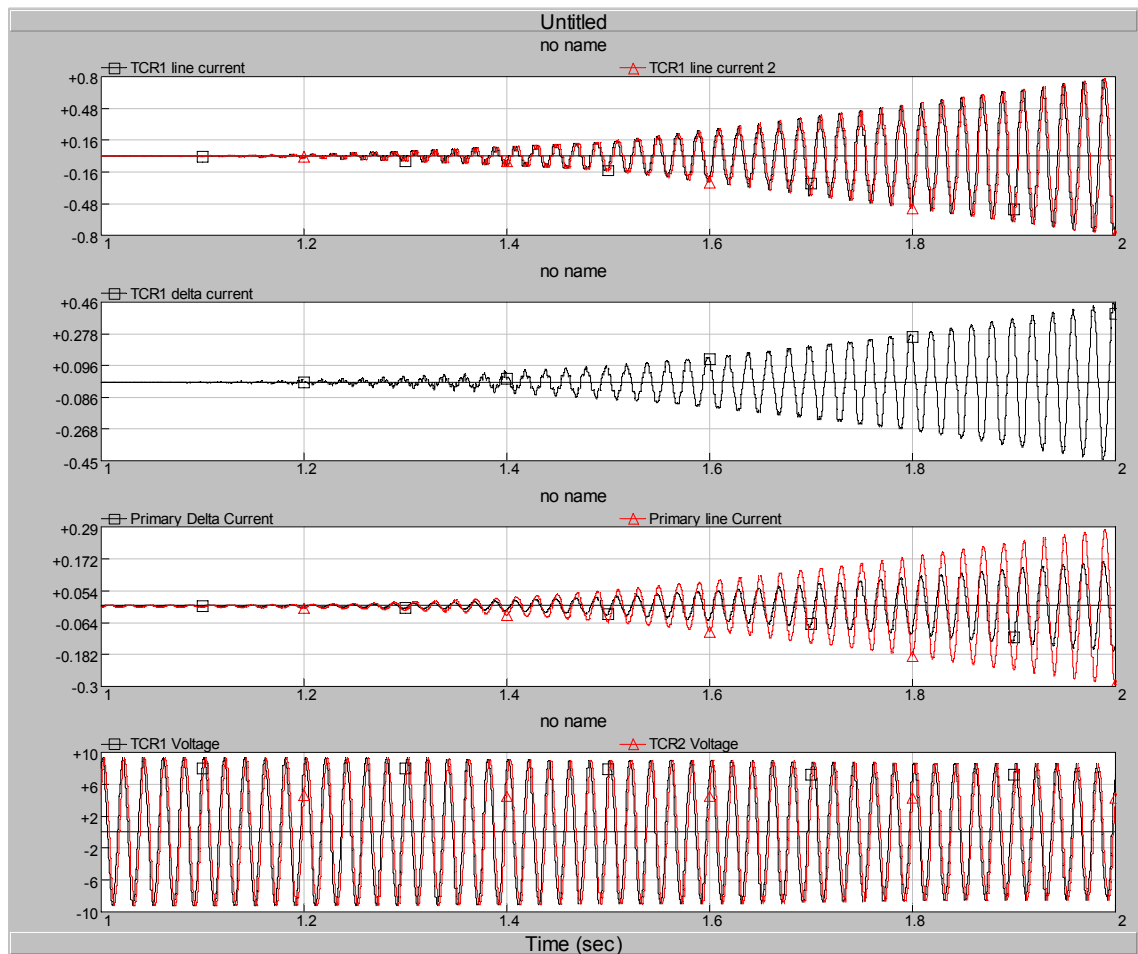
Fig.5.7. TCR Current and Voltage waveforms for 12 pulse TCR simulated on PSCAD for normal operation

Fig.5.8. TCR Current harmonics and TDD waveforms for each 6 pulse TCR of the 12 pulse SVC, simulated on PSCAD for normal operation
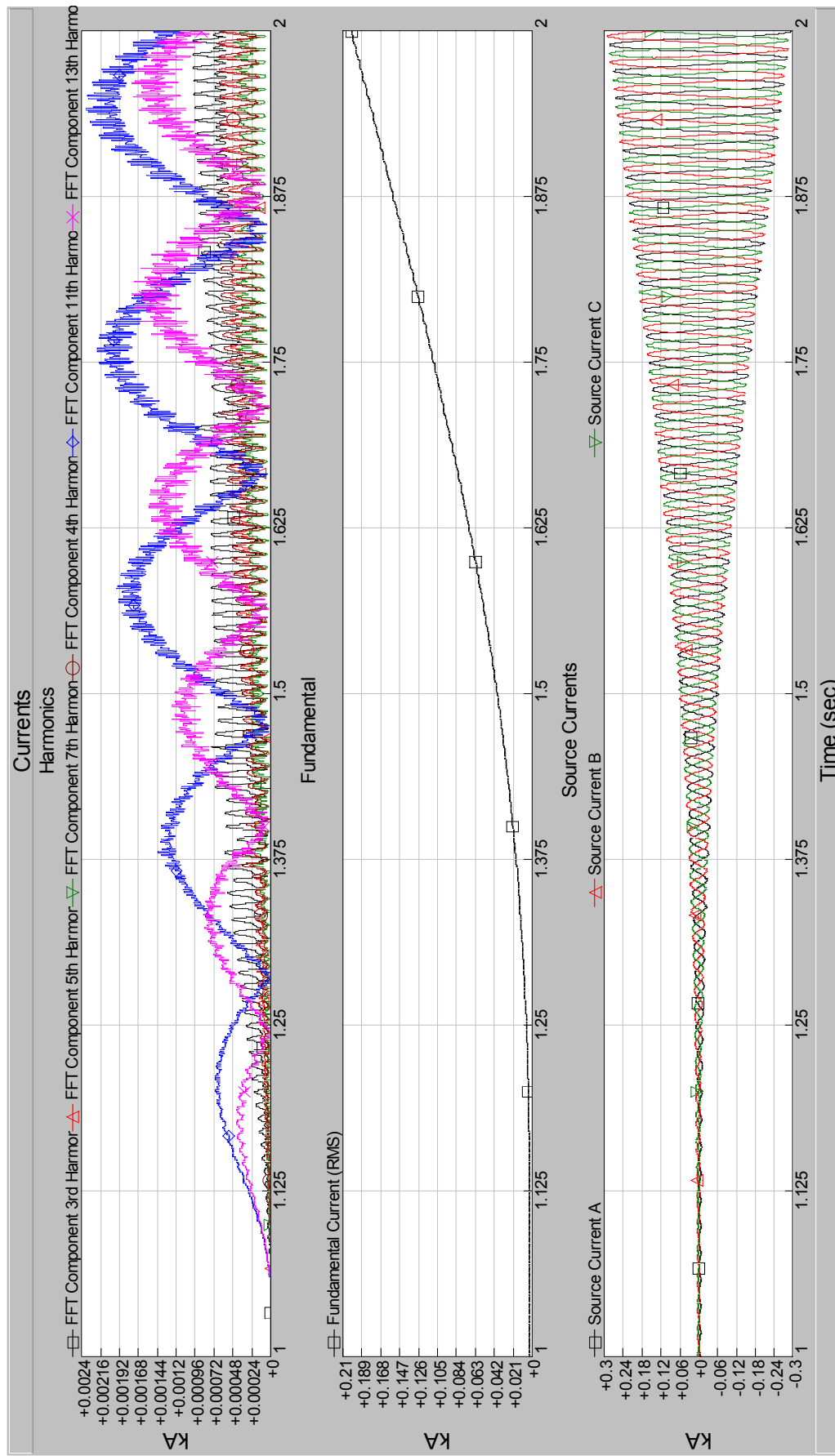
Fig.5.9. TCR Current harmonics in the primary side of the coupling transformers of the 12 pulse SVC, for normal operation:

202

5.2.2.3 5 Degrees Misfiring

The simulation of the circuit in Fig. 5.6 is simulated for firing delay angles that ramp down from 180° to 90°. The second TCR is fired with an extra delay of 5° to simulate possible control system errors. The TCR currents are seen in Fig. 5.10. The harmonic currents of individual 6-pulse TCRs are in Fig.5.11, and harmonic spectrum of the overall system is in Fig.5.12. A maximum of %1.2 5th harmonic and 0.7% 7th harmonic appeared in the overall current at the primary side of the coupling transformers.
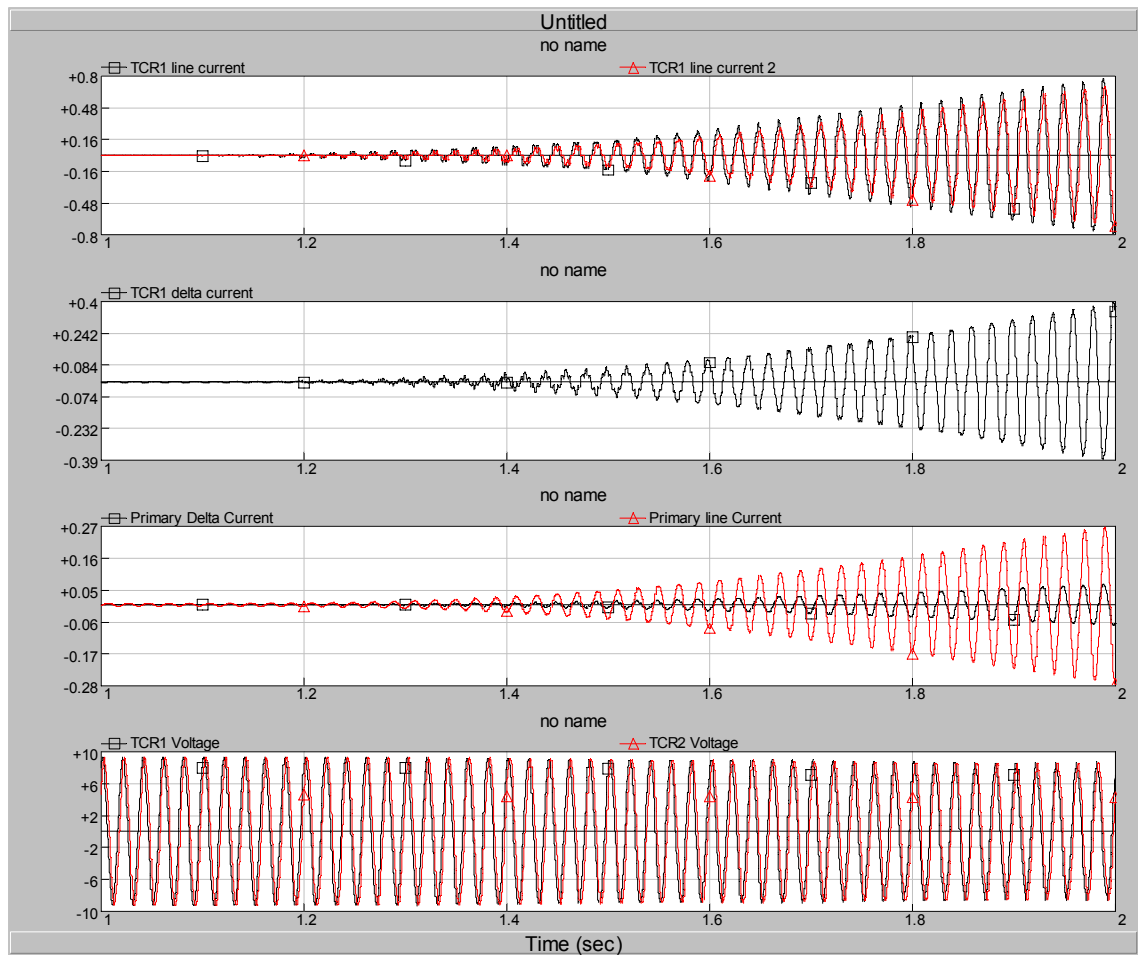
Fig.5.10. TCR Current and Voltage waveforms for 12 pulse TCR simulated on PSCAD for 5 degrees misfiring
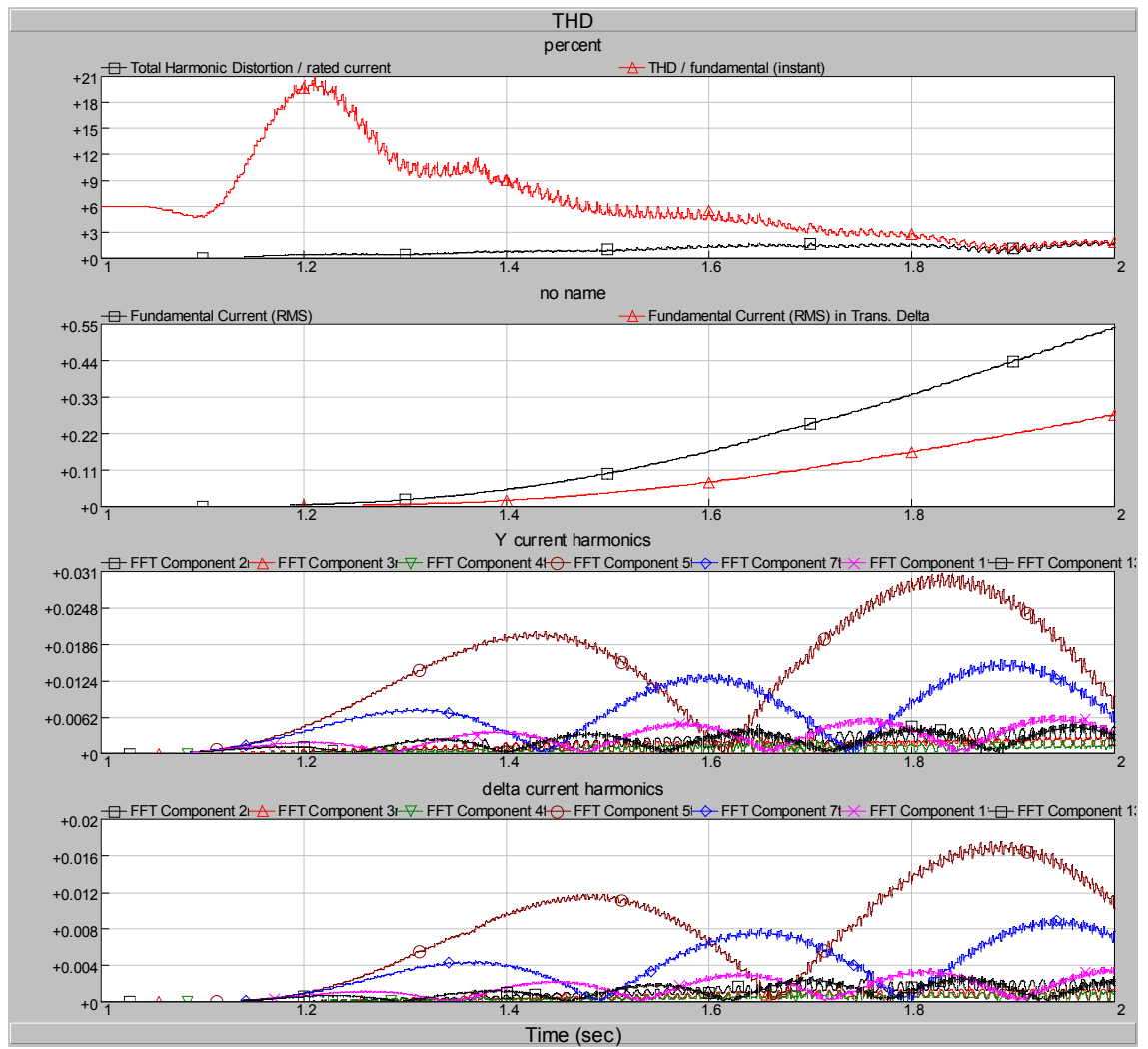
Fig.5.11. TCR Current harmonics and TDD waveforms for each 6 pulse TCR of the 12 pulse SVC, simulated on PSCAD for 5 degrees misfiring
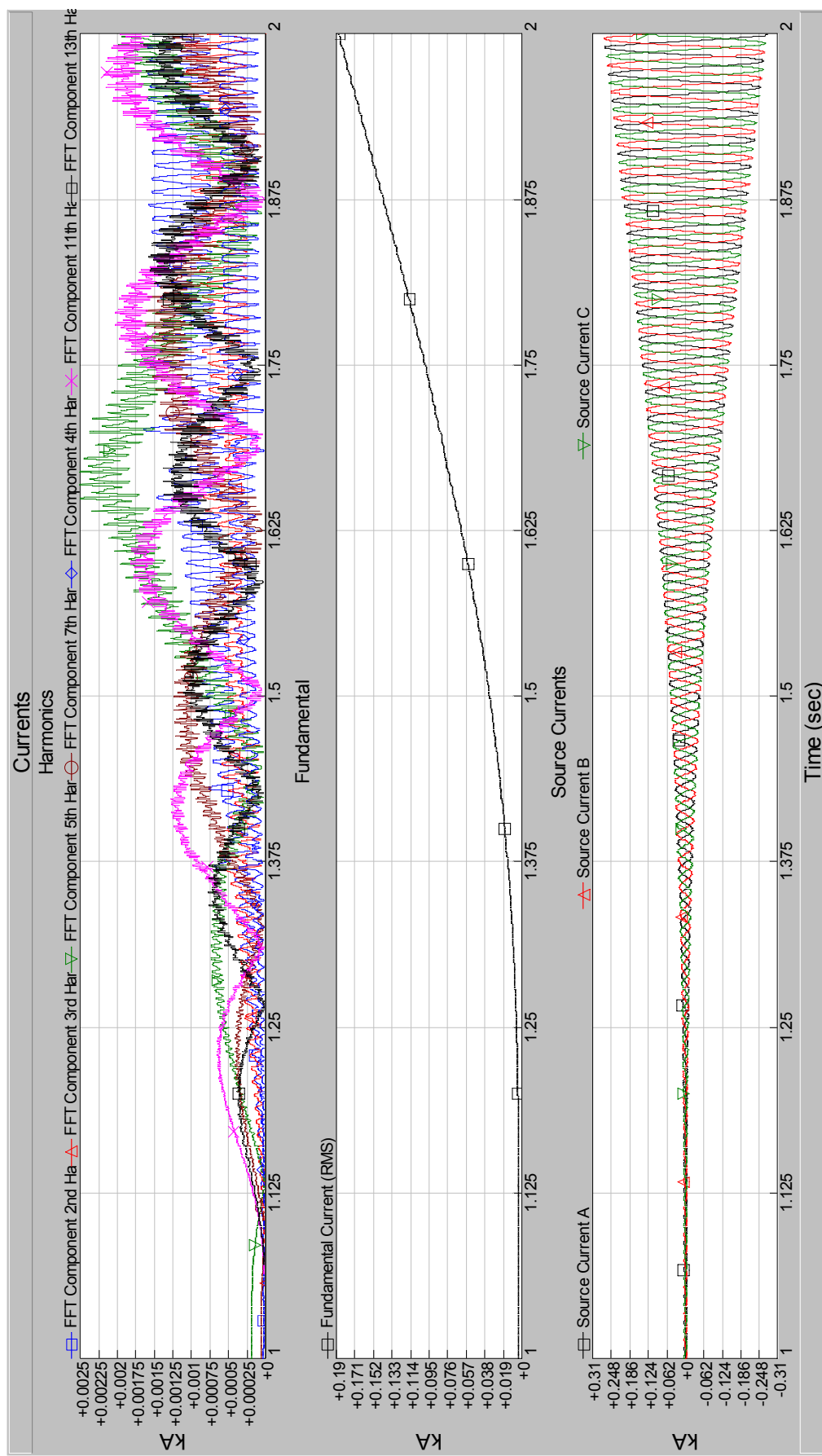
Fig.5.12. TCR Current harmonics in the primary side of the coupling transformers of the 12 pulse SVC, for 5° Misfiring:

5.2.2.4 10% Voltage Rise in the Second Transformer

The simulation of the circuit in Fig. 5.6 is simulated for firing delay angles that ramp down from 180° to 90°. The second coupling transformer secondary voltage is increased 10% in order to simulate possible wrong voltage settings. The TCR currents are seen in Fig. 5.13. The harmonic currents of individual 6-pulse TCRs are in Fig.5.14, and harmonic spectrum of the overall system is in Fig.5.15. A maximum of 5th harmonic and 7th harmonic is less than 0.5% of the overall current at the primary side of the coupling transformers.
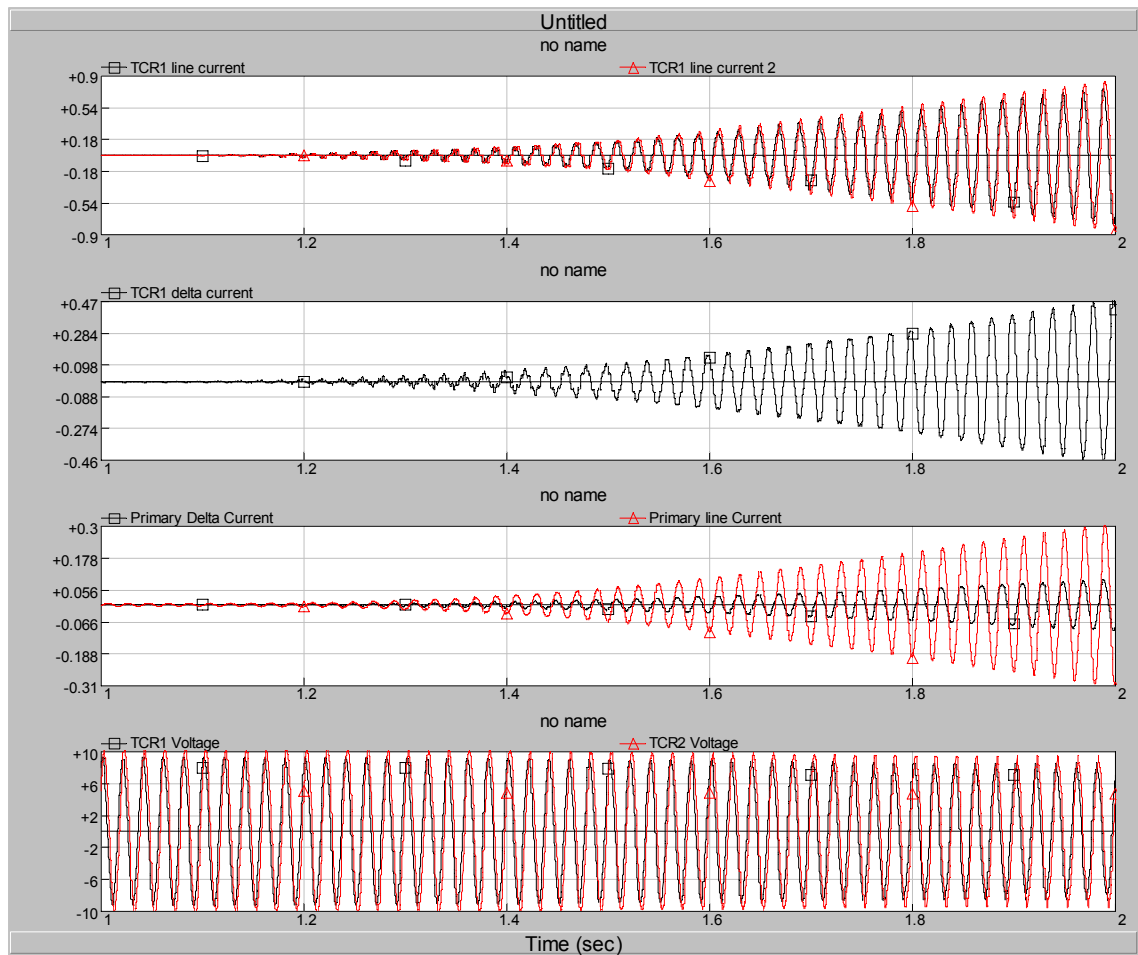
Fig.5.13. TCR Current and Voltage waveforms for 12 pulse TCR simulated on PSCAD for 10% Voltage Rise in the Second Transformer
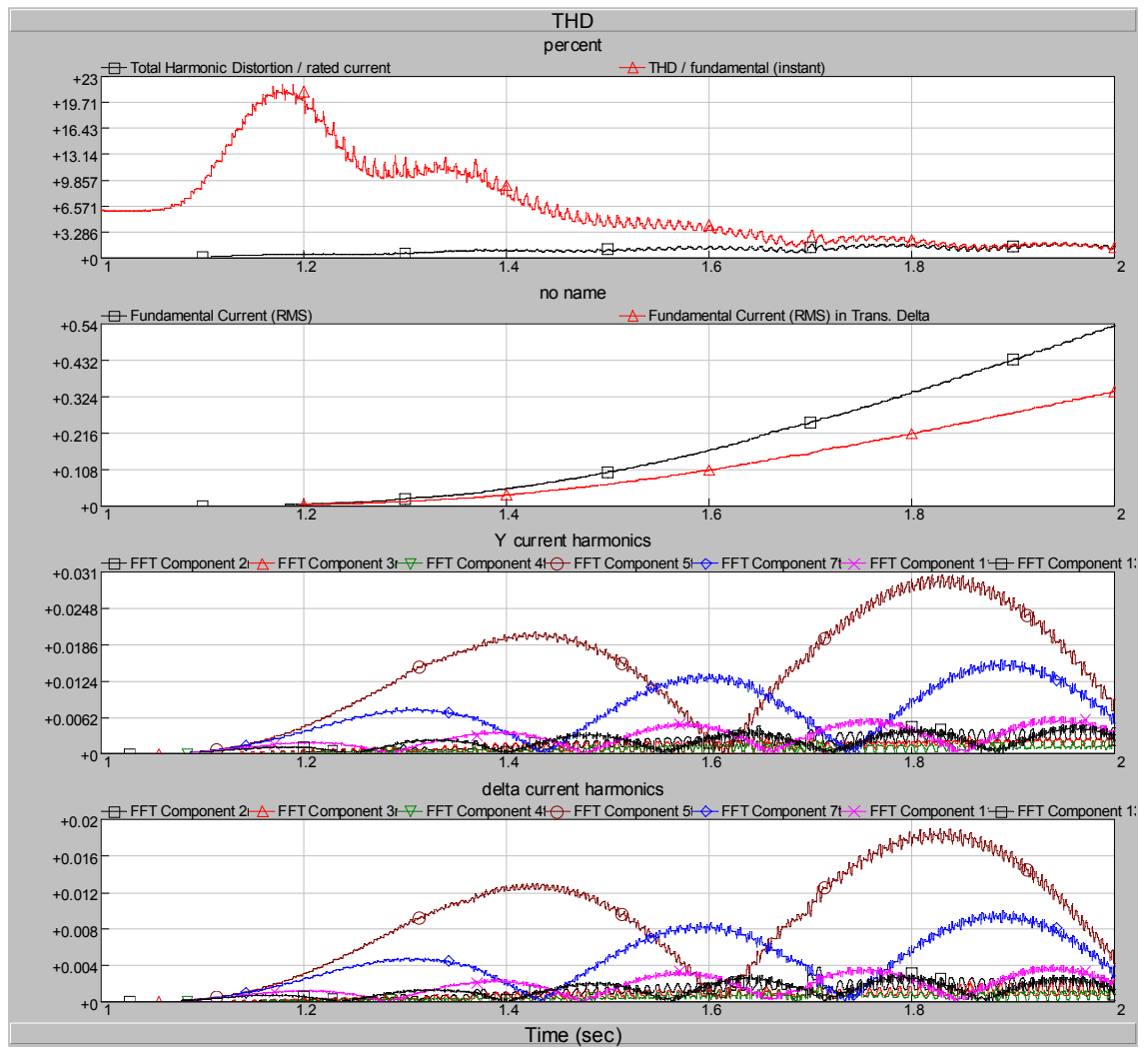
Fig.5.14. TCR Current harmonics and TDD waveforms for each 6 pulse TCR of the 12 pulse SVC, simulated onPSCAD, 10% Voltage Rise in the Second Transformer
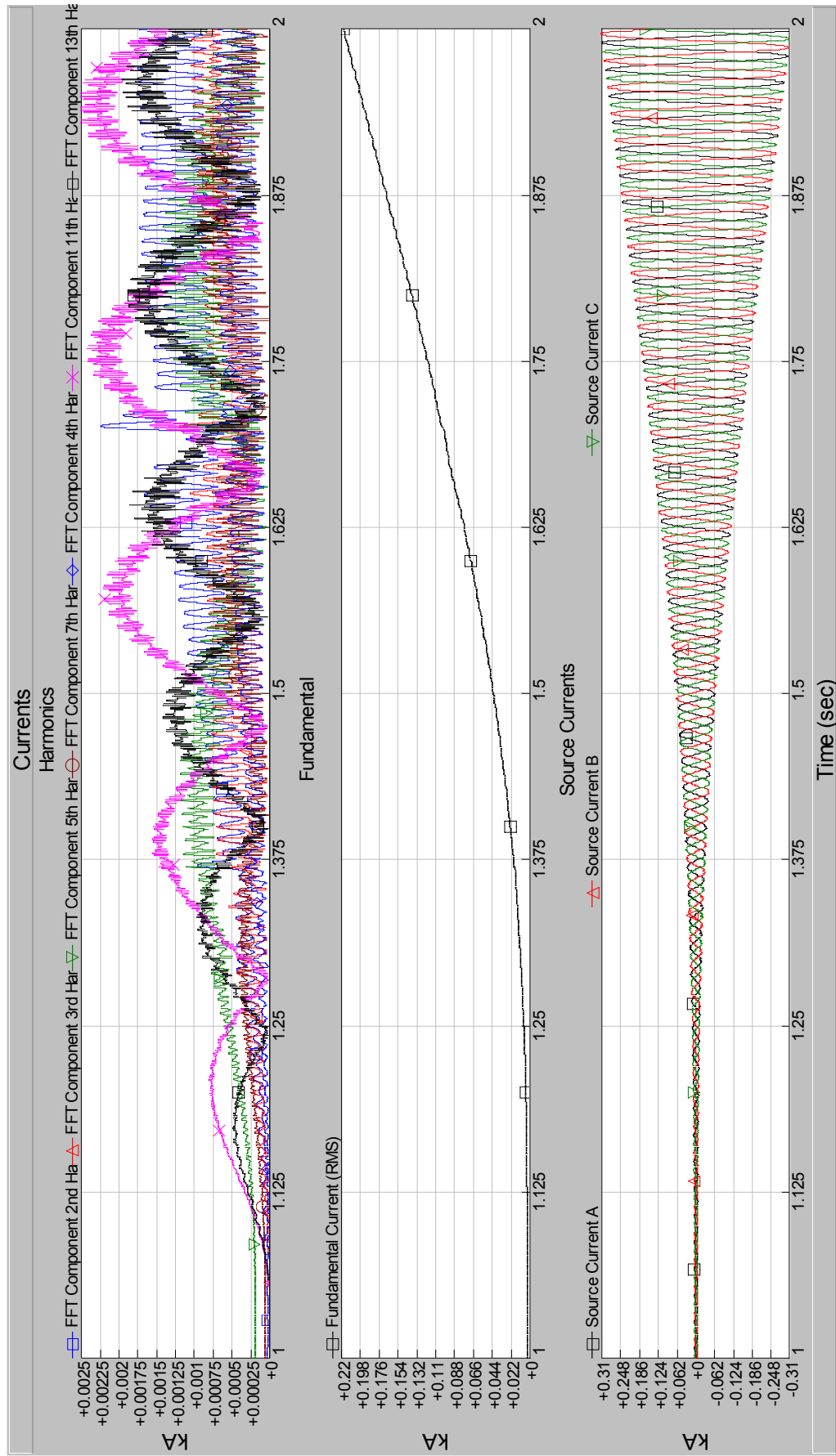
Fig.5.15. TCR Current harmonics in the primary side of the coupling transformers 10% Voltage Rise in the Second Transformer

208

5.2.2.5 2% Change in the Short Circuit Impedance of the Transformer

The simulation of the circuit in Fig. 5.6 is simulated for firing delay angles that ramp down from 180° to 90°. The second coupling transformer short circuit impedance of the transformer (U_k) is increased from 8% to 10% in the rate of 2% in order to simulate dissimilar coupling transformers. The TCR currents are seen in Fig. 5.16. The harmonic currents of individual 6-pulse TCRs is in Fig.5.17, and harmonic spectrum of the overall system are in Fig.5.18. No significant effects are observed in the overall current at the primary side of coupling transformers.
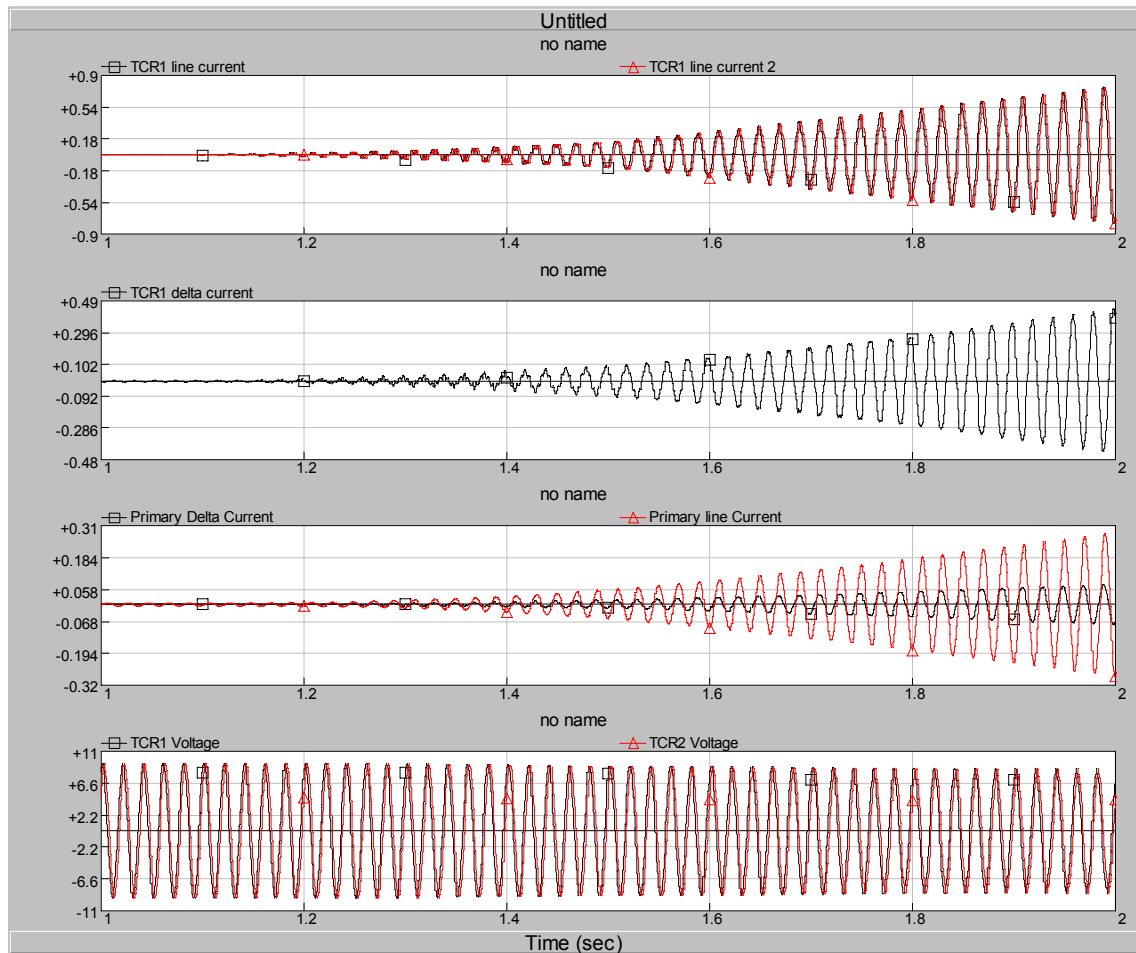
Fig.5.16. TCR Current and Voltage waveforms for 12 pulse TCR simulated on PSCAD for 2% Change In the U_k
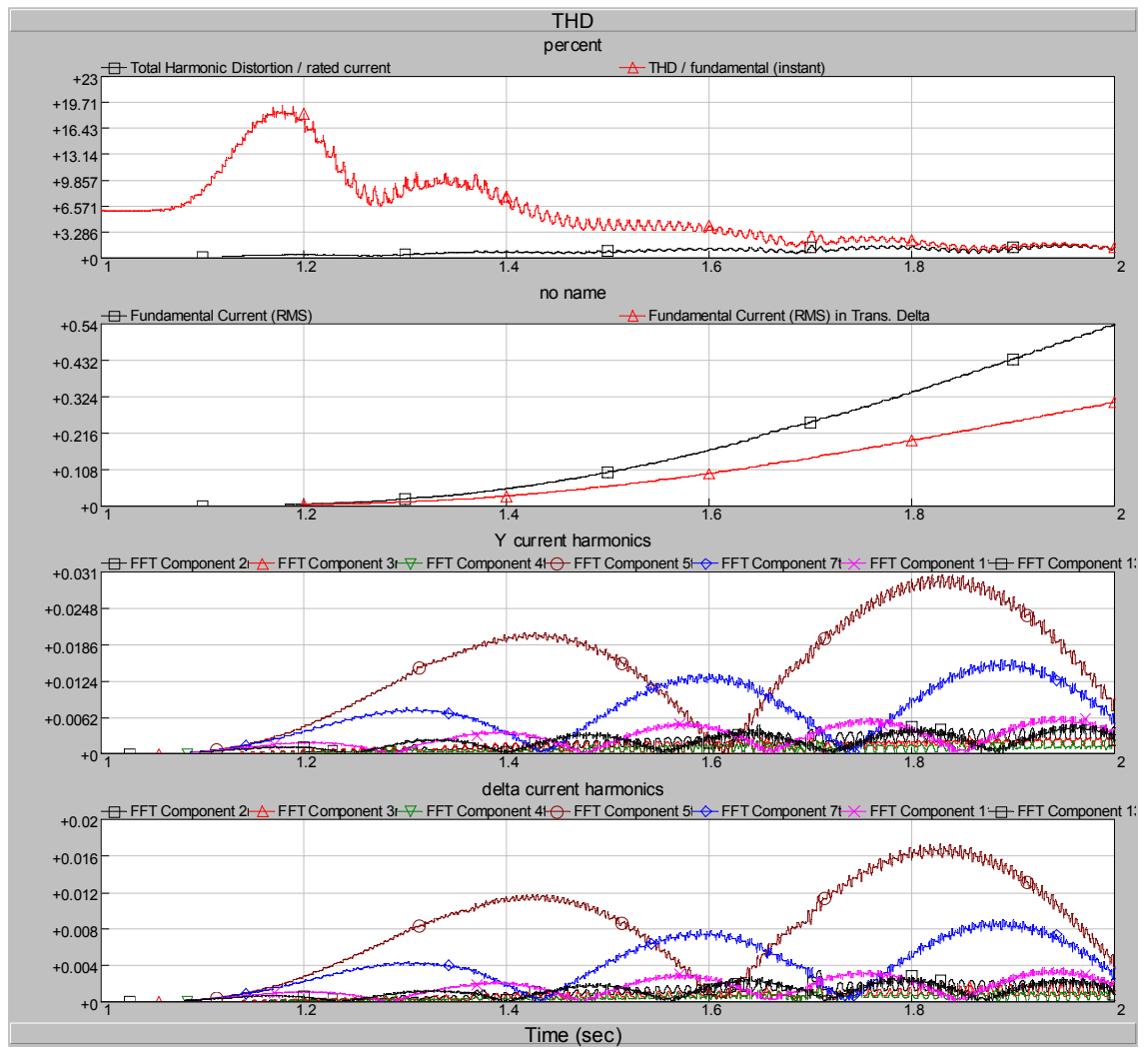
Fig.5.17. TCR Current harmonics and TDD waveforms for each 6 pulse TCR of the 12 pulse SVC, simulated on PSCAD for 2% Change In the U_k
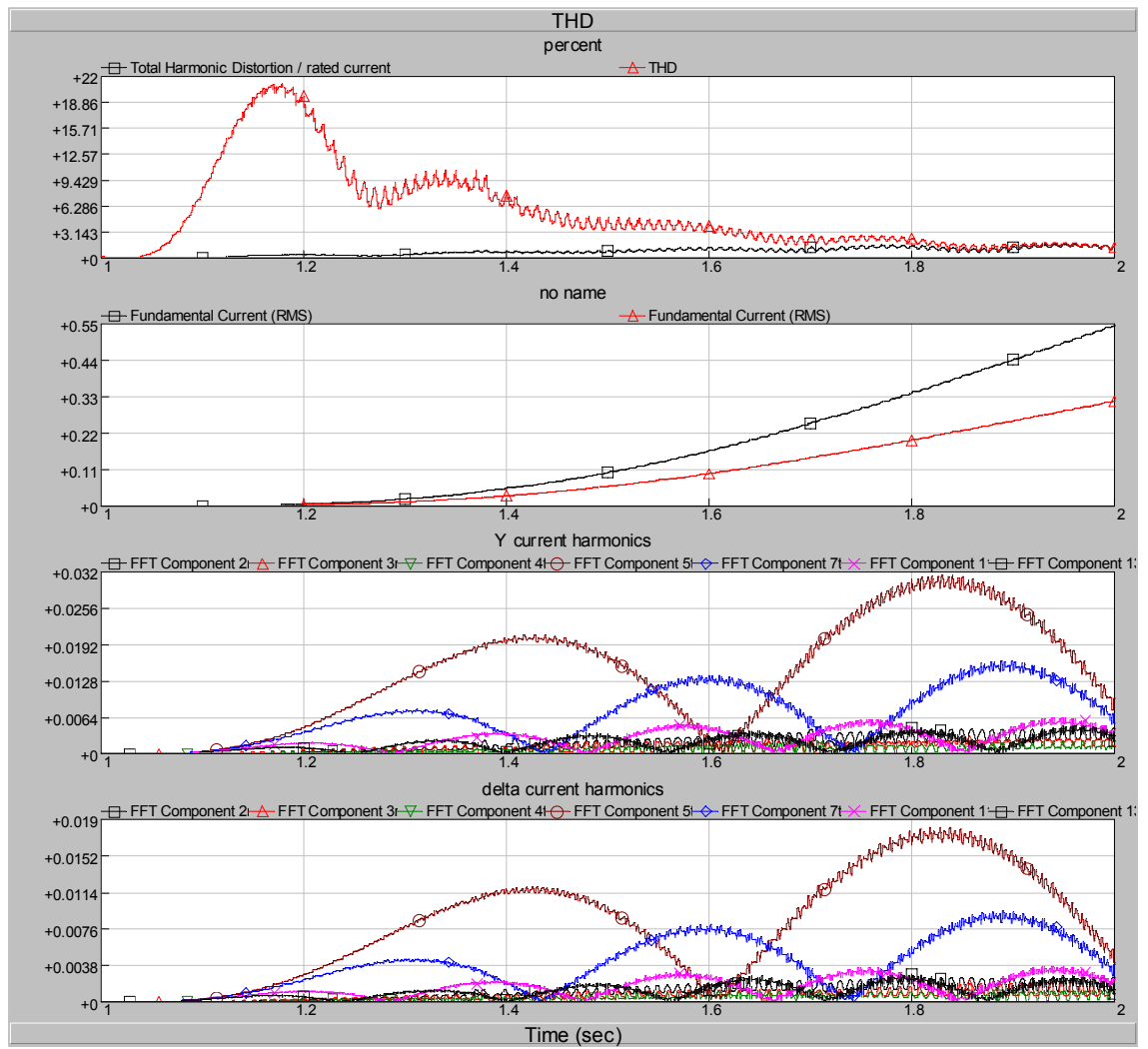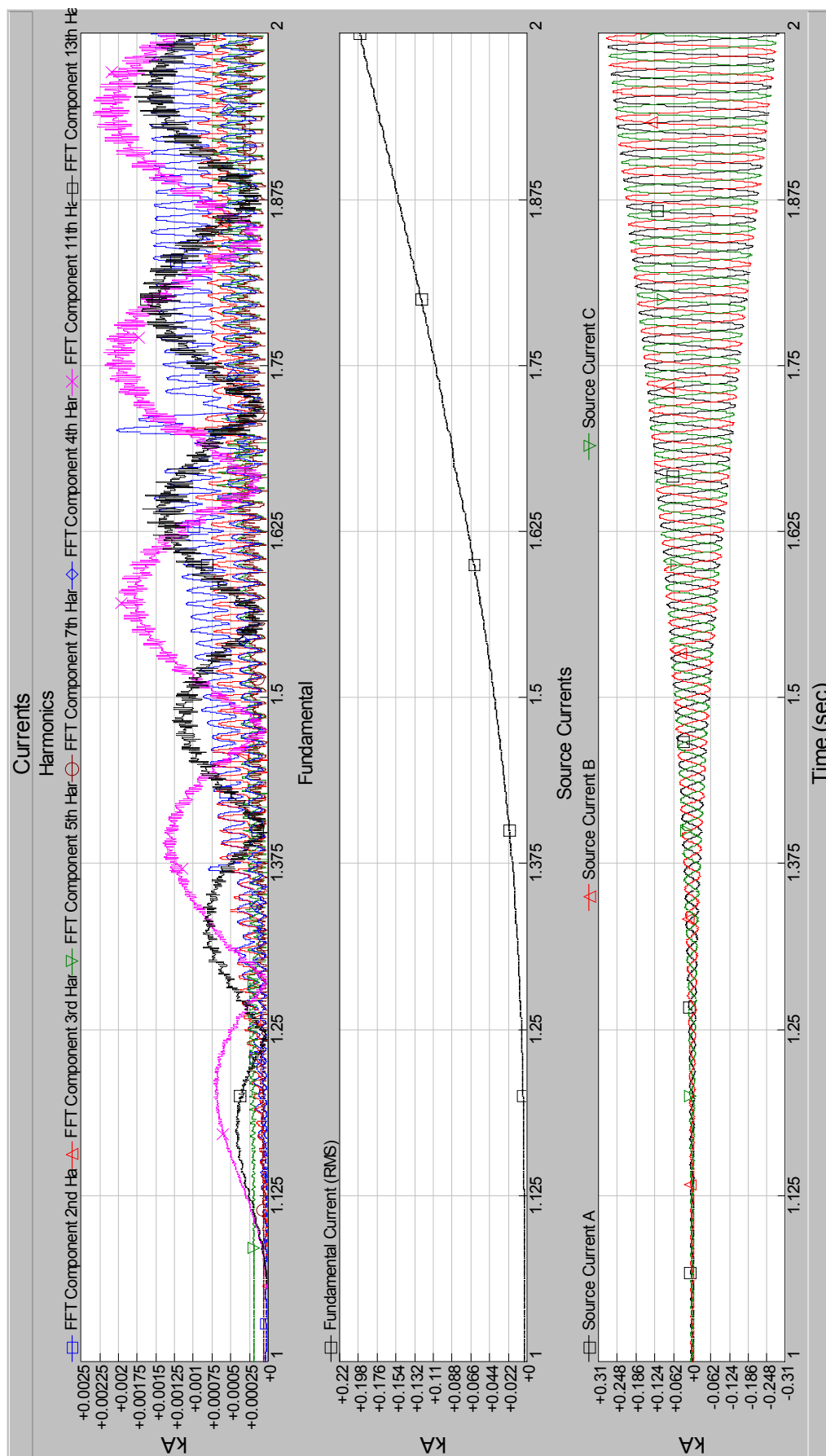
Fig.5.18. TCR Current harmonics in the primary side of the coupling transformers of the 12 pulse SVC, 2% Change In the U_k

211

5.2.3 SVC Coupling Transformer Design

In order to solve the reactive power compensation problem of the ladle furnace, two identical TCRs, each rated at 6 MVAr, 6 kV are connected to 34.5 kV ladle furnace bus via two dissimilar transformers (one is 6/34.5 kV, 8MVA, Y/Δ connected while the other is 6/6/34.5 kV, 12.5/12.5/25 MVA, Δ/Δ/Δ connected). To solve the harmonic problem, the 34.5 kV, 13 MVAr originally installed 3rd harmonic shunt passive filter is preserved by keeping it connected to the ladle furnace bus.

In the existing ladle furnace power system, there was no redundancy in Fig. 5.3 before the implementation of this project. There was only one 40 MVA, 154 / 34.5 kV power transformer (TR-4 in Fig. 5.2) devoted to the ladle furnace. This had caused difficulties in emergency cases and led to interruptions in production during the maintenance periods of the mentioned power transformer. Therefore, an alternative path has been formed in the design phase of the project to supply ladle furnace temporarily during maintenance periods of main power transformer TR-4. This is achieved by designing one of the converter transformers as a unit sufficiently large for the ladle furnace and supplying it from one of the vacant power transformers present in the power system. This is the power transformer TR-3 shown in Fig. 5.2. Since TR-3 has two identical secondary windings, TR-5 should be implemented as a transformer with two identical 6.3 kV windings. The alternative path in supplying ladle furnace when the main transformer TR-4 is out of service is as shown in Fig. 5.3. Furthermore, TR-5 has been designed as a Δ/Δ/Δ connected transformer in order to eliminate any phase shift in voltages between normal and emergency operations of the ladle furnace power system

Table 5.4. Transformers in the Ladle Furnace Distribution System

Transformer Definition	Rating	Ratio	Connection Type	U_k (%)
Main Power Transformer (TR-4)	40 MVA	154/34.5 kV	YN-Δ-11	10
Spare Transformer for Redundancy (TR-3)	32/16/16 MVA	154/6.3/6.3 kV	YN-Δ-Δ-11-11	9.21
Two-folded TCR-1 Power Transformer (TR-5)	25/12.5/12.5 MVA	34.5/6.3/6.3 kV	Δ-Δ-Δ	6.94
TCR-2 Power Transformer (TR-6)	8 MVA	34.5/6.3 kV	Δ-Y	6.84
Ladle furnace transformer	12.087-29 MVA	34.5/0.181-0.315 kV	Δ-Δ	12.9-6.4

(a)   (b)

Fig.5.19. The two dissimilar transformers used in 12-pulse TCR scheme (a) TCR-1 Power Transformer (TR-5) (b) TCR-2 Power Transformer (TR-6)
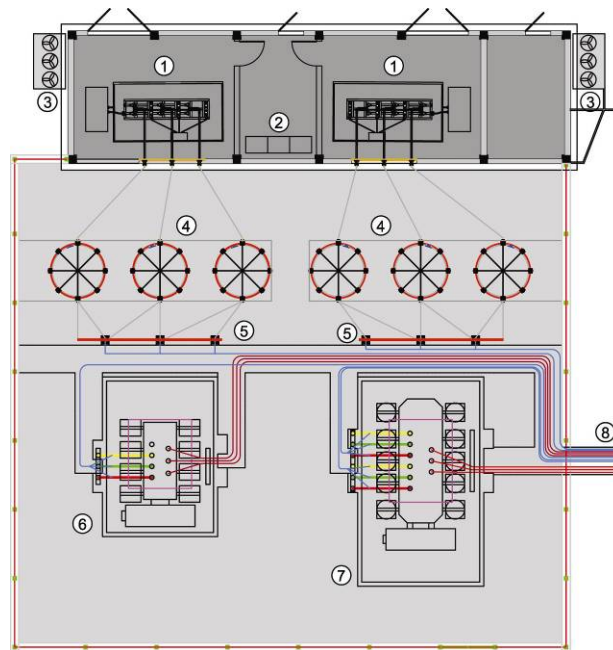
Fig.5.20. Footprint of 12-pulse TCR System excluding distribution switchgear

Fig.5.21. TCR Yard

Fig.5.22. (A) Protection and monitoring panel, (B) Control panel for TCR-1 and (C) Control panel for TCR-2 (If one is chosen as the master control unit the other can act as the slave

Fig. 5.23. Power stage of 6-pulse TCR-2

5.3 Field Tests

The installation and commissioning works of the 12-pulse TCR with dissimilar transformers have been completed by the end of January 2004. The footprint of the system excluding switchgear is as shown in Fig. 5.20. General view of TCR yard is as shown in Fig. 5.21 and some of the main elements in Figures 5.22 and 5.23.

The variations in active, inductive-reactive and capacitive-reactive energy demands of the ladle furnace power system in monthly electric bills after the installation of 12-pulse TCR are as given in Fig. 5.5. Since February-2004 Capacitive Reactive Energy and Inductive Reactive Energy in monthly electric bills have remained at values less than 8 % and 12 % of monthly.
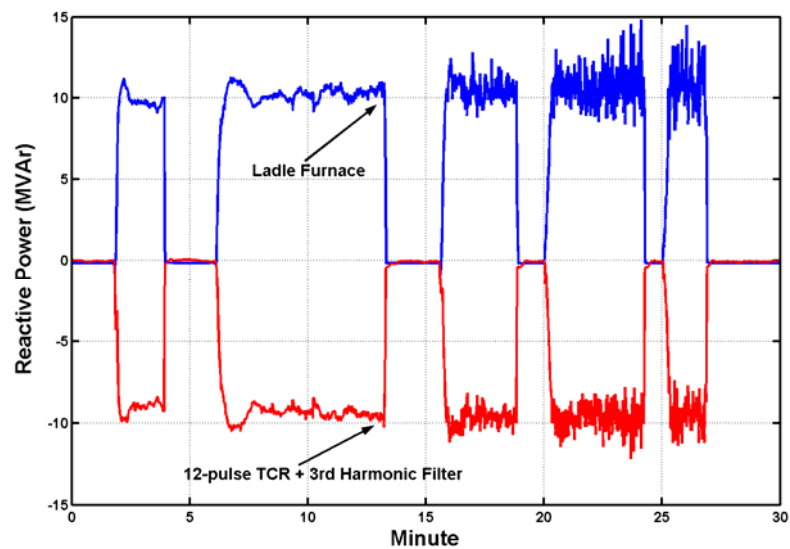
Fig.5.24. Power consumption vs. time records after reactive power compensation (1 sec average field data at points M1 and M2 in Fig. 5.2)

(a)
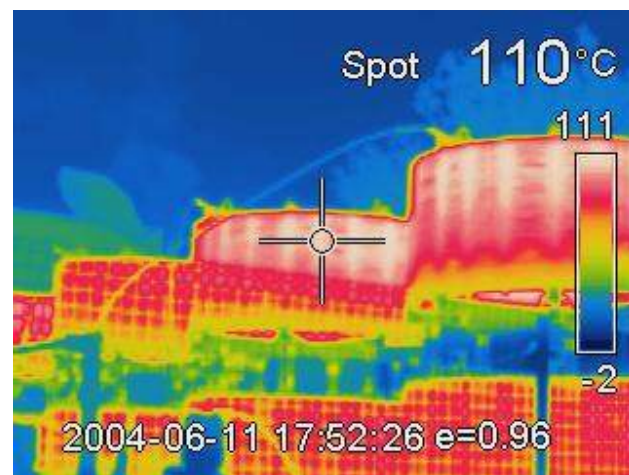
(b)

Fig. 5.25. Sample thermal camera images a. Operating temperatures of deionized cooling water and thyristors are quite low; the dynamic equalizing (snubber) resistors are the hottest points in the image. b. The operating temperature of outdoor type air-core reactors is on the safe side for Class-F insulation and at an ambient temperature of 30°C.

The response of the 12-pulse TCR against the rapid changes in reactive power demand of ladle furnace + fixed 3rd harmonic filter is also obtained in the field. The response given in Fig.5.24 and based on 1 second averaged data shows how successfully the 12-pulse TCR can follow the variations in the reactive power demand of ISDEMIR Ladle Furnace System.

The performance of the thermal management system has been obtained by the use of a thermal camera by taking thermal images of all system components and parts and then comparing them with design values of operating temperatures. Some sample thermal camera images are given in Fig. 5.25.

The major drawback of the overall system is the 2nd harmonic content of current waveform in 154 kV lines in excess of its limit value specified in harmonic standards [35,39]. The maximum values of 2nd and 4th harmonic current components in mains lines can be reduced either by readjustment of PI controller parameters to give a longer response time or by computing reactive power demand over a complete cycle instead of a half cycle.

As an example, the phase of the second current harmonic component produced by the ladle furnace is found to vary in the range from -100 to 135 degrees with respect to the zero crossing point of the actual current waveform in the sample record shown in Fig. 5.26. This is because positive and negative half-cycles of the line current waveform for the ladle furnace are not necessarily symmetrical.

Field tests for the control methods discussed in Chapter 3 are employed in 12-pulse TCR. Power dissipation is seen in Fig.5.27. Equal load sharing method causes less dissipation as expected. This finding can be verified by simple hand calculations on the basis of cupper loss component of air-core reactors. For instance, for partial loads in the range from 0 to 6 MVAr, a reactive current demand of 10 amps/phase-Δ causes $10^2R=100R$ Watts/phase power dissipation in air core reactors for Sequential Load Sharing while the Equal Load Sharing leads to theoretically half of it that is $5^2R+5^2R=50R$ Watts/phase.
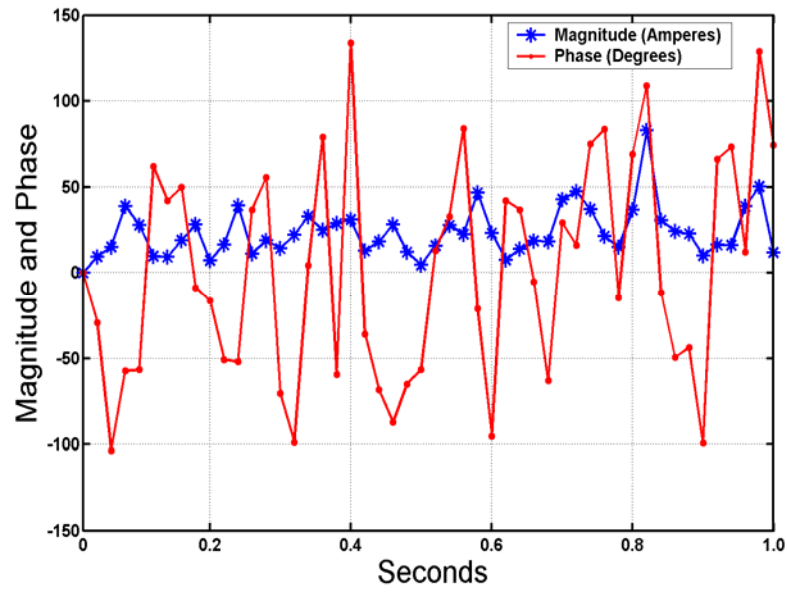
Fig.5.26. Magnitude and phase variation of 2nd harmonic component of Ladle Furnace line current
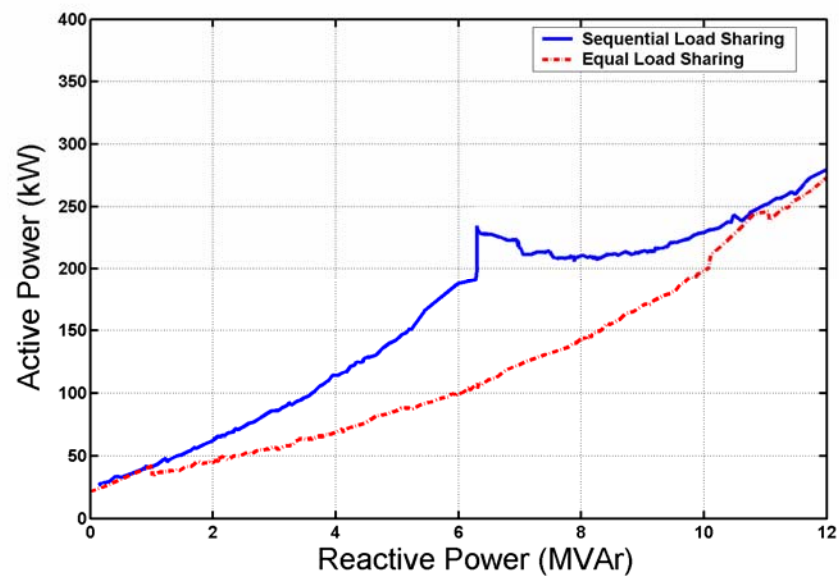
Fig 5.27. Variations in total power loss of the 12-pulse TCR against reactive power for Sequential and Equal Load Sharing Strategies (Field Tests)

5.4 Discussions

The 12-pulse TCR system constitutes a cost effective solution to the reactive power compensation problem of ISDEMIR ladle furnace owing to the use of some components such as 154/6.3 kV power transformer, 6 kV air core reactors, 6 kV circuit breakers, cables existing in the infrastructure of ISDEMIR. By connecting the two 6-pulse TCRs to the ladle furnace bus via two separate and dissimilar transformers instead of a single transformer with Δ and Y connected two identical secondaries, an alternative path is provided to supply ladle furnace in the case of either the maintenance or failure of the main power transformer resulting in redundancy for ladle furnace power system.

Keeping the 3rd harmonic filter originally installed with ladle furnace in the system leads to a significant saving in the cost of upgrading project but introduces some difficulties associated with 2nd harmonic component in complying with the harmonic standards [35, 39, 42].

Although there is no optimum solution to power quality problems of new arc and ladle furnace installations among TCR based schemes [37], the use of 2nd harmonic filter in addition to the 3rd harmonic filter and 12-pulse TCR could be a better solution. However cost reduction aim of the project and unchangeable TCR size made necessary the installation without a 2nd harmonic filter. If there had been new SVC installation instead of upgrading, there would have been more choices. The existing 12 MVArTCRs could have been connected via Δ/Y transformer and a 12 MVAr 34.5 kV TCR could have been installed to the medium voltage bus directly to obtain a 12-pulse TCR with 24 MVAr reactive power. Other possible topologies are also mentioned in [4, 5].

The control strategies of the 12-pulse TCR are described in Chapter 3. In order to increase the redundancy, the TCRs can be operated in the independent mode. By this strategy, the faults in a 6-pulse TCR will not affect the operation of the second 6-pulse TCR. For the reduction of TDD, equal load sharing is the most feasible solution. Sequential load sharing is the best solution for reducing the SVC active power loss.

CHAPTER 6

CONCLUSIONS & FURTHER WORK

This Ph.D. Thesis deals with the design, implementation and engineering aspects of TCR based industrial SVC systems. A systematical approach for the design of industrial SVC systems has been given in view of the long term experience of the author. This approach is in accordance with the updated version of IEEE Std. 1031-2000 which covers only transmission Static VAr Compensators.

In this thesis, two original contributions have been made in the application of TCR based SVCs to industrial plants at distribution voltage level. These are summarized as follows:

1. **For Mining Industry:** The first conceptual design of relocatable, unified and extendible TCR based SVCs for various open cast lignite mines of the Turkish Coal Enterprises (TKİ) to compensate electrical excavators' rapidly changing reactive power demand. Ease of demounting, transportation, erection, and commissioning constitute the major features of the system as a relocatable compensator. The unified compensator can be connected to an overhead line or load bus of different voltage levels with minor modifications, and is designed to operate satisfactorily under different environmental/climatic conditions. The system is designed to be a flexible and extendable one in order to meet the possible future needs of the enterprises. Reactive power demand of each load bus before and after compensation has shown the validity of the proposed design method based on PSCAD/EMTDC simulations of various excavator loads of enterprises, using actual data obtained by means of a data acquisition system in the field.

2. **For Metal Industry:** It is the first reported 12-pulse TCR based SVC implementation for power quality improvement of ISDEMIR ladle furnace.It

has been shown that 12-pulse TCR eliminates $5^{th}, 7^{th}, 17^{th}, 19^{th} \ldots$ (in general $6k+/-1$, $k=1,3,5,7 \ldots$) successfully in both dynamic and steady state thus yielding much better harmonic performance than its 6-pulse counterpart. This improvement is at the expense of employing a single or two transformers with Δ and Y secondaries. At the present time, iron and steel industry in the country is rapidly growing, therefore at a certain dirty bus new SVC installations seem to be needed. The existing SVC installations in iron and steel plants meet neither flicker nor the 2nd harmonic and TDD requirements [37]. Instead of directly connecting a new 6-pulse SVC to the same dirty-bus the 6-pulse TCR of the new SVC can be connected via a Δ/Y connected coupling transformer thus constituting a 12-pulse SVC configuration. This design approach may lead to lessen both harmonic and flicker problems of the iron and steel plants.

6.1 Conclusions

Following conclusions are drawn from the experience gained in these industrial case studies:

1. Excavator loads are usually being filtered out by odd order harmonic filters, however from Case Study 1, it has been observed from the field measurements that considerable even order harmonic currents are injected into the supply during the operation of the motor drives. In addition to this, the transient operation of TCR also generates even order harmonics. These even order harmonics, if not properly taken into account in the design of harmonic filter stages, may lead to a serious parallel resonance problem

2. Especially in arc and ladle furnace operation in iron and steel plants, it has been observed from the extensive field measurements, and from the design experience gained at Case Study 2, that the combination of 2nd and 3rd harmonic filters is not sufficient to reduce the 2nd harmonic currents below the standard limits. In most of the cases, even amplification of this 2nd harmonic component occurs in the presence of the passive filters only. Furthermore the reactive power variations in an arc furnace (EAF) are much more rapid and unbalanced line current phenomenon is more severe than

222

those of excavator loads and ladle furnaces. Field measurements have also shown that TCR in such applications produces significant 2nd and higher order even harmonics because TCR operates in dynamic state almost all the time in order to follow the rapid variations of arc furnace quantities . Some typical records obtained in the iron and steel plants in Aliağa region are given in Fig.6.1. These are the responses of professional SVCs with power ratings in the range of 60-100 MVAr produced by multinational companies. However in our application this was not the case because the loads are less fluctuating and less unbalanced.

3.   A qualitative comparison of SVC system designed for mining applications with the traditional SVC systems developed by multinational companies is given in Table 6.1.

Table 6.1. Comparison of traditional SVCs and SVC Systems Designed for TKI

	Traditional SVC Systems	SVC Systems Designed for TKI
Reactive Power Compensation	Regular systems will need design changes to fulfill the new regulations of Energy Market Authorities	Modularity enables easy change of installed capacity, easily adapted for new regulations of Energy Market Authorities
Ease of relocation	Designed for a specific load and utility grid, not designed primarily for relocation	Relocation and commissioning in a few days. 4 systems in TKİ ELİ and TKİ BLİ are already relocated
Extendibility	In general not extendible, upgrading needs redesigning some parts especially harmonic filters	Modular and easily upgradeable
Robustness	Thyristor and control cubicles are robust but this is not the case for TCR and harmonic filter yards	Designed for harsh environment and unmanned operation

223
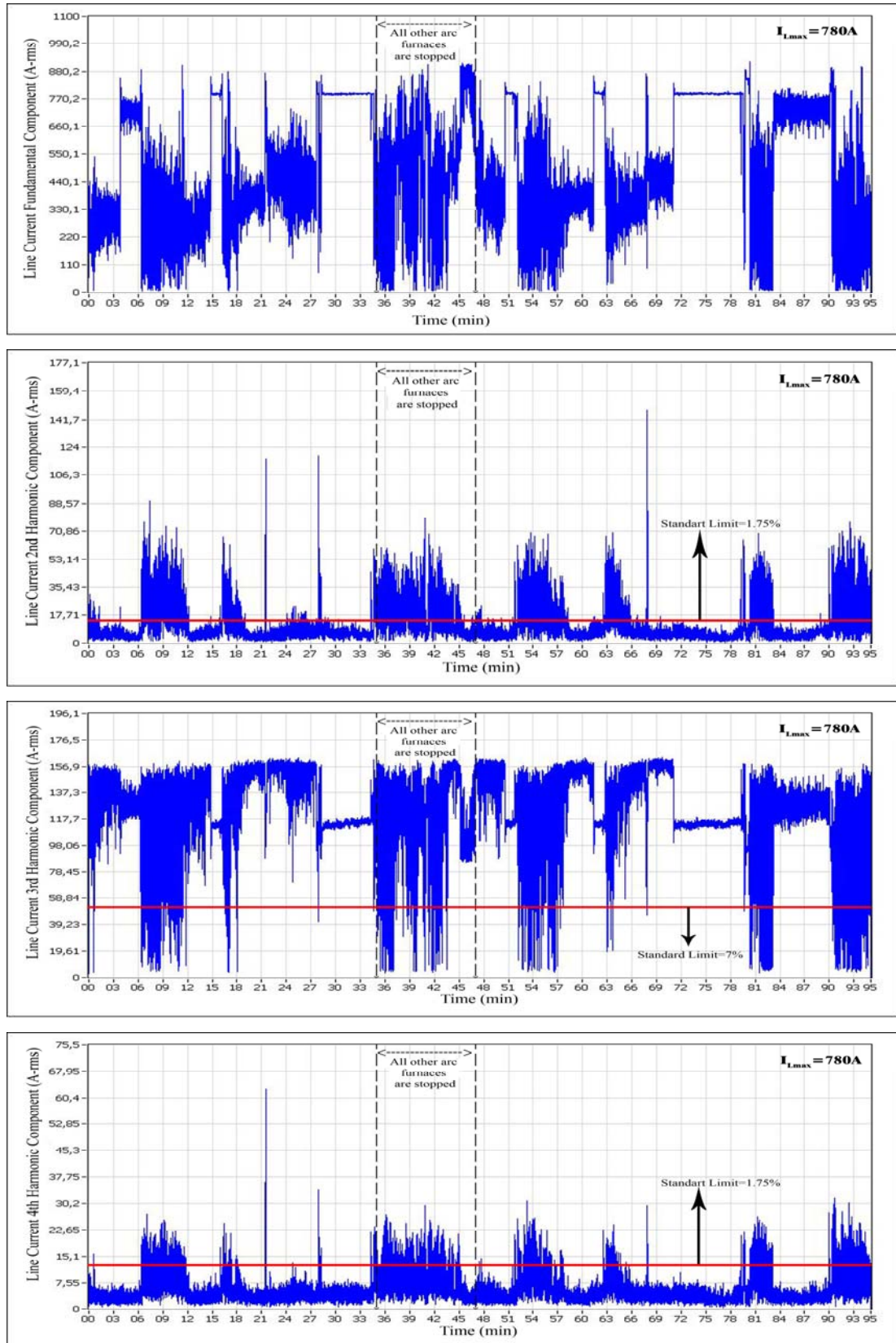
Fig. 6.1. Fundamental, 2nd, 3rd and 4th harmonic current components of TCR based SVC installed for an arc furnace plant in Aliağa region.

224

During this research work, it has been observed that the definition of harmonics in various harmonic standards such as [33], [34], [35],[39] and [42] is not clear. However IEC Std. 61000-4-7 [42] separates harmonics into three classes: Single line, group and subgroup. It has been assumed for the rapidly changing loads that the penalty limits specified in many harmonic standards should be applied in the sense of harmonic subgroup as defined in [42].In the case studies described in this thesis neither the flicker nor the 2nd harmonic and TDD problems are observed. However power quality measurements conducted in various iron and steel plants have shown that both of these problems are existing although those plants are equipped with TCR based SVCs. Furthermore, the operation of existing SVCs makes the light flicker more problematic in comparison to arc furnaces operating without SVC [37]. In order to find out whether this is an inherent disability of an SVC, some analysis work based on Steinmetz equation (2.48) has been carried out in Chapter 2.

The results have shown that:

a)   A higher harmonic filter installation than maximum reactive power demand of the arc furnace (nearly 1.577 times) is required.

b)   Higher installed TCR capacity then installed harmonic filter capacity (nearly 2.154 times reactive power demand of EAF) is needed

However the existing SVCs for EAF installations had much lower TCR and harmonic filter capacities than the required level to mitigate flicker. Even the installation of larger capacities for TCR and harmonic filters may not be successful because the TCR response may be in the order of (30ms-100ms).

For rapidly changing unbalanced loads, a portion of the 3rd harmonic current produced by TCR can not circulate in the Δ connected TCR phases but reflects to the supply lines. These currents will increase the loading on the 3rd harmonic passive shunt filters; therefore it should be taken into consideration in the design.

A reduction in the cost of TCR can be achieved by using reactor in each phase of TCR in one piece instead of two equal pieces for the limitation of short circuit current. This may be permissible for large SVC installations because non-repetitive on state surge currents of large disc-type thyristors may withstand short circuit currents for short durations.

6.2 Further Work

The use of iron core TCR reactors and harmonic filter reactors when they are placed in the containers can make SVC more compact and the resulting SVC can be relocated more easily and rapidly. This is also valid for coupling transformer which can be designed as dry type and placed in the container. However this new design philosophy increases the required cooling capability and makes the overall system more costly. As another alternative for the improvement of relocation process, whole system can be placed permanently placed on trailer(s). Here again, this new approach increases the cost of the system.

In medium voltage thyristor stacks in which several thyristors are connected in series for each forward or backward connected strings, the use of Light Triggered Thyristors (LTT) makes the power stage more compact and safe against EMI because the connection between the control system and power stage will only be the fiber optical cables. Moreover, internal break over diode (BOD) of LTT eliminates the need for overvoltage protection circuit which should be connected across each thyristor. However the use of LTT in TCR based SVC makes the system more costly and may introduce survivability problem because of the single supplier of LTT. An improved EMC can be obtained by using fiber optical triggering of the conventional thyristors as compared to power stacks employing electronic circuits via magnetic coupling.

It has been observed that response time of TCR based SVC is not short enough to follow rapid variation of the unbalanced loads such as EAF to improve successfully light flicker figures. One of the attempts in shortening the response time may be the use of theory of instantaneous power [69] in measuring reactive power consumed from the supply instead of classical reactive power measurement averaged over half cycle. It is worth noting that this can save us only 10ms time in the response. Another contribution may be the increased use of feed-forward controller, but this choice makes necessary very precise measurement of voltage and current waveforms and furthermore possible stability problems are to be solved.

REFERENCES

[1] T.J.E. Miller, "Reactive Power Control In Electric Systems,", John Wiley&Sons, 1982.

[2] J.Arrilaga, N.R. Watson, "Power System Harmonics", Wiley, 1982

[3] B. Mutluer, I. Çadırcı, M.Ermiş, A. Çetin, B. Gültekin, N. Özay, N. Köse, C. Ermiş, M. İnan, Ö.Ünver, V. Ünal, 'A Unified Relocatable SVC for Open-Cast Lignite Mining in Turkey', IEEE Transactions on Industry Applications Vol. 40, no.2, March/April 2004, pp.650-663

[4] N. Köse, B. Mutluer, A. Terciyanlı, B. Gültekin, A. Çetin, F. Bilgin, M. Ermiş, S. Hasbay, E. Akgül, Y. Bahtiyaroğlu, T. Ahi, M. Keyifli, 'Design and Implementation of a 12-Pulse TCR for a Ladle Furnace in ISDEMIR Iron & Steel Works, ACEMP 2004, Istanbul, Turkey, May 2004, pp.438-445

[5] N. Köse, B. Mutluer, A. Terciyanlı, B. Gültekin, A. Çetin, F. Bilgin, M. Ermiş, S. Hasbay, E. Akgül, Y. Bahtiyaroğlu, T. Ahi, M. Keyifli, 'Two-Folded Implementation of a 12-Pulse TCR with Dissimilar Transformers for a Ladle Furnace: Reactive Power Compensation and Power System Redundancy', IEEE IAS 39th Meeting, October 3-7, 2004, Seattle, USA

[6] A.Terciyanlı, M. Ermiş, B. Gültekin, O.B.Tör, M. Yörükoğlu, 'EMC Considerations in the Design of a Unified Relocatable SVC for Open Cast Lignite Mining in Turkey', IEEE Symposium on EMC, 2003, 16-18 May 2003, İstanbul, Turkey

[7] K.Habur,D. O'Leary "FACTS for Cost Effective and Reliable Transmission of Electrical Energy", SİEMENS 2004

[8] C. Schauder , M. Gernhardt , E. Stacey, T. Lemak, L. Gyugyi, W.T. Cease, A. Edris , ''Development of a ±100 MVAr static condenser for voltage control of

transmission systems'', IEEE Transactions on Power Delivery, vol.10, no.3, pp.1486 – 1496, 1995

[9]   Siemens, ''Power Compensation In Transmission Systems'', Siemens Power Engineering Guide, Transmission and Distribution, 4th editionFACTS

[10]   Understanding FACTS Gyugyi, L.;Hingorani, N. G.;December 1999

[11]   Thyristor-Based FACTS Controllers for Electrical Transmission Systems Varma, R. K.;Mathur, R. M.;February 2002

[12]   Mutale, J.; Strbac, G.; **"Transmission network reinforcement versus FACTS: an economic assessment"** IEEE Transactions on Power Systems, Volume 15, Issue 3, Aug. 2000 pp. 961 - 967

[13]   Paserba, J.J.; How FACTS controllers benefit AC transmission systems" IEEE Power Engineering Society General Meeting, 2004. 6-10 June 2004 Vol.2 pp.1257 - 1262

[14]   FACTS Terms & Definitions Task Forceof the DC and FACTS Subcommittee, "Proposed terms and definitions for flexible AC transmission system (FACTS)" IEEE Transactions on Power Delivery, Volume 12, Issue 4, Oct. 1997 pp.1848 - 1853

[15]   L.Gyugyi,"Power Electronics in Electric Utilities: Static Var Compensators", Proceeidngs of the IEEE Vol.76, No.4i April 1988 pp.483-494.

[16]   Gotham, D.J.; Heydt, G.T.; "Power flow control and power flow studies for systems with FACTS devices"IEEE Transactions on Power Systems, Volume 13, Issue 1, Feb. 1998 pp.60 - 65

[17]   P.C.Buddingh, "Even Harmonic Resonance – An Unusual Problem",IEEE Transactions on Industry Applications, vol.39, no.4, July/August 2003 pp.1181-1186

[18]   J.A. Orr,A.E. Emanuel, "On the Need for Strict Second Harmonic Limits" IEEE Transactions On Power Delivery, vol. 15 no. 3, July 2000, pp. 967-971.

[19]   http://www.iue.tuwien.ac.at/phd/park/node13.html

[20]   N. Mohan, "Power Electronics", Wiley, John & Sons, Oct. 2002

[21]   Tomas Larsson "Voltage Source Converters for Mitıgation Of Flicker Caused by Arc Furnaces " PhD Thesis, KTH,Sweden

[22]   IEEE 141," IEEE Recommended Practice for Electric Power Distribution for Industrial Plants", 1993

[23]   IEC 61000-4-30, "Testing and measurement techniques - Power quality measurement methods"

[24]   T. Keppler, N. R. Watson, S. Chen and J. Arrillaga *Digital Flickermeter* Realisations in The Time And Frequency Domains , 2001

[25]   IEC60038,'IEC standard voltages', 1983.

[26]   Web page, Wolfgang Meusel, Metals & Mining, November 2007, http://www.industry.siemens.com/metals/en/news/newsletter/mm_02_2004/art09.htm

[27]   Web page, ABB SVC reference List, January 2008, http://search.abb.com/library/ABBLibrary.asp?DocumentID=SVC_Q%20Ref&LanguageCode=en&DocumentPartID=&Action=Launch

[28]   Johnson, E. R. et al, "Static High Speed Var Control for Arc Furnace Flicker Reduction", Proceedings of the American Power Conference, 1972.

[29]   Frank, H. and Landstrom, B., "Power-Factor Correction With Thyristor-Controlled Capacitors", ASEA Journal, 1971, Vol. 44.No. 6.

[30]   L. Gyugyi et al," Prıncıples And Applıcatıons Of Statıc, Thyrıstor-Controlled Shunt Compensators",IEEE Transactions on Power Apparatus and Systems, Vol. PAS-97, No. 5, Sept/Oct 1978

[31]   "IEEE Guide for the Functional Specification of Transmission Static Var Compensators" IEEE Std 1031-1991)

[32]   Bilgin, H.F.; Ermis, M.; Kose, K.N.; Cetin, A.; Cadirci, I.; Acik, A.; Terciyanli, A.; Kocak, C.; Yorukoglu, "Reactive power compensation of coal mining excavators by using a new generation STATCOM" M.;Industry Applications Conference, Fourtieth IAS Annual Meeting. Conference Record of the 2005Volume 1, 2-6 Oct. 2005, pp.185 - 197

[33]   Elektrik İletim Sistemi Arz Güvenirliği ve Kalitesi, EPDK,2007

[34]   Elektrik Piyasası Şebeke Yönetmeliği, EPDK, 2007

[35]   IEEE 519, "IEEE Recommended Practices And Requirements for Harmonic Control",1992

[36]   "IEEE Guide for the Functional Specification of Transmission Static Var Compensators" IEEE Std 1031-2000 (Revision ofIEEE Std 1031-1991)

[37]   Salor, O.; Gultekin, B.; Buhan, S.; Boyrazoglu, B.; Inan, T.; Atalik, T.; Acik, A.; Terciyanli, A.; Unsar, O.; Altintas, E.; Akkaya, Y.; Ozdemirci, E.; Cadirci, I.; Ermis, M.; **"Electrical Power Quality of Iron and Steel Industry in Turkey"**; Industry Applications Conference, 2007. 42nd IAS Annual Meeting. Conference Record of the 2007 IEEE 23-27 Sept. 2007 pp. 404 - 423

[38]   M.V. Utalay, "Design and Implementation of a Medium Voltage Thyristor Controlled Reactor", MSc. Thesis, METU, Jan.1996

[39]   'Harmonic Constraints for Customers Disturbing the Electrical Power System', Turkish Electricity Council, 1993 (Bozucu Etki Yaratan Müşterilerin Uymak Zorunda Olduğu Koşullar, TEK, 1993, in Turkish)

[40]   ANSI/IEEE standard C57.110, "IEEE recommended practice for establishing transformer capability when supplying nonsinusoidal load currents ",1988

[41]   Tabandeh, M.; Alavi, M.H.; Marami, M.; Dehnavi, G.R.; "Design and Implementation of TSC Type SVC Using A New Approach For Electrical Quantities Measurement Power Tech Proceedings, 2001 IEEE Porto, Vol. 2, 10-13 Sept. 2001 pp.6

[42]   IEC Std. 61 000-4-7, General Guide on Harmonics and Interharmonics Measurement and Instrumentation for Power Supply Systems and Equipment Connected Thereto, 2002

[43]   Semikron Power Electronics Catalogue,Semikron Inc. Germany, 10/1998.

[44]   Lawatsch, H.M.; Vitins, J.; "Protection of thyristors against overvoltage with breakover diyotes", IEEE Transactions on Industry Applications Volume 24, Issue 3, May-June 1988 pp. 444 – 448

[45]   TS 831, "Standard Voltages in THE Distribution Systems" , 1979

[46]   "Effects of Temperature on Thyristor Performance" Application Note AN4870, Dynex Semiconductors, January 2000.

[47]   "Gate Triggering and Gate Characteristics" Application Note AN4840, Dynex Semiconductors, January 2000.

[48]   IEEE Std C57-120 "IEEE Loss Evalution Guide for Power Transformers and Reactors", 1991

[49]   ANSI/IEEE Std. C57-21, "Requirements,Terminology,and Test Code for Shunt Reactors Over 500 kVA", 1981

[50]   ANSI/IEEE Std. C37.109, "IEEE Guide for the Protection of Shunt Reactors" 1988

[51]   IEEE Std. C57-114, "IEEE Seismic Guide for Power Transformers and Reactors", 1990

[52]   IEEE Standard Requirements,Terminology, and Test Code for Shunt Reactors Rated Over 500 kVA, IEEE Std. C57.21-1990

[53]   IEEE Std. C57-125, "IEEE Guide for Failure Investigation, Documentation,and Analysis for Power Transformers and Shunt Reactors" 1991

[54]   "IEEE Loss Evalution Guide for Power Transformers and Reactors" IEEE Std C57-120-1991

[55]   IEC 60289 "Reactors",1988

[56]   IEC 60871, " Shunt capacitors for a.c. power systems having a rated voltage above 1 000 V", 2005

[57]   IEC 61642 Industrial a.c. Networks Affected by Harmonics - Application of Filters and Shunt Capacitors

[58]   IEC 76-1 "Power transformers Part 1: General", 1997

[59]   IEEE, "Guide for loading mineral-oil-immersed transformers,", IEEE Std. C57.91-1995.

[60]   L. W. Pierce, "An investigation of the thermal performance of an oil filled transformer winding," IEEE Trans. Power Delivery, vol. 7, no. 3,pp. 1347–1358, July 1992.

[61]   G. W. Swift et. Al, "Adaptive Transformer Thermal Overload Protection", IEEE Transactions On Power Delivery, Vol. 16, NO. 4, OCTOBER 2001, pp. 516-521

[62]   S.Lu, Y.Liu, J.D. La Ree; "Harmonics Generated from a DC Biased Transformer", IEEE Trans. On Power Delivery, Vol8., No.2, April 1993, pp 725-731

[63]   Alper Çetin "Design and Implementation of a Voltage Source Converter Based STATCOM for Reactive Power Compensation and Harmonic Filtering", Ph.D. Thesis, METU, 2007

231

[64]   Faruk Bilgin "Design and Implementation of a Current Source Converter Based STATCOM for Reactive Power Compensation"PhD. Thesis, METU, 2007

[65]   Web page, EPRI, November 2007,
http://www.epriweb.com/public/000000000001007646.pdf

[66]   Jintakosonwit Et Al.: "Shunt Active Filters For Harmonic Damping Throughout A Power Distribution System" IEEE Transactions On Industry Applications, Vol. 39, No. 2, March/April 2003 Pp.556-564

[67]   Mienski, R.; Pawelek, R.; Wasiak, I.;"Control algorithm for the 12-pulse SVC" 10th International Conference on Harmonics and Quality of Power, 2002. Volume 1, 2002 pp.50 - 55

[68]   Vivas, J.H.; Zambrano, J.D.;"Control of Thyristor Controlled Series Capacitor Based on Instantaneous Power Theory" Transmission & Distribution Conference and Exposition: Latin America, 2006. TDC '06. IEEE/PES Aug. 2006 pp.1 – 5

[69]   H. Akagi, A. Nabae, "The pq Theory in three phase systems under nonlinearconditions ", ETEP, vol. 3, N° 1, pp. 27-31, Jan/Feb. 1993.

[70]   Noroozian, M.; Petersson, A.N.; Thorvaldson, B.; Nilsson, B.A.; Taylor, C.W.; "Benefits of SVC and STATCOM for electric utility application" Transmission and Distribution Conference and Exposition, 2003 IEEE PES

[71]   Kundur, P.; Paserba, J.; Ajjarapu, V.; Andersson, G.; Bose, A.; Canizares, C.; Hatziargyriou, N.; Hill, D.; Stankovic, A.; Taylor, C.; Van Cutsem, T.; Vittal, V.;"Definition and classification of power system stability IEEE/CIGRE joint task force on stability terms and definitions", IEEE Transactions on Power Systems, Volume 19, Issue 3, Aug. 2004 pp.1387 – 1401

[72]   Trujillo, T.V.; Fuerte-Esquivel, C.R.; Hernandez, J.H.T.;"Advanced three-phase static VAr compensator models for power flow analysis"IEE Proceedings-Generation, Transmission and Distribution, Volume 150, Issue 1, Jan. 2003 Page(s):119 – 127

[73]   Kahle K, Larsson T.; "The New 150 Mvar, 18 Kv Static Var Compensator At Cern:Background, Design And Commissioning" 17th International Conference on Electricity Distribution; Barcelona, 12-15 May 2003; Session 2 Paper No 30

[74]   Silva.A, Hultqvist L., Wilcyznski W.; "Steel Plant Performance, Power Supply System Design And Power Quality Aspects", 54th Electric Furnace Conference - Dec. 96.

[75]   Muttik, P.K.; Wang, P.; Minchin, M.W.H.;"Detailed simulation of SVC transient performance using PSCAD" International Conference on Power System Technology, 2000. Proceedings. PowerCon 2000. Volume 2, 4-7 Dec. 2000 pp. 685 - 690

[76]   Knight R C, Young D J and Trainer D R, "Relocatable GTO-Based Static Var Compensator for National Grid Substations", in Proc. 1998 Session of CIGRÉ 14-106 Conf.

[77]   Gole, A.M.; Sood, V.K.;"Development of a state variable-based static compensator model" IEEE Power Electronics Specialists Conference, 1990. PESC '90 Record., 21st Annual 11-14 June 1990 pp.309 – 317

[78]   Y. Xu, W.; Martinich, T.G.; Sawada, J.H.; Mansour, "Harmonics from SVC transformer saturation with direct current ofset", IEEE Transactions on Power Delivery Volume 9, Issue 3, July 1994 pp.1502 – 1509

[79]   A. Açık, A. Çetin, M. Ermiş, A. Terciyanlı, T. Demirci, I. Çadırcı, C. Ermiş, A. Aydınay, 'A Fully Static Solution to Power Quality Problem of Light Rail Transportation System in Bursa, Turkey', ACEMP 2004, İstanbul, Turkey, May 2004, pp. 446-452.

CURRICULUM VITAE

PERSONAL INFORMATION

Surname, Name: Mutluer, Halas Bilge
Nationality: Turkish (TC)
Date and Place of Birth: 3 August 1974 , İzmir
Marital Status: Married
Phone: +90 312 210 13 10
Fax: +90 312 210 13 15
email: bilge.mutluer@uzay.tubitak.gov.tr

EDUCATION

Degree	Institution	Year of Graduation
MS	METU Electrical and Electronics Eng.	1999
BS	METU Electrical and Electronics Eng.	1996
High School	Bornova Anatolian Highschool	1992

WORK EXPERIENCE

Year	Place	Enrollment
2004- Present	TÜBİTAK UZAY	Chief Expert Researcher
2000-2004	TÜBİTAK UZAY	Expert Researcher
1996-2000	TÜBİTAK UZAY	Researcher
1994	PETPOSAN	Intern Engineering Student
1993	GE Medical Systems	Intern Engineering Student

FOREIGN LANGUAGES

Advanced English, Basic German

PUBLICATIONS

- B. Mutluer, I. Çadırcı, M.Ermiş, A. Çetin, B. Gültekin, N. Özay, N. Köse, C. Ermiş, M. İnan, Ö.Ünver, V. Ünal, 'A Unified Relocatable SVC for Open-Cast Lignite Mining in Turkey', IEEE Transactions on Industry Applications Vol. 40, no.2, March/April 2004, pp.650-663
- N. Köse, B. Mutluer, A. Terciyanlı, B. Gültekin, A. Çetin, F. Bilgin, M. Ermiş, S. Hasbay, E. Akgül, Y. Bahtiyaroğlu, T. Ahi, M. Keyifli, 'Design and Implementation of a 12-Pulse TCR for a Ladle Furnace in ISDEMIR Iron & Steel Works, ACEMP 2004, Istanbul, Turkey, May 2004, pp.438-445
- N. Köse, B. Mutluer, A. Terciyanlı, B. Gültekin, A. Çetin, F. Bilgin, M. Ermiş, S. Hasbay, E. Akgül, Y. Bahtiyaroğlu, T. Ahi, M. Keyifli, 'Two-Folded Implementation of a 12-Pulse TCR with Dissimilar Transformers for a Ladle Furnace: Reactive Power Compensation and Power System Redundancy', IEEE IAS 39th Meeting, October 3-7, 2004, Seattle, USA

- Cetin, A.; Bilgin, H. F.; Acik, A.; Demirci, T.; Kose, K. N.; Terciyanli, A.; Gultekin, B.; Aksoy, N.; Mutluer, B.; Cadirci, I.; Ermis, M.; Ongan, K.; Akinci, N.; "Reactive Power Compensation of Coal Conveyor Belt Drives by Using D-STATCOMs", IEEE Industry Applications Conference, 2007. 42nd IAS Annual Meeting. Conference Record of the 2007 ,23-27 Sept. 2007 pp.1731 - 1740
- B.Mutluer "Tiristör Kontrollu Reaktör Tasarımında Akım Harmoniklerinin Değerlendirilmesi", ELECO, Bursa, Aralık 2006

HOBBIES

Guitar, sailing, windsurfing,